Statistical Modelling and Applications Using Weibull and Burr III Distributions

Submitted to

UNIVERSITY OF CALICUT

in partial fulfillment of the requirements

for the award of the Degree of

DOCTOR OF PHILOSOPHY

in

STATISTICS

By

Deepthy G. S

Under the guidance of

Dr Nicy Sebastian

Research and Postgraduate Department of Statistics

St. Thomas College (Autonomous)

Thrissur - 680001, Kerala.

September 2025

CERTIFICATE

This is to certify that all the suggestions recommended by the adjudicators of the PhD thesis of Ms. Deepthy G. S have been incorporated and implemented in the thesis entitled, ***"Statistical Modelling and Applications Using Weibull and Burr III Distributions"***. The content of the thesis in both hard copy and soft copy are one and same.

Thrissur

24 September, 2025

Dr Nicy Sebastian

Supervising Teacher

Dr. Nicy Sebastian
Assistant Professor
P.G. & Research Department of Statistics
St. Thomas' College (Autonomous), Thrissur-1

DECLARATION

I, **Deepthy G. S**, hereby declare that the work presented in the thesis entitled, ***"Statistical Modelling and Applications Using Weibull and Burr III Distributions"***, is based on the original work done by me under the guidance of Dr Nicy Sebastian, Assistant Professer, Department of Statistics, St. Thomas College (Autonomous), Thrissur, Kerala and has not been included in any other thesis submitted previously for the award of any agree. The contents of the thesis are undergone plagiarism check using iThenticate software at C.H.M.K. Library, University of Calicut, and the similarity index found within the permissible limit. I also declare that the thesis is free from AI generated contents.

Deepthy

Thrissur
11 June, 2025

Deepthy G. S

ST. THOMAS COLLEGE (AUTONOMOUS) ESTD 1889 THRISSUR

Dr. Nicy Sebastian
Assistant Professor
P.G. & Research Department of Statistics
St. Thomas' College (Autonomous), Thrissur-1

CERTIFICATE

This is to certify that the thesis titled ***"Statistical Modelling and Applications Using Weibull and Burr III Distributions"*** submitted by **Deepthy G. S** to the **University of Calicut** in partial fulfilment of the requirements for the award of the Degree of ***Doctor of Philosophy in Statistics*** is a record of original research work carried out by her under my supervision. The content of this thesis, in full or in parts, has not been submitted by any other candidate to any other University for the award of any degree or diploma.

Thrissur

11 June, 2025

Dr Nicy Sebastian

Assistant Professor

St. Thomas College (Autonomous)

Thrissur, Kerala

Dr. Nicy Sebastian
Assistant Professor
P.G. & Research Department of Statistics
St. Thomas' College (Autonomous), Thrissur-1

ABSTRACT

Lifetime data analysis is crucial in areas like reliability engineering, survival analysis, and related fields, as it is essential to accurately model time-to-event data for effective risk assessment, reliability evaluation, and informed decision making. However, classical lifetime distributions often struggle with real-world data complexities such as skewness, heavy tails, and diverse hazard rate behaviours. To address these challenges, this thesis focuses on the Weibull and Burr III distributions, known for their flexibility and wide applicability, and develops new models, regression frameworks, and inferential methods to advance lifetime data analysis.

The thesis, titled *Statistical Modelling and Applications Using Weibull and Burr III Distributions*, is organized into ten chapters. Chapter 1 establishes the theoretical background, covering quantile functions, regression models, censoring schemes, and competing risks, alongside a comprehensive literature review. Chapter 2 proposes a new family of distributions combining the quantile functions of Burr III and Weibull, examining their key characteristics and reliability properties. Model parameters are estimated using method of Least Squares and method of L - moments, with performance illustrated through two real-life datasets. Chapter 3 proposes the Burr III Weibull (BIIIW) distribution, analyzes its statistical properties, and develops estimation procedures via maximum likelihood. Its performance is validated through simulations and application to Covid-19 data. Chapter 4 explores the survival features of the Odd Burr III Weibull (OBIIIW) distribution through a comparative analysis between artificial neural networks (ANNs) and the maximum likelihood estimation (MLE) method, showing the promise of ANNs for clinical data modelling.

Chapter 5 develops a parametric regression model using OBIIIW to analyse censored data and complex hazard patterns such as bathtub-shaped failure rates. Estimation is performed using MLE and jackknife methods, with robustness checks via simulations and diagnostics based on influence measures. Chapter 6 investigates stress-strength reliability (SSR) when variables follow Weibull Burr III distributions, using maximum likelihood and Bayesian approaches. The performance of the estimators is validated through a simulation study and two

real-life clinical datasets. Chapter 7 addresses competing risks under generalized type-II hybrid censoring, employing MLE and Bayesian methods for both point and interval estimation, supported by simulation and real-world applications. Chapter 8 extends SSR analysis to multicomponent systems with non-identical strength components under progressive first failure censoring, applying both classical and Bayesian approaches, and illustrates the practical utility with real data.

Chapter 9 summarizes the thesis by highlighting new statistical models, a novel regression model, ANN-based survival analysis, and inferential work on SSR, multicomponent SSR, and competing risk scenarios under censoring framework. Chapter 10 outlines future research directions for extending these methods to more complex data and wider applications.

Keywords: Lifetime data analysis, Maximum Likelihood Estimation, Bayesian Estimation, Censored data, Survival analysis, Competing Risks.

പഠനസംഗ്രഹം

റിലയബിലിറ്റി എഞ്ചിനീയറിംഗ്, സർവൈവൽ അനാലിസിസ് തുടങ്ങിയ മറ്റ് അനുബന്ധ മേഖലകളിലെ ലൈഫ് ടൈം ഡാറ്റ വിശകലനം നിർണായകമായ ഒന്നാണ്. ഫലപ്രദമായ അപകടസാധ്യത വിലയിരുത്തൽ, വിശ്വാസ്യത വിലയിരുത്തൽ, നിർണായകമായ തീരുമാനമെടുക്കൽ എന്നിവയ്ക്കായി ടൈം-ഇവൻറ് ഡാറ്റ കൃത്യമായി മാതൃകയാക്കേണ്ടത് അത്യാവശ്യമാണ്. യഥാർത്ഥ ലോകത്തിൽ നിന്ന് ലഭിക്കുന്ന ലൈഫ് ടൈം ഡാറ്റ സാധാരണയായി സ്കൈനെസ്, ഹെവി ടെയിൽ, വ്യത്യസ്ത ഹസാർഡ് റേറ്റ് പാറ്റേണുകൾ എന്നിവ കാണിക്കുന്നതിനാൽ, ഈ സങ്കീർണ്ണതകളെ പരമ്പരാഗത ഡിസ്ട്രിബ്യൂഷനുകൾക്ക് പൂർണമായി പ്രതിനിധീകരിക്കാൻ കഴിയാതെ വരുന്നു. ഈ വെല്ലുവിളികളെ മറികടക്കുന്നതിനായി വൈവിധ്യമാർന്ന ലൈഫ് ടൈം ഡിസ്ട്രിബ്യൂഷനുകൾ വികസിപ്പിച്ചെടുത്തിട്ടുണ്ട്. അതിൽ വെയ്ബുൾ, ബർ III എന്നീ ഡിസ്ട്രിബ്യൂഷനുകൾ അവയുടെ ഫ്ലെക്സിബിലിറ്റി, വിശകലന-ലാളിത്യം, വിശാലമായ പ്രായോഗികക്ഷമത എന്നിവയാൽ ശ്രദ്ധേയമാണ്. പ്രസ്തുത പ്രബന്ധത്തിൽ നൂതനമായ സ്റ്റാറ്റിസ്റ്റിക്കൽ മോഡലുകൾ സൃഷ്ടിക്കുന്നതിനും, സങ്കീർണ്ണമായ റിലയബിലിറ്റി പ്രശ്നങ്ങൾ പരിഹരിക്കുന്നതിനും, വിവിധ പ്രായോഗിക സാഹചര്യങ്ങളിൽ ലൈഫ് ടൈം ഡാറ്റ വിശകലനത്തിനായി ഫലപ്രദമായ രീതികൾ വാഗ്ദാനം ചെയ്യുന്നതിനും, ഈ രണ്ട് ഡിസ്ട്രിബ്യൂഷൻകളിൽ ശ്രദ്ധ കേന്ദ്രീകരിച്ചിരിക്കുന്നു.

"വെയ്ബുൾ, ബർ III ഡിസ്ട്രിബ്യൂഷനുകൾ ഉപയോഗിച്ചുള്ള സ്റ്റാറ്റിസ്റ്റിക്കൽ മോഡലിംഗും ആപ്ലിക്കേഷനുകളും" എന്ന ശീർഷകത്തിലുള്ള ഈ പ്രബന്ധം പത്ത് അദ്ധ്യായങ്ങളായി ക്രമീകരിച്ചിരിക്കുന്നു. അദ്ധ്യായം 1 ഈ ഗവേഷണത്തെ പിന്തുണയ്ക്കുന്ന അടിസ്ഥാന ആശയങ്ങൾ ഫലപ്രദമായി അവതരിപ്പിക്കുകയും നിലവിലുള്ള പഠനങ്ങളുടെ സമഗ്ര അവലോകനം നൽകുകയും ചെയ്യുന്നു. അദ്ധ്യായം 2-ൽ ബർ III യും വെയ്ബുൾ ഡിസ്ട്രിബ്യൂഷനും, സംയോജിപ്പിച്ച കാണ്ടെൽ ഫംഗ്ഷനുകളുടെ അടിസ്ഥാനത്തിൽ ഒരു പുതിയ ഡിസ്ട്രിബ്യൂഷൻ ഫാമിലിയെ അവതരിപ്പിക്കുന്നു. ഈ അദ്ധ്യായത്തിൽ പുതിയ ഡിസ്ട്രിബ്യൂഷനുകളുടെ വിശ്വാസ്യത, മറ്റ് റിലയബിലിറ്റി സവിശേഷതകൾ, രണ്ട് യഥാർത്ഥ ലൈഫ് ടൈം ഡാറ്റാസെറ്റുകൾ ഉപയോഗിച്ച് മോഡലിൻ്റെ പ്രവർത്തനം എന്നിവ വിശദമായി പരിശോധിക്കുന്നു. അദ്ധ്യായം 3-ൽ, യഥാർത്ഥ ഡാറ്റയുടെ സങ്കീർണ്ണതകൾ മനസിലാക്കുവാൻ വേണ്ടി ബർ III വെയ്ബുൾ ഡിസ്ട്രിബ്യൂഷൻ അവതരിപ്പിക്കുന്നു. ഈ മോഡൽ വിവിധ വാർദ്ധക്യ ഘട്ടങ്ങൾ, ഫെയ്ലിയർ പാറ്റേണുകൾ എന്നിവയെ ഉൾക്കൊള്ളുന്നതുകൊണ്ട് റിലയബിലിറ്റിക്കും സർവൈവൽ വിശകലനത്തിനും ഉപയോഗപ്രദമാണ്. മാക്സിമം ലൈക്ലിഹുഡ് എസ്റ്റിമേഷൻ (MLE) ഉപയോഗിച്ച് പാരാമീറ്ററുകൾ കണക്കാക്കുകയും, കോവിഡ്-19 ഡാറ്റ ഉപയോഗിച്ച് ഈ മോഡലുകളുടെ പ്രായോഗികത ദൃശ്യമാക്കുകയും ചെയ്തിരിക്കുന്നു.

ആർട്ടിഫിഷ്യൽ ന്യൂറൽ നെറ്റ്വർക്കുകളും (ANN-കൾ) MLE രീതിയും തമ്മിലുള്ള താരതമ്യ വിശകലനത്തിലൂടെ ഓഡ് ബർ III വെയ്ബുൾ (OBIIIW) ഡിസ്ട്രിബ്യൂഷൻ്റെ സർവൈവൽ സവിശേഷതകൾ അദ്ധ്യായം 4-ൽ പര്യവേക്ഷണം ചെയ്യുന്നു. ഈ അധ്യായത്തിലെ കണ്ടെത്തലുകൾ പ്രകാരം ക്ലിനിക്കൽ ഡാറ്റ വിശകലനത്തിന് ന്യൂറൽ നെറ്റ്വർക്കുകൾ വളരെ പ്രതീക്ഷ നൽകുന്നതാണ്. അദ്ധ്യായം 5-ൽ OBIIIW ഡിസ്ട്രിബ്യൂഷനെ അടിസ്ഥാനമാക്കി ഒരു പാരാമെട്രിക് ലൊക്കേഷൻ-സ്കെയിൽ റിഗ്രഷൻ ഫ്രെയിംവർക്ക് അവതരിപ്പിക്കുന്നു. ഇത് വിവിധ ഫെയ്ലിയർ റേറ്റ് സ്വഭാവങ്ങളെ ഫലപ്രദമായി മോഡൽ ചെയ്യുന്നു. മോഡലിൻ്റെ പ്രായോഗിക പ്രയോജനം യഥാർത്ഥ ഡാറ്റാസെറ്റ് ഉപയോഗിച്ചു തെളിയിക്കുന്നു.

വെയ്ബുൾ ബർ III ഡിസ്ട്രിബ്യൂഷൻ്റെ സ്ട്രെസ്-സ്ട്രെങ്ത് റിലയബിലിറ്റി (SSR) കണക്കാക്കുന്നതിലാണ് അദ്ധ്യായം 6 ശ്രദ്ധ കേന്ദ്രീകരിക്കുന്നത്. MLE, ബയേഷ്യൻ സാങ്കേതിക വിദ്യകൾ ഉപയോഗിച്ചാണ് എസ്റ്റിമേറ്റുകൾ പരിശോധിക്കുന്നത്. രണ്ട് ക്ലിനിക്കൽ ഡാറ്റാസെറ്റുകൾ ഉപയോഗിച്ച് ഈ സാങ്കേതിക വിദ്യകളുടെ ഫലപ്രാപ്തി തെളിയിക്കപ്പെടുന്നു.വെയ്ബുൾ ഡിസ്ട്രിബ്യൂഷൻ പിന്തുടരുന്ന ലെയ്റ്റന്റ് ഫെയ്ലിയർ ടൈംസ് ഒരു കോംപിറ്റിങ് റിസ്ക് മാതൃകയിലൂടെ, അദ്ധ്യായം 7-ൽ പഠിക്കുന്നു. സാമാന്യവൽക്കരിച്ച ടൈപ്പ്-II ഹൈബ്രിഡ്

സെൻസറിംഗ് സ്കീമിന് കീഴിൽ ഫെയ്ലിയറിന്റെ സമയവും, കാരണങ്ങളും ഭാഗികമായി നിരീക്ഷിക്കുകയും ചെയുന്നു. യഥാർത്ഥ ലോകത്തിലെ ഒരു കേസ്സ് സ്റ്റഡിയും ഉദാഹരണത്തിന് ഉൾപ്പെടുത്തിയിട്ടുണ്ട്. സ്ലെങ്ത് ഘടകങ്ങൾ ഒരുപോലെയല്ലാത്ത ഒരു മൾട്ടികോമ്പോണൻറ് സിസ്റ്റത്തിൽ SSR-നെക്കുറിച്ചുള്ള അനുമാനങ്ങൾ ഉണ്ടാക്കുന്നതിലാണ് അദ്ധ്യായം 8 ശ്രദ്ധ കേന്ദ്രീകരിക്കുന്നത്. വെയ്ബുൾ ഡിസ്ട്രിബ്യൂഷനിൽ നിന്ന് ഉരുത്തിരിഞ്ഞ പ്രോഗ്രസിവ് ഫസ്റ്റ് ഫെയ്ലൂർ സെൻസർ ചെയ്ത ഡാറ്റയാണ് വിശകലനത്തിനായി ഉപയോഗിക്കുന്നത്. മൾട്ടികോമ്പോണൻറ് SSR മോഡലിന്റെ പ്രായോഗികത തെളിയിക്കുന്നതിനായി ഒരു സമീപകാല ഡാറ്റാസെറ്റ് ഉപയോഗപ്പെടുത്തിയിട്ടുണ്ട്,

അദ്ധ്യായം 9-ൽ പ്രബന്ധത്തിൽ ഉൾപ്പെടുത്തിയ പ്രധാന കണ്ടെത്തലുകളുടെ സാരാംശം അവതരിപ്പിക്കുന്നു. പുതിയ സ്റ്റാറ്റിസ്റ്റിക്കൽ മോഡലുകളുടെ വികസനം, ഒരു പുതിയ റിഗ്രഷൻ മോഡലിന്റെ പരിചയം, സർവൈവൽ വിശകലനത്തിൽ ANN-കളുടെ പ്രയോഗം എന്നിവയ്ക്ക് പ്രത്യേകമായ ശ്രദ്ധ നൽകുന്നു, കൂടാതെ വിവിധ സെൻസറിംഗ് ചട്ടക്കൂടുകൾക്കുള്ളിലെ മൾട്ടികോമ്പോണന്റ് SSR, കോംപിറ്റിങ് റിസ്ക് സാഹചര്യങ്ങൾ എന്നിവയുടെ ആഴത്തിലുള്ള അനുമാന വിശകലനം വാഗ്ദാനം ചെയ്യുന്നു. നിർദ്ദിഷ്ട മോഡലുകൾ കൂടുതൽ സങ്കീർണ്ണമായ ഡാറ്റാ ഘടനകളിലേക്കും വിശാലമായ ആപ്ലിക്കേഷൻ മേഖലകളിലേക്കും വ്യാപിപ്പിക്കുന്നതിനുള്ള ഭാവി ദിശകളും അദ്ധ്യായം 10 നൽകുന്നു.

പ്രധാന വാക്കുകൾ: ലൈഫ്ടൈം ഡാറ്റ വിശകലനം, മാക്സിമം ലൈക്ലിഹുഡ് എസ്റ്റിമേഷൻ, ബയേഷ്യൻ എസ്റ്റിമേഷൻ, സെൻസേർഡ് ഡാറ്റ, സർവൈവൽ അനാലിസിസ്, കോംപിറ്റിങ് റിസ്ക്.

To My Family

ACKNOWLEDGEMENTS

I would like to express my deepest gratitude to everyone who has supported and guided me throughout my Ph.D. journey.

First and foremost, I am forever indebted to God, whose grace and strength sustained me during the challenging times and inspired me to persevere in my research. His presence has been my constant source of comfort and motivation.

I want to thank my supervisor, Dr Nicy Sebastian, Assistant Professor in the Department of Statistics at St. Thomas College (Autonomous) in Thrissur, for her invaluable guidance and mentorship throughout my research journey. Her guidance, constant encouragement, and patient supervision have been instrumental in shaping the direction and depth of this work. I am truly grateful for the freedom she provided to explore ideas independently while always being available with thoughtful advice and unwavering support. It has been a great privilege to work under her guidance.

I would like to thank Dr Fr Martin K. A., our Principal, for his continuous support during my research. I'm also grateful to St. Thomas College (Autonomous) for the essential infrastructure that aided my work, and to Mr. Sanjo Jose, our librarian, for his prompt assistance with my academic inquiries.

I would like to express my sincere gratitude to Dr Sajesh T. A., Head of the Department, and Dr V. M. Chacko, Professor, in the Department of Statistics, for their unwavering moral support and encouragement throughout my research journey. I also thank all the faculty and staff in the Department of Statistics for their support and for creating an encouraging academic environment during my doctoral studies.

I would like to express my sincere appreciation to my collaborators, Dr Navin Chandra from the Department of Statistics, Ramanujan School of Mathematical Sciences, Pondicherry University, Puducherry, and Dr Sujesh A. S., Assistant Professor at Shri C. Achutha Menon Government College, Kuttanellur, Thrissur. Their insightful input and consistent support have been instrumental in enhancing the depth and quality of my research.

I extend my love and gratitude to all the scholars from our research room who made these years memorable and inspiring. We were like a family, and each

one holds a special place in my heart. While I cannot name everyone here, I am especially grateful to Sini K. P., Lakshmi R., Anakha K K, Jincy Pauly, Ann Sania, Amrutha M., and Abhijith P., for their invaluable encouragement and unwavering support.

I was able to complete this journey because of the love and support of my family. A special thanks to my husband, Akhilraj N. S., whose steady support and patience helped me through every stage of this work. His encouragement, understanding, and sacrifices allowed me to stay focused and keep going, even during difficult times. I am deeply grateful to my parents, whose love, prayers, and endless support have always guided me forward, and for lovingly caring for my sons during my research journey a support that was truly instrumental in helping me complete this work. A special note of love goes to my dear sons, Anayraj and Anirudh, whose innocent smiles, love, and presence gave me happiness and kept me strong throughout this journey. I also thank my sister Divya, her husband, and their sons for their love, support, and care, which always made me feel encouraged and positive throughout this journey.

Deepthy G. S

Contents

List of Figures

List of Tables

Contents

ABSTRACT

Lifetime data analysis is crucial in areas like reliability engineering, survival analysis, and related fields, as it is essential to accurately model time-to-event data for effective risk assessment, reliability evaluation, and informed decision making. However, classical lifetime distributions often struggle with real-world data complexities such as skewness, heavy tails, and diverse hazard rate behaviours. To address these challenges, this thesis focuses on the Weibull and Burr III distributions, known for their flexibility and wide applicability, and develops new models, regression frameworks, and inferential methods to advance lifetime data analysis.

The thesis, titled *Statistical Modelling and Applications Using Weibull and Burr III Distributions*, is organized into ten chapters. Chapter 1 establishes the theoretical background, covering quantile functions, regression models, censoring schemes, and competing risks, alongside a comprehensive literature review. Chapter 2 proposes a new family of distributions combining the quantile functions of Burr III and Weibull, examining their key characteristics and reliability properties. Model parameters are estimated using method of Least Squares and method of L - moments, with performance illustrated through two real-life datasets. Chapter 3 proposes the Burr III Weibull (BIIIW) distribution, analyzes its statistical properties, and develops estimation procedures via maximum likelihood. Its performance is validated through simulations and application to Covid-19 data. Chapter 4 explores the survival features of the Odd Burr III Weibull (OBIIIW) distribution through a comparative analysis between artificial neural networks (ANNs) and the maximum likelihood estimation (MLE) method, showing the promise of ANNs for clinical data modelling.

Chapter 5 develops a parametric regression model using OBIIIW to analyse censored data and complex hazard patterns such as bathtub-shaped failure rates. Estimation is performed using MLE and jackknife methods, with robustness checks via simulations and diagnostics based on influence measures. Chapter 6 investigates stress-strength reliability (SSR) when variables follow Weibull Burr III distributions, using maximum likelihood and Bayesian approaches. The performance of the estimators is validated through a simulation study and two

real-life clinical datasets. Chapter 7 addresses competing risks under generalized type-II hybrid censoring, employing MLE and Bayesian methods for both point and interval estimation, supported by simulation and real-world applications. Chapter 8 extends SSR analysis to multicomponent systems with non-identical strength components under progressive first failure censoring, applying both classical and Bayesian approaches, and illustrates the practical utility with real data.

Chapter 9 summarizes the thesis by highlighting new statistical models, a novel regression model, ANN-based survival analysis, and inferential work on SSR, multicomponent SSR, and competing risk scenarios under censoring framework. Chapter 10 outlines future research directions for extending these methods to more complex data and wider applications.

Keywords: Lifetime data analysis, Maximum Likelihood Estimation, Bayesian Estimation, Censored data, Survival analysis, Competing Risks.

പഠനസംഗ്രഹം

റിലയബിലിറ്റി എഞ്ചിനീയറിംഗ്, സർവൈവൽ അനാലിസിസ് തുടങ്ങിയ മറ്റ് അനുബന്ധ മേഖലകളിലെ ലൈഫ് ടൈം ഡാറ്റ വിശകലനം നിർണായകമായ ഒന്നാണ്. ഫലപ്രദമായ അപകടസാധ്യത വിലയിരുത്തൽ, വിശ്വാസ്യത വിലയിരുത്തൽ, നിർണായകമായ തീരുമാനമെടുക്കൽ എന്നിവയ്ക്കായി ടൈം-ടു-ഇവൻറ് ഡാറ്റ കൃത്യമായി മാതൃകയാക്കേണ്ടത് അത്യാവശ്യമാണ്. യഥാർത്ഥ ലോകത്തിൽ നിന്ന് ലഭിക്കുന്ന ലൈഫ് ടൈം ഡാറ്റ സാധാരണയായി സ്കൂനെസ്, ഹെവി ടെയിൽ, വ്യത്യസ്ത ഹസാർഡ് റേറ്റ് പാറ്റേണുകൾ എന്നിവ കാണിക്കുന്നതിനാൽ, ഈ സങ്കീർണ്ണതകളെ പരമ്പരാഗത ഡിസ്ട്രിബ്യൂഷനുകൾക്ക് പൂർണമായി പ്രതിനിധീകരിക്കാൻ കഴിയാതെ വരുന്നു. ഈ വെല്ലുവിളികളെ മറികടക്കുന്നതിനായി വൈവിധ്യമാർന്ന ലൈഫ് ടൈം ഡിസ്ട്രിബ്യൂഷനുകൾ വികസിപ്പിച്ചെടുത്തിട്ടുണ്ട്. അതിൽ വെയ്ബുൾ, ബർ III എന്നീ ഡിസ്ട്രിബ്യൂഷനുകൾ അവയുടെ ഫ്ലെക്സിബിലിറ്റി, വിശകലന-ലാളിത്യം, വിശാലമായ പ്രായോഗികക്ഷമത എന്നിവയാൽ ശ്രദ്ധേയമാണ്. പ്രസ്തുത പ്രബന്ധത്തിൽ നൂതനമായ സ്റ്റാറ്റിസ്റ്റിക്കൽ മോഡലുകൾ സൃഷ്ടിക്കുന്നതിനും, സങ്കീർണ്ണമായ റിലയബിലിറ്റി പ്രശ്നങ്ങൾ പരിഹരിക്കുന്നതിനും, വിവിധ പ്രായോഗിക സാഹചര്യങ്ങളിൽ ലൈഫ് ടൈം ഡാറ്റ വിശകലനത്തിനായി ഫലപ്രദമായ രീതികൾ വാഗ്ദാനം ചെയ്യുന്നതിനും, ഈ രണ്ട് ഡിസ്ട്രിബ്യൂഷൻകളിൽ ശ്രദ്ധ കേന്ദ്രീകരിച്ചിരിക്കുന്നു.

"വെയ്ബുൾ, ബർ III ഡിസ്ട്രിബ്യൂഷനുകൾ ഉപയോഗിച്ചുള്ള സ്റ്റാറ്റിസ്റ്റിക്കൽ മോഡലിംഗും ആപ്ലിക്കേഷനുകളും" എന്ന ശീർഷകത്തിലുള്ള ഈ പ്രബന്ധം പത്ത് അദ്ധ്യായങ്ങളായി ക്രമീകരിച്ചിരിക്കുന്നു. അദ്ധ്യായം 1 ഈ ഗവേഷണത്തെ പിന്തുണയ്ക്കുന്ന അടിസ്ഥാന ആശയങ്ങൾ ഫലപ്രദമായി അവതരിപ്പിക്കുകയും നിലവിലുള്ള പഠനങ്ങളുടെ സമഗ്ര അവലോകനം നൽകുകയും ചെയ്യുന്നു. അദ്ധ്യായം 2-ൽ ബർ III യും വെയ്ബുൾ ഡിസ്ട്രിബ്യൂഷനും, സംയോജിപ്പിച്ച കാണ്ടെൽ ഫംഗ്ഷനുകളുടെ അടിസ്ഥാനത്തിൽ ഒരു പുതിയ ഡിസ്ട്രിബ്യൂഷൻ ഫാമിലിയെ അവതരിപ്പിക്കുന്നു. ഈ അദ്ധ്യായത്തിൽ പുതിയ ഡിസ്ട്രിബ്യൂഷനുകളുടെ വിശ്വാസ്യത, മറ്റ് റിലയബിലിറ്റി സവിശേഷതകൾ, രണ്ട് യഥാർത്ഥ ലൈഫ് ടൈം ഡാറ്റാസെറ്റുകൾ ഉപയോഗിച്ച് മോഡലിൻറെ പ്രവർത്തനം എന്നിവ വിശദമായി പരിശോധിക്കുന്നു. അദ്ധ്യായം 3-ൽ, യഥാർത്ഥ ഡാറ്റയുടെ സങ്കീർണ്ണതകൾ മനസിലാക്കുവാൻ വേണ്ടി ബർ III വെയ്ബുൾ ഡിസ്ട്രിബ്യൂഷൻ അവതരിപ്പിക്കുന്നു. ഈ മോഡൽ വിവിധ വാർദ്ധക്യ ഘട്ടങ്ങൾ, ഫെയ്ലിയർ പാറ്റേണുകൾ എന്നിവയെ ഉൾക്കൊള്ളുന്നതുകൊണ്ട് റിലയബിലിറ്റിക്കും സർവൈവൽ വിശകലനത്തിനും ഉപയോഗപ്രദമാണ്. മാക്സിമം ലൈക്ലിഹുഡ് എസ്റ്റിമേഷൻ (MLE) ഉപയോഗിച്ച് പാരാമീറ്ററുകൾ കണക്കാക്കുകയും, കോവിഡ്-19 ഡാറ്റ ഉപയോഗിച്ച് ഈ മോഡലുകളുടെ പ്രായോഗികത ദൃശ്യമാക്കുകയും ചെയ്തിരിക്കുന്നു.

ആർട്ടിഫിഷ്യൽ ന്യൂറൽ നെറ്റ്വർക്കുകളും (ANN-കൾ) MLE രീതിയും തമ്മിലുള്ള താരതമ്യ വിശകലനത്തിലൂടെ ഓഡ് ബർ III വെയ്ബുൾ (OBIIIW) ഡിസ്ട്രിബ്യൂഷൻറെ സർവൈവൽ സവിശേഷതകൾ അദ്ധ്യായം 4-ൽ പര്യവേക്ഷണം ചെയ്യുന്നു. ഈ അധ്യായത്തിലെ കണ്ടെത്തലുകൾ പ്രകാരം ക്ലിനിക്കൽ ഡാറ്റ വിശകലനത്തിന് ന്യൂറൽ നെറ്റ്വർക്കുകൾ വളരെ പ്രതീക്ഷ നൽകുന്നതാണ്. അദ്ധ്യായം 5-ൽ OBIIIW ഡിസ്ട്രിബ്യൂഷനെ അടിസ്ഥാനമാക്കി ഒരു പാരാമെട്രിക് ലൊക്കേഷൻ-സ്കെയിൽ റിഗ്രഷൻ ഫ്രെയിംവർക്ക് അവതരിപ്പിക്കുന്നു. ഇത് വിവിധ ഫെയ്ലിയർ റേറ്റ് സ്വഭാവങ്ങളെ ഫലപ്രദമായി മോഡൽ ചെയ്യുന്നു. മോഡലിൻറെ പ്രായോഗിക പ്രയോജനം യഥാർത്ഥ ഡാറ്റാസെറ്റ് ഉപയോഗിച്ചു തെളിയിക്കുന്നു.

വെയ്ബുൾ ബർ III ഡിസ്ട്രിബ്യൂഷൻറെ സ്ട്രെസ്-സ്ട്രെങ്ത് റിലയബിലിറ്റി (SSR) കണക്കാക്കുന്നതിലാണ് അദ്ധ്യായം 6 ശ്രദ്ധ കേന്ദ്രീകരിക്കുന്നത്. MLE, ബയേഷ്യൻ സാങ്കേതിക വിദ്യകൾ ഉപയോഗിച്ചാണ് എസ്റ്റിമേറ്റുകൾ പരിശോധിക്കുന്നത്. രണ്ട് ക്ലിനിക്കൽ ഡാറ്റാസെറ്റുകൾ ഉപയോഗിച്ച് ഈ സാങ്കേതിക വിദ്യകളുടെ ഫലപ്രാപ്തി തെളിയിക്കപ്പെടുന്നു.വെയ്ബുൾ ഡിസ്ട്രിബ്യൂഷൻ പിന്തുടരുന്ന ലെയ്റ്റന്റ് ഫെയ്ലിയർ ടൈംസ് ഒരു കോംപിറ്റിങ് റിസ്ക് മാതൃകയിലൂടെ, അദ്ധ്യായം 7-ൽ പഠിക്കുന്നു. സാമാന്യവൽക്കരിച്ച ടൈപ്പ്-II ഹൈബ്രിഡ്

സെൻസറിംഗ് സ്കീമിന് കീഴിൽ ഫെയ്ലിയറിന്റെ സമയവും, കാരണങ്ങളും ഭാഗികമായി നിരീക്ഷിക്കുകയും ചെയുന്നു. യഥാർത്ഥ ലോകത്തിലെ ഒരു കേസ്സ് സ്റ്റഡിയും ഉദാഹരണത്തിന് ഉൾപ്പെടുത്തിയിട്ടുണ്ട്. സ്ലെങ്ത് ഘടകങ്ങൾ ഒരുപോലെയല്ലാത്ത ഒരു മൾട്ടികോമ്പോണൻറ് സിസ്റ്റത്തിൽ SSR-നെക്കുറിച്ചുള്ള അനുമാനങ്ങൾ ഉണ്ടാക്കുന്നതിലാണ് അദ്ധ്യായം 8 ശ്രദ്ധ കേന്ദ്രീകരിക്കുന്നത്. വെയ്ബുൾ ഡിസ്ട്രിബ്യൂഷനിൽ നിന്ന് ഉരുത്തിരിഞ്ഞ പ്രോഗ്രസിവ് ഫസ്റ്റ് ഫെയ്ലൂർ സെൻസർ ചെയ്ത ഡാറ്റയാണ് വിശകലനത്തിനായി ഉപയോഗിക്കുന്നത്. മൾട്ടികോമ്പോണൻറ് SSR മോഡലിന്റെ പ്രായോഗികത തെളിയിക്കുന്നതിനായി ഒരു സമീപകാല ഡാറ്റാസെറ്റ് ഉപയോഗപ്പെടുത്തിയിട്ടുണ്ട്,

അദ്ധ്യായം 9-ൽ പ്രബന്ധത്തിൽ ഉൾപ്പെടുത്തിയ പ്രധാന കണ്ടെത്തലുകളുടെ സാരാംശം അവതരിപ്പിക്കുന്നു. പുതിയ സ്റ്റാറ്റിസ്റ്റിക്കൽ മോഡലുകളുടെ വികസനം, ഒരു പുതിയ റിഗ്രഷൻ മോഡലിന്റെ പരിചയം, സർവൈവൽ വിശകലനത്തിൽ ANN-കളുടെ പ്രയോഗം എന്നിവയ്ക്ക് പ്രത്യേകമായ ശ്രദ്ധ നൽകുന്നു, കൂടാതെ വിവിധ സെൻസറിംഗ് ചട്ടക്കൂടുകൾക്കുള്ളിലെ മൾട്ടികോമ്പോണന്റ് SSR, കോംപിറ്റിങ് റിസ്ക് സാഹചര്യങ്ങൾ എന്നിവയുടെ ആഴത്തിലുള്ള അനുമാന വിശകലനം വാഗ്ദാനം ചെയ്യുന്നു. നിർദ്ദിഷ്ട മോഡലുകൾ കൂടുതൽ സങ്കീർണ്ണമായ ഡാറ്റാ ഘടനകളിലേക്കും വിശാലമായ ആപ്ലിക്കേഷൻ മേഖലകളിലേക്കും വ്യാപിപ്പിക്കുന്നതിനുള്ള ഭാവി ദിശകളും അദ്ധ്യായം 10 നൽകുന്നു.

പ്രധാന വാക്കുകൾ: ലൈഫ്ടൈം ഡാറ്റ വിശകലനം, മാക്സിമം ലൈക്ലിഹുഡ് എസ്റ്റിമേഷൻ, ബയേഷ്യൻ എസ്റ്റിമേഷൻ, സെൻസേർഡ് ഡാറ്റ, സർവൈവൽ അനാലിസിസ്, കോംപിറ്റിങ് റിസ്ക്.

Chapter 1

Introduction and Basic Concepts

1.1 Introduction

Lifetime data, also known as survival or reliability data, indicates the time until a specific event happens, such as the failure of a mechanical part or the death of a patient. This data is significant in a variety of fields including engineering, medicine, economics, and social sciences, since it facilitates accurate prediction of time-to-event outcomes for effective decision making and risk assessment.

The modeling of lifetime data through statistical methods offers crucial insights into risk mechanisms, system reliability, and overall performance or behavior of systems over time. Nonetheless, lifetime data often exhibits complex features such as skewness, heavy tails, and various failure rate patterns, varying from increasing, decreasing and bathtub shaped or unimodal shapes. These complexities indicate the necessity of flexible probability distributions that can accurately capture this variability. While traditional models like the exponential and gamma distributions are frequently utilized, due to their straightforward analytical characteristics, they often lack in flexibility when addressing the complex nature of real world datasets.

Lifetime data is modeled using a variety of distributions, including the exponential, Weibull, Pareto, Burr III, Lomax, Log-Logistic families, among others. Of these, the Weibull and Burr III distributions stand out among them due to their adaptability and flexibility to model a wide range of hazard shapes. The Weibull distribution is known for its versatility and interpretability in reliability

and survival analysis (Karim et al. (2019)), while the Burr III distribution is notable for its ability to span a wide region of the skewness-kurtosis plane, providing significant flexibility in capturing heavy tails, high skewness, and modeling extreme values and complex failure behaviors (Rodriguez (1977)).

While the Weibull and Burr III distributions are valuable tools in analyzing lifetime data, they may not be suitable for every situation. Real world data can be complicated, with changing patterns, strong skewness, or extreme values. To enhance the modeling for such data, statisticians often create new distributions by incorporating the features of existing ones. By combining the Weibull and Burr III models, it is possible to create a more adaptable distribution that can represent a wider range of data patterns, thereby addressing the limitations of the individual parent models. This enhanced model has practical applications in fields such as healthcare, engineering, and risk management, where accurate modeling of lifetime data is essential.

When standard approaches fall short in delivering useful insights, the quantile function (QF) serves as a valuable alternative. It describes the probability distribution as same as the distribution function but provides a distinct interpretation. The distribution function may not consistently perform well in data modeling, especially if it lacks a simple closed form or cannot generate necessary insights. In contrast, quantile-based methods provide enhanced flexibility and easier to interpret. The QF, possesses several distinct properties that enhance its practical utility. These include the simplicity of generating random numbers from QF and the explicit general distribution forms contained in the QF of order statistics.

Survival data can exhibit complex hazard trends, such as the "bathtub" curve, where the risk of failure changes over time. Traditional regression models are typically designed for simpler hazard structures and may struggle to represent this type of behavior accurately. This highlights the importance of developing new regression methods that are better for handling bathtub-shaped hazard functions. These models provide deeper insights into how various factors influence survival time and enhance the accuracy of predictions in practical applications.

Statistical inference is essential for evaluating the performance and reliabil-

ity of models in real world applications. Inference on stress-strength reliability analysis helps to quantify the probability that a system or component will operate effectively under varying stress conditions. Inference in multicomponent stress-strength models facilitates the analysis of systems composed of multiple components, providing a clearer understanding of overall system reliability. Similarly, inference on competing risks models helps in identifying the underlying cause of failure when multiple risk factors are present.

The entire thesis is focused on the application and analysis of the Weibull and Burr III distributions, with a particular focus on their use in developing a new flexible distribution, a novel parametric regression model, the application of artificial neural networks in survival analysis as well as in constructing stress-strength reliability models, Weibull-based multicomponent stress-strength, and competing risks models. These developments aim to address various challenges in lifetime data modeling and provide more adaptable tools for real world applications.

1.2 Foundational Concepts and Review of Literature

1.2.1 Lifetime Models

A lifetime model is a mathematical framework used to represent the duration until a specific event occurs, such as the failure of a machine component or the death of an individual. It is crucial to realize that a model is not an exact description of reality, but serve as approximations that capture the essential characteristics of the process under study. These models are particularly significant in reliability engineering and survival analysis, where they help in analyzing the lifetimes of products, systems, or living beings and in making conclusions about the population based on observed data. In recent years, researchers have concentrated on developing, new lifetime distributions that are more flexible and efficient than traditional ones. A key concept in lifetime analysis is the hazard function, which shows how the failure rate changes over time. Each lifetime dataset shows distinct hazard patterns, guiding the selection of appropriate models based on the nature of the hazard in the probability distribution function. For instance, if the data shows an decreasing hazard rate, a distribution with a decresing hazard is

more suitable for modeling that particular dataset. Thus, the shape of the hazard function offers useful guidance in choosing the right lifetime distribution for analyzing the data. Among the various lifetime distributions, the most widely employed lifetime distributions consist of exponential, Weibull, log-normal, and Burr families, and so on. The lifetime distributions, explored in this research include the Weibull and Burr III distributions, each outlined below.

Weibull Distribution

The Weibull distribution, introduced by Weibull in (1951), is one of the most popular and adaptable distributions for analyzing lifetime data. Its flexibility is due to the wide variety of shapes it can assume by varying its shape parameters. The cumulative distribution functions (CDF) and probability density function (PDF) of the two parameter Weibull distribution is provided by:

$$f(x) = \frac{b}{a}\left(\frac{x}{a}\right)^{b-1}\exp\left(-\left(\frac{x}{a}\right)^{b}\right), \quad x>0,\, a>0,\, b>0, \tag{1.1}$$

$$F(x) = 1-\exp\left(-\left(\frac{x}{a}\right)^{b}\right), \quad x>0,\, a>0,\, b>0, \tag{1.2}$$

where a and b are the scale and shape parameters. Figure 1.1 presents the plot of the hazard rate function (HRF) for the Weibull distribution. This image illustrates that when $b = 1$, the hazard rate remains constant over time, which is consistent with the behavior of the exponential distribution's hazard rate. When $b > 1$, the hazard rate increases over time, suggesting that the probability of failure grows as time progresses. Conversely, when $b < 1$, the hazard rate decreases monotonically, indicating a declining failure probability over time.

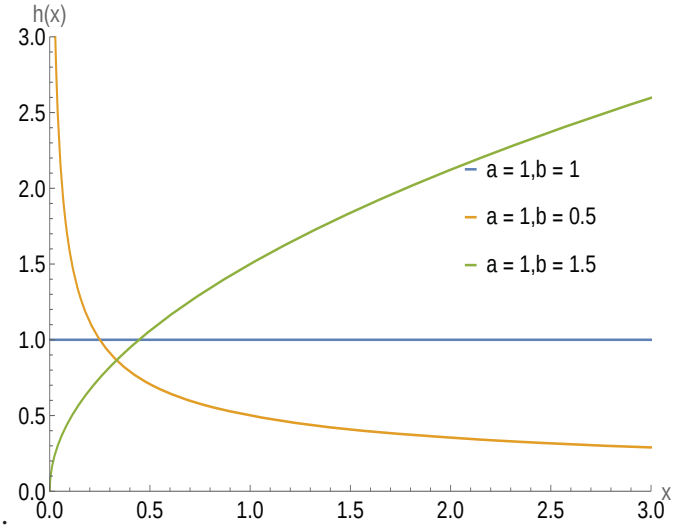

Figure 1.1: Plot for hazard rate of Weibull distribution.

The Weibull family is often employed to model systems with monotone failure rates. However, it is inappropriate for modeling lifetime data, that exhibits a bathtub-shaped hazard function, such as human mortality and the life cycles of machines. However, in reliability analysis, data spanning the entire life cycle of a product can exhibit different patterns including high initial failure rates and later high failure rates due to aging and wearout. This indicates a bathtub-shaped failure rate which cannot be adequately captured by the Weibull distribution.

Many researchers have suggested extensions of the Weibull distribution to increase its adaptability and more effectively model different kinds of lifetime data. One of the earlier developments was the exponentiated Weibull distribution presented by Mudholkar and Hutson (1996), which offered greater control over the shape of the hazard function. Later, Xie et al. (2002) proposed the modified Weibull extension, which demonstrated the capability to model data exhibiting a distinct bathtub-shaped hazard rate. This was followed by the the beta Weibull distribution by Lee et al. (2007) and the generalized modified Weibull distribution introduced by Carrasco et al. (2008), both offering greater flexibility in lifetime modeling. Saboor et al. (2016) introduced another form of the modified Weibull distribution, contributing to the growing family of Weibull based models. Subsequently, Ahmad et al. (2019) proposed the extended alpha power transformed Weibull distribution, adding an extra parameter to further enhance

the models ability to capture various failure behaviors. In more recent developments, attention has turned to exploring Weibull distribution under censoring schemes, a critical aspect of real life data analysis. Zhu (2020) investigated inference procedures for the Weibull distribution within a generalized progressively hybrid censored (GPHC) data and, Nassar and Elshahhat (2024) addressed inference in competing risks models using improved adaptive progressive Type-II censoring.

Burr III Distribution

Burr (1942) proposed a family of distributions based on the distribution function $F(x)$, presenting twelve unique CDF's specifically designed for modelling lifetime data. Among these distributions, the Burr XII and Burr III (BIII) models have gained significant popularity. A key advantage of these distributions is their simple mathematical form combined with the ability to take on many shapes, allowing them to effectively model a variety of situations across different scientific fields.

The PDF and corresponding CDF of the BIII distribution are defined as,

$$f(x) = ckx^{-(c+1)}(1+x^{-c})^{-(k+1)}, \quad x>0,\, c>0,\, k>0, \tag{1.3}$$

$$F(x) = (1+x^{-c})^{-k}, \quad x>0,\, c>0,\, k>0 \tag{1.4}$$

respectively. Here c and k are the shape parameters. If X follows a Burr XII distribution, then the BIII distribution can be obtained through a simple transformation involving $\frac{1}{X}$. Figure 1.2 shows the different shapes of hazard functions for the BIII distribution, based on various parameter values. Its HRF displays two distinct shapes: a decreasing and unimodal pattern. These different HRFs make the BIII distribution useful in many areas, including environmental studies (Lindsay et al. (1996)), economics (Cordeiro et al. (2014)), reliability and survival analysis (Olobatuyi (2017)), each offering unique interpretations and insights relevant to their respective domains. In addition to its use as the BIII distribution, this distribution is referred by different names in various fields of study. In meteorological studies it is commonly referred to as the Kappa distri-

bution (Mielke (1973)), while in the actuarial literature it is referred to as the inverse Burr distribution (Kleiber (2003)). In studies related to income, wage, and wealth distribution, it is known as the Dagum (2008) distribution. The BIII distribution is notable for covering a substantial range of the skewness-kurtosis plane, comparable to established distributions like the gamma and log-normal, (Rodriguez (1977)) and (Tadikamalla (1980)).

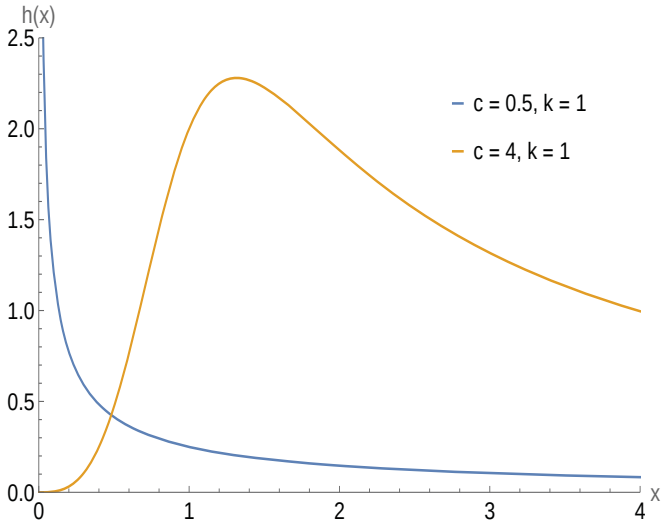

Figure 1.2: Plot for hazard rate of Burr III distribution.

Several authors have investigated flexible generalizations of the BIII distribution. For instance, an extended form of the BIII distribution was proposed by Shao et al. (2008), Domma (2010) analyzed the dependence structure of the bivariate BIII distribution. To enhance model flexibility, Jamal et al. (2017) developed a new family of distributions constructed using the odd BIII transformation. Modi and Gill (2020) proposed a Unit BIII distribution, while Haq et al. (2020) introduced a Modified BIII distribution, including its characterisations and validation tests. Additionally, Jamal et al. (2021) also presented a modified BIII distribution, discussing its structural properties and demonstrating its applicability to real-life data. Furthermore, several studies have been conducted on the BIII distribution within the framework of various censoring plans. Singh et al. (2022) discussed the multicomponent stress-strength model for the unit BIII distribution under progressive censoring (PC), Hassan et al. (2023) investigated statistical inference for the BIII distribution using a joint PC approach. Yadev

et al. (2024) examined parameter estimation of the BIII distribution within the framework of GPHC scheme. Dutta and Kayal (2024) concentrated on estimation and prediction for the BIII distribution based on a unified progressive hybrid censoring approach, among other related studies.

1.2.2 Censoring Schemes

In life testing experiments and survival studies, it is often challenging to scrutinize the exact failure times of all test units. These limitations may arise due to practical constraints such as limited time, high costs, or environmental conditions. To address such challenges, censoring techniques are commonly employed. These methods allow researchers to draw inferences from partially observed data, where complete information on all units is unavailable. Censoring typically occurs when an experiment concludes before all units have failed or when some units are deliberately withdrawn from the study prior to failure. Based on the nature of data loss, censoring is broadly classified into three main categories: left censoring, right censoring and interval censoring. Left censoring is seldom used because it happens when some events have already taken place before the experiment begins, or when the initial occurrence of an event cannot be recorded. Right censoring, the most common type, happens when the exact failure time is unknown but exceeds a certain observed time, such as when a study concludes at a fixed point or a subject leaves before the event occurs. Interval censoring is when the failure time is unknown but lies within a specific time interval, often arising from discrete observation points. In certain cases, experimental units are deliberately withdrawn from the study to reduce the overall testing duration, particularly when some units are expected to take an excessively long time to fail. These censoring concepts are widely used in survival analysis, and for a more detailed understanding, one may refer to Lawless (1982), Lee et al. (2003) and Klein and Moeschberger (2006). In this thesis, only right censoring is utilized for lifetime analysis. A brief overview of commonly used right censoring schemes is provided below:

Type-I and Type-II Censoring

In the Type-I censoring scheme, a group of n identical units, such as mechanical devices or biological samples, are put through a life test in a controlled setting, which results in independent and identically distributed (i.i.d) failure lifetimes. This experiment is conducted with a predetermined time T_0, after which no further events are recorded. Over a fixed period of time, the lifetimes of the units that are failed (s items) are noted, while the remaining $(n - s)$ units continue to operate. This approach is especially useful in situations where time or budget limitations exist, as it enables experiments to be carried out for a fixed duration.

In Type-II censoring, the number of failures to be observed, denoted by s, is set in advance. The experiment continues until the s^{th} failure is reached, at which time the experiment is halted. The lifetimes of the s failed units are recorded, while the remaining $n - s$ units are treated as censored at the time of the last observed failure. This method ensures a fixed number of failure events are included, although the total duration of the test remains random. Type-II censoring is especially useful when a specific number of failures is needed for analysis, allowing for more efficient use of limited experimental units.

For further details on Type-I and Type-II censoring methods, see Meeker (1984), Gupta and Kundu (1998), Yu and Peng (2013), Hyun et al. (2016), Algarni et al. (2020) and Aboul-Fotouh Salem et al. (2024).

Hybrid Censoring

In life-testing experiments, both Type-I and Type-II censoring schemes have certain practical drawbacks. With Type-I censoring, if only a small number of units fail before the set termination time, T_0, the number of observed failures may be limited, which can reduce the statistical efficiency of the test. Conversely, Type-II censoring guarantees a fixed number of failures s, but the duration of the experiment becomes uncertain, as the s^{th} failure might take a long time to occur. To overcome these challenges, Epstein (1954) proposed a more adaptable method known as the hybrid censoring (HC) scheme, which combines the features of both Type-I and Type-II censoring. Due to its blended nature, the approach is referred to as "hybrid" censoring. HC schemes are typically divided into two

categories: Type-I hybrid and Type-II hybrid, each designed to meet different testing requirements. In Type-I HC, the study concludes at $T_1 = \min(T_0, X_{s:n})$, where $X_{s:n}$ represents the time of the s^{th} failure among n units. This approach ensures that the experiment will not extend beyond time T_0, although it can end earlier if the necessary number of failures is achieved sooner. Conversely, Type-II HC sets the stopping time as $T_2 = \max(T_0, X_{s:n})$. This means that the experiment must continue until at least s failures are observed, guaranteeing a certain level of data efficiency, even if the actual duration of the study surpasses T_0.

1.2.3 Quantile Function (QF)

A probability distribution can be characterized either through its distribution function or its QF. Although both convey equivalent information about the underlying distribution, they differ in interpretation. Traditional statistical theory has primarily focused on distribution functions. However, quantile-based methods have become increasingly relevant, especially in situations where classical techniques encounter challenges or fail to produce satisfactory outcomes. QFs possess distinct properties that distribution functions lack, which enhances their applicability in various practical situations. Key features include: (a) the sum or product of two QFs is still a QF, (b) random numbers can be easily generated from QFs, (c) QFs for order statistics often have general explicit forms, and (d) statistical inference using quantiles is generally more robust than methods based on moments. In many applications, QF offer clearer analytical insights, and in some cases, such as characterizations, solutions can only be derived through QFs that do not invert to yield distribution functions. The properties outlined above are generally not applicable to distribution functions, underscoring the benefits of using QF in the modeling and analysis of diverse statistical data. For additional information on the theoretical and applied aspects of QFs, refer to Gilchrist (2000) and Nair et al. (2013).

Definition and Properties of the QF

For a real-valued random variable X with a right continuous CDF $F(x)$, the QF $Q(u)$ is defined as follows:

$$Q(u) = F^{-1}(x) = \inf\{x : F(x) \geq u\}, 0 \leq u \leq 1. \tag{1.5}$$

For $-\infty < x < \infty$ and $0 < u < 1$, we have $F(x) \geq u$ if and only if $Q(u) \leq x$. Hence, if there is an x for which $F(x) = u$, then $F(Q(u)) = u$ and $Q(u)$ represents the smallest value of x satisfying the condition $F(x) = u$. Considering a continuous random variable X, equation (1.5) simplifies to

$$Q(u) = \inf\{x : F(x) = u\}$$

Furthermore, if $F(x)$ is also strictly increasing, $Q(u)$ represents the unique value of x such that $F(x) = u$. In this case, the QF is represented by solving $F(x) = u$ for x in terms of u, yielding $Q(u) = F^{-1}(u)$.

A major development in the early use of QFs to represent statistical distributions was introduced by Hastings et al. (1947), who proposed a class of distributions defined directly through QFs. Further enhancements were made by Ramberg and Schmeiser (1972), Ramberg (1975) and Govindarajulu (1977), who developed flexible QFs used in various fields. Since then, several innovative methods have emerged to develope new distributions using quantile based formulations. Gilchrist (2000) undertook a detailed analysis of the use of QFs in statistical data modeling. Hankin and Lee (2006) discussed the power-Pareto distribution by considering it as the product of the QFs of the power and Pareto distributions. Similarly, Sankaran et al. (2016) developed an innovative QF derived using the sum of generalized Pareto and Weibull distributions. Meanwhile, Sankaran and Dileep (2018) introduced a new class of distributions that merges half logistic and exponential geometric distributions.

1.2.4 Competing Risk

In life-testing experiments, it is common to encounter scenarios where items or organisms may undergo the event of interest due to multiple causes, some of

which may be identified while others remain unknown. For instance, an electric appliance might fail either due to ageing or as a result of sudden voltage fluctuations occurring during its operational phase. Similarly, patient might be exposed to two or more mutually exclusive causes, and their death could result from any one of these distinct causes or occur due to natural circumstances. Such scenarios, where units face multiple risks of experiencing the event of interest but ultimately encounter the event due to the first cause that occurs, are referred to as competing risk (CR) situations. Under CRs scenarios, the data can be represented as a bivariate distribution, consisting of the time to the event and the associated cause of failure. The analysis of data from CR scenarios differs from that of lifetime data resulting from a single failure mode. In CRs, the observed lifetime is the minimum of multiple unobserved lifetimes, each linked to a specific failure mode. Clearly, the model for characterizing the observed lifetimes will be based on the models of multiple unobserved lifetimes, and the resulting framework is referred to as a CR model. To provide a clearer explanation, let us assume that a unit is subjected to the possibility of experiencing the event due to s risks. When the operation of the unit commences, these s risks generate s lifetimes, denoted as $T_1, T_2, \ldots, T_s$, where T_i represents the lifetime associated with the i^{th} risk. Furthermore, it is assumed that the unit fails as soon as any one of these lifetimes is observed. More specifically, if T represents the observed lifetime of the unit, it can be defined as,

$$T = \min(T_1, T_2, \ldots, T_s).$$

A practical method for modeling lifetime observations in a CR scenario is to assume that each mode of failure is independent of the other failure modes and is determined by a particular lifetime distribution. Consequently, if the reliability and hazard functions of T_i are denoted as $R_i(t)$ and $h_i(t)$ for $i = 1, 2, \ldots, s$,

respectively, the reliability and hazard function of T can be derived as follows:

$$R(t) = \prod_{i=1}^{s} R_i(t), \tag{1.6}$$

$$h(t) = \sum_{i=1}^{s} h_i(t) \tag{1.7}$$

The corresponding PDF of T can be obtained as follows:

$$f(t) = h(t) \times R(t). \tag{1.8}$$

The resulting model of T characterized as above is known as the independent CR model or the CR model (Series system model). Models of CRs are widely utilized across numerous disciplines, such as healthcare (Varadhan et al. (2010)), economics (Hachen (1988)), industrial engineering (Bocchetti et al. (2009)), and reliability analysis (Kundu and Basu (2000)).

Inference of CRs models have garnered significant attention in the literature, with numerous notable contributions. The first work on CRs was presented by Cox (1959), who discussed the study of exponential lifetime data involving two failure types. Then, Berger and Sun (1993) performed a Bayesian analysis of the poly-Weibull distribution, where the observed failure time corresponds to the minimum of several independent Weibull failure times from CR. For reliability analysis, Xie and Lai (1996) adopted an additive Weibull model exhibiting a bathtub-shaped failure rate. Kundu and Basu (2000) estimates the parameters of the CRs model when the data may be incomplete using exponential and Weibull distributions. Pareek et al. (2009) developed inference methods for CR models under a PC scheme, assuming Weibull distributed latent failure times. Cramer and Schmiedt (2011) discussed progressively Type-II censored CRs data based on Lomax distributions. Almalki and Yuan (2013) proposed a generalized Weibull model from a series system, where one component follows a Weibull distribution and another follows a modified Weibull distribution, enhancing the analysis of complex reliability systems. Koley et al. (2017) and Koley and Kundu (2017) conducted classical and Bayesian inference of CRs data, assuming exponential distributions for the competing causes of failure, under Type-II hybrid

and GPHC schemes. Chacko and Mohan (2019) analyzed CRs data under PC, assuming the number of units removed at each stage follows a binomial distribution. Almarashi et al. 2020 conducted statistical analysis of CRs lifetime data from the Nadarajah and Haghighi distribution under Type-II censoring. Du and Gui (2022) investigated statistical inference of the Burr XII distribution under adaptive Type-II progressive censored schemes with CRs. More recently, Zheng et al. (2024) developed a CR model under progressive censored data using the inverted exponentiated half-logistic distribution.

1.2.5 Stress-Strength Reliability

Stress-strength reliability (SSR) has significant importance in today's world, especially in fields where ensuring the safe and efficient functioning of systems and components is critical. Some devices can withstand a certain amount of stress due to their inherent strength. However, when the stress exceeds this strength, the devices are likely to fail. Let's denote the random stress applied to a device as Y, and the random strength it can withstand as X. The system is considered to have failed if, at any point, the applied stress surpasses the strength. Therefore, a system's reliability may be quantified as $R = P(X > Y)$. Stress-strength analysis is a widely used technique in engineering and manufacturing systems (Barbiero (2013)), but its application is not confined to these fields alone. SSR is gaining attention in various areas such as finance (Biswas et al. (2021)), economics (Susam and Hudaverdi (2024)), medical research (Sharma et al. (2015)) and so on.

The concept of stress-strength was initially introduced by Birnbaum et al. (1956) and further enhanced by Birnbaum and McCarty (1958). The applications of SSR have been investigated by many authors, including Chung (1982), Kundu and Gupta (2005), Krishnamoorthy et al. (2007), Biswas et al. (2021), Kundu and Gupta (2006) etc. Recently, the estimation of SSR from Exponentiated Inverse Rayleigh distribution was studied by Rao et al. (2019), Xavier and Jose (2021b) discuss the SSR using a generalization of the power transformed half-logistic distribution, Al-Babtain et al. (2022) mentioned the Bayesian and non-Bayesian reliability estimation of the stress-strength model for power-modified Lindley distribution. Also, Agiwal (2023) developed Bayesian estimation of SSR

from the inverse Chen distribution.

1.2.6 Multicomponent Stress-Strength Reliability

An advancement of the classical SSR model is the multicomponent stress-strength reliability (MSSR) approach, designed for systems that consist of several strength bearing components subjected to a shared stress. While the traditional model is adequate for scenarios involving only one strength component, numerous practical applications involve arrangements where multiple components collaborate to function correctly.

The MSSR model assesses the reliability of a system with k independent strength components under a common stress. Thus, the system is considered reliable if at least s out of the k strength components exceed the stress. This model is known as the G - system: s out of k system. The G - system is utilized in many real world scenarios. For example, consider an automobile engine consists of eight cylinders, and it is designed to function effectively even when only four of those cylinders are operational. This configuration is referred to as a 4 out of 8 system. Another example is a power plant with eight units generating electricity. A common challenge faced by this system is the demand for electricity, while the functioning generators, such as wind turbines, represent the strength components. If the plant requires a minimum of 6 out of the 8 units to operate effectively and generate power, it is classified as a 6 out of 8: G - system. The pioneering work in this area was carried out by Bhattacharyya and Johnson (1974), who formulated the multicomponent reliability expression as follows:

$$\begin{aligned} R_{s,k} &= P(\text{atleast } s \text{ of the } X_i \text{ exceed } Y) \\ &= \sum_{p=s}^{k} \binom{k}{p} \int_{-\infty}^{\infty} (1 - F_X(y))^p \, (F_X(y))^{k-p} \, dG_Y(y), \end{aligned} \tag{1.9}$$

where, $X_1, X_2, \ldots, X_k$ represent i.i.d strength variables characterized by the distribution function $F(x)$, while Y signifies the stress variable described by the distribution function $G(y)$. The evaluation of reliability in multicomponent stress-strength (MSS) systems has gained significant research interest, similar to

single-component models. Many studies have expanded the MSS framework by using various lifetime distributions to capture real-world failure complexities. For example Rao and Kantan (2008) studied reliability estimation in MSS systems using the log-logistic distribution. Gadde (2012) later explored the generalized exponential distribution, highlighting its adaptability for various failure rates. Nadar and Kızılaslan (2015) and Dey et al. (2017) further assessed the reliability model in MSS using the Marshall-Olkin bivariate Weibull and Kumaraswamy distribution. Recently, Kohansal (2019) focused on estimating MSSR using the Kumaraswamy distribution based on PC sample. In a similar area, Xavier and Jose (2021a) analyzed MSSR with the power transformed half-logistic distribution. Saini et al. (2022) studied multicomponent reliability for the Burr XII distribution, using progressively first-failure censored samples for their analysis. Lio et al. (2022) and Ahmed et al. (2022) worked on formulating the inference for MSSR concerning the Burr XII and power Lomax distribution. Finally, Zhang et al. (2022) introduced Bayesian analysis for system reliability in MSS models based on the Marshall-Olkin Weibull distribution.

1.2.7 Regression Approaches in Survival Analysis

In survival analysis, explanatory variables (or covariates) play a crucial role in explaining the heterogeneity observed within a population. One of the primary goals of survival studies is to investigate how these covariates influence the lifetime variable, which is typically the time until an event such as failure or death occurs. To explore this relationship, various regression models are employed, enabling researchers to assess the impact of covariates on survival time. In some contexts, covariate values may vary over time, in which case they are termed time-varying or time-dependent covariates. Depending on the nature of the data and underlying assumptions, both parametric and semi-parametric techniques can be utilized. Parametric models assume a specific distribution for survival time conditioned on covariates, whereas semi-parametric models, such as the Cox proportional hazards model, offer greater flexibility by not requiring a specified form for the baseline hazard. In applied contexts involving censored or incomplete survival data, choosing a suitable regression framework is crucial for reliable inference. Among parametric methods, the location-scale regression

model (LSRM) is notable for its adaptability and is commonly used in fields like clinical research. As discussed by Lawless (1982), this model enhances interpretability by allowing both the location and scale of survival times to be functions of explanatory variables, enabling a more detailed representation of survival dynamics.

The LSRM has been widely studied over the years due to its broad applicability in fields such as engineering, hydrology, and survival analysis. Barros et al. (2008) introduced a class of lifetime regression models assuming errors follow the generalized Birnbaum-Saunders (BS) distribution, while Carrasco et al. (2008) proposed a regression model based on the modified Weibull distribution. Silva et al. (2008) examined a LSRM using the Burr XII distribution, and later Silva et al. (2009 further discussed a LSRM designed for fitting censored survival times with bathtub shaped hazard rates. Hashimoto et al. (2010) introduced the log-exponentiated Weibull regression model for analyzing interval censored data and Ortega et al. (2012) investigated the log-exponentiated generalized gamma regression model within the context of censored data. Pescim et al. (2013) proposed a LSRM based on the beta generalized half-normal distribution, and Ortega et al. (2015) introduced a power-series beta Weibull regression model for the prediction of breast carcinoma. Recently, Pescim et al. (2017) developed a log-linear regression model based on the odd log-logistic generalized half normal distribution, while Eliwa et al. (2021) proposed the log odd- Lindley-half-logistic regression model as a valuable tool for analyzing survival data, highlighting its potential applicability in survival analysis.

1.3 Statistical Inference Methods

Statistical inference is essential in data analysis, as it enables conclusions to be drawn about population characteristics using information obtained from a sample. This approach improves our comprehension of data trends and helps in making well-informed decisions through statistical modeling techniques. Several estimation procedures are available in the literature to meet different analytical needs, with prominent methods including the method of moments, method of least squares, maximum likelihood estimation (MLE), and Bayesian estimation,

each offering unique advantages depending on the context of the analysis.

1.3.1 Maximum Likelihood Estimation

MLE stands is one of the most effective and widely used technique for estimating the parameters of a statistical model. The basic concept of MLE is to identify the parameter values that maximize the likelihood of the observed data under the assumed model. MLE is favored for its desirable statistical properties, it yields estimators that are efficient, consistent, and sufficient, while also possessing notable properties such as invariance and asymptotic behavior.

Consider a random sample consisting of size n, denoted as $x = (x_1, \ldots, x_n)$, drawn from a population with a density function $f(x; \theta)$, where θ is the parameter to be estimated. The likelihood function for the sample data is defined as the joint PDF of the random variables $x_1, \ldots, x_n$, represented as:

$$L(\theta) = L(\theta|x) = \prod_{i=1}^{n} f(x_i, \theta)$$

The concept of the maximum likelihood (ML) estimator involves selecting the value of the unknown parameter θ that maximizes the likelihood of obtaining the sample x based on the given density $f(x; \theta)$. Maximizing the likelihood function is tedious since it involves the product of n quantities $f(x_i; \theta)$. Consequently, we can simplify our task by maximizing the log-likelihood function, $\ln L(\theta|x)$, which is a monotonic increasing function and reaches its maximum at the same point as the likelihood function. The statistic $t = t(x) \in \Theta$ is considered the ML estimator of θ if the maximum value of $\ln L(\theta|x)$ is attained at $t(x)$. It is important to note that the ML estimator is not always unique, and when it is unique, it depends on sufficient statistics of θ.

1.3.2 Bayesian Estimation

In the Bayesian inference framework, the unknown parameter θ of the model is considered a random variable instead of being regarded as a constant value. This method incorporates prior beliefs about the parameter by representing them through a probability distribution. Bayesian statistics aims to represent prior uncertainty about model parameters through a probability distribution. This initial

uncertainty is then updated with observed data, resulting in a posterior probability distribution for the parameter with diminished uncertainty. The theoretical basis for this process is Bayes theorem. For a continuous parameter θ, the posterior distribution, which represents the revised belief about the parameter, is given as follows:

$$\pi(\theta|\underline{x}) = \frac{L(\theta|\underline{x})\pi(\theta)}{\int L(\theta|\underline{x})\pi(\theta)\, d\theta}, \tag{1.10}$$

where $\pi(\theta)$ represents the prior knowledge about the parameters θ and $L(\theta|\underline{x})$ denotes the likelihood function of the unknown parameter associated with the observed sample. The explanation above clearly shows that, the posterior distribution results from updating the prior distribution. The prior distribution holds a critical role in Bayesian analysis. A well-chosen prior leads to effective results from the posterior, whereas a poorly chosen prior can result in misleading inferences. Thus, selecting an appropriate prior distribution presents a challenging task. For further information on prior selection, refer to Box and Tiao (2011) and Berger (2013). Priors are typically classified into two categories based on the information available to the experimenter: informative and non-informative priors. A non-informative prior (NIP) is used when there is limited or uncertain prior knowledge about the parameters, whereas an informative prior (IP) is based on substantial available information. However, in the absence of information about θ, a NIP may provide more reliable results than a poorly selected IP.

Another key goal of Bayesian analysis is to reduce the posterior expected loss function. In statistical inference, the objective is to uncover accurate information, leading either to the successful discovery of the truth or to a situation of loss if the inference diverges from reality. The loss function quantifies the deviation from the truth, and its selection depends on the specific estimation problem. The literature outlines several loss functions for point estimation, typically categorized as symmetric or asymmetric. Symmetric loss functions focus on the magnitude of errors, ignoring their direction, while asymmetric loss functions consider both magnitude and direction. Various symmetric and asymmetric loss functions, such as the squared error loss function (SELF), quadratic loss, LINEX loss (LLF), general entropy loss (GELF), and absolute error loss (AELF), are discussed in the literature. For additional insights, refer to works like Box and

Tiao (2011), Zellner (1986), and others.

Bayesian inference often faces challenges in deriving explicit posterior distributions, especially when dealing with complex and high-dimensional models where the posterior includes incomplete integrals that are not analytically solvable. Consequently, numerical methods become necessary, although they can be resource-intensive. To address this issue, Markov Chain Monte Carlo (MCMC) techniques are utilized to sample from the posterior distribution. Among the most widely utilized MCMC methods are the Metropolis-Hastings (M-H) algorithm and the Gibbs sampler. In this thesis, M-H methods are employed to efficiently derive the Bayes estimates (BEs).

1.3.3 Model Selection Techniques

Model selection is a key concept of statistical analysis, particularly when multiple competing distributions are available for modeling a dataset. The goal is to identify, a most suitable model that achieves an optimal balance between goodness-of-fit (GoF) and model complexity. The Kolmogorov-Smirnov (K-S) test and the Chi-square (χ^2) test are common methods used to check how well a distribution fits the data. Additionally, measures like the Akaike Information Criterion (AIC) and Bayesian Information Criterion (BIC) are used to assess model performance, with smaller values indicating better performance.

Kolmogorov–Smirnov test

The K–S test is a non-parametric method used to assess how well a continuous distribution fits a given dataset. It focuses on the maximum absolute deviation between the empirical distribution function (EDF) derived from the sample and the CDF of the hypothesized model. The test statistic defined as:

$$D_n = \sup_x |F_n(x) - F(x)|$$

In this equation, $F_n(x)$ represents the EDF, while $F(x)$ denotes the theoretical CDF of the proposed distribution. A small value of D_n indicates a better fit, and its corresponding p - value is used to determine whether to reject the null hypothesis that the data follow the specified distribution.

Chi-square test

The Chi-square GoF test is a popular statistical method used to assess how well an observed data set aligns with a theoretical distribution. The process starts by partitioning the interval of u in (0, 1) into m equal segments defined by $u_i = \frac{i}{m}$ for $i = 1, 2, \ldots, m-1$, with $u_0 = 0$ and $u_m = 1$. Let f_i represent the number of observations that fall within the interval $(\hat{Q}(u_{i-1}), \hat{Q}(u_i))$, which serves as the observed frequency O_i for the i^{th} interval. The expected frequency E_i is $\frac{n}{m}$ for each interval. Using this information, we can form the test statistic:

$$\chi^2 = \sum_{i=1}^{m} \frac{(O_i - E_i)^2}{E_i} = \sum_{i=1}^{m} \frac{(f_i - \frac{n}{m})^2}{\frac{n}{m}}.$$

This statistic approximately follows a χ^2 distribution with $m-1$ degrees of freedom. It is evident from the test statistic that the χ^2 value tends to be smaller when the observed data closely aligns with the fitted QF.

Akaike Information Criterion

The AIC, introduced by Akaike (1973), is a widely used method for choosing model in likelihood-based statistical analysis. It helps to identify the model that strikes the best balance between fitting the data well and model simplicity. AIC is calculated as:

$$\text{AIC} = -2\log(L) + 2k,$$

where, L is the ML function value, while k represents the number of parameters to be estimated. AIC quantifies the relative amount of information a model may lose; thus, a lower AIC indicates better model quality. This criterion is especially effective for comparing different models, focusing on the selection of a model that offers good predictive performance without unnecessary complexity.

Bayesian Information Criterion

The BIC, introduced by Schwarz (1978), is a method for model selection that determines how well models fit the data while accounting for their complexity.

BIC is calculated as:

$$\text{BIC} = -2\log(L) + k\log(n),$$

where L is the ML estimate, k is the number of parameters, and n is the sample size. BIC is effective at preventing overfitting, particularly in large datasets, and a lower BIC value indicates a better model. Unlike AIC, BIC applies a stronger penalty for complexity, making it more conservative in model selection. It is also asymptotically consistent, meaning it is more likely to identify the true model with larger sample sizes.

1.4 Objectives of the Study

1. To introduce a new flexible lifetime model using quantile functions of Burr III and Weibull distribution.

2. To propose a new distribution based on the competing risks approach by incorporating the Burr III and Weibull lifetime distributions and to examine its statistical characteristics and survival (or reliability) properties.

3. To develop a new regression model using a bathtub-shaped distributions for analyzing lifetime data.

4. To investigate a stress-strength reliability models based on Burr III - Weibull distribution and develop its inferential procedures.

5. To explore potential applications of the developed distributions across survival and reliability studies.

6. To model partially observed competing risk data using the Weibull distribution.

1.5 Outline of the Thesis

The thesis consists of 10 Chapters. Chapter 1 provides an overview of the research topic, including a concise review of relevant literature and a summary of the contributions made in this work. Chapter 2 presents a new family of distributions developed using a quantile-based approach, where the QF is constructed

by adding the QFs of the Burr III and Weibull distributions. The Chapter examines the statistical properties and reliability characteristics of the proposed model. Parameter estimation is performed using the Method of Least Squares and the Method of L - moments. To illustrate the model's practical applicability, it is applied to two real life datasets. The content of this Chapter is based on the author's published article: "Applications of Burr III - Weibull quantile function in reliability analysis (Deepthy et al. (2023))" in ***Statistical Theory and Related Fields***.

Chapter 3 presents a novel model known as the Burr III Weibull (BIIIW) distribution, specifically formulated to accommodate a variety of ageing patterns and failure behaviors. The Chapter details the statistical properties of the distribution, offering valuable insights into its behavior and characteristics. Parameter estimation is carried out using the ML method. To evaluate the model's fit, a modified Chi-squared GoF test is proposed using the Nikulin–Rao–Robson statistic (Y^2) for complete data. A simulation study is also conducted to assess the performance of the BIIIW model's estimators. The practical applicability of the proposed distribution is illustrated through its implementation on three real-life datasets, demonstrating its effectiveness in modeling complex lifetime data. This work was presented at the International Conference on Statistics for the Twenty-First Century - 2022, organized by the International Statistics Fraternity (ISF), the School of Physical and Mathematical Sciences, and the Department of Statistics, University of Kerala, Trivandrum, during 16–19 December 2022, under the title "Burr III Weibull Distribution: Properties, Applications, and Characterizations."

Chapter 4 focuses on the modeling and survival analysis of relief periods in arthritic patients by integrating traditional statistical estimation techniques with modern artificial intelligence approaches. The Chapter highlights the use of the odd Burr III Weibull (OBIIIW) distribution to effectively describe survival functions, hazard rates, and other related survival measures. A comparative analysis is performed by applying both MLE and artificial neural networks (ANNs) to estimate survival metrics. The predictive capabilities of both approaches are examined using real clinical data. Overall, this Chapter showcases the potential

of ANN as a reliable tool for survival analysis, especially in healthcare settings where prediction accuracy is of great importance. This work has been published as "A Comprehensive Analysis Using Maximum Likelihood Estimation and Artificial Neural Networks for Modeling Arthritic Pain Relief Data (Deepthy et al. (2024))" in *Stochastics and Quality Control*.

Chapter 5 presents a LSRM based on the OBIIIW distribution, designed to capture various failure rate behaviors in lifetime data. Key statistical properties of the log-transformed model are discussed, and parameters are estimated using ML and jackknife techniques. Simulation studies assess estimator stability under different parameter combinations. The Chapter also incorporates diagnostic tools like global influence, martingale, and modified deviance residuals for model validation. The practical performance of the suggested regression model is demonstrated through the analysis of a real-life dataset. This work has been accepted for publication in the journal *Statistics and Applications*.

In Chapter 6, the SSR $R = P(X > Y)$ is estimated assuming, X and Y follow independent Weibull-Burr III random variables with the same shape and different scale parameters. Estimations of R are done using ML and Bayesian methods, including informative and non-informative approaches. To construct confidence intervals, the Chapter employs the asymptotic confidence intervals, Highest posterior density (HPD) credible intervals, and bootstrap confidence intervals. A simulation study evaluates the effectiveness of these estimates, and the relevance of the model is shown through two clinical datasets. This work was presented at International Conference on Knowledge Discoveries on Statistical Innovations and Recent Advances in Optimization (ICON-KSRAO), Department of Statistics, Andra University, Visakhapatnam on 29th and 30th December 2022, under the title "Estimation of Stress Strength Reliability for Weibull Burr III Distribution".

A statistical inference for a CRs model is discussed in Chapter 7, where failure causes are partially observed and latent failure times are assumed to follow Weibull distributions. The analysis is carried out under generalized Type-II hybrid censoring scheme. Parameter estimation is performed using both ML and Bayesian methods, with interval estimates derived from asymptotic confidence

and HPD credible intervals. Bayesian estimation utilizes the MCMC method along with importance sampling. The accuracy of the estimators is assessed through Monte Carlo simulations, and the Chapter concludes with a real dataset analysis to illustrate practical application. This work has been published as "Inference on Partially Observed Competing Risks Models Using Generalized Type-II Hybrid Censoring Scheme (Deepthy et al. (2025))" in *Austrian journal of Statistics*.

Chapter 8 addresses the inference of MSSR in systems with non-identical strength components. The study uses progressively first-failure censored data, with both stress and strength modeled by the Weibull distribution. Estimation is performed using ML and Bayesian methods, with interval estimates obtained through asymptotic confidence intervals and HPD credible intervals. The accuracy and behavior of the estimators are examined via Monte Carlo simulations, and the method's effectiveness is demonstrated through analysis of a real-world dataset.

Chapter 9 outlines the major findings of the thesis, highlighting the creation of innovative statistical models, the formulation of a novel regression model, the relevance of ANNs in clinical studies and detailed inferential analysis for SSR, MSSR, and CR scenarios under different censoring frameworks, all supported by validation through real-world data applications. The results contribute to the theoretical advancement of survival and reliability modeling while also offering practical methodologies applicable across diverse fields such as engineering, clinical research and biostatistics. Chapter 10 discusses the recommendations or future directions for the implementation and further development of the proposed models and methods.

Chapter 2

Burr III - Weibull Quantile Function

2.1 Introduction

The main goal of quantile-based reliability analysis is to create new quantile functions (QFs) that can effectively model and analyze lifetime data sets. In this Chapter, we introduce a flexible family of distributions defined by a QF that does not have closed-form expression for its distribution function. QFs exhibit several features that are not supported by distribution function. For instance, the sum (product) of two QFs results in another QF. A more comprehensive discussion on the properties and definition of QFs is provided in Chapter 1, offering the necessary theoretical foundation for their use in reliability analysis. The objective of this Chapter is to present a novel QF formed by adding the QFs of the Burr III and Weibull distributions. This new class offers a diverse range of distribution shapes depending on the selected parameters.

This Chapter is organized primarily as follows: A new family of distributions and their basic characteristics are presented in Section 2.2. Section 2.3 discusses several well-known distributions that are either belongs to the suggested class of distributions or have been derived through appropriate transformations applied to the proposed QF. The distributional characteristics of the proposed QF are addressed in Section 2.4. The reliability properties of the proposed class is presented in Section 2.5. Section 2.6 examines the inference procedures related to the model's parameters and illustrates the application of the associated class of distributions in a real-life context. In conclusion, Section 2.7 presents the key

findings of this Chapter.

2.2 Burr III - Weibull QF

The suggested QF is obtained by taking the sum of QFs of Burr III and Weibull distributions. The survival and QF of Burr III (BIII) distribution are respectively given by,

$$\bar{F}(x) = 1 - (1 + x^{-c})^{-k}, \quad c > 0, k > 0, \tag{2.1}$$

and

$$Q_1(u) = (u^{-\frac{1}{k}} - 1)^{-\frac{1}{c}}, \quad c > 0, k > 0, \tag{2.2}$$

where c and k are the shape parameters. The survival and QF of Weibull (W) distribution are respectively given by,

$$\bar{G}(x) = e^{-\left(\frac{x}{\sigma}\right)^{\lambda}}, \quad \sigma > 0, \lambda > 0 \tag{2.3}$$

and

$$Q_2(u) = \sigma \left[-\log(1-u)\right]^{\frac{1}{\lambda}}, \quad \sigma, \lambda > 0. \tag{2.4}$$

The new class of distributions called Burr III-Weibull (BIIIW) QF is obtained by making use of the property that the sum of two positive QFs is again a QF.

$$Q(u) = \sigma \left[-\log(1-u)\right]^{\frac{1}{\lambda}} + (u^{-\frac{1}{k}} - 1)^{-\frac{1}{c}}, \quad 0 < u < 1, \quad c, k, \sigma, \lambda > 0. \tag{2.5}$$

The quantile density function is obtained as,

$$q(u) = \frac{\sigma \left[-\log(1-u)\right]^{\frac{1}{\lambda}-1}}{\lambda(1-u)} + \frac{\left(u^{-\frac{1}{k}} - 1\right)^{-\frac{1}{c}-1} u^{-\frac{1}{k}-1}}{ck}. \tag{2.6}$$

The distribution function for the class of distributions (2.5) cannot be expressed in closed form, hence it has to be numerically evaluated. However we may express

(2.6) using the density function $f(x)$ and distribution function $F(x)$ as,

$$f(x) = \frac{ck\lambda(1-F(x))}{ck\sigma[-\log(1-F(x))]^{\frac{1}{\lambda}-1}+\lambda(1-F(x))\left((F(x))^{-\left(\frac{1}{k}\right)}-1\right)^{-\left(\frac{1}{c}+1\right)}(F(x))^{-\left(\frac{1}{k}+1\right)}}. \tag{2.7}$$

The QF (2.5) describes a family of distributions with varying shapes depending on the parameter values. For various parameter values, the shapes of density functions are shown in Figure 2.1. It can be observed that the family comprises decreasing, unimodal, positive and negatively skewed models for appropriate parameter values.

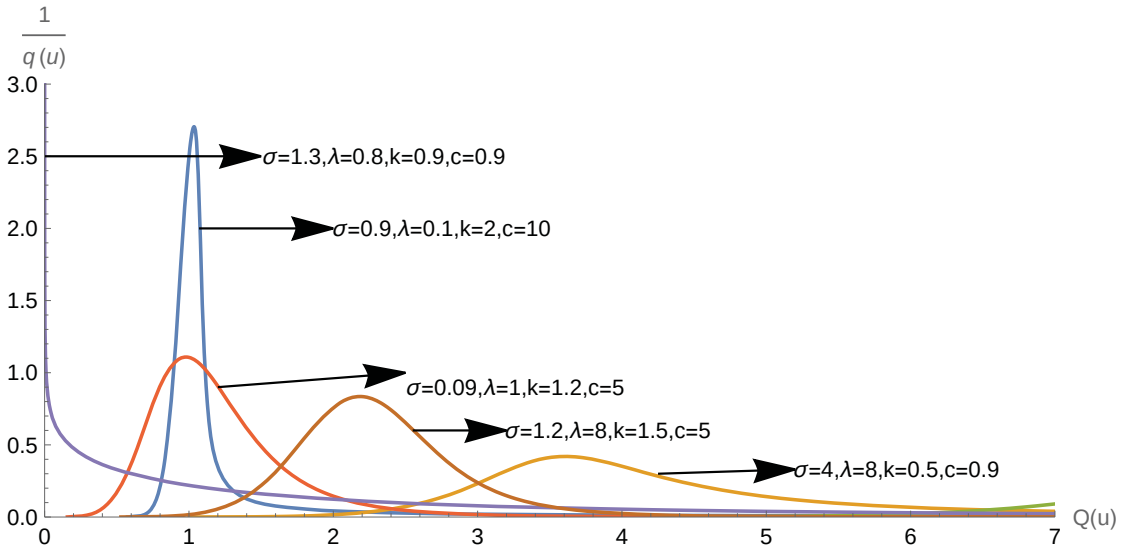

Figure 2.1: Plots of the density function for various parameter values.

2.3 Members of the Family

The suggested family of distributions (2.5) includes several well-known distributions for various parameter values is given below;

Case 1: $\sigma = 0$, $c > 0$, $k > 0$

$$Q(u) = (u^{-\frac{1}{k}} - 1)^{-\frac{1}{c}},$$

is the QF of the Burr III distribution.

Case 2: $c = 1$, $\sigma = 0$

$$Q(u) = (u^{-\frac{1}{k}} - 1)^{-1},$$

is the QF of the Inverse Lomax distribution.

Case 3: $k = 1$, $\sigma = 0$

$$Q(u) = (u^{-1} - 1)^{-\frac{1}{c}},$$

is the QF of the Log-Logistic distribution with scale parameter $\alpha = 1$.

Case 4: $c \to 0$

$$Q(u) = \sigma \left[-\log(1-u)\right]^{\frac{1}{\lambda}},$$

is the QF of Weibull distribution. Also by making use of some transformations mentioned in Gilchrist (2000), we can obtain some other well distributions from the proposed model.

Case 5 - Logarithmic Transformation: Using logarithmic transformation in (2.5), with $\sigma = 0$, $k = 1$ we have

$$Q(u) = -s \log(u^{-1} - 1),$$

where $s = \dfrac{1}{c}$, belongs to Logistic distribution with location parameter $\mu = 0$,

Case 6 - Reciprocal Transformation : Using reciprocal transformation $Q(u) = \frac{1}{Q(1-u)}$ in (2.5), with $\sigma = 0$, $c > 0$ and $k > 0$, the QF becomes,

$$Q(u) = \left((1-u)^{-\alpha} - 1\right)^{\eta},$$

with $\alpha = \frac{1}{k}$ and $\eta = \frac{1}{c}$. This is the QF of Burr XII distribution.

As we already know, the sum of two QFs is again a QF. But the random variable associated with the QF of the sum is not clearly established in the literature. The theorem below can be used to determine the random variable associated with the new model (2.5).

Theorem 1. *If $X \sim W(\lambda, \sigma)$, then the random variable*

$Y = X + \left(\left[1 - e^{-\left(\frac{X}{\sigma}\right)^{\lambda}}\right]^{-\frac{1}{k}} - 1\right)^{-\left(\frac{1}{c}\right)}$ *has BIIIW(c, k, σ, λ) distribution.*

Proof. Let $Q_S(u)$ and $Q_V(u)$ be the appropriate QFs for the two random variables S

and V with distribution function $F_S(x)$ and $F_V(x)$.

Then, we know that sum of two QF is again a QF. Hence $Q^*(u) = Q_S(u) + Q_V(u)$.

The random variable corresponding to the QF $Q^*(u)$ is $S + Q_V(F_S(S))$ and $V + Q_S(F_V(V))$ (given in Sankaran et al. (2016)).

Consider $Z \sim BIII(c,k)$ and $X \sim W(\lambda,\sigma)$ then $X + Q_Z(F_X(X)) \sim BIIIW(c,k,\sigma,\lambda)$ distribution.

Given $Q_Z(u) = \left(u^{-(\frac{1}{k})} - 1\right)^{-\frac{1}{c}}$ and $F_X(X) = 1 - e^{-\left(\frac{X}{\sigma}\right)^{\lambda}}$ then,

$$X + Q_Z(F_X(X)) = X + \left(\left[1 - e^{-\left(\frac{X}{\sigma}\right)^{\lambda}}\right]^{-\frac{1}{k}} - 1\right)^{-\left(\frac{1}{c}\right)}.$$

Hence the proof. □

Theorem 2. *If* $Y \sim BIII(c,k)$*, then the random variable* $X = Y + \sigma\left[-\log\left(1 - (1 + Y^{-c})^{-k}\right)\right]^{\frac{1}{\lambda}}$ *has BIIIW*(c,k,σ,λ) *distribution.*

Proof. : The proof works the same way as Theorem 1. □

2.4 Distributional Characteristics

The quantile based measures of the distributional characteristics such as location, dispersion, skewness, and kurtosis have wide applications in statistical analysis. It eliminates the requirement to define a distribution using its moments. These measures are used to estimate model parameters by equating population and sample characteristics. For the model (2.5), the basic descriptive measures such as the median (M), interquartile range (IQR), Galton's coefficient of skewness (S), and Moor's coefficient of kurtosis (T) are given below.

The median is a measure of location given by,

$$\mathrm{M} = Q\left(\frac{1}{2}\right) = \sigma\left[\log(2)\right]^{\frac{1}{\lambda}} + \left((0.5)^{-\frac{1}{k}} - 1\right)^{-\frac{1}{c}}. \tag{2.8}$$

The interquartile range is a measure of dispersion given by,

$$\begin{aligned} IQR &= Q\left(\frac{3}{4}\right) - Q\left(\frac{1}{4}\right) \\ &= \sigma\left([\log(4)]^{\frac{1}{\lambda}} - [-\log(0.75)]^{\frac{1}{\lambda}}\right) \\ &+ \left((0.75)^{-\frac{1}{k}} - 1\right)^{-\frac{1}{c}} - \left((0.25)^{-\frac{1}{k}} - 1\right)^{-\frac{1}{c}}. \end{aligned} \tag{2.9}$$

Galton's coefficient of skewness (S) is used to measure skewness,

$$\mathrm{S} = \frac{Q(\frac{3}{4}) + Q(\frac{1}{4}) - 2\ \text{Median}}{IQR}$$

$$= \frac{\sigma\left([\log(4)]^{\frac{1}{\lambda}} + [-\log(0.75)]^{\frac{1}{\lambda}} - 2[\log(2)]^{\frac{1}{\lambda}}\right) + \mathrm{A}}{\sigma\left([\log(4)]^{\frac{1}{\lambda}} - [-\log(0.75)]^{\frac{1}{\lambda}}\right) + \left((0.75)^{-\frac{1}{k}} - 1\right)^{-\frac{1}{c}} - \left((0.25)^{-\frac{1}{k}} - 1\right)^{-\frac{1}{c}}}, \tag{2.10}$$

where $\mathrm{A} = \left((0.75)^{-\frac{1}{k}} - 1\right)^{-\frac{1}{c}} + \left((0.25)^{-\frac{1}{k}} - 1\right)^{-\frac{1}{c}} - 2\left((0.5)^{-\frac{1}{k}} - 1\right)^{-\frac{1}{c}}$.

The Moor's coefficient of kurtosis (T) is used to measure kurtosis,

$$\mathrm{T} = \frac{Q(0.875) - Q(0.625) + Q(0.375) - Q(0.125)}{IQR}$$

$$= \frac{\sigma\left([-\log(0.125)]^{\frac{1}{\lambda}} - [-\log(0.375)]^{\frac{1}{\lambda}} + [-\log(0.625)]^{\frac{1}{\lambda}} - [-\log(0.875)]^{\frac{1}{\lambda}}\right) + \mathrm{B}}{\sigma\left([\log(4)]^{\frac{1}{\lambda}} - [-\log(0.75)]^{\frac{1}{\lambda}}\right) + \left((0.75)^{-\frac{1}{k}} - 1\right)^{-\frac{1}{c}} - \left((0.25)^{-\frac{1}{k}} - 1\right)^{-\frac{1}{c}}}, \tag{2.11}$$

where $\mathrm{B} = ((0.875)^{-\frac{1}{k}} - 1)^{-\frac{1}{c}} - ((0.625)^{-\frac{1}{k}} - 1)^{-\frac{1}{c}} + ((0.375)^{-\frac{1}{k}} - 1)^{-\frac{1}{c}} - ((0.125)^{-\frac{1}{k}} - 1)^{-\frac{1}{c}}$.

2.4.1 L-moments

L-moments are frequently found to be preferable to conventional moments in specifying the characteristics of distributions. Hosking (1990) developed a coherent theory and a comprehensive investigation on L-moments, investigated the properties of L-moments, their use in summarising and identifying probability distributions, estimation techniques based on L-moments etc. L-moments are the expected value of the linear combinations of order statistics. L-moments are more stable against outliers and have lower sample variances, it also provide better asymptotic approximations to sampling distributions.

The r^{th} L moment is given by,

$$L_r = \int_0^1 \sum_{k=0}^{r-1} (-1)^{r-1-k} \binom{r-1}{k} \binom{r-1+k}{k} u^k Q(u) du.$$

The first L-moment (L_1) is the mean of the distribution, given by,

$$\begin{aligned} L_1 &= \int_0^1 Q(u)du \\ &= \sigma\Gamma(1+\frac{1}{\lambda}) + \Gamma(1-\frac{1}{c})\left[\frac{\Gamma(k+\frac{1}{c})}{\Gamma k}\right]. \end{aligned} \tag{2.12}$$

The second L-moment is,

$$\begin{aligned} L_2 &= \int_0^1 (2u-1)\,Q(u)du \\ &= \sigma\Gamma(1+\frac{1}{\lambda})\left[1-2^{-\frac{1}{\lambda}}\right] + \Gamma(1-\frac{1}{c})\left[\frac{\Gamma(2k+\frac{1}{c})}{\Gamma(2k)} - \frac{\Gamma(k+\frac{1}{c})}{\Gamma k}\right]. \end{aligned} \tag{2.13}$$

Similarly, the third and fourth L-moments respectively are the following:

$$\begin{aligned} L_3 &= \int_0^1 \left(6u^2-6u+1\right) Q(u)du \\ &= \sigma\Gamma(1+\frac{1}{\lambda})\left[1-3\times 2^{-\frac{1}{\lambda}}+2\times 3^{-\frac{1}{\lambda}}\right] \\ &+ \Gamma(1-\frac{1}{c})\left[\frac{\Gamma(k+\frac{1}{c})}{\Gamma k} - \frac{3\Gamma(2k+\frac{1}{c})}{\Gamma(2k)} + \frac{2\Gamma(3k+\frac{1}{c})}{\Gamma(3k)}\right]. \end{aligned} \tag{2.14}$$

$$\begin{aligned} L_4 &= \int_0^1 \left(20u^3-30u^2+12u-1\right) Q(u)du \\ &= \sigma\Gamma(1+\frac{1}{\lambda})\left[1-3\times 2^{1-\frac{1}{\lambda}}+10\times 3^{-\frac{1}{\lambda}}-5\times 4^{-\frac{1}{\lambda}}\right] \\ &+ \Gamma(1-\frac{1}{c})C, \end{aligned} \tag{2.15}$$

$$\text{where} \quad C = \left[\frac{5\Gamma(4k+\frac{1}{c})}{\Gamma(4k)} - \frac{10\Gamma(3k+\frac{1}{c})}{\Gamma(3k)} + \frac{6\Gamma(2k+\frac{1}{c})}{\Gamma(2k)} - \frac{\Gamma(k+\frac{1}{c})}{\Gamma(k)}\right] \tag{2.16}$$

The L-coefficient of variation (τ_2), L-coefficient of skewness (τ_3) and L-coefficient of kurtosis (τ_4) for the model (2.5), is given below,

$$\begin{aligned}\tau_2 &= \frac{L_2}{L_1} \\ &= \frac{\sigma\Gamma(1+\frac{1}{\lambda})\left[1-2^{-\frac{1}{\lambda}}\right]+\Gamma(1-\frac{1}{c})\left[\frac{\Gamma(2k+\frac{1}{c})}{\Gamma(2k)}-\frac{\Gamma(k+\frac{1}{c})}{\Gamma k}\right]}{\sigma\Gamma(1+\frac{1}{\lambda})+\Gamma(1-\frac{1}{c})\left[\frac{\Gamma(k+\frac{1}{c})}{\Gamma k}\right]}.\end{aligned} \tag{2.17}$$

$$\begin{aligned}\tau_3 &= \frac{L_3}{L_2} \\ &= \frac{\sigma\Gamma(1+\frac{1}{\lambda})\left[1-3\times 2^{-\frac{1}{\lambda}}+2\times 3^{-\frac{1}{\lambda}}\right]+\Gamma(1-\frac{1}{c})D}{\sigma\Gamma(1+\frac{1}{\lambda})\left[1-2^{-\frac{1}{\lambda}}\right]+\Gamma(1-\frac{1}{c})\left[\frac{\Gamma(2k+\frac{1}{c})}{\Gamma(2k)}-\frac{\Gamma(k+\frac{1}{c})}{\Gamma k}\right]},\end{aligned} \tag{2.18}$$

$$\text{where} \quad D=\left[\frac{\Gamma(k+\frac{1}{c})}{\Gamma k}-\frac{3\Gamma(2k+\frac{1}{c})}{\Gamma(2k)}+\frac{2\Gamma(3k+\frac{1}{c})}{\Gamma(3k)}\right].$$

$$\begin{aligned}\tau_4 &= \frac{L_4}{L_2} \\ &= \frac{\sigma\Gamma(1+\frac{1}{\lambda})\left[1-3\times 2^{1-\frac{1}{\lambda}}+10\times 3^{-\frac{1}{\lambda}}-5\times 4^{-\frac{1}{\lambda}}\right]+\Gamma(1-\frac{1}{c})\mathrm{C}}{\sigma\Gamma(1+\frac{1}{\lambda})\left[1-2^{-\frac{1}{\lambda}}\right]+\Gamma(1-\frac{1}{c})\left[\frac{\Gamma(2k+\frac{1}{c})}{\Gamma(2k)}-\frac{\Gamma(k+\frac{1}{c})}{\Gamma k}\right]},\end{aligned} \tag{2.19}$$

where C is given in (2.16).

2.4.2 Order Statistics

Order statistics have a wider application in many areas. One of them is system reliability. Let $X_{i:n}$ be the i^{th} order statistic of a random sample of size n, then the density function of $X_{i:n}$ is given as follows,

$$f_i(x)=\frac{1}{B(i,n-i+1)}f(x)F^{i-1}(x)(1-F(x))^{n-i},$$

where $B(a,b)$ is the beta function. Substituting (2.7), we have,

$$f_i(x) = \frac{ck\lambda(F(x))^{i-1}(1-F(x))^{n-i+1}}{B(i,n-i+1)\left(ck\sigma[-\log(1-F(x))]^{\frac{1}{\lambda}-1}+\lambda(1-F(x))\left((F(x))^{-(\frac{1}{k})}-1\right)^{-\left(\frac{1}{c}+1\right)}(F(x))^{-\left(\frac{1}{k}+1\right)}\right)}.$$

Hence

$$E(X_{i:n}) = \frac{1}{B(i,n-i+1)}\int_0^\infty x f_i(x)dx.$$

In quantile terms, we have

$$E(X_{i:n}) = \frac{1}{B(i,n-i+1)}\int_0^1 \frac{Q(u)u^{i-1}(1-u)^{n-i}}{q(u)}du.$$

The QF of first order statistic $X_{1:n}$ for the model (2.5) is given by,

$$\begin{aligned} Q_{1^*}(u) &= Q(1-(1-u)^{\frac{1}{n}}) \\ &= \sigma\left[-\log(1-u)^{\frac{1}{n}}\right]^{\frac{1}{\lambda}} + \left[(1-(1-u)^{\frac{1}{n}})^{-\frac{1}{k}}-1\right]^{-\frac{1}{c}}, \end{aligned} \tag{2.20}$$

and the QF of n^{th} order statistic $X_{n:n}$ is,

$$\begin{aligned} Q_{n^*}(u) &= Q(u^{\frac{1}{n}}) \\ &= \sigma\left[-\log\left(1-u^{\frac{1}{n}}\right)\right]^{\frac{1}{\lambda}} + \left(u^{-\frac{1}{kn}}-1\right)^{-\frac{1}{c}}. \end{aligned} \tag{2.21}$$

2.5 Reliability Properties

There are several functions available for modelling and analysis of lifetime data such as the HRF, the mean residual life function etc. Nair and Sankaran (2009) defined the hazard QF in a quantile structure, which is identical to the hazard rate. Hazard rate can be defined as the conditional probability of a unit failing in the next small interval of time given that the unit has survived age x. The hazard QF, $H(u)$ is defined as,

$$H(u) = h(Q(u)) = [(1-u)q(u)]^{-1}. \tag{2.22}$$

Note that $H(u)$ uniquely determines the distribution using the identity,

$$Q(u) = \int_0^u \frac{dp}{(1-p)H(p)}. \tag{2.23}$$

The hazard QF of Weibull and Burr III distribution respectively are,

$$H_1(u) = \lambda\sigma^{-1}\left[-\log(1-u)\right]^{1-\frac{1}{\lambda}} \tag{2.24}$$

$$\text{and} \quad H_2(u) = ck\,(1-u)^{-1}\left(u^{-\frac{1}{k}}-1\right)^{1+\frac{1}{c}} u^{1+\frac{1}{k}}. \tag{2.25}$$

Since the suggested class of distributions is the sum of QFs of Weibull and Burr III QFs, Equations (2.22) and (2.23) give,

$$\frac{1}{H(u)} = \frac{1}{H_1(u)} + \frac{1}{H_2(u)}.$$

For the class of distributions (2.5) the hazard QF has the form,

$$H(u) = \frac{ck\lambda}{\lambda(1-u)(u^{-\frac{1}{k}}-1)^{-\frac{1}{c}-1}u^{-\frac{1}{k}-1} + ck\sigma\left[-\log(1-u)\right]^{\frac{1}{\lambda}-1}} \tag{2.26}$$

which allows increasing, decreasing, linear, bathtub and upside-down bathtub shapes for different choices of parameters. Figure 2.2 shows plots of the hazard QF for various parameter values. Using the derivative of $H(u)$ we can obtain the shape of the hazard function, obtained as,

$$H^{'}(u) = \frac{h^{'}(u)}{\left[\lambda(1-u)(u^{-\frac{1}{k}}-1)^{-\frac{1}{c}-1}u^{-\frac{1}{k}-1} + ck\sigma\left[-\log(1-u)\right]^{\frac{1}{\lambda}-1}\right]^2}.$$

Since $\left[\lambda(1-u)(u^{-\frac{1}{k}}-1)^{-\frac{1}{c}-1}u^{-\frac{1}{k}-1} + ck\sigma\left[-\log(1-u)\right]^{\frac{1}{\lambda}-1}\right]^2 > 0$ for all values of the parameters, the sign of $H^{'}(u)$ depends on $h^{'}(u)$ given by,

$$\begin{aligned} h^{'}(u) &= \frac{(c+1)(u-1)\left(u^{-\frac{1}{k}}-1\right)^{-\frac{1}{c}}\lambda^2}{u^2\left(u^{\frac{1}{k}}-1\right)^2} + \frac{c(k+1)(u-1)\left(u^{-\frac{1}{k}}-1\right)^{-\frac{1}{c}}\lambda^2}{u^2\left(u^{\frac{1}{k}}-1\right)} \\ &- \frac{ck\left(u^{-\frac{1}{k}}-1\right)^{-\frac{1}{c}}\lambda^2}{u\left(u^{\frac{1}{k}}-1\right)} - \frac{c^2k^2\left(\frac{1}{\lambda}-1\right)\lambda\sigma\left[-\log(1-u)\right]^{-2+\frac{1}{\lambda}}}{1-u}. \end{aligned}$$

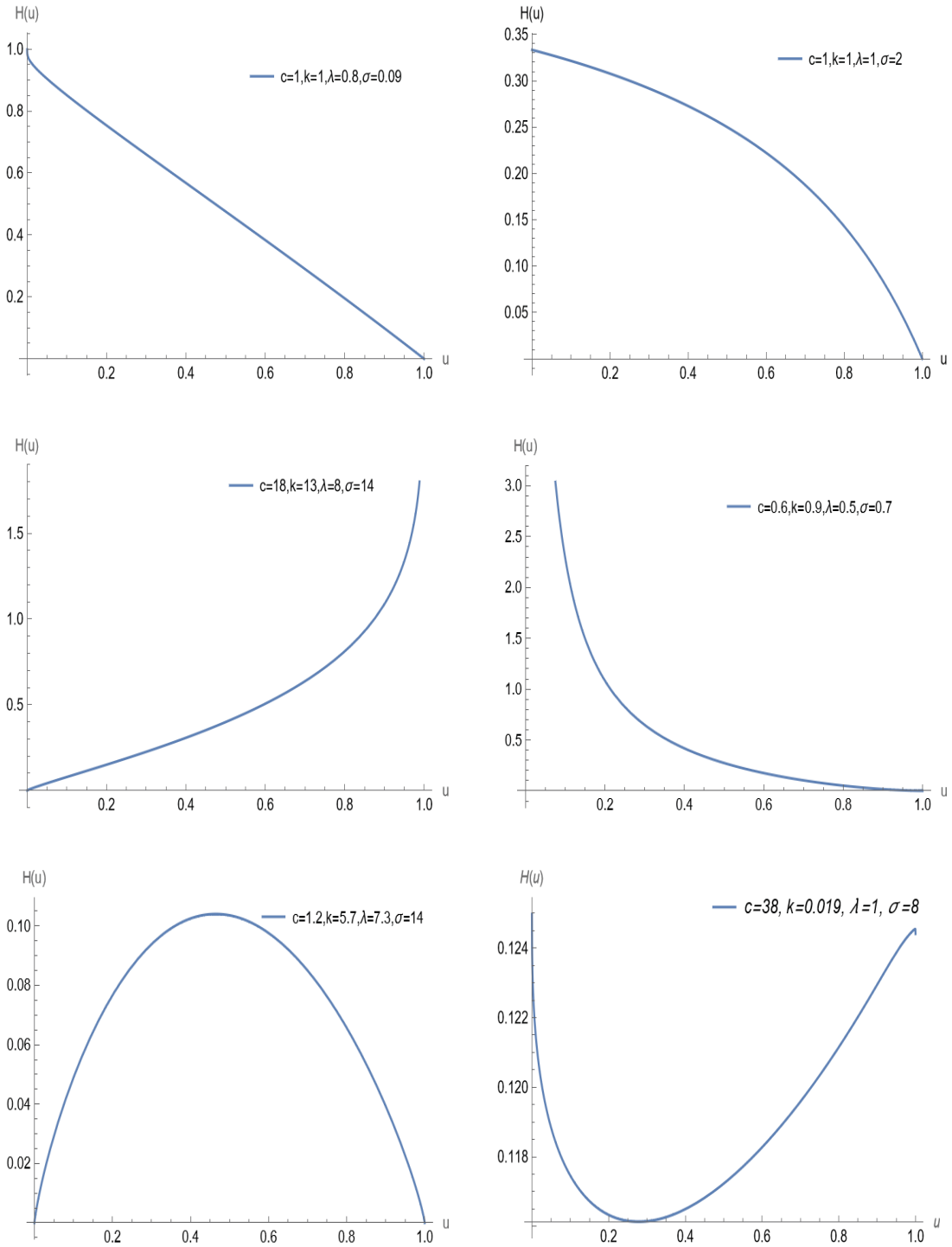

Figure 2.2: Plots of the hazard QF for various parameter values.

Let u_0 be the critical point of $H(u)$ satisfying the non-linear equation $h^{'}(u_0) = 0$. Since u_0 has no closed-form, we need to use any mathematical software for its numerical evaluation. Also, we know that the sign of $h^{''}(u_0)$ represents the nature of u_0: u_0 is local minimum if $h^{''}(u_0) > 0$ and local maximum if $h^{''}(u_0) < 0$.
In reliability analysis, the mean residual function is a well-known statistic that has been widely used for modelling lifetime data. The average remaining life of a system given that the system has lasted upto a specific age is called the mean residual life. The quantile version of the mean residual function proposed by Nair and Sankaran (2009) is given by,

$$M(u) = \frac{1}{1-u}\int_u^1 (Q(p) - Q(u))\, dp.$$

For the model (2.5), $M(u)$ has the form,

$$\begin{aligned} M(u) &= \frac{\sigma\Gamma(\frac{1}{\lambda}+1, -\log(1-u))}{1-u} - \sigma\left(-\log(1-u)\right)^{\frac{1}{\lambda}} \\ &+ \frac{k}{1-u}\left[B\left(k+\frac{1}{c}, 1-\frac{1}{c}\right) - B_{u^{\frac{1}{k}}}\left(k+\frac{1}{c}, 1-\frac{1}{c}\right)\right] \\ &- \left(u^{-\frac{1}{k}}-1\right)^{-\frac{1}{c}}, \qquad Re\left(\frac{1}{c}\right) < 1, \end{aligned} \tag{2.27}$$

where $B_u(a,b) = \int_0^u x^{a-1}(1-x)^{b-1}dx$ is the incomplete beta and
$\Gamma(s,t) = \int_t^1 x^{s-1}e^{-x}dx$ is the upper incomplete gamma function.
The hazard QF and mean residual QF defined in reverse time has the expression,

$$\begin{aligned} \Lambda &= (uq(u))^{-1}, \\ &= \frac{ck\lambda(1-u)}{u\left[ck\sigma\left(-\log(1-u)\right)^{\frac{1}{\lambda}-1} + \lambda(1-u)\left(u^{-\frac{1}{k}}-1\right)^{-\frac{1}{c}-1}u^{-\frac{1}{k}-1}\right]} \end{aligned} \tag{2.28}$$

$$\begin{aligned} R(u) &= \frac{1}{u}\int_0^u [Q(u) - Q(p)]dp. \\ &= \sigma\left(-\log(1-u)\right)^{\frac{1}{\lambda}} - \frac{\sigma\gamma(\frac{1}{\lambda}+1, -\log(1-u))}{u} \\ &+ \left(u^{-\frac{1}{k}}-1\right)^{-\frac{1}{c}} - \frac{k}{u}\left[B_{u^{\frac{1}{k}}}\left(k+\frac{1}{c}, 1-\frac{1}{c}\right)\right], \quad \mathrm{Re}\left(\frac{1}{c}\right) < 1, \end{aligned} \tag{2.29}$$

where $B_u(a,b) = \int_0^u x^{a-1}(1-x)^{b-1}dx$ is the incomplete beta and $\gamma(s,t) = \int_0^t x^{s-1}e^{-x}dx$ is the lower incomplete gamma function. $R(u)$ represents the time elapsed since the failure of a unit given that its lifetime is at most x. The total time on the test transform (TTT) is a well-known statistical method with numerous applications in reliability analysis Lai and Xie (2006). The quantile-based TTT proposed by Nair et al. (2008) takes the following form:

$$T(u) = \int_0^u (1-p)q(p)dp.$$

Another relationship between total time on test transform and reversed mean residual QF (see Nair et al. (2008)) has the expression,

$$\begin{aligned} T(u) &= Q(u) - uR(u), \\ &= \sigma\left(-\log(1-u)\right)^{\frac{1}{\lambda}}[1-u] + (u^{-\frac{1}{k}}-1)^{-\frac{1}{c}}[1-u] \\ &+ \sigma\gamma\left(\frac{1}{\lambda}+1, -\log(1-u)\right) + kB_{u^{\frac{1}{k}}}\left(k+\frac{1}{c}, 1-\frac{1}{c}\right). \end{aligned} \tag{2.30}$$

The total time in the test statistic is the sum of all observed and incomplete life durations. As the number of units on test approaches infinity, the limit of this statistic is known as the total time on test transform (TTT).

2.6 Inference and Applications

The most commonly used methods for estimating the parameters of QF are method of percentiles, method of L-moments, method of least squares, method of ML etc. Here method of least square and method of L-moments are employed to estimate the parameters of the model (2.5).

2.6.1 Method of Least Square Estimation (LSE)

Let $X_1, X_2, ..., X_n$ be a random sample of size n from a population of lifetime with quadratic hazard QF. Consider $X_{(i)}$ be the i^{th} order statistics of random sample of size n. The random variable $X_{(i)}$ has the same distribution as the random variable $Q(u_i, \hat{\theta})$, where $u_{(i)}$ be the order statistics of the sample following uniform distribution and $\hat{\theta}$ be the estimate of the model's parameter vector. The method of least squares, estimates the unknown parameters $(\theta_1, \theta_2, \ldots, \theta_n)$ by

minimising the sum of squares of theoretical and empirical quantile differences (Hankin and Lee (2006)). The function for which we compute the minimum then takes the following form,

$$S(\theta_1, \theta_2, \ldots, \theta_n) = \sum_{i=1}^{n} \left(X_{(i)} - Q(u_{(i)}, \theta) \right)^2 .$$

2.6.2 Method of L moments (MLM)

In this method, the sample L-moments are equated to the population L-moments. Let $X_1, X_2, \ldots, X_n$ be a random sample of size n from the population having QF (2.5), then the corresponding sample L-moments are:

$$\begin{aligned}
l_1 =& \frac{1}{n} \sum_{i=1}^{n} X_{(i)} \\
l_2 =& \binom{1}{2} \binom{n}{2}^{-1} \sum_{i=1}^{n} \left(\binom{i-1}{1} - \binom{n-i}{1} \right) X_{(i)} \\
l_3 =& \binom{1}{3} \binom{n}{3}^{-1} \sum_{i=1}^{n} \left(\binom{i-1}{2} - 2\binom{i-1}{1}\binom{n-i}{1} + \binom{n-i}{2} \right) X_{(i)}
\end{aligned}$$

$$l_4 = \tbinom{1}{4} \tbinom{n}{4}^{-1} \sum_{i=1}^{n} \left(\tbinom{i-1}{3} - 3\tbinom{i-1}{2}\tbinom{n-i}{1} + 3\tbinom{i-1}{1}\tbinom{n-i}{2} - \tbinom{n-i}{3} \right) X_{(i)},$$

where $X_{(i)}$ denotes the i^{th} order statistic. We equate the first four sample L moments with the corresponding population L moments for obtaining the estimates of the parameters c, k, λ, σ. Hence, we have

$$l_r = L_r; \quad r = 1, 2, 3, 4.$$

2.6.3 Applications

Here we consider two real datasets to compare the proposed estimation techniques and to demonstrate the applicability of the BIIIW QF. χ^2 Goodness of fit and quantile-quantile (Q-Q) plot techniques were used to determine the effectiveness of the proposed model. The Q-Q plot indicates the physical closeness of the model. The first data is taken from Nadarajah and Kotz (2008) represents fracture toughness of Alumina, (Al_2O_3) (in the units of MPa $m^{\frac{1}{2}}$) presented in

Table 2.1. The second data deals with the number of consecutive failures of jet airplanes air conditioning system (for details see Huang and Oluyede (2014)) given in Table 2.2.

Table 2.1: Fracture toughness data of Alumina (Al_2O_3)

5.5	5	4.9	6.4	5.1	5.2	5.2	5	4.7	4
4.5	4.2	4.1	4.56	5.01	4.7	3.13	3.12	2.68	2.77
2.7	2.36	4.38	5.73	4.35	6.81	1.91	2.66	2.61	1.68
2.04	2.08	2.13	3.8	3.73	3.71	3.28	3.9	4	3.8
4.1	3.9	4.05	4	3.95	4	4.5	4.5	4.2	4.55
4.65	4.1	4.25	4.3	4.5	4.7	5.15	4.3	4.5	4.9
5	5.35	5.15	5.25	5.8	5.85	5.9	5.75	6.25	6.05
5.9	3.6	4.1	4.5	5.3	4.85	5.3	5.45	5.1	5.3
5.2	5.3	5.25	4.75	4.5	4.2	4	4.15	4.25	4.3
3.75	3.95	3.51	4.13	5.4	5	2.1	4.6	3.2	2.5
4.1	3.5	3.2	3.3	4.6	4.3	4.3	4.5	5.5	4.6
4.9	4.3	3	3.4	3.7	4.4	4.9	4.9	5	

For the computation of the MLM method, the sample L moments are calculated for both of the datasets which are described in Table 2.3. The Newton-Raphson technique is used to solve the four nonlinear equations, which are formed by equating the values of sample L moments with the corresponding population L moments given in (2.12)-(2.15). The value of the parameters which are obtained using the LSE technique are used as the initial values for the Newton Raphson procedure. The descriptive statistics for the datasets are shown in Table 2.4. The estimated values, χ^2 with degree of freedom (dof) and p - values obtained using the two estimation techniques are shown in Table 2.5. The results were obtained using the MATHEMATICA software.

Table 2.2: Number of failures for the air conditioning system of the Jet airplanes.

194	413	90	74	55	23	97	50	359	50
130	487	57	102	15	14	10	57	320	261
51	44	9	254	493	33	18	209	41	58
60	48	56	87	11	102	12	5	14	14
29	37	186	29	104	7	4	72	270	283
7	61	100	61	502	220	120	141	22	603
35	98	54	100	11	181	65	49	12	239
14	18	39	3	12	5	32	9	438	43
134	184	20	386	182	71	80	188	230	152
5	36	79	59	33	246	1	79	3	27
201	84	27	156	21	16	88	130	14	118
44	15	42	106	46	230	26	59	153	104
20	206	5	66	34	29	26	35	5	82
31	118	326	12	54	36	34	18	25	120
31	22	18	216	139	67	310	3	46	210
57	76	14	111	97	62	39	30	7	44
11	63	23	22	23	14	18	13	34	16
18	130	90	163	208	1	24	70	16	101
52	208	95	62	11	191	14	71		

Table 2.3: The sample L-moment values for dataset 1 and dataset 2.

	l_1	l_2	l_3	l_4
DataSet-1	4.3253	0.5688	-0.0500	0.0919
DataSet-2	92.0745	51.3599	22.0285	11.062

Table 2.4: The basic descriptive statistics of the two datasets.

	Median	IQR	Skewness (S)	Kurtosis (T)
Dataset-1	4.3566	1.3232	-0.0358	1.246
Dataset-2	55.1305	107.198	0.3477	1.4241

From the χ^2 values shown in the Table 2.5, it is evident that the MLM estimation technique is found to be the best fit in both cases. The Figures 2.3 and 2.4 represent the Q-Q plots of the datasets corresponding to LSE and MLM techniques. That is, Q-Q plots also guarantees the result obtained using the χ^2

Table 2.5: GoF statistics corresponding to the two datasets.

	DataSet 1			DataSet 2		
	Parameters	χ^2(dof)	p - value	Parameters	χ^2(dof)	p - value
LSE	c = 7.084 k = 0.5882 λ = 6.2665 σ = 3.8404	19.2516(13)	0.115	c = 2.2448 k =16.8983 λ = 0.8285 σ = 82.7944	16.6332(16)	0.409
MLM	c = 7.4363 k = 0.4457 λ = 5.6163 σ = 3.7564	9.3154(13)	0.748	c = 1.9101 k = 16.9201 λ = 0.7971 σ= 78.9684	11.8295(16)	0.7556

values. As a result, of the two described estimation methods, the MLM is found to be the most suitable estimation method for each of the datasets.

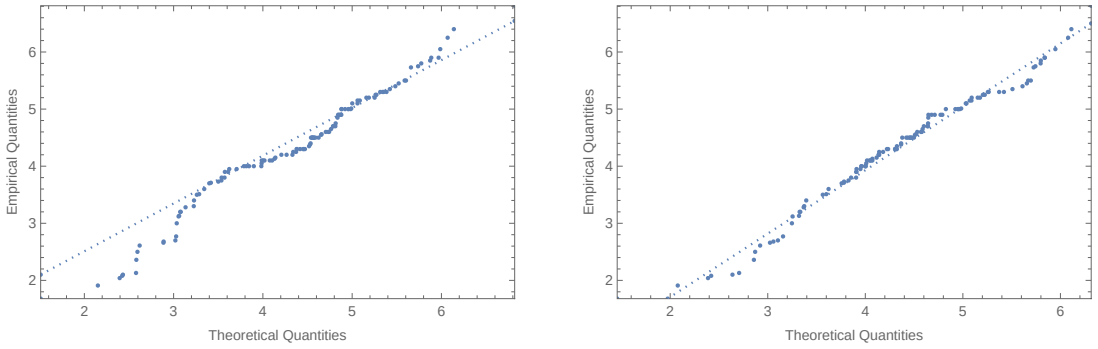

Figure 2.3: Q-Q plot corresponing to LSE and MLM estimates for the first dataset.

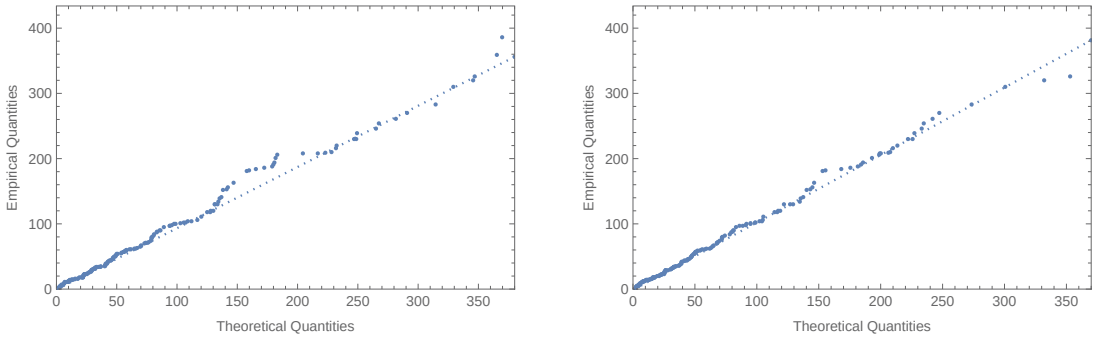

Figure 2.4: Q-Q plot corresponing to LSE and MLM estimates for the second dataset.

The proposed model is then compared against the Weibull (W) and Burr

III (BIII) models. MLM technique is used to find the estimates of comparable models. Figure 2.5 displays the histogram of the datasets and the estimated density for the BIIIW, W and BIII models. This demonstrates that in both cases, our proposed distribution provides a better fit than the other two models.

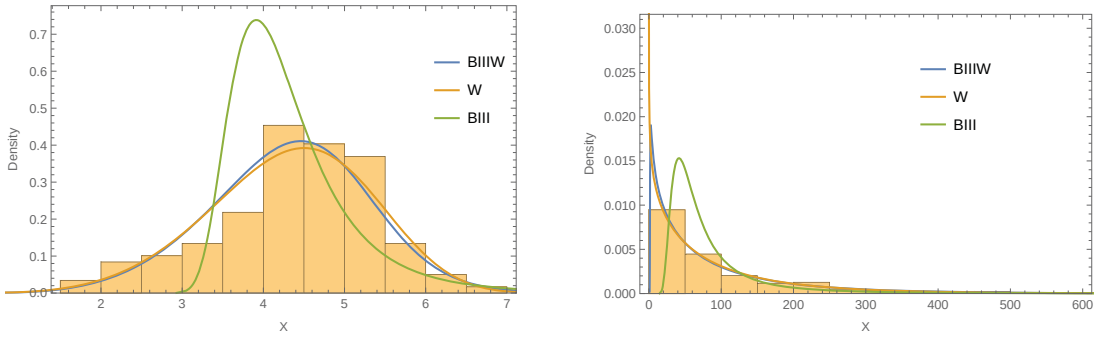

Figure 2.5: (a) The fitted density of the first dataset. (b) The fitted density of the second dataset.

The χ^2 value and p - value obtained for the models BIIIW, W and BIII are given in Table 2.6. Based on the χ^2 values also, we can conclude that our model gives a better fit.

Table 2.6: The χ^2 with p - values for the datasets.

	Dataset 1		Dataset 2	
Models	χ^2	p - value	χ^2	p - value
BIIIW	9.31543	0.7487	11.8295	0.7556
W	12.4163	0.4938	14.4481	0.5653
BIII	18.8007	0.1294	21.5262	0.1591

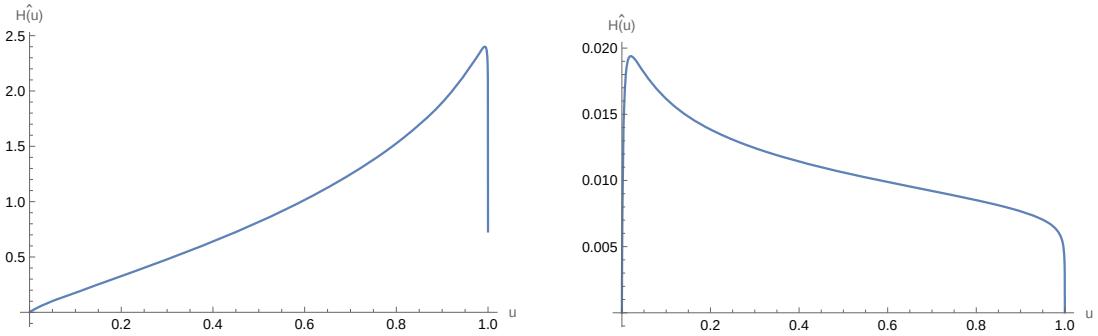

Figure 2.6: (a) Hazard quantile plot of the first dataset. (b) Hazard quantile plot of the second dataset.

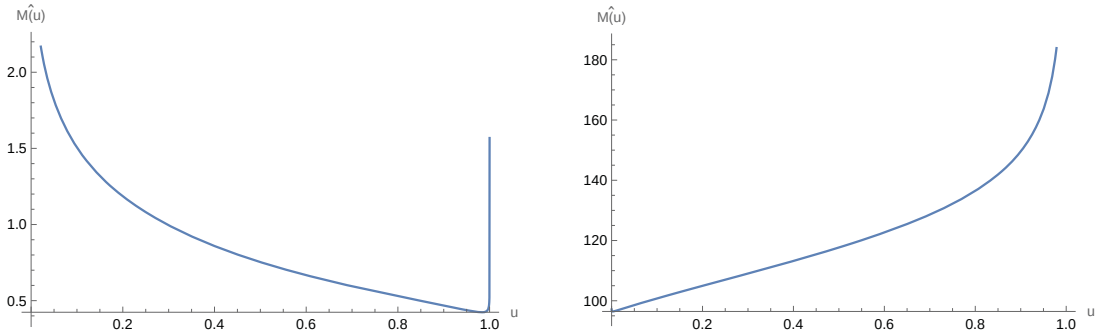

Figure 2.7: (a) Mean residual plot of the first dataset. (b) Mean residual plot of the second dataset.

The Figure 2.6 and 2.7 describes the flexible nature of the hazard QF and mean residual function for different estimates. It is obvious from the shapes of $\hat{H}(u)$, that the new model may be applied to examine a variety of lifetime data.

2.7 Summary

In this Chapter, we introduced a new QF called the BIIIW QF, which is the sum of the QFs of Burr III and Weibull distributions. The new model has several sub-models such as Inverse-Lomax, Logistic, Weibull, Log-Logistic etc. Different reliability properties of the suggested class is discussed. The new model achieves several interesting behaviours for the hazard QF. The estimation of parameters of the model is conducted using the LSE and MLM. The applications of the proposed model were studied with the use of two real life datasets. From the two applications, it is clear that the proposed model provides a better fit than the other competing models. The flexible nature of the hazard QF makes the model effective for fitting many types of lifetime data.

Chapter 3

A Competing Risks Based Burr III Weibull Distribution and its Applications to COVID-19 Data

3.1 Introduction

Developing new probability distributions is crucial in lifetime data analysis, where accurately modeling of event timings like failure or death is vital. Existing distributions may lack the flexibility to capture complex real-world phenomena, such as non-monotonic hazard rates, multi-modality, or varying skewness in empirical data. This necessitates, the exploration of innovative models that offer better data fits and deeper insights into risk factors and failure mechanisms, leading to more informed decisions.

Compounding, or the competing risks (CRs) approach, is vital as it integrates multiple independent failure processes into a single model. By merging survival functions from various baseline distributions, the compounded model retains features from each while allowing flexibility to represent different hazard rate behaviors. This method not only includes standard distributions but also enables the development of adaptable models for various data patterns, making it a key asset in reliability engineering, biostatistics, and quality control. This Chapter discusses a new lifetime distribution by combining the Weibull and Burr III distributions in a serial system. The hazard function of this new distribution

is obtained as the sum of the hazard functions from the Weibull and Burr III distributions. The motivation is to address limitations of the Weibull and Burr III distributions in modeling various types of data such as bathtub-shaped hazard rates. While neither parent distribution can accommodate this shape, the Burr III-Weibull (BIIIW) distribution fills this gap, supporting diverse hazard rate forms including decreasing, increasing, and bathtub shape. Also BIIIW distribution can exhibit a bimodal shape, unlike the Weibull and Burr III distributions. This makes it a valuable model for accurately representing and capturing the patterns and characteristics of bimodal data.

This Chapter is structured as follows. Section 3.1 presents an introduction of the Chapter. In Section 3.2, the newly proposed BIIIW model is developed. The statistical properties of this model are examined in Section 3.3. Sections 3.4 and 3.5 address the order statistics and Rényi entropy associated with the BIIIW distribution, respectively. Characterizations of the proposed model are also discussed in Section 3.6. Section 3.7 explores the autoregressive time series framework based on the proposed distribution. The ML estimation method is described in Section 3.8. Section 3.9 investigates the efficiency of the estimators through a simulation study. In Section 3.10, the applicability of the model is demonstrated using three real-world datasets. Section 3.11 presents model validation using the NRR statistic, and the final conclusions are summarized in Section 3.12.

3.2 Burr III-Weibull Distribution

As previously noted, the Weibull (W) distribution is a significant lifetime model capable of representing monotone hazard rate behaviors. Due to its extensive versatility, it has been widely applied to characterize both early-stage and aging-related failures. The PDF of its basic two-parameter form, denoted as $W(a, b)$, is given by,

$$f_W(x|a,b) = \frac{b}{a}\left(\frac{x}{a}\right)^{b-1} \exp\left(-\left(\frac{x}{a}\right)^{b}\right), \quad x > 0,\, a > 0,\, b > 0,$$

where a and b are scale and shape parameters. The PDF of Burr III (BIII) distribution is given by,

$$f_{BIII}(x|c,k) = ckx^{-(c+1)}(1+x^{-c})^{-(k+1)}, \quad x>0,\, c>0,\, k>0,$$

where c and k are shape parameters. A CRs model incorporating, Weibull and Burr III distribution can be defined as follows. Let X_1 be a random variable following $W(a,b)$ and X_2 be another random variable following $BIII(c,k)$. A CR Burr III Weibull (BIIIW) model can then be described by the random variable $X = \min(X_1, X_2)$, characterized by the four parameters c, k, a, b. The survival function of BIIIW distribution is given by,

$$\bar{F}_{BIIIW}(x) \;=\; [1-(1+x^{-c})^{-k}]e^{-\left(\frac{x}{a}\right)^b}.$$

Then the corresponding CDF of BIIIW distribution is given as follows,

$$F_{BIIIW}(x) = 1-[1-(1+x^{-c})^{-k}]e^{-\left(\frac{x}{a}\right)^b}, \quad x>0, \tag{3.1}$$

where $c, k, b, a > 0$ are non-negative with c, k and b being shape parameters and a being scale parameters.
The PDF of BIIIW distribution is given by,

$$f_{BIIIW}(x) \;= e^{-\left(\frac{x}{a}\right)^b}\left\{ck(1+x^{-c})^{-(k+1)}x^{-(c+1)} + \tfrac{b}{a^b}x^{b-1}(1-(1+x^{-c})^{-k})\right\}, \quad x>0, c>0, k>0, a>0, b>0. \tag{3.2}$$

An alternative formulation could be,

$$f_{BIIIW}(x) = [h_{BIII}(x;c,k) + h_W(x;a,b)]S_{BIII}(x;c,k)S_W(x;a,b).$$

where S_W and h_W represent the survival and hazard functions of the Weibull distribution, while S_{BIII} and h_{BIII} represent the survival and hazard functions of the Burr III distribution respectively. The significance of (3.1) is that it includes numerous well-known distributions as special models. When $b = 1$, model (3.1) becomes Burr III exponential distribution (BIIIE), which is not previously

known in the literature. For $b = 2$, it reduces to Burr III Rayleigh distribution (BIIIR). For $c = 1$, the model reduces to Inverse Lomax Weibull (ILW) distribution. For $k = 1$, it reduces to Log-Logistic Weibull distribution (LLW). When $k \to \infty$, it becomes Weibull distribution. The PDF of the BIIIW distribution can exhibit various shapes including decreasing, unimodal, bimodal, left-skewed, nearly symmetrical, or right-skewed. Figure 3.1 illustrates these different shapes of the BIIIW density function.

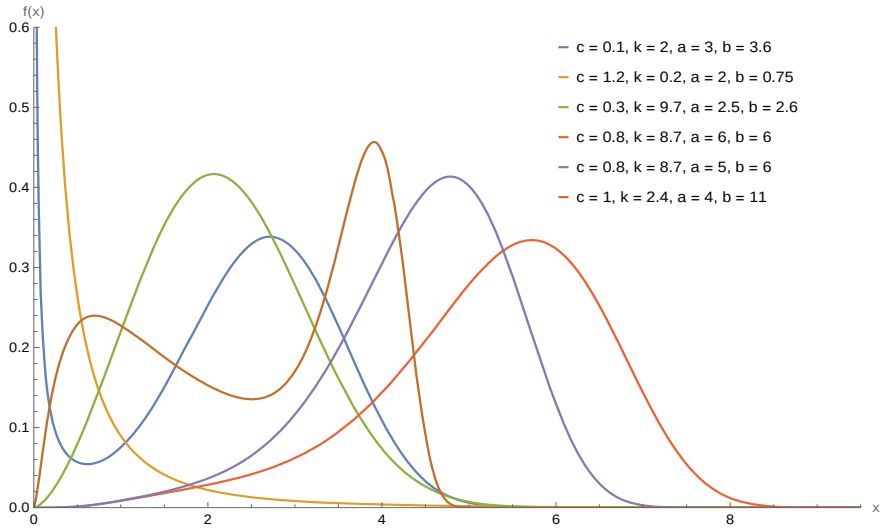

Figure 3.1: Plot for PDF curves of the BIIIW distribution.

3.3 Statistical Properties

The HRF, $h(x)$ of BIIIW distribution is given as follows,

$$h_{BIIIW}(x) = \frac{ck(1+x^{-c})^{-k-1}x^{-c-1} + \frac{b}{a^b}x^{b-1}(1-(1+x^{-c})^{-k})}{1-(1+x^{-c})^{-k}}. \quad (3.3)$$

Additionally, (3.3) may be written as,

$$h_{BIIIW}(x) = h_{BIII}(x) + h_W(x).$$

Hence, the HRF of the BIIIW distribution is obtained by adding together the HRFs of the Burr III and Weibull distributions. This can be interpreted as a configuration of a serial system comprising two independent components. One of the components follows the Weibull distribution with parameters a and b, while

the other component follows the Burr III distribution with parameters c and k. From Figure 3.2 it is evident that, the HRF of the BIIIW distribution exhibits various patterns such as decreasing, increasing, unimodal and bathtub-shaped which overcomes the limitation of parent distributions. This implies that the newly introduced family of distributions which consists of four parameters, is highly versatile and can be employed effectively for analyzing survival data.

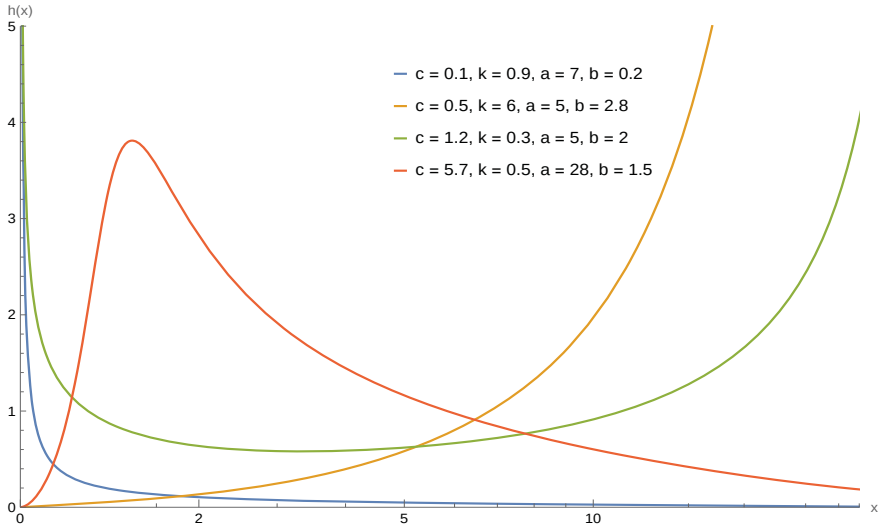

Figure 3.2: Plot for HRF of the BIIIW distribution.

3.3.1 Quantile Function

The real solution of the non-linear equation corresponds to the quantile (x_q) of the BIIIW distribution is given by,

$$\log[1-(1+x_q^{-c})^{-k}]-\left(\frac{x_q}{a}\right)^b=\log(1-q),\quad 0<q<1. \tag{3.4}$$

Hence, in order to obtain the quantiles for (3.4), numerical techniques need to be employed as there is no closed form solution available for x_q.

3.3.2 Moments and Incomplete Moments

Moments are frequently used to assess a probability distribution's mean, variance, skewness, and kurtosis. If X follows the BIIIW distribution, then the r^{th}

moment of X is given by,

$$\begin{aligned} E(X^r) &= \int_0^\infty x^r f(x)dx \\ &= \int_0^\infty x^r e^{-(x/a)^b}\left[ck(1+x^{-c})^{-k-1}x^{-c-1} + \frac{b}{a^b}x^{b-1}(1-(1+x^{-c})^{-k})\right]dx. \end{aligned}$$

Using the expansion of binomial, exponential and generalised gamma expression we get,

$$\begin{aligned} E(X^r) &= k\sum_{m=0}^{\infty}\frac{(-1)^m}{a^{(mb)}m!}B\left(k+\frac{r}{c}+\frac{mb}{c}, 1-\frac{r}{c}-\frac{mb}{c}\right) + a^r\Gamma\left(\frac{r}{b}+1\right) \\ &- a^{r-ct}\sum_{t=0}^{\infty}(-1)^t\binom{k+t-1}{t}\Gamma\left(\frac{r+b-ct}{b}\right) \text{ where } r<c, m\beta<c, \end{aligned} \tag{3.5}$$

where $B(\alpha,\beta) = \int_0^1 t^{\alpha-1}(1-t)^{\beta-1}dt$ and $\int_0^\infty x^{d-1}e^{-(x/\alpha)^p}dx = \frac{\Gamma\left(\frac{d}{p}\right)}{\frac{p}{\alpha^d}}$ is the beta and the generalised gamma function respectively. The first six moments ($\mu_1^{'}$, $\mu_2^{'}$, $\mu_3^{'}$, $\mu_4^{'}$, $\mu_5^{'}$, $\mu_6^{'}$), standard deviation (SD), coefficient of variation (CV), coefficient of skewness (CS) and coefficient of kurtosis (CK) for different selected values of the BIIIW distribution parameters are listed in Table 3.1.

Table 3.1: Moments of BIIIW for selected parameter values.

	(c, k, a, b)				
Moments	(5, 2.5, 0.5, 1.5)	(1, 1, 0.2, 0.9)	(2, 3, 0.4, 0.8)	(3, 1.2, 0.8, 1.5)	(0.4, 0.2, 1, 2)
$\mu_1^{'}$	0.44431	0.17564	0.21448	0.60806	0.14926
$\mu_2^{'}$	0.28101	0.06958	0.12327	0.50286	0.14075
$\mu_3^{'}$	0.21902	0.04434	0.12371	0.51011	0.17208
$\mu_4^{'}$	0.19687	0.03965	0.18929	0.60844	0.24533
$\mu_5^{'}$	0.19695	0.04618	0.41159	0.83411	0.39184
$\mu_6^{'}$	0.21481	0.06674	1.20954	1.29465	0.68564
SD	0.28913	0.19680	0.27797	0.36486	0.34419
CV	0.65073	1.12047	1.29601	0.60003	2.30597
CS	0.82234	2.42891	2.98560	0.87391	2.83748
Ck	3.37007	12.34781	18.5636	4.12879	11.39373

The findings in Table 3.1 indicate that the BIIIW distribution displays positive skewness and exhibits a range of kurtosis characteristics, including platykurtic, mesokurtic, and leptokurtic behaviors. The s^{th} incomplete moment is given

by,

$$\begin{aligned}\phi_s(t) &= \int_0^t x^s f(x)dx \\ &= k\sum_{m=0}^{\infty}\frac{(-1)^m}{a^{(mb)}m!}B_{(1+t^{-c})^{-1}}\left(k+\frac{s}{c}+\frac{mb}{c},1-\frac{s}{c}-\frac{mb}{c}\right)+a^s\gamma\left(\frac{s}{b}+1,\left(\frac{t}{a}\right)^b\right) \\ &- a^{s-cp}\sum_{p=0}^{\infty}(-1)^p\binom{k+p-1}{p}\gamma\left(1+\frac{s}{b}-\frac{cp}{b},\left(\frac{t}{a}\right)^b\right), \qquad (3.6)\end{aligned}$$

where $B_u(\alpha,\beta)=\int_0^u x^{\alpha-1}(1-x)^{\beta-1}dx$ and $\gamma(\alpha,t)=\int_0^t x^{\alpha-1}e^{-x}dx$ denotes the incomplete beta and lower incomplete gamma function.

3.3.3 Mean Deviation

Measuring the deviations from the mean and from the median, helps to determine how much spread there is in a population. The mean deviations of X about mean $\mu=E(X)$ and median M can be expressed ,

$$\delta_1(X) = \int_0^{\infty} \mid x-\mu \mid dF(x|c,k,a,b),$$

and

$$\delta_2(X) = \int_0^{\infty} \mid x-M \mid dF(x|c,k,a,b).$$

The following results can be used to evaluate the quantities $\delta_1(X)$ and $\delta_2(X)$.

$$\begin{aligned}\delta_1(x) &= 2\left[\mu F(\mu)-\int_0^{\mu}xf(x)dx\right]=2\left[\mu F(\mu)-\phi_s(\mu)\right], \\ \delta_2(x) &= \mu-2\int_0^{M}xf(x)dx=\mu-2\phi_s(M),\end{aligned}$$

where $\phi_s(t)=\int_0^t xf(x)dx$ given in (3.6).

3.3.4 Inequality Measures

The Lorenz and Bonferroni curves initially developed as inequality measures in economics are widely utilized to visually depict the distribution of income or wealth within a specific population. In addition to representing the distribution

of income and wealth, the Lorenz and Bonferroni curves can also be employed to illustrate the distribution of assets. The Lorenz curve offers a comprehensive view of inequality or concentration across the entire distribution, providing insights into how wealth or resources are spread across a population. In contrast, the Bonferroni curve focuses on the lower tail of the distribution, shedding light on the segment of the population with the least wealth or income. Together, these curves help economists understand different aspects of inequality and asset distribution. These curves are also widely applied in industries such as reliability, healthcare, and insurance, where they assist in analyzing statistical distributions. Then Lorenz and Bonferroni curve are given by,

$$B(p) = \frac{1}{p\mu} I(q) \quad \text{and} \quad L(p) = \frac{1}{\mu} I(q),$$

where $I(q) = \int_0^q x f(x) dx$ and $q = F^{-1}(p)$ for $0 \leq p \leq 1$.

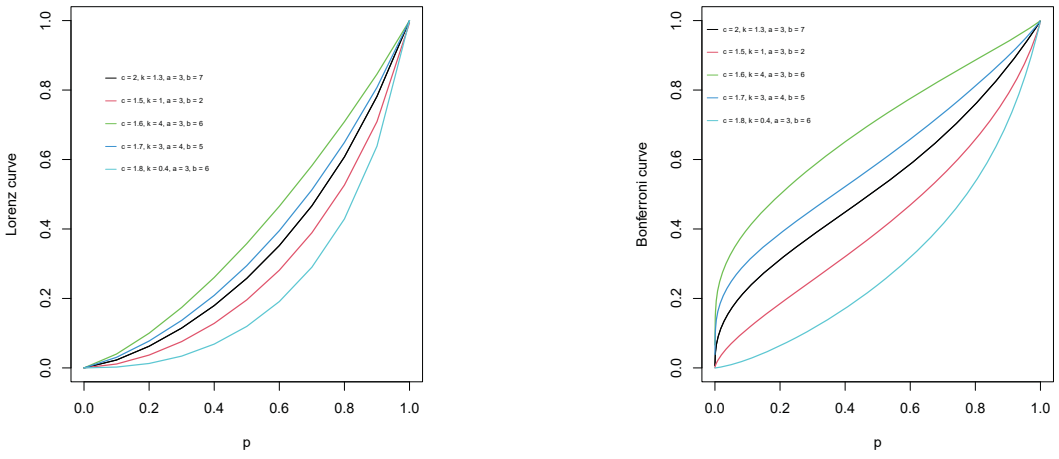

Figure 3.3: Plot of Lorenz and Bonferroni curves of BIIIW distribution.

Figure 3.3 presents the Lorenz and Bonferroni curves for various parameter values, illustrating the distributional inequality under different scenarios.

3.4 Order Statistics

The density function $f_{i:m}(x)$ of the i^{th} order statistic for $i = 1, 2, 3, \ldots, m$ from i.i.d random variables $X_1, X_2, \ldots, X_m$ following BIIIW distribution is given by,

$$\begin{aligned} f_{i:m}(x) &= \frac{m! f_{BIIIW}(x)}{(i-1)!(m-i)!}[F_{BIIIW}(x)]^{i-1}[1-F_{BIIIW}(x)]^{m-i} \\ &= \frac{m! f_{BIIIW}(x)}{(i-1)!(m-i)!}\sum_{j=0}^{m-i}(-1)^j\binom{m-i}{j}[F_{BIIIW}(x)]^{j+i-1} \end{aligned} \tag{3.7}$$

Using the binomial expansion $[1-F(x)]^{m-i} = \sum_{j=0}^{m-i}\binom{m-i}{j}(-1)^j[F(x)]^j$ and the PDF and CDF of BIIIW distribution in (3.7) we have,

$$\begin{aligned} f_{i:m}(x) &= \frac{m! f_{BIIIW}(x)}{(i-1)!(m-i)!}\sum_{j=0}^{m-i}(-1)^j\binom{m-i}{j}\left(1-\left[1-\left(1+x^{-c}\right)^{-k}\right]\left[e^{-\left(\frac{x}{a}\right)^b}\right]\right)^{j+i-1} \\ &= \sum_{j=0}^{m-i}(-1)^j\frac{m!}{(i-1)!(m-i-j)!(j)!}\left(1-\left[1-\left(1+x^{-c}\right)^{-k}\right]\left[e^{-\left(\frac{x}{a}\right)^b}\right]\right)^{j+i-1} \\ &\times\ e^{-\left(\frac{x}{a}\right)^b}\left(ck\left(1+x^{-c}\right)^{-k-1}x^{-c-1}+\frac{b}{a^b}x^{b-1}\left(1-\left(1+x^{-c}\right)^{-k}\right)\right). \end{aligned}$$

The PDF of the 1^{st} and n^{th} order statistic is given by,

$$\begin{aligned} f_{1:m}(x) &= \sum_{j=0}^{m-1}(-1)^j\frac{m!}{(m-1-j)!(j)!}\left(1-\left[1-\left(1+x^{-c}\right)^{-k}\right]\left[e^{-\left(\frac{x}{a}\right)^b}\right]\right)^{j} \\ &\times\ e^{-\left(\frac{x}{a}\right)^b}\left(ck\left(1+x^{-c}\right)^{-k-1}x^{-c-1}+\frac{b}{a^b}x^{b-1}\left(1-\left(1+x^{-c}\right)^{-k}\right)\right). \end{aligned} \tag{3.8}$$

$$\begin{aligned} f_{n:m}(x) &= \sum_{j=0}^{m-n}(-1)^j\frac{m!}{(n-1)!(m-n-j)!(j)!}\left(1-\left[1-\left(1+x^{-c}\right)^{-k}\right]\left[e^{-\left(\frac{x}{a}\right)^b}\right]\right)^{j+n-1} \\ &\times\ e^{-\left(\frac{x}{a}\right)^b}\left(ck\left(1+x^{-c}\right)^{-k-1}x^{-c-1}+\frac{b}{a^b}x^{b-1}\left(1-\left(1+x^{-c}\right)^{-k}\right)\right). \end{aligned} \tag{3.9}$$

3.5 Rényi Entropy

The Rényi entropy of the BIIIW distribution is determined in this section. An entropy is a measure of uncertainty or variation of a random variable. Rényi entropy is an extension of Shannon entropy. In the case of BIIIW distribution

Rényi entropy is defined to be

$$I_R(v) = \frac{1}{1-v}\log\left(\int_0^\infty [f_{BIIIW}(x;c,k,a,b)]^v dx\right), v \neq 1, v > 0.$$

Rényi entropy tends to Shannon entropy as $v \to 1$. Note that $[f(x;c,k,a,b)]^v = f^v_{BIIIW}(x)$ can be written as ,

$$\begin{aligned} f^v_{BIIIW}(x) &= e^{-v(x/a)^b}\left[ck\left(1+x^{-c}\right)^{-k-1}x^{-c-1} + \frac{b}{a^b}x^{b-1}\left(1-\left(1+x^{-c}\right)^{-k}\right)\right]^v \\ &= \sum_{j=0}^{\infty}\frac{(-1)^j v^j (\frac{x}{a})^{bj}}{j!}\left[ckx^{-c-1}(1+x^{-c})^{-k-1} + \frac{b}{a^b}x^{b-1}\left(1-(1+x^{-c})^{-k}\right)\right]^v \\ &= \sum_{j=0}^{\infty}\sum_{p=0}^{v}\sum_{w=0}^{p}\frac{(-1)^{j+w}v^j b^p}{a^{(bj+bp)}j!}(ck)^{v-p}\binom{v}{p}\binom{p}{w}x^{bj+cp+p-cv-v+pb-p} \\ &\times (1+x^{-c})^{kp+p-kv-v-kw}. \end{aligned}$$

Now,

$$\begin{aligned} \int_0^\infty f^v_{BIIIW}(x)dx &= \sum_{j=0}^{\infty}\sum_{p=0}^{v}\sum_{w=0}^{p}\frac{(-1)^{j+w}v^j b^p}{a^{(bj+pb)}j!}(ck)^{v-p}\binom{v}{p}\binom{p}{w} \\ &\times \int_0^\infty x^{bj+cp+p-cv-v+pb-p}(1+x^{-c})^{kp+p-kv-v-kw}dx. \end{aligned}$$

Put $u = (1+x^{-c})^{-1}$,

$$\begin{aligned} \int_0^\infty f^v_{BIIIW}(x)dx &= \sum_{j=0}^{\infty}\sum_{p=0}^{v}\sum_{w=0}^{p}\frac{(-1)^{j+w}v^j\ b^p}{a^{(bj+pb)}\ j!}\ (ck)^{v-p}\ \binom{v}{p}\ \binom{p}{w}\ \frac{1}{c} \\ &\times \int_0^\infty u^{\gamma-1}(1-u)^{\delta-1}du, \\ &= \sum_{j=0}^{\infty}\sum_{p=0}^{v}\sum_{w=0}^{p}\frac{(-1)^{j+w}\ v^j\ b^p}{a^{(bj+pb)}\ j!}\ (ck)^{v-p}\ \binom{v}{p}\ \binom{p}{w}\ \frac{1}{c} \times B(\gamma,\delta), \end{aligned}$$

where

$$\begin{aligned} \gamma &= \frac{1}{c}(pb+bj+cp-cv-v) + \frac{1}{c} - kp - p + kv + v + kw, \\ \delta &= \frac{1}{c}(cv+v-pb-bj-cp) - \frac{1}{c}. \end{aligned}$$

Then,

$$I_R(v) = \frac{1}{1-v}\log\left(\sum_{j=0}^{\infty}\sum_{p=0}^{v}\sum_{w=0}^{p}\frac{(-1)^{j+w}\ v^j\ b^p}{a^{(bj+pb)}\ j!}\ (ck)^{v-p}\ \binom{v}{p}\ \binom{p}{w}\ \frac{1}{c}B(\gamma,\delta)\right), \tag{3.10}$$

for $v \neq 1$ abd $v > 0$.

3.6 Characterizations Based on Two Truncated Moments

The characterization of probability distributions plays a vital role in statistical studies, serving as a crucial tool to evaluate whether a proposed model meets the requirements of a given distribution. The characterization using truncated moments, as proposed by Glänzel (1987), limits the observations, thereby saving both time and cost. The proposed characterization may benefit those working in the fields of natural and applied sciences.

Theorem 3. *Let (Ω, $\mathcal{F}$, $\mathcal{P}$) be a given probability space and let $H = [a, b]$ be an interval for some $a < b$ ($a = -\infty$, $b = \infty$ might as well be allowed). Let X: $\Omega \to H$ be a continuous random variable with the distribution function F and let Q_1 and Q_2 be two real functions defined on H such that*

$$E[Q_2(X)|X \geq x] = E[Q_1(X)|X \geq x]\xi(x), \quad x \in H$$

is defined with some real function ξ. Assume that $Q_1, Q_2 \in C^1(H)$, $\xi \in C^2(H)$ and F is twice continuously differentiable and strictly monotone function on the set H. Finally, assume that the equation $\xi Q_1 = Q_2$ has no real solution in the interior of H. Then F is uniquely determined by the functions Q_1, Q_2 and ξ, particularly

$$F(x) = \int_a^x C\Big|\frac{\xi^{'}(u)}{\xi(u)Q_1(u) - Q_2(u)}\Big|\exp(-s(u))du,$$

where the function s is a solution of the differential equation $s^{'} = \frac{\xi^{'}Q_1}{\xi Q_1 - Q_2}$ and C is the normalization constant, such that $\int_H dF = 1$.

Proposition 1. *Let X:* $\Omega \to$ *(0,*∞*) be a continuous random variable and let* $Q_1(x)$ = $e^{-\left(\frac{x}{a}\right)^b} \frac{bx^{b-1}}{a^b} \left[ck(1+x^{-c})^{-(k+1)}x^{-(c+1)} + \frac{b}{a^b}x^{b-1}(1-(1+x^{-c})^{-k})\right]^{-1}$ *and* $Q_2(x)$= $Q_1 e^{-\left(\frac{x}{a}\right)^b}$ *for* $x > 0$*. The random variable X then contains PDF* (3.2) *if and only if the function* ξ *has the form*

$$\xi(x) = \frac{2}{3}e^{-\left(\frac{x}{a}\right)^b}, x > 0.$$

Proof. Consider of X as a random variable with PDF (3.2), then

$$(1-F(x))E[Q_1(x)|X \geq x] = \frac{1}{2}e^{-2\left(\frac{x}{a}\right)^b}, x > 0.$$

and

$$(1-F(x))E[Q_2(x)|X \geq x] = \frac{1}{3}e^{-3\left(\frac{x}{a}\right)^b}, x > 0.$$

and so,

$$\xi(x)Q_1(x) - Q_2(x) = -\frac{1}{3}e^{-\left(\frac{x}{a}\right)^b}Q_1(x) \neq 0 \text{ for } x > 0.$$

Conversely, if ξ has the above form, then

$$s^{'}(x) = \frac{\xi^{'}(x)Q_1(x)}{\xi(x)Q_1(x) - Q_2(x)} = \frac{2bx^{b-1}}{a^b}.$$

and hence

$$s = 2\left(\frac{x}{a}\right)^b, x > 0.$$

Now, in view of Theorem 3, X has density (3.2). □

Corollary 1. *Let X:* $\Omega \to (0,\infty)$ *be a continuous random variable and let* $Q_1(x)$ *be as in Proposition 1. The PDF of X is* (3.2) *if and only if there exist functions* Q_2 *and* ξ *defined in Theorem 3 satisfying the differential equation,*

$$\frac{\xi^{'}(x)Q_1(x)}{\xi(x)Q_1(x) - Q_2(x)} = \frac{2bx^{b-1}}{a^b}. \tag{3.11}$$

The general solution of the differential equation given in Corollary 1 is

$$\xi(x) = e^{2\left(\frac{x}{a}\right)^b}\left[-\int \frac{2bx^{b-1}}{a^b}e^{-2\left(\frac{x}{a}\right)^b}(Q_1(x))^{-1}Q_2(x)dx + D\right]$$

where D is a constant. Note that a set of functions satisfying the above differential

equation is given in Proposition 1 with D = 0. It should be noted that more triplets (Q_1, Q_2, ξ) exist that meet Theorem 3 requirements.

3.7 Autoregressive Time Series Modeling

The autoregressive model represents a stochastic process commonly employed in statistical modeling, where future values are predicted based on a weighted combination of previous values. This concept is grounded in the belief that past values influence current outcomes. Gaver and Lewis (1980) introduced a first-order autoregressive time series model characterized by an exponential stationary marginal distribution. In recent years, various researchers, including Jayakumar and Babu (2015) and Gillariose and Tomy (2023), have created different autoregressive models incorporating minification structures. Here we analyse the first order autoregressive (AR(1)) minification process using the BIIIW distribution as the marginal distribution.

Consider the structure of an AR(1) minification process,

$$X_n = \begin{cases} \xi_n \quad \text{with} \quad \text{probability } \delta \\ min(X_{n-1,\ \xi_n}) \text{ with} \quad \text{probability} \quad 1-\delta,\ 0<\delta<1,\ n \geq 1 \end{cases} \tag{3.12}$$

where $\{\xi_n\}$ is a sequence of i.i.d random variables.

Marshall and Olkin (1997) introduced a new generalized distribution family, known as the Marshall-Olkin (MO) family, by incorporating an additional parameter into an existing distribution family $H(x)$. Hence, the survival function takes the form:

$$\bar{F}(x;\alpha) = \frac{\alpha \bar{H}(x)}{1-\bar{\alpha}\bar{H}(x)}, -\infty < x < \infty,\ \alpha > 0.$$

We require the following definition to create the time series model with BIIIW marginal distribution,

Definition 1. *A random variable X on (0,∞) is said to have MO Burr III Weibull*

distribution $X \stackrel{d}{=}$ MOBIIIW(α, c, k, a, b) , if it has the survival function,

$$\begin{aligned}\bar{F}_X(x) &= \frac{\alpha\left[(1-(1+x^{-c})^{-k})e^{-\left(\frac{x}{a}\right)^b}\right]}{1-(1-\alpha)\left[(1-(1+x^{-c})^{-k})e^{-\left(\frac{x}{a}\right)^b}\right]} \\ &= \frac{1}{1+\frac{1}{\alpha}\left\{\left[(1-(1+x^{-c})^{-k})e^{-\left(\frac{x}{a}\right)^b}\right]^{-1}-1\right\}}. \end{aligned} \tag{3.13}$$

Theorem 4. *In an AR (1) process with structure* (3.12) *describes an AR(1) stationary minification process if and only if $\{\xi_n\}$'s are i.i.d MOBIIIW(δ^{-1}, c, k, a, b) with $X_0 \stackrel{d}{=}$ BIIIW(c, k, a, b).*

Proof. In terms of survival function, the model (3.12) is,

$$P(X_n > x) = P(\xi_n > x)[\delta + (1-\delta)P(X_{n-1} > x)].$$

Hence

$$\bar{F}_{X_n}(x) = \bar{F}_{\xi_n}(x)[\delta + (1-\delta)\bar{F}_{X_{n-1}}(x)]. \tag{3.14}$$

If $\{X_n\}$ is stationary with BIIIW marginals, then,

$$\begin{aligned}\bar{F}_{\xi_n}(x) &= \frac{\bar{F}_X(x)}{\delta+(1-\delta)\bar{F}_X(x)} \\ &= \frac{[1-(1+x^{-c})^{-k}]e^{-\left(\frac{x}{a}\right)^b}}{\delta+(1-\delta)[1-(1+x^{-c})^{-k}]e^{-\left(\frac{x}{a}\right)^b}} \\ &= \frac{1}{1+\delta\left\{\left([1-(1+x^{-c})^{-k}]e^{-\left(\frac{x}{a}\right)^b}\right)^{-1}-1\right\}}. \end{aligned}$$

That is, $\xi_n^{'}s$ are i.i.d MOBIIIW(δ^{-1}, c, k, a, b).

Conversely, if $\xi_n's$ are i.i.d MOBIIIW(δ^{-1}, c, k, a, b) with $X_0 \stackrel{d}{=}$ BIIIW(c, k, a, b), then

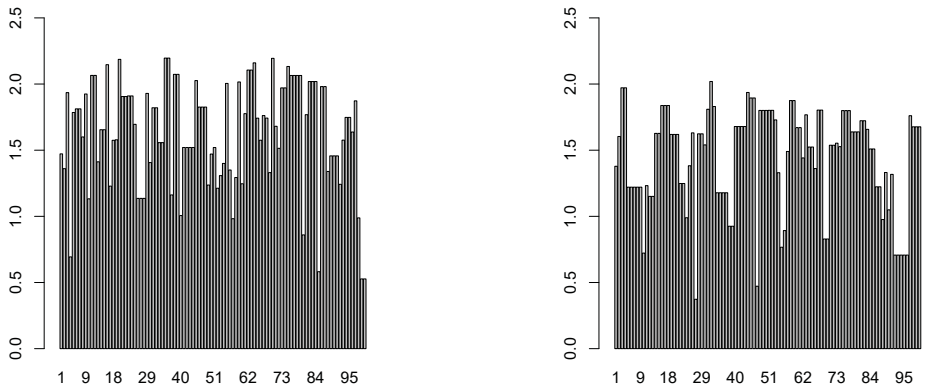

Figure 3.4: Sample path for AR(1) Minification process for $c = 1$, $k = 3$, $a = 2$, $b = 3$ and $\delta = 0.6, 0.7$.

from (3.14), we have,

$$\begin{aligned}
\bar{F}_{X_1}(x) =& \bar{F}_{\xi_1}(x)[\delta + (1-\delta)\bar{F}_{X_0}(x)] \\
=& \delta \left\{ \frac{1}{1+\delta\left\{\left([1-(1+x^{-c})^{-k}]e^{-\left(\frac{x}{a}\right)^b}\right)^{-1} - 1\right\}} \right\} \\
&+(1-\delta)\left\{ \frac{[1-(1+x^{-c})^{-k}]e^{-\left(\frac{x}{a}\right)^b}}{1+\delta\left\{\left([1-(1+x^{-c})^{-k}]e^{-\left(\frac{x}{a}\right)^b}\right)^{-1} - 1\right\}} \right\} \\
=& \left[1-(1+x^{-c})^{-k}\right] e^{-\left(\frac{x}{a}\right)^b}.
\end{aligned}$$

Then $X_1 \stackrel{d}{=}$ BIIIW(c, k, a, b). Assuming $X_{n-1} \stackrel{d}{=}$ BIIIW(c, k, a, b), we can establish by induction that $X_n \stackrel{d}{=}$ BIIIW(c, k, a, b). As a result, we can infer that the sequence $\{X_n\}$ is stationary with BIIIW marginals. The sample path characteristics of the AR(1) models presenting an overview of their distinct characteristics are described in Figure 3.4. □

3.8 ML Estimation

To estimate the unknown parameters of the BIIIW distribution, we utilize the MLE method, which is widely accepted as the most suitable approach. This

method provides the most comprehensive information regarding the properties of the estimated parameters. The log-likelihood function, (L) for an BIIIW model with a random sample of size n say $x_1, x_2, \ldots, x_n$ is as follows,

$$L = -\sum_{i=1}^{n} \left(\frac{x_i}{a}\right)^b + \sum_{i=1}^{n} \ln \left[ck(1+x_i^{-c})^{-(k+1)} x_i^{-(c+1)} + \frac{b}{a^b} x_i^{b-1}(1-(1+x_i^{-c})^{-k}) \right] \quad (3.15)$$

Let $\Theta = (c, k, a, b)'$ represent the parameter vector of interest, then the corresponding score function U is given by,

$$U = \left(\frac{\partial L}{\partial c}, \frac{\partial L}{\partial k}, \frac{\partial L}{\partial a}, \frac{\partial L}{\partial b}\right)',$$

where $\frac{\partial l}{\partial c}, \frac{\partial L}{\partial k}, \frac{\partial L}{\partial a}, \frac{\partial L}{\partial b}$ are the partial derivatives of the log-likelihood function w.r.t. to each parameter and are given by,

$$\begin{aligned}\frac{\partial L}{\partial c} =& \sum_{i=1}^{n} \frac{1}{Z(x_i)} \{ ck(k+1)x_i^{-2c-1}(1+x_i^{-c})^{-k-2} \ln(x_i) - ckx_i^{-(c+1)}(1+x_i^{-c})^{-k-1} \ln(x_i) \\ &+ kx_i^{-(c+1)}(1+x_i^{-c})^{-(k+1)} - kba^{-b}x_i^{-c+b-1}(1+x_i^{-c})^{-(k+1)} \ln(x_i) \},\end{aligned}$$

$$\begin{aligned}\frac{\partial L}{\partial k} =& \sum_{i=1}^{n} \frac{1}{Z(x_i)} \{ cx_i^{-(c+1)}(1+x_i^{-c})^{-(k+1)} - ckx_i^{-(c+1)}(1+x_i^{-c})^{-(k+1)} \ln(1+x_i^{-c}) \\ &+ ba^{-b}x^{b-1}(1+x_i^{-c})^{-k} \ln(1+x_i^{-c}) \},\end{aligned}$$

$$\begin{aligned}\frac{\partial L}{\partial b} =& \sum_{i=1}^{n} \frac{1}{Z(x_i)} \{ a^{-b}x_i^{b-1} \ln(x_i) b - x_i^{b-1} ba^{-b} \ln(a) - x_i^{b-1} \ln(x_i) ba^{-b}(1+x_i^{-c})^{-k} \\ &+ x_i^{b-1} ba^{-b} \ln(a)(1+x_i^{-c})^{-k} + x_i^{b-1}a^{-b} - x_i^{b-1}a^{-b}(1+x_i^{-c})^{-k} \} \\ &+ \sum_{i=1}^{n} \frac{\ln(a)x_i^b - \ln(x_i)x_i^b}{a^b},\end{aligned}$$

$$\frac{\partial L}{\partial a} = \sum_{i=1}^{n} \frac{1}{Z(x_i)} \{ b^2 x_i^{b-1} a^{-b-1}(1+x_i^{-c})^{-k} - b^2 x_i^{b-1} a^{-b-1} \} + \sum_{i=1}^{n} bx_i^b a^{-b-1},$$

where $Z(x_i) = ck(1+x_i^{-c})^{-(k+1)}x_i^{-(c+1)} + \frac{b}{a^b}x_i^{b-1}(1-(1+x_i^{-c})^{-k})$.

The MLE's are then obtained by solving $U(\Theta) = 0$, for each parameter. Iterative techniques, such as the Newton-Raphson algorithm, can be employed in statistical software to numerically solve equations that lack analytical solutions. The asymptotic distribution of $(\hat{\Theta} - \Theta)$ is given as

$$\sqrt{n}(\hat{\Theta} - \Theta) \sim N_4(0, I(\Theta)^{-1}),$$

where $I(\Theta)$ is the expected information matrix. The mentioned asymptotic behavior remains valid when we replace the expected information matrix $I(\Theta)$ with the observed information matrix $J(\hat{\Theta})$, where $\hat{\Theta}$ represents the estimated parameter values. We can utilize the multivariate normal distribution $N_4(0, J(\hat{\Theta})^{-1})$ to create approximate confidence intervals for the parameters.

3.9 Simulation Study

In this section, we evaluate the accuracy of the MLE's of the BIIIW parameters by employing Monte Carlo simulations. The simulation study is conducted by repeating the process 1000 times, with sample sizes of 100, 200, 400, 500, 800 and 1000 from the BIIIW model, considering different combinations of c, k, a, b. Two different parameter combinations are considered: $I : c = 2, k = 3, a = 5, b = 7$, $II : c = 9, k = 7, a = 2, b = 3$. The estimators performance for the unknown parameters of the BIIIW distribution is compared using Bias and Root Mean Squared Error (RMSE).

$$\begin{aligned} Bias &= \frac{1}{N}\sum_{i=1}^{N}(\hat{\Theta} - \Theta), \\ RMSE &= \sqrt{\frac{1}{N}\sum_{i=1}^{N}(\hat{\Theta} - \Theta)^2}. \end{aligned}$$

The estimates, average bias (Bias), RMSE, coverage probability (CP) and average length of confidence interval (AL) of 95% asymptotic confidenc values of the parameters for various sample sizes are shown in Table 3.2. We may infer from the results of Table 3.2 that the Bias and RMSEs decreases with increase

in sample size. Furthermore in each case, the lengths of the estimated confidence intervals decreases as sample sizes increases. The CP of the intervals are quite near to the nominal level of 95%.

Table 3.2: Simulation results: Estimates, Bias, RMSE, CP and AL.

		Set I					Set II				
Parameter	n	Estimates	Bias	RMSE	AL	CP	Estimates	Bias	RMSE	AL	CP
	100	2.0034	0.0034	0.1890	0.7374	0.9480	8.9674	-0.0326	1.0382	4.0904	0.960
c	200	2.0026	0.0026	0.1320	0.5048	0.947	8.9823	-0.0177	0.6861	2.7386	0.971
	400	2.0016	0.0016	0.0896	0.3534	0.945	8.9850	-0.0150	0.4733	1.8790	0.949
	500	1.9993	-0.0007	0.0800	0.3146	0.953	8.9820	-0.0180	0.4229	1.6702	0.956
	800	1.9995	-0.0005	0.0620	0.2477	0.964	8.9863	-0.0137	0.3170	1.3065	0.969
	1000	1.9985	-0.0015	0.0557	0.2212	0.962	8.9894	-0.0106	0.2805	1.1654	0.962
k	100	3.0654	0.0654	0.3509	1.2997	0.951	7.5673	0.5673	2.2225	7.6644	0.935
	200	3.0278	0.0278	0.2315	0.8830	0.953	7.2742	0.2742	1.2689	4.8623	0.965
	400	3.0160	0.016	0.1633	0.6183	0.949	7.1403	0.1403	0.8535	3.2896	0.949
	500	3.0119	0.0119	0.1439	0.5519	0.953	7.1150	0.1150	0.7299	2.9144	0.957
	800	3.0087	0.0087	0.1173	0.4356	0.939	7.0651	0.0651	0.5692	2.2630	0.954
	1000	3.0067	0.0067	0.1023	0.3892	0.938	7.0569	0.0569	0.5031	2.0182	0.958
a	100	4.9526	-0.0474	0.3553	1.1917	0.870	2.2686	0.2686	2.0779	3.8075	0.837
	200	4.9791	-0.0209	0.2351	0.8669	0.910	2.0644	0.0644	0.5150	1.4705	0.871
	400	4.9918	-0.0082	0.1597	0.6290	0.939	2.0110	0.0110	0.2355	0.906	0.917
	500	4.9920	-0.008	0.1477	0.5617	0.948	2.0084	0.0084	0.2114	0.8017	0.905
	800	4.9952	-0.0048	0.1126	0.4452	0.946	2.0058	0.0058	0.1613	0.6272	0.924
	1000	4.9942	-0.0058	0.0996	0.3987	0.958	2.0041	0.0041	0.1452	0.5578	0.929
b	100	10.4208	3.4208	14.1581	17.2737	0.938	3.2335	0.2335	0.9859	3.3253	0.899
	200	8.2049	1.2049	3.6873	9.422	0.949	3.1243	0.1243	0.6643	2.3343	0.913
	400	7.4599	0.4599	1.5881	5.8058	0.967	3.0755	0.0755	0.4363	1.6421	0.944
	500	7.3540	0.3540	1.4135	5.0612	0.959	3.0606	0.0606	0.3890	1.4632	0.937
	800	7.2101	0.2101	1.037	3.8420	0.949	3.0376	0.0376	0.3038	1.1547	0.945
	1000	7.1380	0.1380	0.8762	3.3744	0.948	3.0303	0.0303	0.2677	1.0304	0.941

3.10 Real Data Applications

In this section, we examine data analysis to bring out the importance and need of the BIIIW distribution in real-world data modelling. The usefulness of BIIIW is evaluated by analyzing the Covid-19 datasets. The first data set presents Covid-19 mortality rates for 59 days in Italy from February 27 to 27 April 2020 (Dataset-1). The second dataset which includes 108 observations indicates the mortality rate of patients during the Covid-19 pandemic in Mexico (Dataset-2). These datasets are also examined by Almongy et al. (2021) and Kilai et al. (2022). The datasets are given in Table 3.3 and 3.4. The third dataset represents the case fatality ratio (CFR) expressed in % of India, from 1st February to 1st April of year 2022 due to Covid-19. The data was collected from the site [https://covid19.who.int/ and is presented in Table 3.5.

Table 3.3: Covid-19 Mortality Rates in Italy

4.571	7.201	3.606	8.479	11.41	8.961	10.919	10.908	6.503	18.474
11.01	17.337	16.561	13.226	15.137	8.697	15.787	13.333	11.822	14.242
11.273	14.33	16.046	11.95	10.282	11.775	10.138	9.037	12.396	10.644
8.646	8.905	8.906	7.407	7.445	7.214	6.194	4.64	5.452	5.073
4.416	4.859	4.408	4.639	3.148	4.04	4.253	4.011	3.564	3.827
3.134	2.78	2.881	3.341	2.686	2.814	2.508	2.45	1.518	

Table 3.4: Covid-19 Mortality Rates in Mexico

8.826	6.105	10.383	7.267	13.22	6.015	10.855	6.122	10.685	10.035
5.242	7.63	14.604	7.903	6.327	9.391	14.962	4.73	3.215	16.498
11.665	9.284	12.878	6.656	3.44	5.854	8.813	10.043	7.26	5.985
4.424	4.344	5.143	9.935	7.84	9.55	6.968	6.37	3.537	3.286
10.158	8.108	6.697	7.151	6.56	2.988	3.336	6.814	8.325	7.854
8.551	3.228	3.499	3.751	7.486	6.625	6.14	4.909	4.661	1.867
2.838	5.392	12.042	8.696	6.412	3.395	1.815	3.327	5.406	6.182
4.949	4.089	3.359	2.070	3.298	5.317	5.442	4.557	4.292	2.5
6.535	4.648	4.697	5.459	4.12	3.922	3.219	1.402	2.438	3.257
3.632	3.233	3.027	2.352	1.205	2.077	3.778	3.218	2.926	2.601
2.065	1.041	1.800	3.029	2.058	2.326	2.506	1.923		

Table 3.5: Covid-19 CFR data (in %) of India

1.067	1.757	1.705	1.849	1.131	1.595	1.524	1.014	1.266
1.678	1.758	1.898	1.459	3.37	1.283	1.753	1.84	2.134
2.293	2.217	2.365	1.485	2.603	2.952	2.164	3.142	4.88
2.885	1.513	2.704	3.169	2.485	6.08	2.462	1.508	1.078
3.777	3.407	2.363	5.893	3.421	7.211	2.001	2.087	3.487
3.457	4.925	2.469	10.48	2.514	2.779	2.514	2.285	3.895

The descriptive statistics for the Covid-19 datasets are shown in Table 3.6. The positive skewness value indicates that all the dataset is right-skewed. Also, the first dataset exhibits platykurtic behaviours, whereas the second and third dataset demonstrates leptokurtic characteristics.

Table 3.6: Descriptive statistics for Covid-19 data.

	Mean	Median	Standard Deviation	Skewness	Kurtosis
Dataset-1	8.1577	7.445	4.5258	0.452	2.129
Dataset-2	5.7580	5.1925	3.2541	0.9866	3.6813
Dataset-3	2.7227	2.328	1.6844	2.3610	7.0372

The total time on test (TTT) transform plot appears with a concave shape in Figure 3.5, shows that all datasets exhibit an increasing failure rate. This confirms that the shape of the hazard function shown in Figure 3.2 is appropriate for modelling this kind of data. Thus, it is feasible to consider the BIIIW distribution as a suitable model for perfectly fitting these datasets.

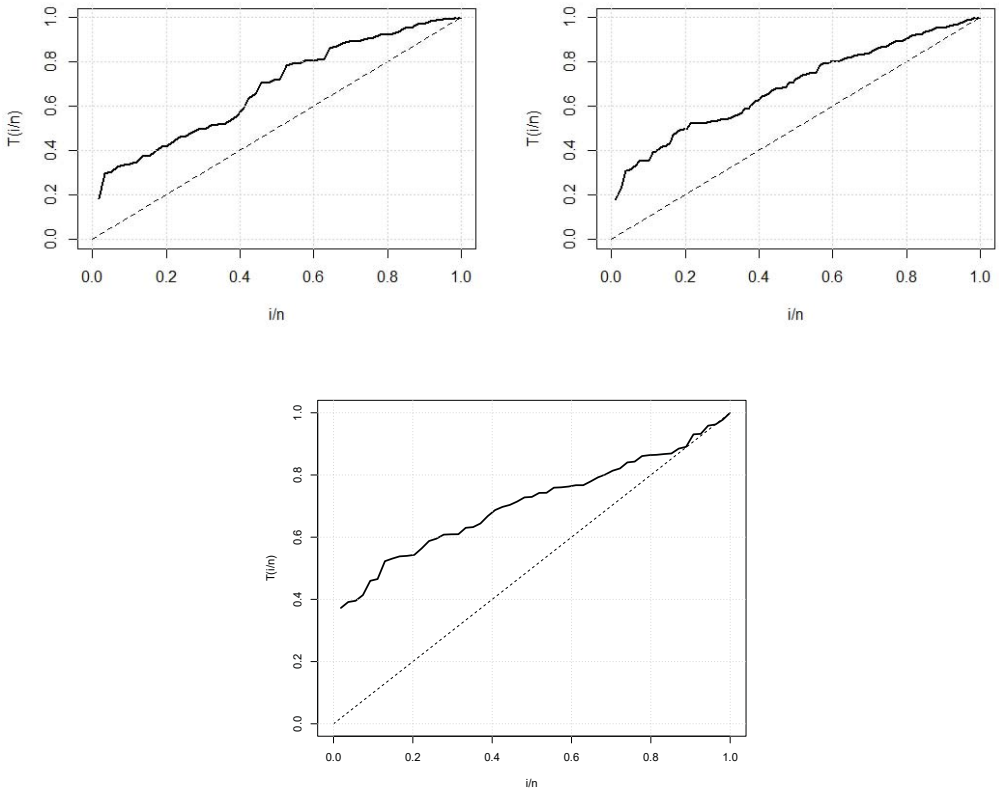

Figure 3.5: TTT-transform plot for (a) Italy mortality rates data (b) Mexico mortality rates data (c) CFR data.

The effectiveness of the Covid datasets for the BIIIW distribution is evaluated by comparing the fitting performance with other competing distributions namely Modified Burr III (MBIII, Jamal et al. (2021)), Weibull Burr XII (WBXII, Nasir et al. (2018)), Weibull Rayleigh (WR, Ganji et al. (2016)), Weibull (W, 1951), Burr III (BIII, 1942), Inverse Lomax Weibull (ILW, Falgore and Doguwa (2020)) and Burr III Exponential (BIIIE, New). Similarly, the CFR dataset is compared with WBXII, WR, W and BIII distribution. The ML estimates of the parameters, the log-likelihood function, and values of the AIC, BIC, K-S statistic along with p - value for the BIIIW distribution are presented in Table 3.7, 3.8 and 3.9. Based on the comparison with various models, it can be determined that BIIIW has the lowest K-S value for all datasets while also having the highest log-likelihood and p - value. As a result, we could conclude that the proposed distribution provides a better fit compared to the other competing

models.

Table 3.8: MLE's, Log-likelihood, information criteria and GoF statistics for Mexico Covid-19 mortality rates data

	Parameters	Est	K-S	p - value	L	AIC	BIC
BIIIW	c	1.4354	0.0470	0.9706	-264.8797	537.7593	548.4878
	k	8.8005					
	b	2.8598					
	a	10.6226					
MBIII	c	0.7552	0.0626	0.7903	-266.223	538.447	546.4930
	k	8.9809					
	l	0.2623					
WBXII	c	1.57396	0.0677	0.7039	-265.936	539.871	550.6000
	k	0.1805					
	α	10.0314					
	β	3.5762					
WR	b	2.3729	0.0735	0.6026	-268.955	543.9108	551.9571
	c	0.9484					
	γ	3.7757					
W	β	1.8968	0.0735	0.5769	-268.955	541.911	547.2750
	λ	6.5209					
BIII	c	1.8068	0.0844	0.4026	-275.213	554.426	559.7900
	k	11.1672					
ILW	α	3.2661	0.0588	0.8482	-265.4865	538.973	549.7016
	λ	0.0581					
	β	0.2394					
	θ	1.5480					
BIIIE	c	1.9445	0.0904	0.34	-273.39	552.7789	560.8253
	k	16.6744					
	λ	42.2097					

Table 3.7: MLE's, Log-likelihood, information criteria and GoF statistics for Italy Covid-19 mortality rates data.

Model	Parameters	Estimates	K-S	p - value	L	AIC	BIC
BIIIW	c	1.3796	0.0779	0.8391	-163.0456	334.0911	342.4013
	k	11.3024					
	b	5.4665					
	a	14.9756					
MBIII	c	0.7038	0.1130	0.4077	-168.2732	342.5463	348.7789
	k	348.7789					
	l	0.1754					
WBXII	c	0.4884	0.1208	0.328	-167.5412	343.082	351.3926
	k	0.1643					
	α	38072.8					
	β	7.0724					
WR	b	3.2380	0.1228	0.3092	-167.6974	341.3949	347.6275
	c	0.9639					
	γ	4.0666					
W	β	1.9278	0.1228	0.3092	-167.697	339.395	343.5500
	λ	9.2344					
BIII	c	1.6990	0.1457	0.1473	-173.549	351.097	355.2520
	k	16.2413					
ILW	α	1.8876	0.1075	0.4703	-167.4136	342.8273	351.1374
	λ	0.0266					
	β	0.4333					
	θ	1.6482					
BIIIE	c	1.7322	0.1490	0.1312	-173.1795	352.359	358.5916
	k	13.4835					
	λ	3.7507					

Table 3.9: MLE's, Log-likelihood, information criteria and GoF statistics for CFR data.

Model	Parameters	Estimates	K-S	p - value	L	AIC	BIC
BIIIW	c	2.6203	0.0541	0.9974	-79.4134	166.827	174.7829
	k	6.0785					
	b	315.703					
	a	10.4802					
WBXII	c	6.9948	0.0608	0.9882	-83.0607	174.1216	182.0775
	k	0.2551					
	α	0.3410					
	β	1.9008					
WR	b	1.8166	0.1397	0.2422	-94.3508	194.7016	200.6686
	c	0.8981					
	γ	1.4431					
W	β	1.7962	0.1397	0.2422	-94.3508	192.7016	196.6796
	λ	3.0863					
BIII	c	2.3800	0.0908	0.7647	-73.8779	151.7558	155.7338
	k	5.4730					

Fitting the histogram for Covid datasets (Figures 3.6) also illustrates the previously stated conclusions. The Likelihood Ratio (LR) statistic can be employed to compare certain specific models with the BIIIW model for Covid mortality datasets. The LR statistic, used to test the null hypothesis $H_0 : \theta_1 = \theta_1^0$ against the alternative hypothesis $H_1 : \theta_1 \neq \theta_1^0$, is defined as $w = 2[l(\hat{\theta})$ - $l(\tilde{\theta})]$, where $l(\hat{\theta})$ and $l(\tilde{\theta})$ represent the estimates under the null and alternative hypotheses, respectively. The distribution of the statistic w is asymptotically χ_k^2 (as $n \to \infty$), where k represents the difference between the number of independent parameters specified in the null hypothesis and the number of independent parameters specified in the alternative hypothesis. Table 3.10 compares the proposed model with a few of its sub-models using LR statistics. For the two tests performed on Dataset 1, we have enough evidence to reject the null hypothesis in favour of a wider distribution. The level of rejection is highly significant, providing strong evidence for the effectiveness of the shape parameters c and b in accurately representing real data. It is evident from the analysis of Dataset 2 that the BIIIW

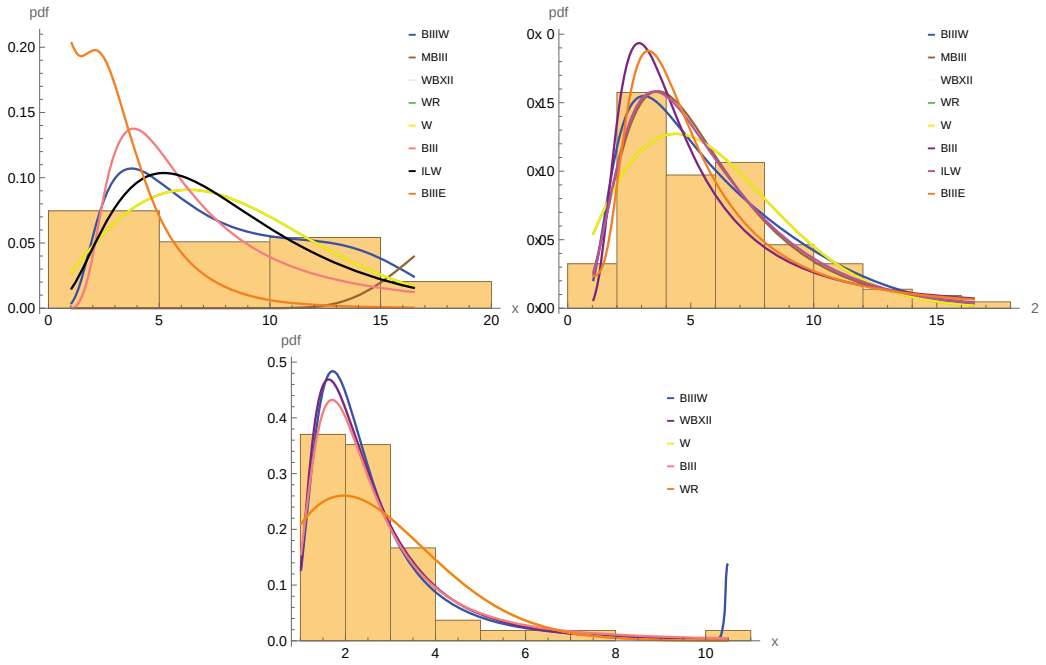

Figure 3.6: Fitted PDF for Italy, Mexico and CFR Covid 19 datasets.

model outperforms the BIIIE model. Furthermore, upon comparing the BIIIW and ILW models, we can conclude that the ILW model is the most suitable option for this particular dataset.

Table 3.10: LR statistic for Covid 19 datasets.

		Dataset1		Dataset2	
Comparison	Hypothesis	LR Statistic	p - value	LR Statistic	p - value
ILW vs BIIIW	H_0: c = 1 vs H_1: c $\neq$ 1	8.736	0.0031	1.2136	0.2706
BIIIE vs BIIIW	H_0: b = 1 vs H_1: b $\neq$ 1	20.2678	< 0.0001	17.02	< 0.0001

Figures 3.7 and 3.8 indicates the plot of profile log-likelihood function for the Covid mortality rate datasets. The P-P plot illustrating the fit of the BIIIW distribution for the entire dataset is presented in Figure 3.9. It is evident from Figure 3.9 how well the BIIIW model fits the data.

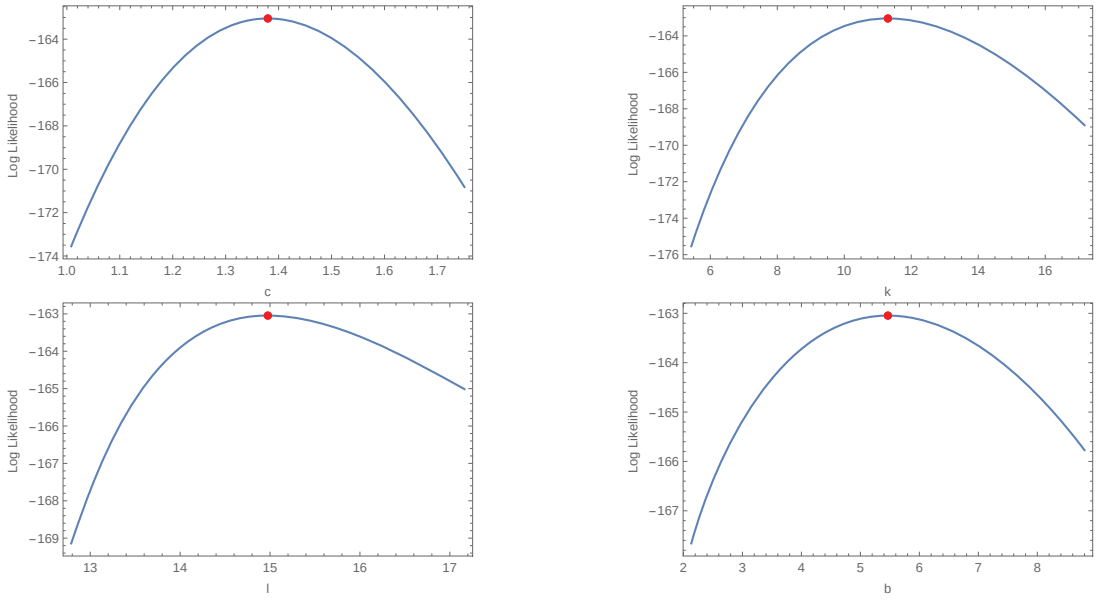

Figure 3.7: Log Likelihood curves of the BIIIW parameters for dataset 1

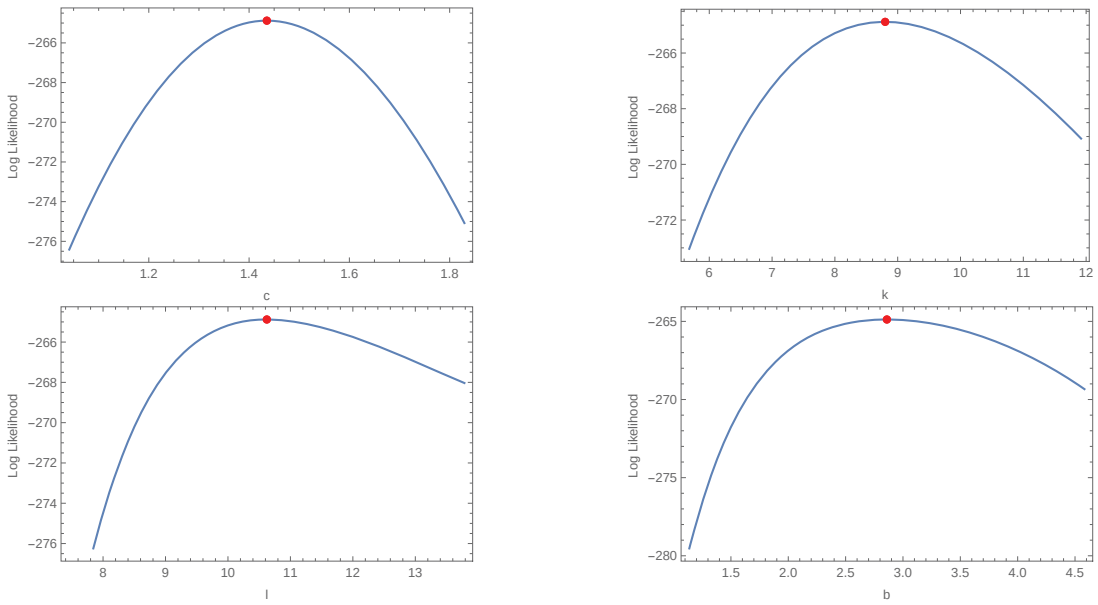

Figure 3.8: Log Likelihood curves of the BIIIW parameters for dataset 2

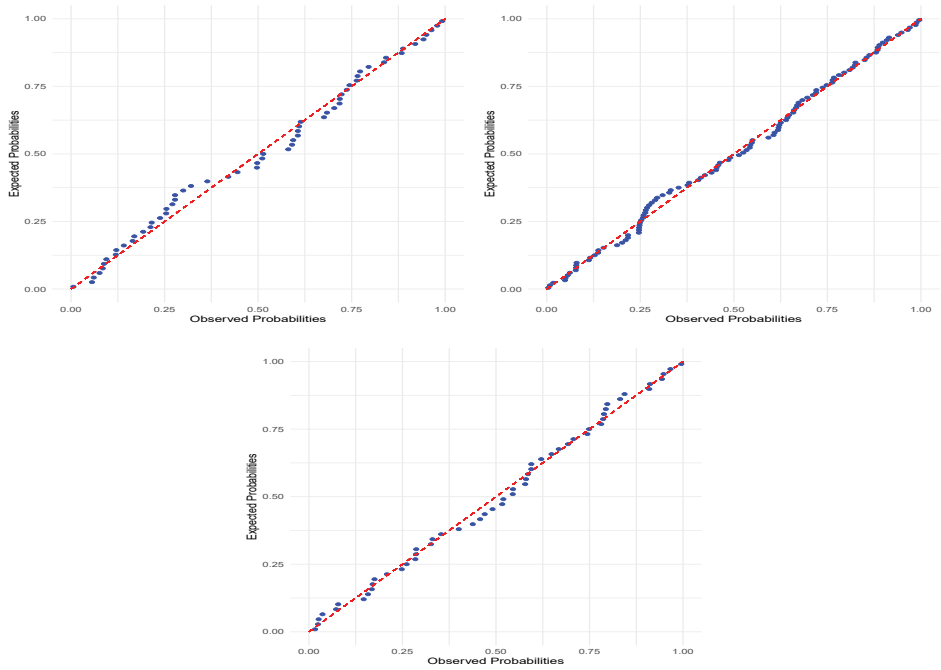

Figure 3.9: Probability Plots for (a) Italy Covid-19 mortality rates data (b) Mexico Covid-19 mortality rates data (c) CFR data.

3.11 Goodness-of-fit Test

When dealing with complete data, several methods are employed to evaluate how well mathematical models fit the observed data. The most often used tests are those based on Pearson's Chi-square statistics. However, these tests are not applicable in all scenarios, especially when the model's parameters are unknown or when the data is censored. Since the middle of the 20^{th} century, researchers have started proposing modifications to existing statistical methods to address both unknown parameters and data censoring. For complete data, Nikulin (1973) and Rao and Robson (1974) each independently developed a statistic that is now referred to as the N.R.R. statistic (Nikulin-Rao-Robson). This statistical test, which adheres to a χ^2 distribution, represents a natural extension of the Pearson statistic.

3.11.1 N.R.R. Statistic Test

To test the hypothesis H_0 that T_1, T_2,..., T_n, an n sample, originates from a parametric family $F(t;\theta)$,

$$H_0 : P\{T_i \leq t\} = F(t,\theta),\ t \in \mathbf{R},\ \theta = (\theta_{\mathbf{1}}, \theta_{\mathbf{2}}, \ldots, \theta_{\mathbf{s}})^{\mathbf{T}},$$

where θ denotes the vector of unknown parameters. Nikulin (1973) and Rao and Robson (1974) introduced Y^2, the N.R.R statistic, defined as follows:
Observations $T_1, T_2, \ldots, T_n$ are categorized into r mutually disjoint subintervals $\boldsymbol{I}_1, \boldsymbol{I}_2, \ldots, \boldsymbol{I}_r$, where $\boldsymbol{I}_j = (a_{j-1}, a_j]$ for $j = 1, \ldots, r$. The limits a_j of the intervals $\boldsymbol{I}_j$ are determined in such a way that,

$$p_j(\boldsymbol{\theta}) = \int_{a_{j-1}}^{a_j} f(t,\boldsymbol{\theta})\, dt \ \text{ for } j = 1, 2, \ldots, r,$$

and

$$a_j = F^{-1}\left(\frac{j}{r}\right)\Bigg|_{j=1,2,\ldots(r-1)}.$$

If $\nu_j = (\nu_1, \nu_2, \ldots, \nu_r)^T$ represents the frequency vector resulting from grouping the data into these $\boldsymbol{I}_j$ intervals.

$$\nu_j = \sum_{i=1}^{n} 1_{t_i \in \mathbf{I_j}}\Big|_{(j=1,\ldots,r)}.$$

Then the N.R.R statistic is given by,

$$Y^2(\hat{\boldsymbol{\theta}}_n) = \chi_n^2(\hat{\boldsymbol{\theta}}_n) + \frac{1}{n}\boldsymbol{L}^T(\hat{\boldsymbol{\theta}}_n)\left(\boldsymbol{I}(\hat{\boldsymbol{\theta}}_n) - \boldsymbol{J}(\hat{\boldsymbol{\theta}}_n)\right)^{-1}\boldsymbol{L}(\hat{\boldsymbol{\theta}}_n),$$

where,

$$\chi_n^2(\theta) = \left(\frac{\nu_1 - np_1(\boldsymbol{\theta})}{np_1(\boldsymbol{\theta})}, \frac{\nu_2 - np_2(\boldsymbol{\theta})}{np_2(\boldsymbol{\theta})}, \ldots, \frac{\nu_r - np_r(\boldsymbol{\theta})}{np_r(\boldsymbol{\theta})}\right)^T,$$

and $\boldsymbol{J(\theta)}$ is the information matrix for the grouped data, defined as

$$\boldsymbol{J(\theta)} = B(\boldsymbol{\theta})^T B(\boldsymbol{\theta}),$$

with,

$$B(\boldsymbol{\theta}) = \left(\frac{1}{\sqrt{p_i}} \frac{\partial p_i(\boldsymbol{\theta})}{\partial \mu}\right)_{r \times s} \quad (\text{for } i = 1, 2, \ldots, r \text{ and } k = 1, \ldots, s),$$

where $\boldsymbol{L(\theta)}$ is given by $\boldsymbol{L(\theta)} = (\boldsymbol{L_1(\theta)}, \ldots, \boldsymbol{L_s(\theta)})^T$, with each component $\boldsymbol{L_k(\theta)}$ defined as

$$\boldsymbol{L_k(\theta)} = \sum_{i=1}^{r} \frac{\nu_i}{p_i} \frac{\partial p_i(\boldsymbol{\theta})}{\partial \boldsymbol{\theta}_k},$$

where $\boldsymbol{I_n(\hat{\theta}_n)}$ denotes the estimated Fisher information matrix, and $\boldsymbol{\hat{\theta}_n}$ is the ML estimator for the parameter vector. The Y^2 statistic follows a χ^2 distribution with $r-1$ degrees of freedom, denoted as χ^2_{r-1}.

3.11.2 N.R.R Statistic for the BIIIW Model

Let $T = (T_1, T_2, \ldots, T_n)^T$ represent a dataset. To assess whether this dataset follows the BIIIW model, defined by $P\{T_i \leq t\} = F_{\text{BIIIW}}(t, \boldsymbol{\theta})$ with unknown parameters $\boldsymbol{\theta} = (c, k, a, b)^T$, a χ^2 GoF test is is employed, utilizing the N.R.R. statistic formulated in the preceding section. The ML estimators $\hat{\boldsymbol{\theta}}_n$ of the unknown parameters of the BIIIW distribution are calculated based on the preliminary data. Since the statistic Y^2 is independent of the parameters, we can utilize the Fisher information matrix estimated as $\boldsymbol{I_n(\hat{\theta}_n)}$

3.11.3 Simulation of N.R.R. statistics

We carry out an extensive analysis using numerical simulations, to validate the findings of this study. To evaluate the null hypothesis H_0 that a given sample follows the BIIIW model, we compute the N.R.R. statistic Y^2 using 10,000 simulated datasets with sample sizes of $n = 35$, 55, 100, 300 and 800 respectively. At various theoretical significance levels ($\eta = 0.02, 0.05, 0.01, 0.1$), we determine the mean count of non-rejections of the null hypothesis. When $Y^2 \leq \chi^2_\eta(r-1)$,

we then provide the findings of corresponding empirical and theoretical levels in Table 3.11. It is evident that the empirical level values computed are nearly identical to their respective theoretical levels. As a result, we can conclude that the proposed test is suited for the BIIIW distribution.

Table 3.11: Empirical levels versus theoretical levels

N = 10000	$\eta = 0.01$	$\eta = 0.02$	$\eta = 0.05$	$\eta = 0.1$
35	0.9922	0.9825	0.9524	0.9051
55	0.9921	0.9814	0.9516	0.9048
100	0.9915	0.9813	0.9512	0.9040
300	0.9911	0.9804	0.9504	0.9028
800	0.9904	0.9802	0.9502	0.9014

3.11.4 Simulated distribution of the N.R.R. statistic for the BIIIW Model

To illustrate that the Y^2 statistic converges to a χ^2 distribution with $s = r - 1$ degrees of freedom in the limit, we perform 10,000 simulations of the $Y^2(\hat{\theta})$ distribution under the null hypothesis H_0. This is done for various parameter values of the BIIIW model (c, k, a, b) and $r = 11$ intervals, comparing the results to a χ^2 distribution with $s = 10$ degrees of freedom. The histograms are illustrated in Figure 3.10, with a comparison to the χ^2 distribution with s degrees of freedom. Figure 3.10 illustrates that the statistical distribution of Y^2 varies with different parameter values and varying numbers s of grouping cells. Ultimately, it approaches a χ^2 distribution with s degrees of freedom, even when considering the statistical errors from the simulations. Similar findings are observed for various numbers of equiprobable grouping intervals and different parameter values. This indicates that the limiting distribution of the generalized chi-squared Y^2 statistic is independent of distribution.

3.11.5 Results of GoF Test

We utilize the N.R.R. statistic to evaluate the null hypothesis H_0 that the Italy Covid-19 data follow a BIIIW distribution. The ML estimates obtained using *nlm* function in R, are $\hat{c} = 1.3796$, $\hat{k} = 11.3024$, $\hat{b} = 5.4664$ and $\hat{a} = 14.9756$.

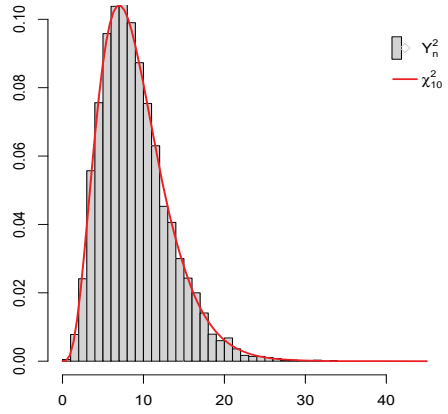

(a) $c = 1.5$, $k = 2.5$, $a = 1.7$, $b = 2.2$

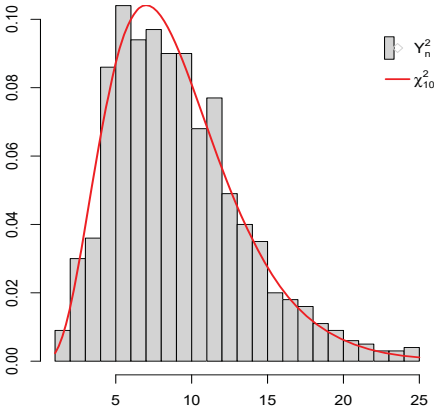

(b) $c = 0.9$, $k = 1.6$, $a = 2$, $b = 1.5$

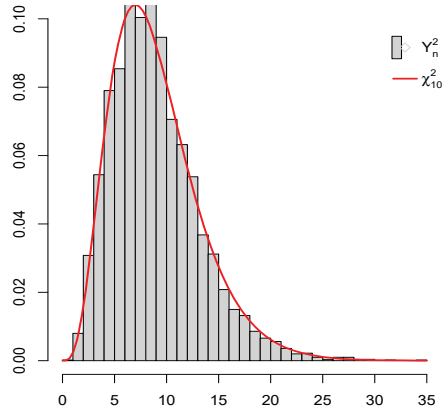

(c) $c = 1.3$, $k = 2$, $a = 3$, $b = 1.7$

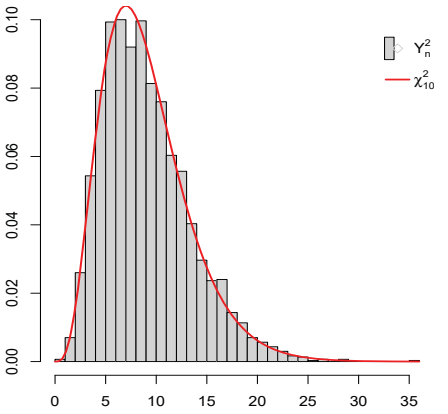

(d) $c = 2$, $k = 0.6$, $a = 1.8$, $b = 3$

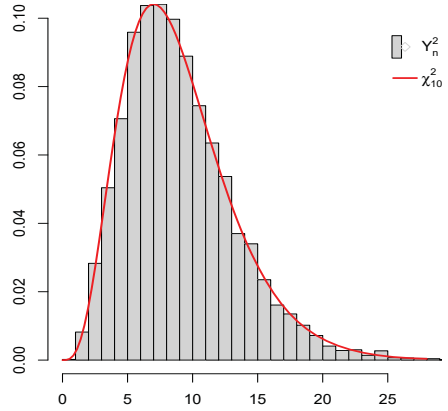

(e) $c = 2.5$, $k = 1$, $a = 4.5$, $b = 4$

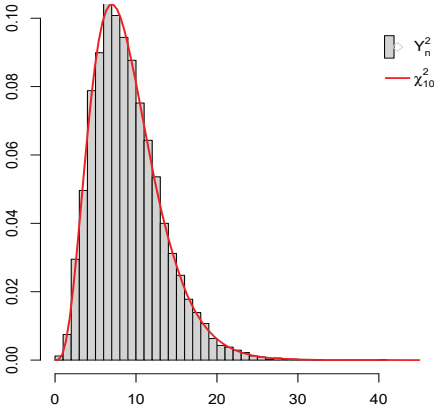

(f) $c = 3$, $k = 3$, $a = 2.5$, $b = 3.3$

Figure 3.10: Simulated distribution of the Y^2 statistic versus χ^2 distribution with 10 degrees of freedom ($n = 150$ and $N = 10,000$)

Then, the corresponding N.R.R Y^2 statistic for $r = 5$, based on these estimates, is $Y^2 = 6.628$. At the significance level of 0.05, the critical value of $\chi^2_{r-1} = 9.4877$. Since the Y^2 statistic value is below the critical value, we conclude that the data aligns well with the BIIIW model.

To test the null hypothesis H_0 that the Mexico Covid-19 follow a BIIIW distribution. The ML estimates obtained are $\hat{c} = 1.4354$, $\hat{k} = 8.8005$, $\hat{b} = 2.8598$ and $\hat{a} = 10.6226$. Based on these estimates, the computed NRR Y^2 statistic for $r = 6$ is 9.1812, which is lower than the corresponding critical value of $\chi^2_{r-1} = 11.0705$ at the 0.05 significance level. Consequently, we do not reject H_0, indicating that the Mexico Covid-19 data align well with the BIIIW model.

Similarly, we evaluate the CFR data using the N.R.R. statistic to test the null hypothesis H_0 that the CFR follow a BIIIW distribution. The estimates obtained are $\hat{c} = 2.6203$, $\hat{k} = 6.0785$, $\hat{b} = 302.0802$ and $\hat{a} = 10.4802$. Then, the NRR statistic computed for $r = 5$ is 2.1107, which is lower than the corresponding critical value of $\chi^2_{r-1} = 9.4877$ at the 0.05 significance level. Consequently, we do not reject H_0, indicating that the CFR data align well with the BIIIW model.

3.12 Summary

A novel distribution derived from the Weibull and Burr III distributions, has been introduced and its properties are studied. Due to the flexibility of the proposed distribution which may display monotone, bathtub-shaped, and unimodal failure rates depending on different parameter combinations, it is envisaged that this model would have broad use in fields like reliability engineering and biological sciences. Through our analysis of real datasets, we have observed that the BIIIW distribution demonstrates a strong fit to the Covid-19 datasets. Finally, we anticipate that the new distribution will be used as an alternative model to other existing models that are already available in the literature for modelling real data in areas such as engineering, survival analysis, hydrology, economics, and so forth. In conclusion, the BIIIW distribution could offer a very adaptable technique for fitting a variety of positive real-world data sets.

Chapter 4

A Comparative Analysis of MLE and ANN Using the Odd Burr III Weibull Distribution for Survival Assessment in Arthritic Pain Relief Data

4.1 Introduction

The application of artificial intelligence (AI) technology has expanded across many fields and has made human life significantly easier. When complex functions cannot be adequately modelled using traditional mathematical techniques, AI algorithms are often used. The use of AI tools for data prediction provides significant time and cost benefits, particularly in scientific studies. One of the AI techniques known as artificial neural networks (ANNs) is capable of high-precision simulations because of its powerful learning algorithms and training capabilities. ANNs serve as potent AI tools that may deliver extremely precise prediction and data estimations due to their robust learning capabilities. They are widely used in many different fields, including pattern recognition, error detection, control and process analysis as discussed by Ariana et al. (2015). Shafiq et al. (2022) and Shafiq et al. (2024) conducted extensive analyses on the use of ANN to optimize the reliability metrics of mixed models, while Çolak et al. (2022) explored the optimization of nonlinear flow of a Darcy-Forchheimer

squeezing fluid in a stratified medium under convective conditions. Additionally Waini et al. (2021) forecasted the Dufour and Soret effects on Al_2O_3 water nanofluid flow over a moving thin needle and Liu et al. (1995) examined to explore the application of a neural network approach for reliability data.

MLE is a well established method, but it relies heavily on predefined assumptions about data distributions which may not hold always in real world scenarios especially with small samples. In such cases, the performance of the MLE can be compromised, resulting in biased or inefficient estimates. In contrast, ANN offer greater flexibility as they do not require prior assumptions about data distribution. This flexibility makes them highly suitable for modeling complex, non-linear relationships that are commonly found in real life data, where underlying hazards or risks may evolve over time or involve intricate interactions between covariates. ANN can learn directly from the data, adapting to these complexities and yielding more accurate reliable predictions. Furthermore, ANN can easily incorporate multiple covariates or time-varying factors providing a more adaptable and comprehensive framework for real life data analysis. Also, ANN's ability to generalize across different datasets means it can capture subtle patterns and interactions that MLE might overlook. For example, in situations where data is missing or incomplete, ANN can impute values or learn from partial data more effectively than MLE. This leads to enhanced model robustness and a better fit to real-world scenarios. By integrating ANN with MLE, researchers can leverage the strengths of both approaches. ANN's flexibility and adaptability can complement MLE's theoretical foundation, resulting in more robust models that perform well even when traditional assumptions do not hold. Several studies in the literature highlight the use of ANN and MLE for optimizing and predicting survival measures in lifetime models. For instance, Shafiq et al. (2022) applied both ANN and MLE to estimate COVID-19 mortality rates. Çolak et al. (2024) performed a comparative analysis of these methods using the new power function distribution to predict the electrical component reliability. Similarly, Sindu et al. (2024) employed the Burr Hatke distribution to explore these techniques for engineering and disease data analysis.

This Chapter is an extension of Usman and Haq (2019), to investigate the

suitability of ANNs models in analyzing and predicting real life data using Odd Burr III Weibull (OBIIIW) distribution and to provide comparison findings using the above two distinct techniques. Although ANN approaches may be used in many different medical fields, this Chapter offers a practical application for predicting clinical data. By doing so, this research aims to bridge a notable gap in the current body of literature.

The Chapter is organized as follows: Section 4.2 introduces the OBIIIW distribution, and Section 4.3 presents key survival metrics based on this model. Section 4.4 discusses MLE of model parameters, while Section 4.5 outlines the design and training of the ANN model for predicting survival characteristics. Section 4.6 evaluates the performance of the MLE and ANN methods using real arthritis data, and Section 4.7 concludes the study by summarizing the findings and highlighting the effectiveness of ANNs in survival modeling.

4.2 Model

Jamal et al. (2017) proposed a method for generating flexible statistical distributions via the CDF. This approach led to the development of the Odd Burr III-G (OBIII-G) family, which provides greater adaptability in modeling diverse data patterns. The CDF of the OBIII-G family is given by:

$$F(x; c, k, \gamma) = \left\{1 + \left[\frac{1 - G(x, \gamma)}{G(x, \gamma)}\right]^{c}\right\}^{-k},$$

where $c > 0$ and $k > 0$ denotes the shape parameters and γ represents the parameters of the baseline distribution.

A novel extension of the Weibull distribution, termed the Odd Burr III Weibull (OBIIIW) distribution, has been introduced by employing the Weibull distribution as the baseline within the OBIII-G family. Usman and Haq (2019) investigated this four-parameter model, referred to as the OBIIIW distribution. Then, the CDF and PDF of OBIIIW distribution with shape parameter c, k, b

and scale parameter a is defined by,

$$F(x;c,k,a,b) = \left\{1+\left[\frac{e^{-(ax)^b}}{1-e^{-(ax)^b}}\right]^c\right\}^{-k}, c,k,a,b>0 \text{ and } x>0, \quad (4.1)$$

$$f(x;c,k,a,b) = ckba^b x^{b-1}\frac{[e^{-(ax)^b}]^c}{[1-e^{-(ax)^b}]^{c+1}}\left\{1+\left[\frac{e^{-(ax)^b}}{1-e^{-(ax)^b}}\right]^c\right\}^{-k-1}, \quad c,k,a,b>0 \text{ and } x>0. \quad (4.2)$$

The OBIIIW distribution finds extensive applications in fields such as biomedical research, reliability analysis, physical engineering, and survival studies due to its adaptability and ability to model skewed data effectively. The shapes of PDF and CDF or Failure Function (FF) are given in Figure 4.1 and Figure 4.2. As seen in Figure 4.1, the PDF has a variety of forms including bimodal, unimodal, decreasing, left and right-skewed (positive and negative skewness). From Figure 4.2, it is evident that the behaviour of FF is monotonically increasing.

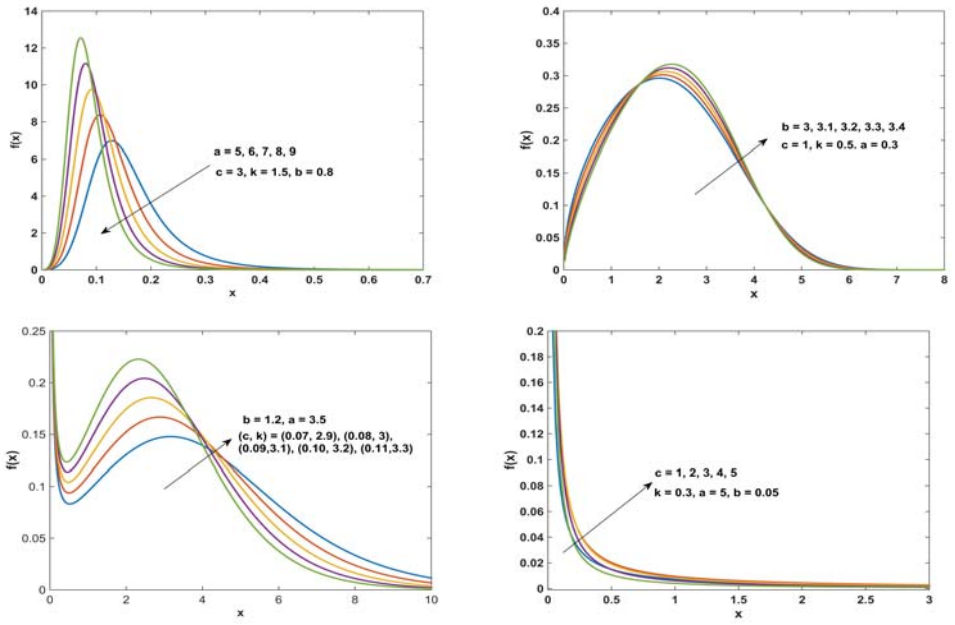

Figure 4.1: Plots of PDF for the OBIIIW distribution at various parameter values.

4.3 Survival Measures

Survival analysis has become increasingly popular and widely used in disciplines like medicine, biology, econometrics, and engineering. It is also referred to as

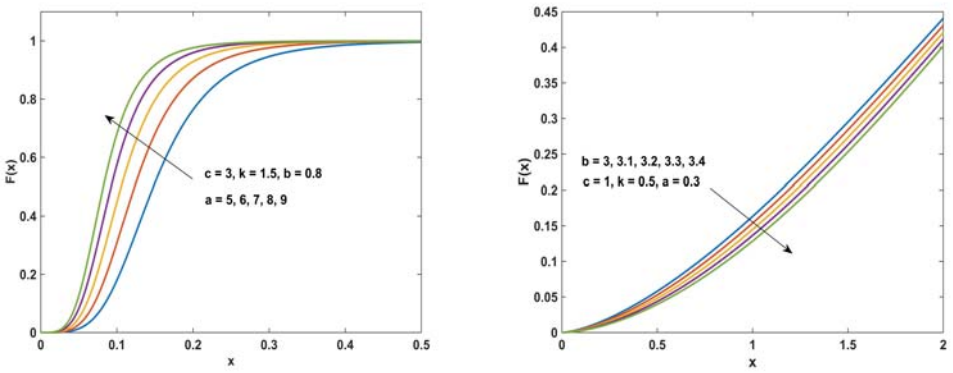

Figure 4.2: Plots of FF for the OBIIIW distribution at various parameter values.

reliability analysis in engineering, is an extremely useful tool that establishes a significant connection between variables and the duration of an event. It analyzes the duration of an event and the factors that affect it, allowing us to make informed decisions and take proactive measures to prevent or mitigate negative outcomes.

4.3.1 Survival Function

The survival (reliability) paradigm often focuses on estimating a systems probability of success or failure. The $R(x) = 1 - F(x)$ evaluates the reliability or survival function (SF) of a random variable X. It is defined as the probability that the system will not fail within a specified time period x. The survival function of the OBIIIW is defined as,

$$R(x; c, k, a, b) = 1 - \left\{1 + \left[\frac{e^{-(ax)^b}}{1 - e^{-(ax)^b}}\right]^c\right\}^{-k}. \tag{4.3}$$

Figure 4.3 shows graphs of the survival function of the proposed distribution for various parameter values. The function exhibit non-increasing behaviour for SF.

4.3.2 Hazard Rate Function

The hazard rate is an essential measure that helps in predicting a patients lifespan. A persons chance of surviving as a function of time is modelled using hazard rate, which captures intervals with different probability of an event occurring.

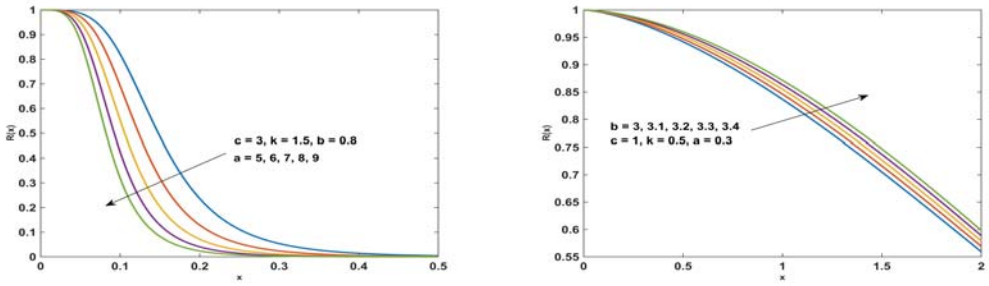

Figure 4.3: Plots of SF for the OBIIIW distribution at various parameter values.

This metric plays a crucial role in guiding healthcare decisions related to medical treatments, interventions and healthcare planning. Having prior knowledge about the shape of the hazard rate can facilitate model selection. This information can guide the selection of appropriate statistical models for analysis and help to make more accurate predictions about a systems future performance. The forms of the HRF are illustrated in Figures 4.4. The HRF can be predicted through various patterns such as bathtub, decreasing, unimodal and increasing, each representing favorable characteristics for any lifetime model. Consequently, this distribution is highly versatile and can be used to model complex data across numerous fields, including engineering, finance, and other disciplines.

$$h(x;c,k,a,b) = \frac{ckba^b x^{b-1}[e^{-(ax)^b}]^c[1-e^{-(ax)^b}]^{-c-1}\left\{1+\left[\frac{e^{-(ax)^b}}{1-e^{-(ax)^b}}\right]^c\right\}^{-k-1}}{1-\left\{1+\left[\frac{e^{-(ax)^b}}{1-e^{-(ax)^b}}\right]^c\right\}^{-k}}. \tag{4.4}$$

4.3.3 Cumulative Hazard Rate Function

The cumulative hazard rate function (CHRF) is another important measure in reliability and survival analyses. It determines the entire amount of risk experienced up to time x.

$$\begin{aligned} H(x;c,k,a,b) &= \int_0^t h(x)dx = -\log[S(t)] \\ &= -\log\left[1-\left\{1+\left[\frac{e^{-(ax)^b}}{1-e^{-(ax)^b}}\right]^c\right\}^{-k}\right]. \end{aligned} \tag{4.5}$$

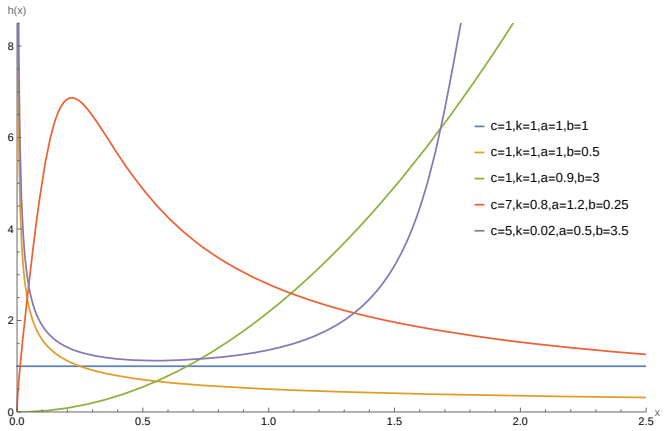

Figure 4.4: Hazard plot of OBIIIW distribution.

Figure 4.5 provides an interpretation of how the parameters affect the CHRF

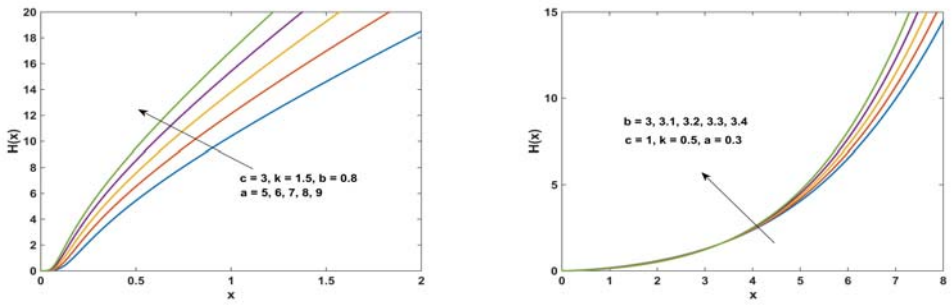

Figure 4.5: Plots of CHRF for the OBIIIW distribution at various parameter values.

of the OBIIIW model. The model exhibits monotonically increasing behaviour for CHRF.

4.3.4 Reversed Hazard Rate Function

The reversed hazard rate function (RHRF) has been introduced as a dual measure of hazard rate. It is the ratio of the PDF to the corresponding CDF. This method is useful for interpreting left censored data and applied in various disciplines including environmental studies, forensic sciences, quality control, survival analysis etc. For further details about the characteristics and definition of the RHRF, see Block et al. (1998), Chandra and Roy (2001) and Finkelstein (2002). Figure 4.6 examines the effects of relevant parameters on the RHRF. The RHRF

exhibit monotonically decreasing behaviour for selected parameter values.

$$\begin{aligned} h^{'}(x;c,k,a,b) &= \frac{f(x)}{F(x)} \\ &= ckba^b x^{b-1} \frac{[e^{-(ax)^b}]^c}{[1-e^{-(ax)^b}]^{c+1}} \left\{1+\left[\frac{e^{-(ax)^b}}{1-e^{-(ax)^b}}\right]^c\right\}^{-1}. \end{aligned} \quad (4.6)$$

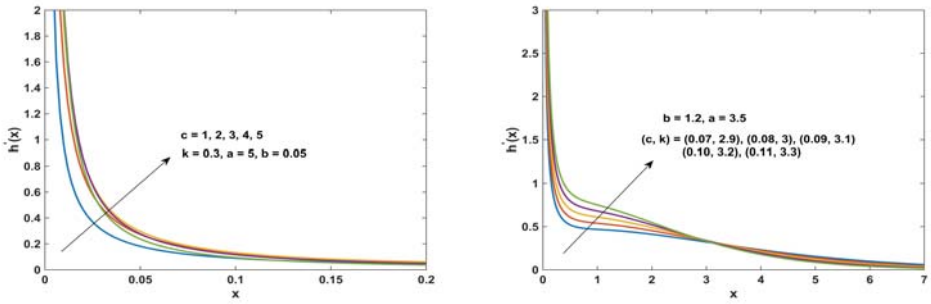

Figure 4.6: Plots of RHRF for the OBIIIW distribution at various parameter values.

4.3.5 Mills Ratio

Mills Ratio (MR) introduced by Mills (1926) is another reliability measure to understand the behavior of failure rates over time. It is a specific technique for evaluating durability. Different forms of MR can be predicted from Figure 4.7 including decreasing, increasing, and upside-down curves. These forms are desirable qualities in a lifetime model as they are versatile and ideal for including both monotonic and non monotonic hazard rate trends that are common in real-life applications.

$$\begin{aligned} MR(x;c,k,a,b) &= \frac{S(x)}{f(x)} \\ &= \frac{1-\left\{1+\left[\frac{e^{-(ax)^b}}{1-e^{-(ax)^b}}\right]^c\right\}^{-k}}{ckba^b x^{b-1}[e^{-(ax)^b}]^c[1-e^{-(ax)^b}]^{-c-1}\left\{1+\left[\frac{e^{-(ax)^b}}{1-e^{-(ax)^b}}\right]^c\right\}^{-k-1}}. \end{aligned} \quad (4.7)$$

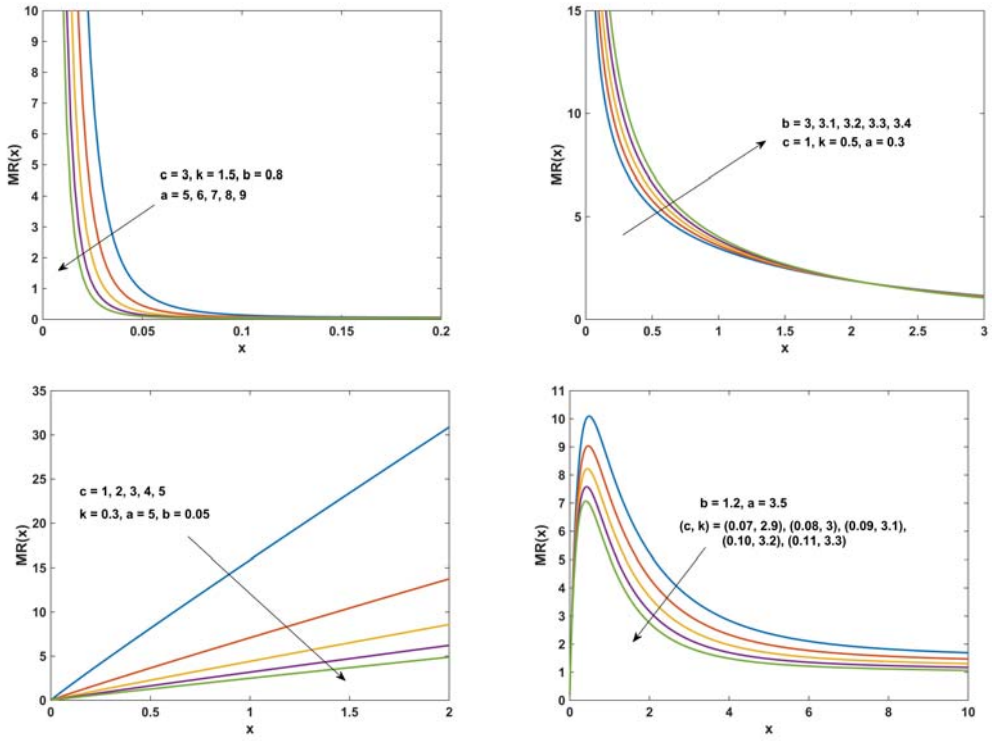

Figure 4.7: Plots of MR for the OBIIIW distribution at various parameter values.

4.3.6 Odd Function

The odd function (OF) is defined as,

$$\begin{aligned} OF(x;c,k,a,b) &= \frac{F(x)}{S(x)} \\ &= \frac{\left\{1+\left[\frac{e^{-(ax)^b}}{1-e^{-(ax)^b}}\right]^c\right\}^{-k}}{1-\left\{1+\left[\frac{e^{-(ax)^b}}{1-e^{-(ax)^b}}\right]^c\right\}^{-k}}. \end{aligned} \tag{4.8}$$

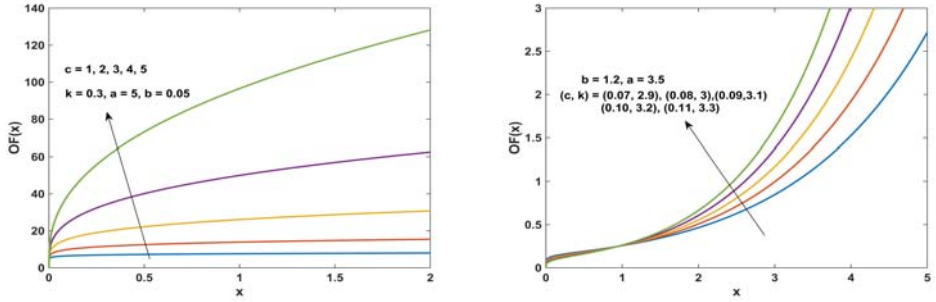

Figure 4.8: Plots of OF for the OBIIIW distribution at various parameter values.

The OF of the OBIIIW model displays a monotonically increasing behavior (see Figure 4.8).

4.4 ML Estimation

It is interesting to note that researchers have devised multiple methods to estimate parameters. However among all the techniques, the ML method stands out as the most popular one. Its wide acceptance in the scientific community serves as evidence of its accuracy and efficiency. The ML estimator is a function of the observed data that maximizes the likelihood function across all potential values of Θ within the parameter space. We thus utilise this technique to estimate the unknown parameters of OBIIIW from complete samples.

Let $x_1, x_2, \ldots, x_n$ represent a random sample from OBIIIW distribution with unknown parameters $\Theta = (c, k, a,\ b)$. The log-likelihood function $L = L(\Theta)$ is given by,

$$\begin{aligned} L &= n\log c + n\log k + n\log b + nb\log a + (b-1)\sum_{i=1}^{n}\log x_i - c\sum_{i=1}^{n}(ax_i)^b \\ &\quad -(c+1)\sum_{i=1}^{n}\log(1-z_i) - (k+1)\sum_{i=1}^{n}\log\left\{1+\left[\frac{z_i}{1-z_i}\right]^c\right\}, \end{aligned} \tag{4.9}$$

where $z_i = e^{-(ax_i)^b}$. The score vector is given by $I(c,k,a,b)=(\frac{\partial L}{\partial c},\ \frac{\partial L}{\partial k},\ \frac{\partial L}{\partial a},\ \frac{\partial L}{\partial b})^T$.

Then,

$$\begin{aligned}
\frac{\partial L}{\partial c} &= \frac{n}{c} - \sum_{i=1}^{n}(ax_i)^b - \sum_{i=1}^{n}\log(1-z_i) - (k+1)\sum_{i=1}^{n}\frac{\left[\frac{z_i}{1-z_i}\right]^c \log\left[\frac{z_i}{1-z_i}\right]}{1+\left[\frac{z_i}{1-z_i}\right]^c}.\\
\frac{\partial L}{\partial k} &= \frac{n}{k} - \sum_{i=1}^{n}\log\left\{1+\left[\frac{z_i}{1-z_i}\right]^c\right\}.\\
\frac{\partial L}{\partial a} &= \frac{nb}{a} - cb\sum_{i=1}^{n}x_i(ax_i)^{b-1} - (c+1)\sum_{i=1}^{n}\frac{bz_ix_i(ax_i)^{b-1}}{1-z_i}\\
&+ (k+1)\sum_{i=1}^{n}\frac{c\left[\frac{z_i}{1-z_i}\right]^{c-1}\left[\frac{bz_i^2x_i(ax_i)^{b-1}}{(1-z_i)^2} + \frac{bz_ix_i(ax_i)^{b-1}}{1-z_i}\right]}{1+\left[\frac{z_i}{1-z_i}\right]^c}.\\
\frac{\partial L}{\partial b} &= \frac{n}{b} + \sum_{i=1}^{n}\log(x_i) - c\sum_{i=1}^{n}(ax_i)^b\log(ax_i) - (c+1)\sum_{i=1}^{n}\frac{z_i(ax_i)^b\log(ax_i)}{1-z_i}\\
&+ (k+1)\sum_{i=1}^{n}\frac{c\left[\frac{z_i}{1-z_i}\right]^{c-1}\left\{\frac{z_i^2(ax_i)^b\log(ax_i)}{[1-z_i]^2}\right\} + \frac{z_i(ax_i)^b\log(ax_i)}{1-z_i}}{1+\left[\frac{z_i}{1-z_i}\right]^c}.
\end{aligned}$$

The estimates for the unknown parameters can be determined by equating the score vector to zero, denoted as $I(\Theta) = 0$. The simultaneous solution of these equations provides the ML estimates $\hat{c}$, $\hat{k}$, $\hat{a}$ and $\hat{b}$. Iterative methods like the Newton-Raphson algorithm can be employed to obtain these estimates numerically.

4.5 ANN Model

A neural network model was developed to analyse the survival measures based on the OBIIIW distribution. The constructed model utilizes a multilayer perceptron (MLP) network model with feedforward back propagation (FF-BP). MLP network models are often recommended neural network models due to their robust structures and learning algorithms, that produce optimal output behavior. A MLP network comprises of three fundamental layers. The first is the input layer which describes the input data. The second is the hidden layer comprises of computational components called neurons and there is at least one hidden layer in every MLP network. Finally, the prediction values are acquired at the output layer. In MLP networks, every layer is directly linked to the next layer. The

prediction values are contained in the output layer of the MLP network model. The process involves inputting data into the input layer which is then processed through the network layer by layer. Then the predicted values generated in the output layer are compared to the target values to determine the accuracy of the model. Error occurs when there are disparities between the prediction and the target values. The backpropagation algorithm is used to adjust the weights and biases in the network with the goal of reducing errors. This cycle continues until the error rate between the predicted and target data is minimized signifying the completion of the training phase for the ANN model.

After the training phase, the performance of the ANN model is analyzed and the model with the highest performance is selected. The desired prediction values are then obtained in the output layer of the selected model. In the input layer of the ANN model, five distinct input parameters were utilized, including the three shape parameters ($\hat{c}$, $\hat{k}$, $\hat{b}$), one scale parameter ($\hat{a}$) and the data (relief period of arthritic patients). The output layer predicts several survival measures, including the PDF, FF, RF, HRF, RHRF, CHRF, OF and MR. The Levenberg-Marquardt training algorithm which is popular because of its outstanding performance was used to train the designed MLP network. A single hidden layer was sufficient for the ANN structure in this study due to the strong performance of the model. Determining the number of neurons for the hidden layer is a hurdle in the development of MLP networks. Therefore, during the design phase, various models with different numbers of neurons were tested and their predictive performance was analyzed. Since there is no universally accepted method for determining the number of neurons, conclusions were drawn by analyzing the performance of models with different numbers of neurons were tested (see Shafiq et al. (2023), Shafiq et al. (2021)). A model with 7 neurons in the hidden layer was ultimately employed in this study. A total of 50 data were employed in the development of the ANN model and these data has been grouped using a highly accurate method, ensuring precision in the progression of the model. Here 70% of the data was utilised for training, 15% for validation, and 15% for testing. Using a total of 50 datasets, 34 were utilized for training, 8 for validation, and 8 for testing in the MLP network model, which was

developed to predict survival measures. The hidden layer employs the Tan-Sig function, while the output layer uses the Purelin function as transfer functions. The specific forms of these transfer functions are as follows:

$$\begin{aligned} f(x) &= \frac{1}{1+\exp(-x)} \\ \text{purelin(x)} &= x. \end{aligned}$$

The performance of the designed ANN models was examined by using Mean Squared Error (MSE), Coefficient of Determination (R^2) and Margin of Deviation (MoD) values. The following are the mathematical formulas used to calculate the performance characteristics.

$$\begin{aligned} MSE &= \frac{1}{N}\sum_{i=1}^{N}(X_{Targ(i)-X_{Pred(i)}})^2. \\ R^2 &= 1-\frac{\sum_{i=1}^{N}(X_{Targ(i)-X_{Pred(i)}})^2}{\sum_{i=1}^{N}(X_{Targ(i)})^2}. \\ MoD(\%) &= \left\{\frac{X_{Targ}-X_{Pred}}{X_{Targ}}\right\}\times 100. \end{aligned}$$

4.6 Comparison Between the ML Method and the ANNs Model

The application of the OBIIIW model for biological data is examined in this section. The data was gained through a clinical trial that was conducted to evaluate the effectiveness of an analgesic is given in Table 4.1. This dataset represents the relief periods (in hours) of 50 arthritis patients on a prescribed dosage of a particular drug. Wingo (1983) carefully examined this data set for fitting the Burr Type XII Distribution. Sindhu et al. (2024) also analyzed this dataset to model Generalized exponentiated unit Gompertz distribution. The MLE's of the parameters along with GoF for the relief periods of arthritic patients are presented in Table 4.2. By using the results obtained, we conducted an analysis to assess the impact of MLE's of relevant parameters on various factors such as PDF, FF, RF, HRF, RHRF, CHRF, MR and OF for arthritic

data. Based on this analysis, we have developed an ANN framework that can accurately forecast these outcomes.

Table 4.1: Duration of relief (hours) for 50 arthritic patients

Data Set
0.70, 0.84, 0.58, 0.50, 0.55, 0.82, 0.59, 0.71, 0.72, 0.61, 0.62, 0.49, 0.54, 0.72, 0.36, 0.71, 0.35, 0.64, 0.85, 0.55, 0.59, 0.29, 0.75, 0.53, 0.46, 0.60, 0.60, 0.36, 0.52, 0.68, 0.80, 0.55, 0.84, 0.70, 0.34, 0.70, 0.49, 0.56, 0.71, 0.61, 0.57, 0.73, 0.75, 0.58, 0.44, 0.81, 0.80, 0.87, 0.29, 0.50

It is essential to confirm that the training process is completed effectively before assessing the accuracy of predictions made by the ANN model. The performance of the designed ANN model is shown in Figure 4.9. The MSE values initially high during the early stages of training phases of MLP networks are anticipated to decrease as the number of epochs increases. The training process of an MLP network concludes when the difference between the predicted values and the target value is minimized. From Figure 4.9, it seems that the MSE values are quite large in the early phases of the training phase. However, as the network progresses through each epoch, the MSE values begin to decrease. This indicates that the error between the predicted values and the target outcomes obtained in the output layer is also decreasing. The training stage of the model concluded upon achieving its highest possible training performance by the 91^{th} epoch, the point at which the smallest error value was determined.

Error histograms are a specialized type of histogram used to examine error values, which indicate the differences between the outputs of an ANN model and the target data. In the error histogram shown in Figure 4.10, error values are presented for each dataset categorized into training, validation and testing groups. Upon evaluating the distributions of the calculated error values, it is clear that the errors cluster closely around the zero error line, typically highlighted

Table 4.2: GoF and estimates of OBIIIW distribution based on the arthritic relief data.

Model	$\hat{c}$	$\hat{k}$	$\hat{a}$	$\hat{b}$	AIC	BIC	K-S
OBIIIW	0.4644	0.3263	1.2689	21.0156	-42.3467	-34.6986	0.1288

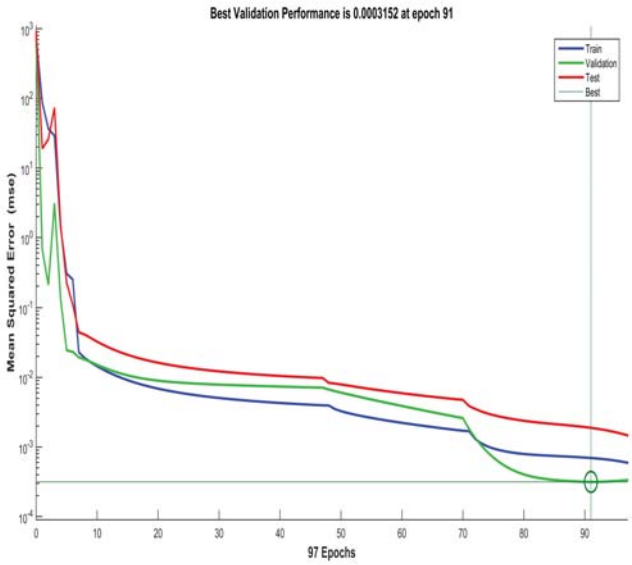

Figure 4.9: The performance of the described ANN model for the arthritic dataset.

in yellow across all three groups. Analyzing the numerical values of the errors along the x-axis reveals that they are relatively low. The findings from the error histogram demonstrate that the errors produced during the training phase of the MLP network model are minimal or remaining within acceptable error thresholds. These results indicate that the training phase of the network model has been effectively completed.

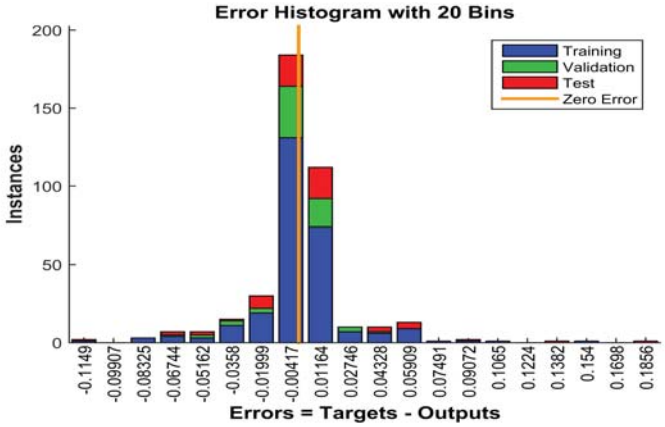

Figure 4.10: Error histogram of the designed ANN model.

The R^2 value quantifies the strength of the relationship between the predicted and actual values, ranging from 0 to 1. An R^2 value of 0 indicates no

relationship between predicted and actual values, while an R^2 value of 1 reflects a perfect match. In this study, the R^2 value of 0.9999 for the ANN model confirms the high accuracy and successful completion of the training phase. Figure 4.11 presents regression plots of the ANN, showing the target data on the x-axis and the normalized predicted output on the y-axis for training, validation, testing and overall datasets. The close alignment of data points along the diagonal line suggests that the predicted values are very close to the target values, indicating strong model performance. This high R^2 value achieved consistently across both training and testing datasets demonstrates the models ability not only to fit the training data but also to generalize well to new unseen data, a crucial feature for robust predictive modeling. The fundamental architectural layout of the neural network that was constructed was shown in Figure 4.12.

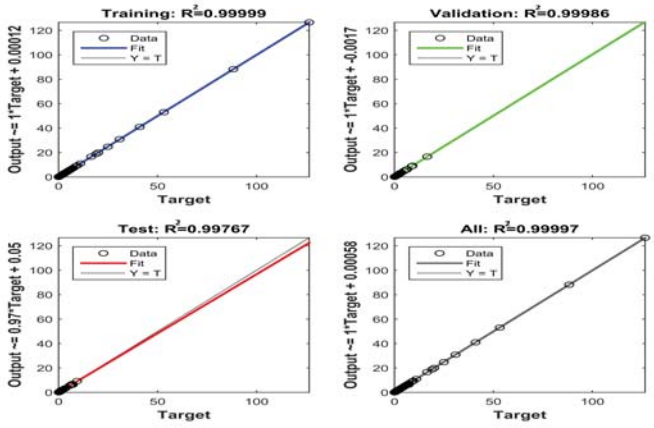

Figure 4.11: Training status of the designed ANN model.

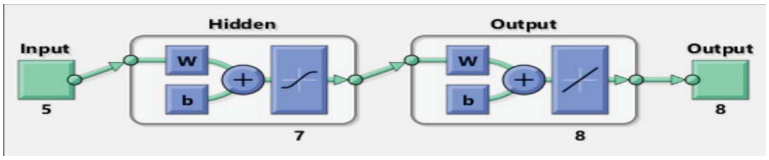

Figure 4.12: The basic architectural structure of the designed ANN.

Figure 4.13 presents the comparing results of the survival measures for the relief periods of arthritic patients obtained from the MLE technique with those predicted by the ANN. Upon monitoring the values associated with each of the data points used in the development of the ANN model, it becomes evident

that the predicted values derived from the ANN model perfectly match with the target values. This indicates that the simulation output shown by the black lines perfectly coincides with the target values represented by the blue squares. As illustrated in Figure 4.13, the reliability function, Mills ratio, and RHRF exhibit a decreasing trend, while the risk function shows an increasing pattern, aligning with the theoretical expectations of these functions. Additionally, both the Odd function and CHRF demonstrate an upward trend as anticipated by the underlying theory.

The computed MoD values for each output are displayed in Fig 4.14. Assessing the proportional deviation between the predicted outputs of the ANN and the target data is an another key for evaluating the predictive accuracy of the model. The deviation results represented by pink triangles, shows that the values are consistently close to the zero error line for each output indicating minimal deviations between the predicted and actual values. Additionally, the average MoD values for each output are notably small highlighting the models precision and consistency. These low deviations confirm that the ANN model can accurately predict the 8 output values with extremely low error, further confirm the model effectiveness and reliability.

Figure 4.15 presents a detailed analysis of the error rates for the proposed MLP neural network. In this figure, the differences between the target data and the predicted output values are calculated for each of the eight output measures across all data points. The small magnitude of these deviations as seen in the Figure 4.15, indicates that the MLP network consistently produces predictions that closely align with the actual target values. This suggests that the MLP network has strong predictive power, reliably capturing the underlying patterns in the data. The obtained results unequivocally demonstrate that the constructed ANN model can predict with exceptional accuracy and minimal errors.

Figure 4.16 illustrates the relationship between the target data (x-axis) and the predicted output from the neural network (y-axis). The figure demonstrates the accuracy of the model by showing that all data points lie close to the zero-error line, indicating a strong alignment between predicted and target values. Furthermore, the data points fall within the 10% error band, highlighting the

models prediction reliability. This close proximity to the zero-error line confirms the ANN's ability to generate predictions with minimal deviation, supporting the conclusion that the model has achieved perfect accuracy.

The R^2 value of 0.999 for the ANN models indicates exceptional predictive accuracy, explaining 99.9% of the variance in relief times and demonstrating that the model has effectively captured the underlying data patterns. This high R^2 value consistent across both training and testing datasets, also shows that the model generalizes well to unseen data. The low MSE and MoD along with the high R^2 value emphasize the ANN's strong generalization across unseen datasets and reliable predictive capability. Performance metrics as shown in Table 4.3, further validate the models strength. This suggests the model is well-suited for survival analysis and also perform effectively on unseen data.

Table 4.3: The calculated performance metrics

Survival Measures	MSE	MoD(%)	R^2
Failure Function	8.35×10^{-07}	-0.0798	0.999
Probability Density Function	2.57×10^{-05}	0.0076	
Reliability Function	8.35×10^{-07}	0.0350	
Hazard Rate Function	1.36×10^{-05}	0.0450	
Cumulative Hazard Rate Function	1.85×10^{-06}	0.0211	
Reversed Hazard Rate Function	1.86×10^{-05}	0.0023	
Mills Ratio	3.51×10^{-05}	0.0195	
Odd Function	5.29×10^{-05}	-0.2930	

4.7 Summary

This Chapter focused on the comparative analysis of the OBIIIW distribution using the ANN model and the ML approach. This groundbreaking model was utilized in a clinical trial aimed at evaluating the efficacy of a pain relief for arthritis patients. Furthermore, this study investigates the impact and outcomes of relevant parameters estimated using the ML method on survival metrics such as PDF, FF, RF, HRF, RHRF, CHRF, MR and OF. The outputs of the ANN

experiments provide more accurate predictions for the survival metrics for the OBIIIW distribution. As the hazard rate increases with longer relief times, it becomes tougher for those with severe arthritis to maintain relief. The values of the survival function appeared to be decreasing as survival time increased, which is aligned with the principles of survival function theory. Furthermore, both the ANN and MLE techniques exhibit consistent patterns as relief time increases. The developed ANN model achieved R^2 value of 0.999, demonstrating high predictive accuracy. The performance metrics, including a high R^2 value and low MSE and MoD values highlight the ANN models excellent fit to the data, suggesting reliable performance and strong generalization across unseen datasets. These findings show that the ANN model is effective for optimization and prediction, making it a powerful tool for analyzing survival and clinical data.

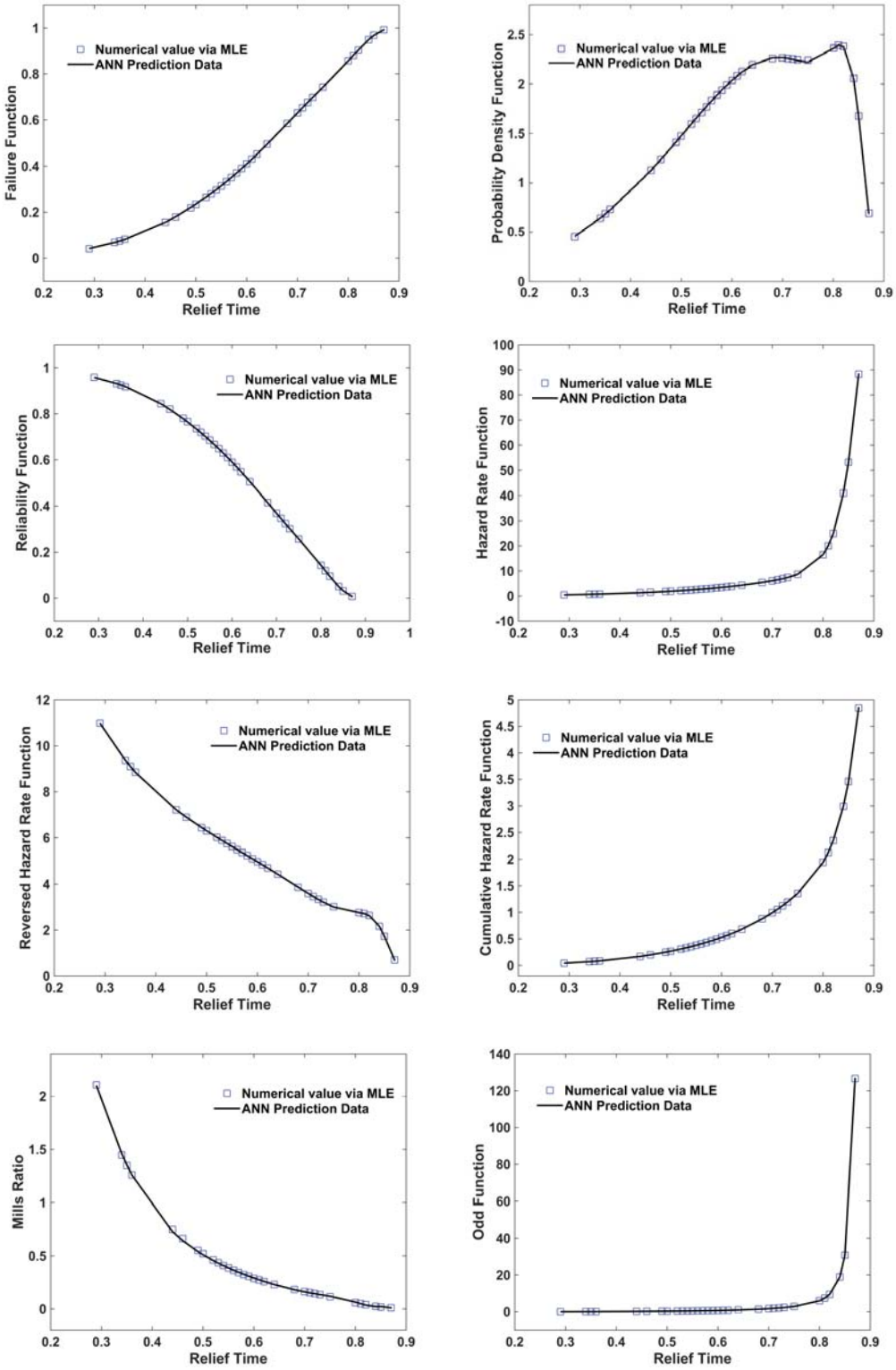

Figure 4.13: ANN predictions vs target values based on the arthritic data.

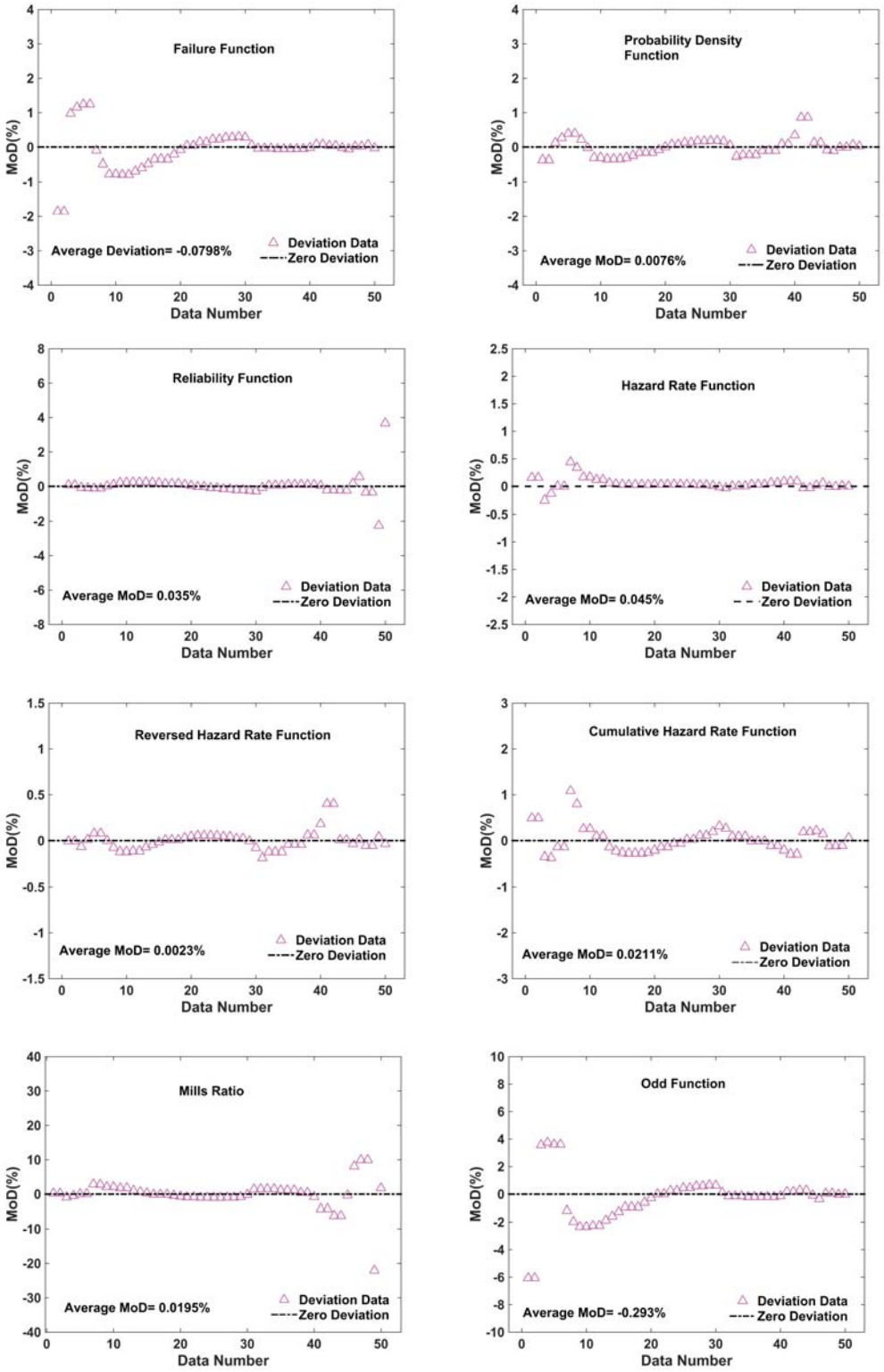

Figure 4.14: Deviation values based on the arthritic data.

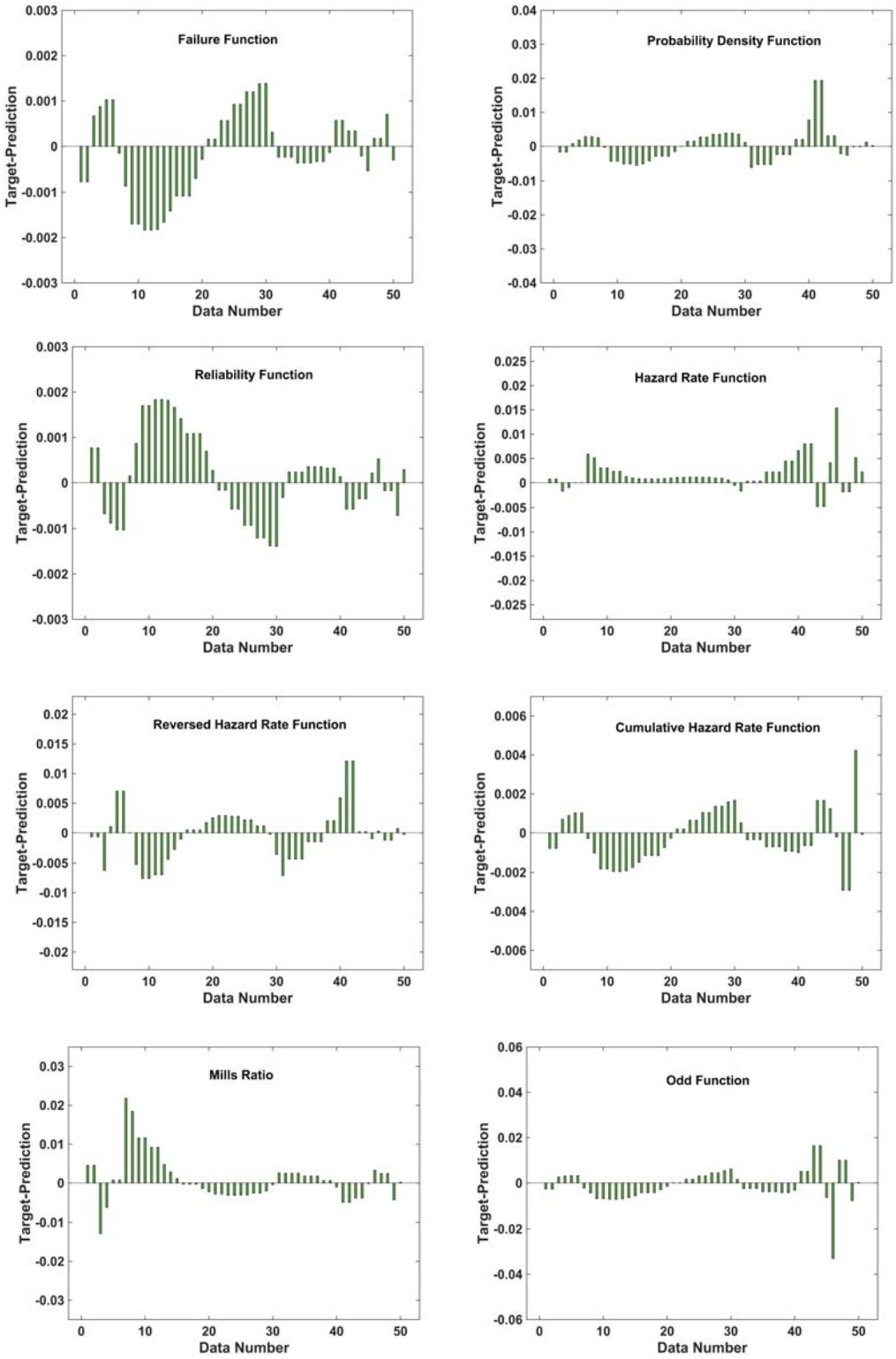

Figure 4.15: The departures between the target data and the predicted values based on the arthritic data.

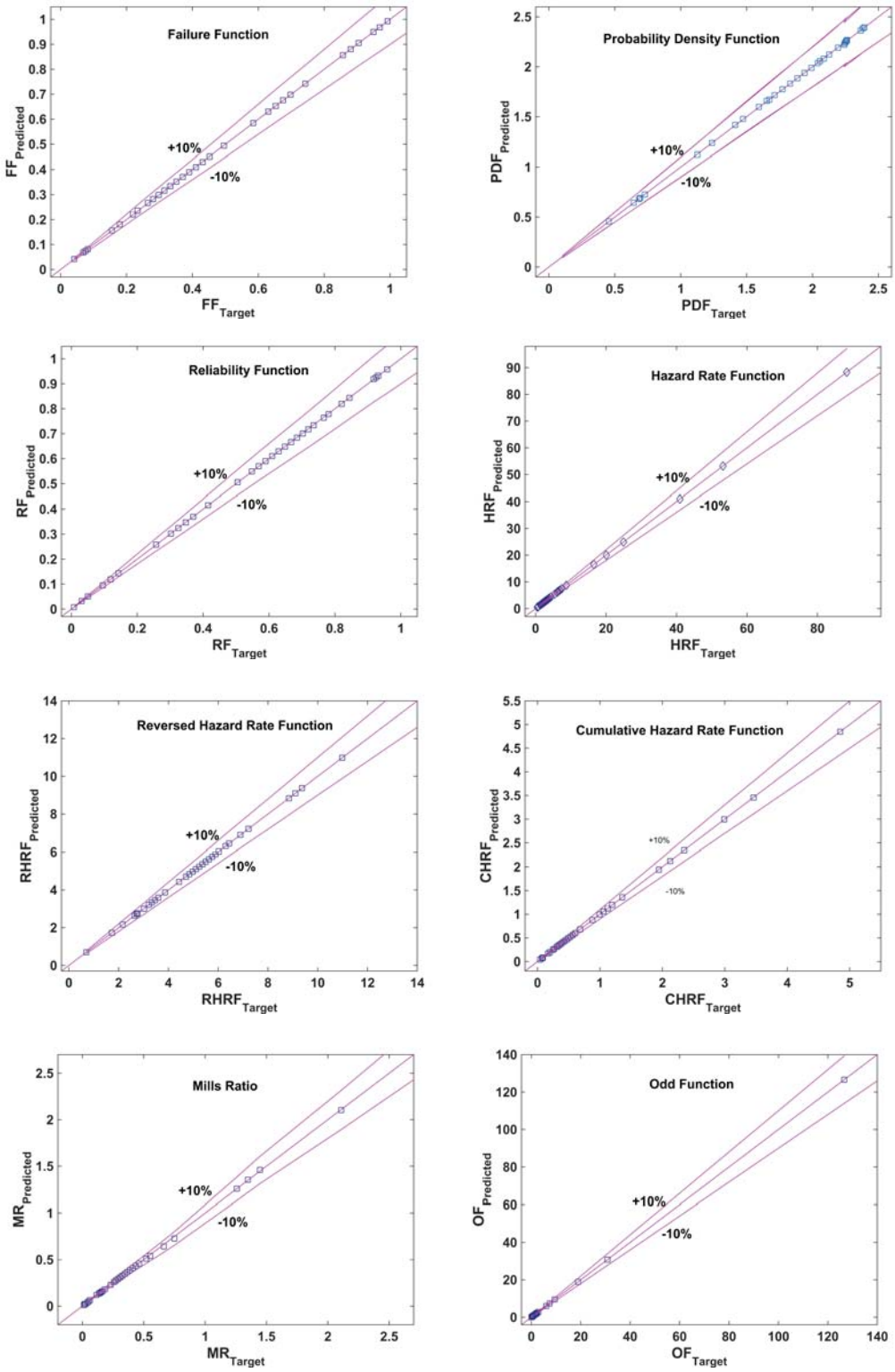

Figure 4.16: ANN predictions versus target values based on the arthritic data.

Chapter 5

On Log Odd Burr III Weibull Regression Model

5.1 Introduction

In practical scenarios, survival time is influenced by multiple factors that can account for the variability in the time of survival. To assess how these factors influence survival time, it is important to employ proper regression model for censored and time-to-failure data. In other words, to design regression models, it is essential to describe a probabilistic model for survival time. Different types of regression models exist for this purpose. The location-scale regression model (LSRM), as highlighted by Lawless (2011) stands out among these and is often utilized in clinical trials. A linear combination is assumed for the log-lifetimes models preserving the characteristics of standard regression models and also incorporating the advantage of handling censored data. A detailed description of the LSRM is provided in Chapter 1.

In this Chapter, we present a new LSRM based on the logarithm of the OBIIIW distribution, referred to as the log Odd Burr III Weibull (LOBIIIW) regression model. The modification in the current distribution results in a LSRM which is apt for modelling censored survival times exhibiting bathtub shaped hazard rates. This offers a practical alternative for the log-logistic and log-Weibull regression model. As a result, we expect that our proposed distribution will be useful in a wide range of applications for analyzing survival and reliability

data.

The Chapter is structured to convey key findings effectively: Section 5.2 defines the OBIIIW and LOBIIIW distributions and their properties. Section 5.3 develops the LOBIIIW regression model, while Section 5.4 discusses parameter estimation techniques. Section 5.5 addresses global influence diagnostics, and Section 5.6 focuses on residual analysis. Section 5.7 applies the model to heart transplant data, and Section 5.8 summarizes the key conclusions.

5.2 Log Odd Burr III Weibull Distribution

The PDF of OBIIIW distribution (which is detailed in Chapter 4) is defined by,

$$\begin{aligned} f(x;c,k,a,b) &= ckba^b x^{b-1}\frac{[e^{-(ax)^b}]^c}{[1-e^{-(ax)^b}]^{c+1}}\left\{1+\left[\frac{e^{-(ax)^b}}{1-e^{-(ax)^b}}\right]^c\right\}^{-k-1}, \\ & x>0 \text{ and } c,k,a,b>0, \end{aligned} \tag{5.1}$$

where c, k and b are the shape parameters, and a is the scale parameter. The survival function associated with equation (5.1) is given as follows:

$$S(x;c,k,a,b) = 1-\left\{1+\left[\frac{e^{-(ax)^b}}{1-e^{-(ax)^b}}\right]^c\right\}^{-k}.$$

The hazard function of the OBIIIW distribution exhibits remarkable flexibility by accommodating various hazard rate patterns including constant, decreasing, increasing, unimodal and bathtub shaped hazard rates (see Figure 4.4 in Chapter 4). This flexibility holds particular significance in reliability analysis, where non-monotone hazard rates are frequently encountered in real world data sets.

If X is a random variable with the OBIIIW density function (5.1), then $Y=\log(X)$ is a random variable with the log odd Burr III Weibull (LOBIIIW) distribution. Its density function, parameterized with $a=e^{-\mu}$ and $b=\sigma^{-1}$, can be formulated as follows:

$$f(y;c,k,\mu,\sigma) = \frac{ck}{\sigma}\frac{\exp\left[\left(\frac{y-\mu}{\sigma}\right)-c\exp\left(\frac{y-\mu}{\sigma}\right)\right]}{\left[1-\exp(-\exp(\frac{y-\mu}{\sigma}))\right]^{c+1}}\left\{1+\left(\frac{\exp[-\exp(\frac{y-\mu}{\sigma})]}{1-\exp[-\exp(\frac{y-\mu}{\sigma})]}\right)^c\right\}^{-k-1}, \tag{5.2}$$

where $-\infty < y < \infty$, $c > 0$, $k > 0$, $\sigma > 0$ and $-\infty < \mu < \infty$. We refer to Equation (5.2) as representing the distribution of $Y \sim LOBIIIW(c, k, \mu, \sigma)$, where μ indicates the location parameter, σ is scale parameter, and c and k are the shape parameters. Figure 5.1 displays graphs depicting the density function (5.2) for various parameter values. These findings suggest that this distribution serves as a suitable choice for effectively modeling both left-skewed, right-skewed, and symmetric datasets related to lifetimes.

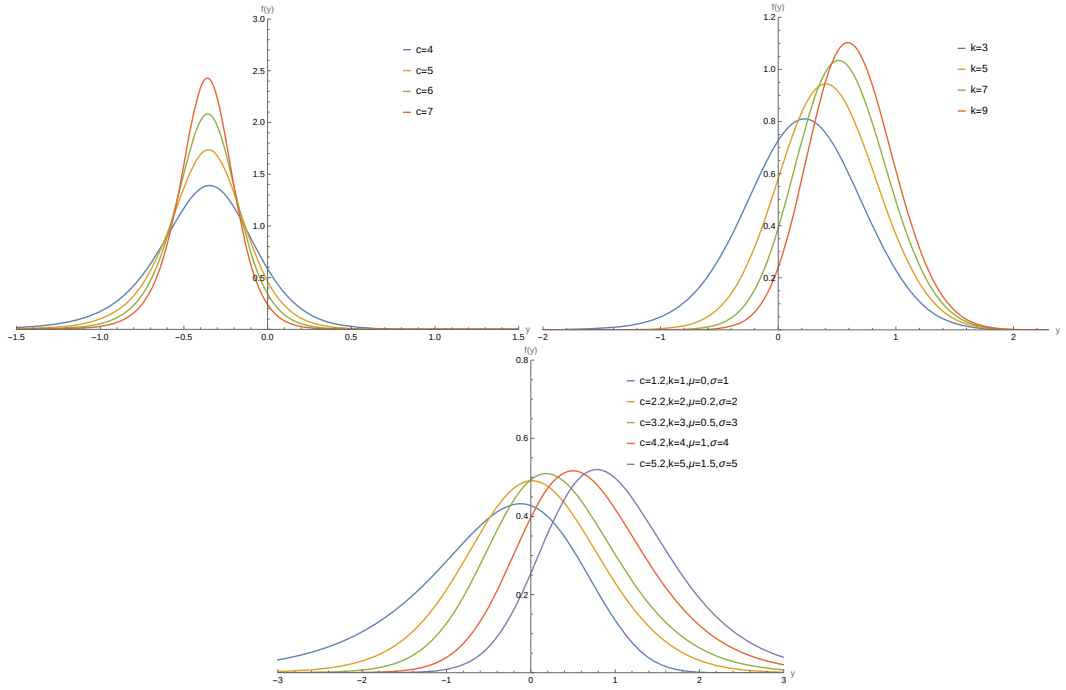

Figure 5.1: Plots of the LOBIIIW PDF for parameter values (a) k = 1, μ = 0, σ = 1. (b) c = 1.5, μ = 0, σ = 1.

The survival function associated with Equation (5.2) can be expressed as,

$$S(y; c, k, \mu, \sigma) = 1 - \left\{1 + \left[\frac{\exp[-\exp(\frac{y-\mu}{\sigma})]}{1 - \exp[-\exp(\frac{y-\mu}{\sigma})]}\right]^{c}\right\}^{-k}. \tag{5.3}$$

Then the standardized random variable $Z = \frac{Y-\mu}{\sigma}$, which is characterized by the density function is given as follows:,

$$\pi(z; c, k) = ck\frac{\exp\left[z - c\exp\left(z\right)\right]}{[1 - \exp(-\exp(z))]^{c+1}}\left\{1 + \left(\frac{\exp[-\exp(z)])}{1 - \exp(-\exp(z))}\right)^{c}\right\}^{-k-1}, \; -\infty < z < \infty. \tag{5.4}$$

The r^{th} ordinary moment of the standardized distribution (5.4) is,

$$\begin{aligned}\mu'_r &= E(Z^r) \\ &= ck\int_{-\infty}^{\infty} z^r \frac{\exp\left[z - c\exp\left(z\right)\right]}{\left[1-\exp(-\exp(z))\right]^{c+1}}\left\{1+\left(\frac{\exp[-\exp(z)])}{1-\exp(-\exp(z))}\right)^c\right\}^{-k-1}\mathrm{d}z.\end{aligned}$$

Expanding the binomial terms and substituting $m = \exp(z)$, we obtain the following expression,

$$\mu'_r = ck\sum_{i=j=0}^{\infty}(-1)^i\binom{k+i}{i}\binom{c+ci+j}{j}\int_0^{\infty}[\log m]^r\exp(-m(c+ci+j))\mathrm{d}m.$$

The above integral can be computed using the equation 2.6.21.1 provided in Prudnikov et al. (1986).

$$\mu'_r = ck\sum_{i=j=0}^{\infty}(-1)^i\binom{k+i}{i}\binom{c+ci+j}{j}\left(\frac{\partial}{\partial\alpha}\right)^r\left[(c+ci+j)^{-\alpha}\Gamma(\alpha)\right]\Big|_{\alpha=1}.$$

5.3 The Log Odd Burr III Weibull Regression Model

Researchers and statisticians have been investigating flexible regression models aimed at effectively capturing non-monotone failure rates, frequently encountered in fields such as reliability and biology. To overcome the limitations of the Weibull distribution in modelling such patterns, a LSRM utilizing the LOBIIIW distribution can be used instead. This model is particularly beneficial for analyzing data characterized by increasing, decreasing and bathtub shaped hazard failures. The importance of the newly developed regression model is its capability to extend the commonly used Weibull distribution to more complex scenarios through continuous extension. This generalization opens up new possibilities for applications that require more sophisticated statistical analysis. Moreover, it is crucial to examine the impact of various explanatory variables on lifetimes such as cholesterol levels, weight, blood pressure etc. Researchers can gain valuable insights into the relationship between the lifetime and the explanatory factors using regression models specifically location scale models.

We have now introduced a linear regression model using the LOBIIIW dis-

tribution to analyze the relationship between the response variable y_i and the explanatory variable vector $\mathbf{x_i} = (\mathrm{x}_1, \mathrm{x}_2, \ldots, \mathrm{x}_p)^T$ in the following way:

$$y_i = \mathbf{x_i^T}\boldsymbol{\beta} + \sigma z_i, i = 1, 2, \ldots, n, \tag{5.5}$$

where the error term z_i follows the density function (5.4), $\boldsymbol{\beta} = (\beta_1, \beta_2, \ldots, \beta_p)^T$, $c > 0$ and $k > 0$ are the unknown parameters. The explanatory variable vector $\mathbf{x_i^T} = (x_{i1}, x_{i2}, \ldots, x_{ip})$ is associated with the location parameter μ_i. The vector $\boldsymbol{\mu}$ $= (\mu_1, ..., \mu_n)^T$ of LOBIIIW regression model represents the location parameters and is indicated as linear model $\boldsymbol{\mu} = \boldsymbol{X}\boldsymbol{\beta}$ where $\boldsymbol{X} = (\mathrm{x}_1, \ldots, \mathrm{x}_n)^T$ is a predefined model matrix. New opportunities for fitting several kinds of data are made possible by the LOBIIIW model (5.5).

By employing the log linear model given in Equation (5.5), the survival function $Y_i|\mathrm{x}$ simplifies to,

$$S(y_i|\mathrm{x}) = 1 - \left\{1 + \left[\frac{\exp[-\exp(\frac{y_i - \mathbf{x_i^T}\boldsymbol{\beta}}{\sigma})]}{1 - \exp[-\exp(\frac{y_i - \mathbf{x_i^T}\boldsymbol{\beta}}{\sigma})]}\right]^c\right\}^{-k}.$$

When $k = 1$, the regression model (5.5) simplifies to the log-odd logistic regression model, and when $c = k = 1$, it further diminishes to the log-Weibull regression model.

5.4 Estimation of the LOBIIIW Regression Model

5.4.1 MLE method

Consider a sample of n independent observations $(y_1, \mathrm{x}_1), (y_2, \mathrm{x}_2), \ldots, (y_n, \mathrm{x}_n)$, where $y_i = \min\{\log(T_i), \log(C_i)\}$, and x_i represents the explanatory variable vector linked to the i^{th} individual. We consider that the observed lifetimes $(\log(T_i))$ and censoring times (C_i) are independent and the censorship is non-informative. The log-likelihood function for the vector of parameters $\boldsymbol{\eta}$ $=(c, k, \sigma, \boldsymbol{\beta}^T)^T$ is given by,

$$l(\boldsymbol{\eta}) = \sum_{i \in F} l_1(c, k, z_i) + \sum_{i \in C} l_2(c, k, z_i) \tag{5.6}$$

where,

$$l_1(c,k,z_i) = \log\left[\frac{ck}{\sigma}\frac{\exp\left[z_i - c\exp\left(z_i\right)\right]}{\left[1-\exp(-\exp(z_i))\right]^{c+1}}\left\{1+\left(\frac{\exp[-\exp(z_i)])}{1-\exp(-\exp(z_i))}\right)^{c}\right\}^{-k-1}\right],$$

$$l_2(c,k,z_i) = \log\left[1-\left\{1+\left[\frac{\exp[-\exp(z_i)]}{1-\exp[-\exp(z_i)]}\right]^{c}\right\}^{-k}\right].$$

and $z_i = \frac{y_i - \mathbf{x_i}^T\boldsymbol{\beta}}{\sigma}$. The set F represents individuals for whom y_i corresponds to log-lifetime, whereas C designates individuals subject to right censoring.

The ML estimates for the parameter vector $\boldsymbol{\eta}$ can be obtained by maximizing the likelihood function (5.6). The estimates are obtained by using the R software, specifically utilizing the MAXLIK package. Assuming the standard regularity conditions hold, the asymptotic distribution of $(\hat{\boldsymbol{\eta}} - \boldsymbol{\eta})$ follows a multivariate normal distribution $N_{p+3}\{0, \boldsymbol{I(\eta)}^{-1}\}$, where $\boldsymbol{I(\eta)})$ defines the expected information matrix. The asymptotic covariance matrix denoted as $\boldsymbol{I(\eta)}^{-1}$ of $\hat{\boldsymbol{\eta}}$ can be estimated by approximating the inverse of the $(p+3)\times(p+3)$ observed information matrix denoted as $-\ddot{\boldsymbol{L}}(\boldsymbol{\eta})$, with its elements evaluated numerically. Hence, it is possible to generate approximate confidence regions for the $\hat{\boldsymbol{\eta}}$ by using the multivariate normal distribution $N_{p+3}\{0, -\ddot{\boldsymbol{L}}(\boldsymbol{\eta})^{-1}\}$.

Additionally, the Likelihood Ratio (LR) statistic can be used to evaluate the LOBIIIW model against specific sub-models. The LR statistic for testing specific models within the LOBIIIW regression model can be constructed by calculating the maximum log-likelihood values for both the unrestricted and constrained models.

5.4.2 Jackknife Method

Jackknifing is a technique that converts the task of estimating a population parameter to that of estimating a population mean. When appling this method, estimating a mean value is approached from a distinct perspective. Lipsitz et al. (1990) offered a significant contribution for executing the jackknife method by proposing an alternative robust estimator for the covariance matrix. This estimator relies on the jackknife method and is valid for analyzing data from repeated measure analyses. This technique can be employed as an alternative

method to estimate population parameters.

Suppose $X_1, X_2, \ldots, X_n$ be a random sample of size n and $\bar{X} = \sum_{i=1}^{n} \frac{X_i}{n}$ be the sample mean used to estimate the population mean. Let $\hat{\eta}$ be the estimated parameter vector of η based on each of the n observations and $\hat{\eta}_{-i}$ for $i = 1, 2, \ldots, n$ be the estimated η value after the i^{th} observation was removed from the sample. Hence, the pseudo-values are obtained by;

$$\hat{\eta}_i^* = n\hat{\eta} - (n-1)\hat{\eta}_{-i}, \quad i = 1, 2, \ldots, n.$$

Thus, the jackknife estimator of η is given by,

$$\hat{\eta}^* = \frac{\sum_{i=1}^{n} \hat{\eta}_i^*}{n}$$

Manly (2018) proposed that an approximate $100(1-\gamma)\%$ confidence interval for each η is provided by $\hat{\eta}^* \pm t_{\frac{\gamma}{2},n-1} \frac{s}{\sqrt{n}}$, which eliminates bias of order n^{-1}. Here s represents the standard deviation of the pseudo-values and $t_{\frac{\gamma}{2},n-1}$ is the upper $(1 - \frac{\gamma}{2})$ point of t distribution with $n-1$ degrees of freedom.

5.4.3 Simulation

We execute a Monte Carlo simulation analysis to examine how the ML estimators of c, k, σ, β_0 and β_1 behave in finite sample ($n = 50$, 100 and 300). The samples are obtained using the true parameter values: $c = 2$, $k = 4$, $\sigma = 1.5$, $\beta_0 = 3$ and $\beta_1 = 2$ with varying levels of censoring generally at censoring percentages (CP), CP = 0%, 10% and 30%. The log-lifetimes $\log(T_1)$, ..., $\log(T_n)$ are simulated from the LOBIIIW regression model (5.5), where $\mathbf{x}_i^T \boldsymbol{\beta} = \beta_0 + \beta_1 x_i$ and x_i are sampled from a uniform distribution within the interval (0, 1). The censored times C_1, C_2, ..., C_n are drawn from a uniform distribution over the interval (n, τ), where τ represents the censoring percentages. Then, 1000 samples are generated for every combination of n, c, k, σ, β_0, β_1 and censoring percentages. Each dataset generated was fitted with the LOBIIIW regression model (5.5), where $\mu_i = \beta_0 + \beta_1 x_i$. Table 5.1 displays the average estimates (AEs) and MSEs for the MLEs of c, k, σ, β_0, β_1 based on the simulation results. We can see from the data in Table 5.1 that MSEs increase along with an increase in the

censoring percentages. Additionally as predicted, the MSEs decline with sample size increases. These facts indicate that the asymptotic normal distribution accurately approximates the distribution of the estimates from a finite sample.

Table 5.1: AEs and MSEs (in parentheses) for the parameters of the LOBIIIW regression model.

CP	Parameter	Sample Size		
		50	100	300
0%	c	2.0489(0.0479)	2.0195(0.0210)	2.0086(0.0072)
	k	4.1593(0.5196)	4.0676(0.2080)	4.0195(0.0682)
	σ	1.3882(0.1946)	1.4689(0.0856)	1.4981(0.0384)
	β_0	3.1711(0.1313)	3.2008(0.0937)	3.2220(0.0688)
	β_1	2.3465(0.2200)	2.3294(0.1647)	2.3203(0.1273)
10%	c	2.0174(0.0494)	1.9894(0.0228)	1.9824(0.0078)
	k	4.3935(0.7953)	4.2926(0.3593)	4.2337(0.1380)
	σ	1.3016(0.3028)	1.3745(0.1242)	1.4457(0.0507)
	β_0	3.1143(0.1505)	3.1500(0.0777)	3.1571(0.0497)
	β_1	2.3528(0.2171)	2.3168(0.1409)	2.2673(0.0913)
30%	c	1.8797(0.0593)	1.8464(0.0437)	1.8328(0.0348)
	k	4.9652(1.8927)	4.8063(0.9988)	4.7374(0.6627)
	σ	1.0040(0.8286)	1.0962(0.4321)	1.0828(0.3557)
	β_0	3.0172(0.2901)	3.0948(0.1148)	3.1736(0.0844)
	β_1	2.4716(0.3867)	2.4157(0.2480)	2.3849(0.1784)

5.5 Sensitivity analysis: Global Influence

The initial technique for performing sensitivity analysis involves global influence through case-deletion as outlined in Cook (1977). Case deletion is a widely utilized technique for assessing the effect of removing the i^{th} record from the dataset. In the context of model (5.5), the case-deletion process is defined as

follows:

$$Y_l = \mathrm{x}_l^T \boldsymbol{\beta} + \sigma Z_l, \quad l = 1, 2, ..., n, \quad l \neq i. \tag{5.7}$$

The term indexed by "i" represents the actual expression with the exclusion of the i^{th} record. The log-likelihood function for model (5.7) is represented as $l_{(i)}(\boldsymbol{\eta})$ and let $\hat{\boldsymbol{\eta}}_i = (\hat{c}_i, \hat{k}_i, \hat{\sigma}_i, \hat{\boldsymbol{\beta}}_i^T)^T$represent the corresponding estimate of $\boldsymbol{\eta}$. To assess the influence of the i^{th} observation on the ML estimate $\hat{\boldsymbol{\eta}} = (\hat{c}, \hat{k}, \hat{\sigma}, \hat{\boldsymbol{\beta}}^{\boldsymbol{T}})^T$, the basic concept is to examine the disparity between $\hat{\boldsymbol{\eta}}_i$ and $\hat{\boldsymbol{\eta}}$. More consideration should be provided to an observation, if its exclusion substantially affects the estimates. Therefore, if $\hat{\boldsymbol{\eta}}_i$ significantly varies from $\hat{\boldsymbol{\eta}}$, this observation is considered influential observation. An initial measure for assessing global influence is the widely recognized generalized Cook distance (GCD), which is described as,

$$GCD_i(\boldsymbol{\eta}) = (\hat{\boldsymbol{\eta}}_i - \hat{\boldsymbol{\eta}})^T \{-\ddot{\boldsymbol{L}}(\hat{\boldsymbol{\eta}})\}(\hat{\boldsymbol{\eta}}_i - \hat{\boldsymbol{\eta}}).$$

Another established measure used to quantify the distinction between $\hat{\boldsymbol{\eta}}_i$ and $\hat{\boldsymbol{\eta}}$ is the likelihood displacement (LD) defined as:

$$LD_i(\boldsymbol{\eta}) = 2\{l(\hat{\boldsymbol{\eta}}) - l(\hat{\boldsymbol{\eta}}_i)\}.$$

5.6 Residual Analysis

Residual analysis is a essential stage after fitting a statistical model to the dataset. It serves for various purposes such as validating the data, evaluating the data to unveil valuable information, and confirming the assumptions of the model. Residual analysis can also help to review any deviation from the error assumption and to determine the existence of outliers. Different kinds of residual analysis have been offered in literature to execute these objectives. For instance, Collett (2023), McCullagh (2019), Fleming and Harrington (2013) and Ortega et al. 2008 have discussed about various residual analyses. This study assesses two types of residuals: martingale-type residual and deviance component residual. The martingale residual (MR) in parametric lifetime models may be defined as $r_{Mi} = \delta_i + \log[S(y_i, \hat{\boldsymbol{\eta}})]$, where $\delta_i = 0(\delta_i = 1)$ signifies censored (uncensored) observation and $S(y_i, \hat{\boldsymbol{\eta}})$ refers to the estimated survival function as specified by

(5.3). In fact, r_{Mi} spans from a minimum of $-\infty$ to maximum of $+1$. Thus, the MR for the LOBIIIW model assumes the following expression:

$$r_{Mi} = \begin{cases} 1 + \log\left\{1 - \left(1 + \left[\frac{\exp[-\exp(\hat{z}_i)]}{1-\exp[-\exp(\hat{z}_i]}\right]^{\hat{c}}\right)^{-\hat{k}}\right\} & \text{if } \delta_i = 1, \\ \log\left\{1 - \left(1 + \left[\frac{\exp[-\exp(\hat{z}_i)]}{1-\exp[-\exp \hat{z}_i]}\right]^{\hat{c}}\right)^{-\hat{k}}\right\} & \text{if } \delta_i = 0, \end{cases}$$

where $\hat{z}_i = \frac{y_i - \mathrm{x}_i^T\hat{\boldsymbol{\beta}}}{\hat{\sigma}}$.

The drawback of the MR is its significant skewness, indicating that it does not closely resemble a normal distribution. To address this issue, Therneau et al. (1990) proposed the modified deviance residual (MDR), which transforms the MR to reduce skewness. The advantage of the MDR is that its distribution approximates a normal distribution as closely as possible, facilitating more effective residual analysis, which can be formulated as:

$$r_{Di} = \text{sign}(r_{Mi})\{-2[r_{Mi} + \delta_i \log(\delta_i - r_{Mi})]\}^{1/2},$$

where r_{Mi} is the MR.

5.6.1 Simulation studies

A simulation study was executed to examine the empirical distributions of residuals r_{Mi} and r_{Di} for the values $n = 50$, 100 and 300 and censoring percentages 0%, 10%, and 30%. Here, the log-lifetimes $\log(T_1)$, $\log(T_2)$, ..., $\log(T_n)$ are obtained from the LOBIIIW model with $\mathrm{x}_i^T\boldsymbol{\beta} = \beta_0 + \beta_1 x_i$ (x_i is drawn from uniform distribution (0, 1)) using parameters values $c = 2$, $k = 4$, $\sigma = 1.5$, $\beta_0 = 3$, $\beta_1 = 2$. The censoring times C_1, C_2,...,C_n are obtained from uniform distribution over the interval $(0, \tau)$ where τ indicates the percentage of censoring. The lifetimes are computerd for each fit as follows: $y_i = \min\{\log(C_i), \log(T_i)\}$. A total of 1000 samples are generated for every combination of n, c, k, σ, β_0, β_1 and censoring percentages. We fit the LOBIIIW regression model (5.5), for each simulated dataset and find the residuals r_{Mi} and r_{Di}. Finally, the ordered residuals were plotted against the expected quantiles of the standard normal distribution. Figure 5.2 and 5.3 shows the graphs of the residuals r_{Mi} and r_{Di} plotted against the

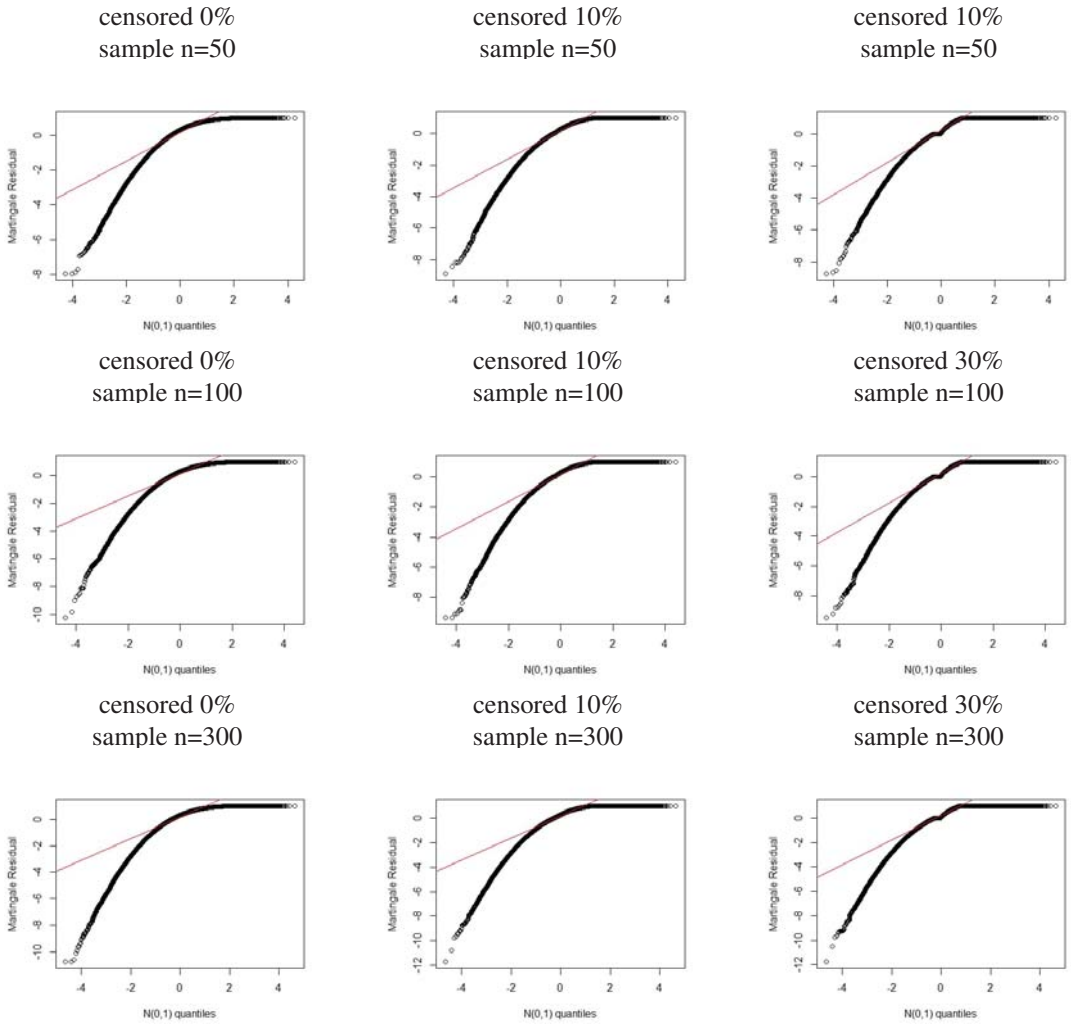

Figure 5.2: Normal probability plots for the residuals r_{Mi} for parameter values c = 2, k = 4, σ = 1.5, β_0 = 3, β_1 = 2.

expected quantiles of the standard normal distribution. Following conclusions can be drawn by observing Figure 5.2 and 5.3:

1. The empirical distribution of the residuals r_{Mi} exhibits asymmetry around zero and generally shows pronounced kurtosis.

2. The empirical distribution of the MDR closely matches the standard normal distribution, indicating a strong agreement.

3. The empirical distribution of the MDR tends to converge towards the standard normal distribution as the CP decreases or the sample size increases.

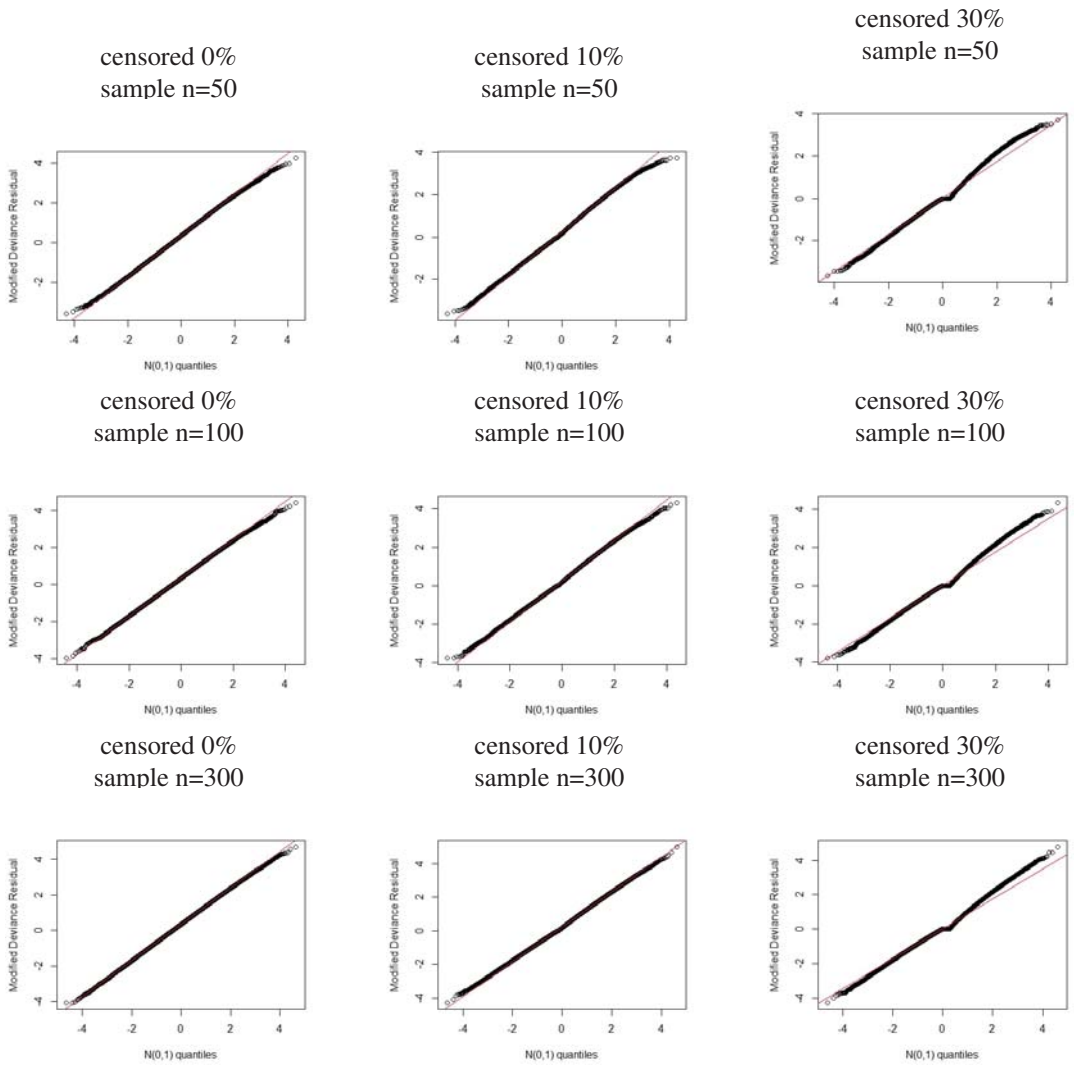

Figure 5.3: Normal probability plots for the residuals r_{Di} for parameter values c = 2, k = 4, σ = 1.5, β_0 = 3, β_1 = 2.

5.7 Application

The heart transplant dataset documented in the book by Kalbfleisch and Prentice (2011), encompassing records up to April 1st, 1974. During this timeframe, certain patients passed away before a suitable heart became available. Out of the 103 patients, 69 underwent heart transplant surgeries, with 75 deaths reported. The remaining 28 patients provided censored survival time data. Each patient ($i = 1, 2, \ldots, 103$) was related to the following explanatory variables.

- y_i = Survival times from patient entry (The duration in days from acceptance into the transplantation program to both the transplant and death was recorded for each patient) in the study.
- ν_{i1} = Age at acceptance (in years).
- ν_{i2} = Prior surgery (marked as 1 for yes and 0 for no).
- ν_{i3} = Transplant (0 = no; 1 = yes).

The TTT plot can be utilized to analyze the empirical behavior of the HRF as depicted in Figure 5.4. Figure 5.4 reveals that the dataset exhibits a clear monotonically increasing pattern. Hence, the LOBIIIW distribution is appropriate for modeling this dataset.

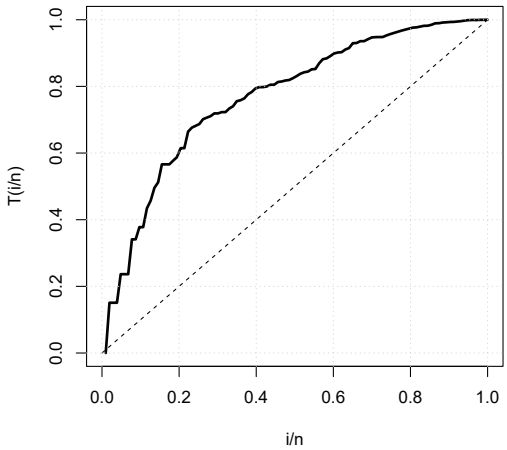

Figure 5.4: TTT plot on stanford heart transplant data.

Now, we demonstrate the results obtained from fitting the LOBIIIW regression model:

$$y_i = \beta_0 + \beta_1 \nu_{i1} + \beta_2 \nu_{i2} + \beta_3 \nu_{i3} + \sigma z_i,$$

where the errors z_i are independent random variables with a density function (5.4).

5.7.1 Results of ML and Jackknife Estimation

The MLEs for the parameters of the LOBIIIW, Log Odd Log Logistic Weibull (LOLLW), and Log Weibull (LW) regression models were computed using the R statistical software. Table 5.2 presents the parameter estimates along with their standard errors, p - values, and model selection criteria (AIC, CAIC, and BIC statistics). A comparative analysis of these models shows that the LOBIIIW model consistently yields lower values across the model selection criteria. Moreover, Table 5.3 provides the jackknife estimates of the model parameters. The results from the LOBIIIW regression model indicate that the explanatory variables ν_1, ν_2, and ν_3 are statistically significant at the 5% level for both estimation techniques. Both methods presented nearly identical estimates. The results of LOBIIIW regression model in Table 5.2 reveal that the covariates ν_1, ν_2, and ν_3 have a significant impact. We can analyze the estimated coefficients in the following way: the expected survival time is expected to decreases by approximately 94.08% ($e^{-0.061} \times 100\%$) when the age at acceptance (ν_1) increases by one unit. Variables ν_2 and ν_3 might also be interpreted in the same way.

Table 5.2: The parameter estimates for the LOBIIIW, LOLLW and LW regression models fitted to the heart transplant data.

Models	c	k	σ	β_0	β_1	β_2	β_3
LOBIIIW	1.813	2.378	3.506	5.604	-0.061	1.450	2.580
	(0.722)	(1.114)	(1.153)	(1.254)	(0.019)	(0.589)	(0.378)
				[< 0.001]	[0.001]	[0.013]	[< 0.001]
		AIC = 346.722		BIC = 365.165		CAIC=347.901	
LOLLW	4.628		6.203	8.744	-0.076	1.405	2.591
	(3.530)		(4.685)	(1.760)	(0.019)	(0.574)	(0.388)
				[< 0.001]	[< 0.001]	[0.016]	[< 0.001]
		AIC = 347.595		BIC = 363.404		CAIC = 348.470	
LW			1.465	7.974	-0.092	1.214	2.537
			(0.1314)	(0.933)	(0.020)	(0.647)	(0.373)
				[< 0.001]	[< 0.001]	[0.063]	[< 0.001]
		AIC = 353.420		BIC = 366.594		CAIC = 354.039	

Table 5.3: Jackknife estimates fitted to the heart transplant data

Parameter	Estimates	SE	95%CI	p-value
c	1.8790	0.7775	(0.3550, 3.4028)	0.0156
k	2.6486	1.2789	(0.1419, 5.1553)	0.0383
σ	3.7520	1.2375	(1.3264, 6.1775)	0.0024
β_0	5.6791	1.3454	(3.0420, 8.3161)	< 0.001
β_1	-0.0649	0.0192	(-0.1297, -0.0271)	< 0.001
β_2	1.5309	0.5878	(0.3788, 2.68290)	0.0091
β_3	2.5511	0.3804	(1.8055, 3.2967)	< 0.001

The Cox regression model, also known as the proportional hazards model, is a widely used statistical method for analyzing survival data, particularly when dealing with censored observations. This model assesses the effect of explanatory variables on the hazard rate, which represents the instantaneous risk of an event (e.g., failure or death) occurring at a given time. A key feature of the Cox model is that it does not require the specification of the baseline hazard function, making it a semi-parametric approach. Instead, it assumes that covariates have a multiplicative effect on the hazard, maintaining the proportional hazards assumption. This flexibility allows for robust estimation of covariate effects while accommodating complex survival patterns commonly seen in medical, reliability, and engineering studies. Table 5.4 shows estimates, standard errors, and p - values for the Cox regression model. The Cox regression model also exhibits that all explanatory variables are marginally significant at the 5% level, aligning with the the results of the LOBIIIW regression model. Furthermore, the LR

Table 5.4: Cox regression model estimates fitted to the heart transplant data

Parameter	Estimate	SE	p - value	CI
β_1	0.05919	0.01494	<0.0001	(0.0299, 0.0884)
β_2	-0.74266	0.44225	0.0931	(-1.6094, 0.1241)
β_3	-1.66121	0.27588	<0.0001	(-2.2019, -1.1204)
	AIC	BIC	CAIC	
	554.3522	561.3047	554.6902	

statistic is employed to compare the LOBIIIW and LW regression models by testing the hypotheses $H_0 : c = k = 1$ against $H_1 : H_0$ is not true. The test yielded a test statistic value of $w = 2(-166.3611 - (-171.7112)) = 10.7002$, with a corresponding p - value of 0.0047. These results signify a favorable indication towards the LOBIIIW regression model.

5.7.2 Results of Sensitivity and Residual Analysis

To identify the influential observations in the LOBIIIW regression model fitted to the present dataset, we have computed the global influence measures $GCD_i(\eta)$ and $LD_i(\eta)$. Figure 5.5 shows the index plots of influence measures, which signifies that the possible influential observations are 18 and 99. Another way for detecting potential outliers in the LOBIIIW regression model involves plotting the MDR (r_{Di}) against the adjusted values, as shown in Figure 5.6(a). Upon examining the MDR plot, a residual analysis indicates that observations 8 and 99 are identified as potential outliers.

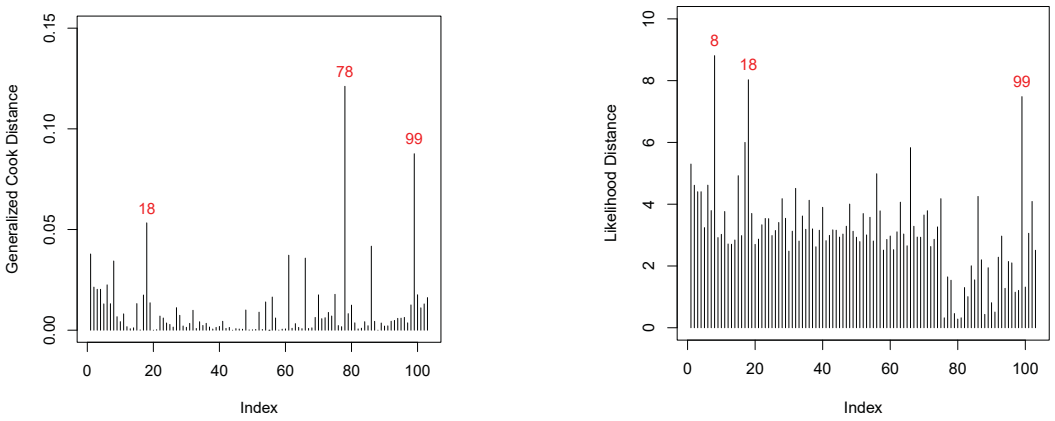

Figure 5.5: The index plot of (a) $GD_i(\eta)$ and (b) $LD_i(\eta)$ for the LOBIIIW regression model.

Both sensitivity and residual analysis determined observations 99 as the most frequently occurring possible influential points. Observation 99 indicates the longest survival time within the present censored dataset. To determine whether this observations had a significant effect on the parameter estimates, we revised the model by removing the observations. The Table 5.5 illustrates the

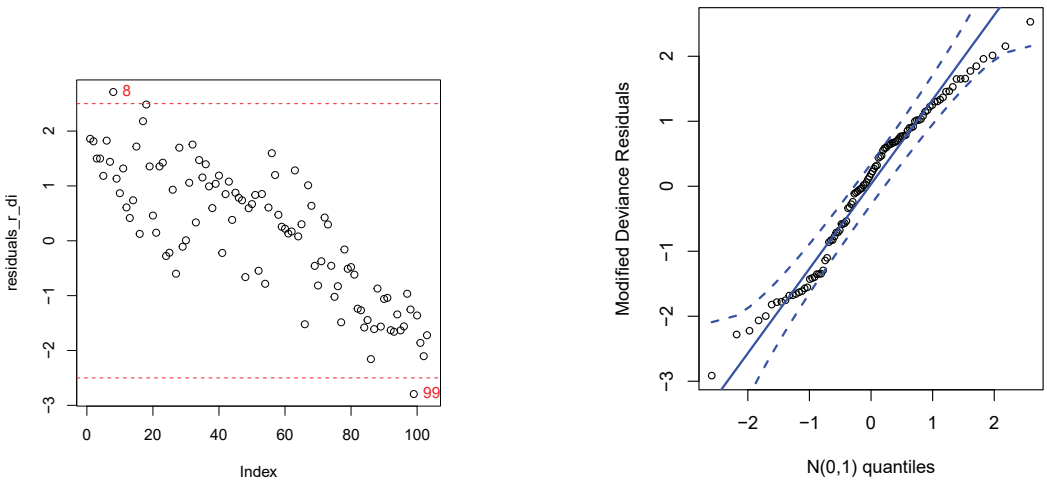

Figure 5.6: (a) Index plot of the deviance residual and (b) normal probability plot of rD_i with envelopes.

relative change in the estimated parameters, given by the formula $R = \frac{\hat{\eta}_j - \hat{\eta}_{j(i)}}{\hat{\eta}_j}$. Here, $\hat{\eta}_{j(i)}$ represents the MLEs calculated excluding the i^{th} record. We evaluate the robustness of the parameters in the LOBIIIW regression model, considering that the covariates ν_1, ν_2 and ν_3 have significance in the fitted model. Thus, the inference remains unchanged when the observation identified as potentially influential in the diagnostic plots is removed.

Table 5.5: Relative changes (expressed in percentages) along with the estimates and corresponding p-values for the datssets.

Dropped Observation	$\hat{c}$	$\hat{k}$	$\hat{\sigma}$	$\hat{\beta}_0$	$\hat{\beta}_1$	$\hat{\beta}_2$	$\hat{\beta}_3$
None	-	-	-	-	-	-	-
	1.8136	2.3785	3.5062	5.6040	-0.0610	1.4501	2.5804
				(< 0.001)	(0.0013)	(0.0138)	(< 0.001)
#99	[-2.2618]	[-12.2317]	[-2.6506]	[3.8708]	[0.2569]	[-6.734]	[-1.4363]
	1.8546	2.6694	3.5991	5.3871	-0.0609	1.5478	2.6175
				(< 0.001)	(< 0.001)	(0.0066)	(< 0.001)

In order to determine potential deviations from the assumed error distribution in model (5.5) and to detect any outliers, we depict in Figure 5.6(b) a normal probability plot of the MDR along with the generated envelope. The plot in Figure 5.6(b) recommends that the LOBIIIW regression model appears to adequately fit the dataset, with no observations occurring as possible outliers.

5.8 Summary

This Chapter presents an innovative LOBIIIW regression model designed for analyzing survival data, particularly when dealing with censored observations. The model is effective when the hazard function displays a bathtub shape. The ML and jackknife estimation techniques were utilized to estimate the parameters of a new regression model. The assumptions of the model were verified by utilizing MR and MDR. Through the use of simulation study, it has been observed that the empirical distribution of MDR approximates a standard normal distribution. In addition, GCD and LD measures were introduced to detect influential observations in the regression model. Additionally, we demonstrate the effectiveness of the model by analyzing a real dataset.

Chapter 6

Estimation of Stress-Strength Reliability Based on Weibull Burr III Distribution

6.1 Introduction

Stress-strength reliability (SSR) has become increasingly applicable across various fields. In this context, stress encompasses all factors that lead to system failure, while strength refers to all the characteristics that give stress resistance. Stress can arise from a range of circumstances that cause the system to fail, such as environmental issues, excess voltage, or temperature. In the reliability aspect, if X represents strength and Y defines stress then SSR, $R = P(X > Y)$ determines the probability that a components random strength X exceeds its stress Y. Then $1 - R$ measures the probability of system failure. The detailed discussion of SSR is presented in Chapter 1.

Bourguignon et al. (2014) introduced another Weibull generalized family of distributions using the odds ratio $\frac{G(x)}{1-G(x)}$. Then, the corresponding CDF and PDF of the Weibull generalized family introduced by Bourguignon et al. (2014)

are as follows,

$$
\begin{aligned}
F(x;\alpha,\beta) &= 1-\exp\left\{-\alpha\left[\frac{G(x,\xi)}{\bar{G}(x,\xi)}\right]^{\beta}\right\}; x>0, \alpha>0, \beta>0,\\
f(x;\alpha,\beta) &= \alpha\beta g(x,\xi)\frac{[G(x,\xi)]^{\beta-1}}{[\bar{G}(x,\xi)]^{\beta+1}}\exp\left\{-\alpha\left[\frac{G(x,\xi)}{\bar{G}(x,\xi)}\right]^{\beta}\right\}; x>0, \alpha>0, \beta>0,
\end{aligned}
$$

where $G(x;\xi)$ is a baseline CDF which depends on a parameter vector ξ, α is the scale and β is the shape parameters.

The Weibull Burr III (WBIII) distribution was formulated by Yakubu and Doguwa (2017) by using the Weibull generator concept proposed by Bourguignon (2014). Yakubu and Doguwa (2017) comprehensively discussed the essential properties of WBIII distribution such as moments, order statistics, and Rényi entropy. This distribution is a preferred choice for modeling various reliability scenarios due to its ability to represent increasing, decreasing, and bathtub-shaped curves. The CDF and PDF of WBIII distribution are defined as follows,

$$
\begin{aligned}
F_{WBIII}(x;c,k,\alpha,\beta) &= 1-\exp\left\{-\alpha[(1+x^{-c})^{k}-1]^{-\beta}\right\},\\
f_{WBIII}(x;c,k,\alpha,\beta) &= \begin{cases} \alpha\beta ckx^{-c-1}\frac{(1+x^{-c})^{-(k\beta+1)}}{[1-(1+x^{-c})^{-k}]^{\beta+1}}\exp\left\{-\alpha[(1+x^{-c})^{k}-1]^{-\beta}\right\}; \\ \qquad\qquad x>0,\ c>0,\ k>0,\quad \beta>0,\ \alpha>0 \\ 0; \quad \text{otherwise}, \end{cases} \qquad (6.1)
\end{aligned}
$$

where α is the scale and β, c, k are the shape parameters.

Various aspects of the stress-strength model have been examined by researchers, however there has been no discussion on estimating stress strength when both X and Y have WBIII and the model needs to be considered in the Bayesian framework. The analysis of the WBIII model suggest that the model can be used to evaluate the diagnostic accuracy of a new device for assessing Aortic luminal diameter (ALD) in distinguishing between individuals with low and high rupture risk and also for examining the survival rates of two groups undergoing two different treatment methods for head neck cancer (HNC) datasets. The main objective of this Chapter is to address the challenges of estimating SSR for both ALD and HNC datasets that follow the WBIII model.

The following is how the Chapter is structured. Section 6.2 deals with the expression of R. Section 6.3 includes different estimation techniques and its subsections discusses ML and Bayesian estimation. Section 6.4 compares the performance of the ML and Bayes estimators using a simulation study. Section 6.5 illustrates the models application using ALD and HNC datasets. A summary of the key findings is offered in Section 6.6.

6.2 Stress-Srength Reliability

Let X and Y be two independent random variable following WBIII distribution with parameters (α_1, β, c, k) and (α_2, β, c, k) then,

$$\begin{aligned} R &= P(Y < X) = \int_0^\infty \left[\int_0^x f_Y(y)\right] f_X(x)dx \\ &= \int_0^\infty F_Y(x) f_X(x)dx \\ &= \int_0^\infty \frac{\alpha_1 \beta c k x^{-c-1}}{\left[1 - e^{-\alpha_2[(1+x^{-c})^k - 1]^{-\beta}}\right]^{-1}} \frac{(1+x^{-c})^{-(k\beta+1)}}{[1-(1+x^{-c})^{-k}]^{\beta+1}} e^{-\alpha_1[(1+x^{-c})^k-1]^{-\beta}} dx \\ &= \frac{\alpha_2}{\alpha_1 + \alpha_2}. \end{aligned} \tag{6.2}$$

R is independent of the shape parameters β, c and k.

6.3 Estimation of SSR

6.3.1 ML Estimation

Let $(X_1, X_2, ..., X_n)$ and $(Y_1, Y_2, ..., Y_m)$ are two independent random variables following WBIII distributions with parameters (α_1, β, c, k) and (α_2, β, c, k). Then the likelihood function of $\alpha_1, \alpha_2, \beta, c, k$ for the observed samples is given as follows,

$$L = \prod_{i=1}^{n} f(x_i) \prod_{j=1}^{m} f(y_j).$$

$$
\begin{aligned}
L &= \alpha_1^n \alpha_2^m \beta^{n+m} c^{n+m} k^{n+m} \prod_{i=1}^{n} x_i^{-c-1} \frac{(1+x_i^{-c})^{-(k\beta+1)}}{[1-(1+x_i^{-c})^{-k}]^{\beta+1}} \\
&\quad \times \prod_{j=1}^{m} y_j^{-c-1} \frac{(1+y_j^{-c})^{-(k\beta+1)}}{[1-(1+y_j^{-c})^{-k}]^{\beta+1}} \\
&\quad \times \exp\left\{ -\alpha_1 \sum_{i=1}^{n} [(1+x_i^{-c})^k - 1]^{-\beta} - \alpha_2 \sum_{j=1}^{m} [(1+y_j^{-c})^k - 1]^{-\beta} \right\}.
\end{aligned}
$$

The log-likelihood function of $\alpha_1, \alpha_2, \beta, c$ and k is obtained as follows,

$$
\begin{aligned}
l = \ln \mathrm{L} &= n\ln(\alpha_1) + m\ln(\alpha_2) + (n+m)\ln(\beta) + (n+m)\ln(c) + (n+m)\ln(k) \\
&- (c+1)\sum_{i=1}^{n} \ln(x_i) - (c+1)\sum_{j=1}^{m} \ln(y_j) - (k\beta+1)\sum_{i=1}^{n} \ln(1+x_i^{-c}) \\
&- (k\beta+1)\sum_{j=1}^{m} \ln(1+y_j^{-c}) - (\beta+1)\sum_{i=1}^{n} \ln[1-(1+x_i^{-c})^{-k}] \\
&- (\beta+1)\sum_{j=1}^{m} \ln[1-(1+y_j^{-c})^{-k}] - \alpha_1 \sum_{i=1}^{n} [(1+x_i^{-c})^k - 1]^{-\beta} \\
&- \alpha_2 \sum_{j=1}^{m} [(1+y_j^{-c})^k - 1]^{-\beta}.
\end{aligned}
$$

MLE's of α_1, α_2, β, c and k say $\hat{\alpha}_1$, $\hat{\alpha}_2$, $\hat{\beta}$, $\hat{c}$ and $\hat{k}$ can be obtained by solving the following equations.

$$
\frac{\partial l}{\partial \alpha_1} = 0 \implies \frac{n}{\alpha_1} - \sum_{i=1}^{n} [(1+x_i^{-c})^k - 1]^{-\beta} = 0. \tag{6.3}
$$

$$
\frac{\partial l}{\partial \alpha_2} = 0 \implies \frac{m}{\alpha_2} - \sum_{j=1}^{m} [(1+y_j^{-c})^k - 1]^{-\beta} = 0. \tag{6.4}
$$

$$\begin{aligned}
\frac{\partial l}{\partial \beta} &= 0 \implies \frac{n+m}{\beta} - k\sum_{i=1}^{n}\ln(1+x_i^{-c}) - k\sum_{j=1}^{m}\ln(1+y_j^{-c}) \\
&- \sum_{i=1}^{n}\ln(1-(1+x_i^{-c})^{-k}) - \sum_{j=1}^{m}\ln(1-(1+y_j^{-c})^{-k}) \\
&+ \alpha_1\sum_{i=1}^{n}[(1+x_i^{-c})^k-1]^{-\beta}\ln((1+x_i^{-c})^k-1) \\
&+ \alpha_2\sum_{j=1}^{m}[(1+y_j^{-c})^k-1]^{-\beta}\ln((1+y_j^{-c})^k-1) = 0. \qquad (6.5)
\end{aligned}$$

$$\begin{aligned}
\frac{\partial l}{\partial c} &= 0 \implies \frac{n+m}{c} - \sum_{i=1}^{n}\ln(x_i) - \sum_{j=1}^{m}\ln(y_j) \\
&+ (k\beta+1)\sum_{i=1}^{n}\frac{x_i^{-c}\ln(x_i)}{1+x_i^{-c}} + (k\beta+1)\sum_{j=1}^{m}\frac{y_j^{-c}\ln(y_j)}{1+y_j^{-c}} \\
&+ (\beta+1)\sum_{i=1}^{n}\frac{k(1+x_i^{-c})^{-k-1}}{[1-(1+x_i^{-c})^{-k}]}x_i^{-c}\ln(x_i) \\
&+ (\beta+1)\sum_{j=1}^{m}\frac{k(1+y_j^{-c})^{-k-1}}{[1-(1+y_j^{-c})^{-k}]}y_j^{-c}\ln(y_j) \\
&- \sum_{i=1}^{n}\alpha_1\beta k[(1+x_i^{-c})^k-1]^{-\beta-1}(1+x_i^{-c})^{k-1}x_i^{-c}\ln(x_i) \\
&- \sum_{j=1}^{m}\alpha_2\beta k[(1+y_j^{-c})^k-1]^{-\beta-1}(1+y_j^{-c})^{k-1}y_j^{-c}\ln(y_j) = 0. \qquad (6.6)
\end{aligned}$$

$$\begin{aligned}
\frac{\partial l}{\partial k} &= 0 \implies \frac{n+m}{k} - \beta\sum_{i=1}^{n}\ln(1+x_i^{-c}) - \beta\sum_{j=1}^{m}\ln(1+y_j^{-c}) \\
&- (\beta+1)\sum_{i=1}^{n}\frac{(1+x_i^{-c})^k\ln(1+x_i^{-c})}{[1-(1+x_i^{-c})^{-k}]} \\
&- (\beta+1)\sum_{j=1}^{m}\frac{(1+y_j^{-c})^k\ln(1+y_j^{-c})}{[1-(1+y_j^{-c})^{-k}]} \\
&+ \alpha_1\beta\sum_{i=1}^{n}[(1+x_i^{-c})^k-1]^{-\beta-1}(1+x_i^{-c})^k\ln(1+x_i^{-c}) \\
&+ \alpha_2\beta\sum_{j=1}^{m}[(1+y_j^{-c})^k-1]^{-\beta-1}(1+y_j^{-c})^k\ln(1+y_j^{-c}) = 0. \qquad (6.7)
\end{aligned}$$

From equation (6.3) and (6.4), we have

$$\hat{\alpha}_1 = \frac{n}{\sum_{i=1}^{n}[(1+x_i^{-c})^k - 1]^{-\beta}} \tag{6.8}$$

$$\hat{\alpha}_2 = \frac{m}{\sum_{j=1}^{m}[(1+y_j^{-c})^k - 1]^{-\beta}}, \tag{6.9}$$

and $\hat{\beta}, \hat{c}$ and $\hat{k}$ can be obtained by solving the non-linear equations (6.5), (6.6) and (6.7) using $\hat{\alpha}_1$ and $\hat{\alpha}_2$ instead of α_1 and α_2, then solve the equations using Newton-Raphson method. Hence the MLE of R becomes,

$$\hat{R} = \frac{\hat{\alpha_2}}{\hat{\alpha_1} + \hat{\alpha_2}}. \tag{6.10}$$

Here we suggest the asymptotic approach of MLE and parametric bootstrap method for the construction of the actual confidence interval of R.

6.3.1.1 Asymptotic Confidence Interval

This section deals with obtaining the asymptotic distribution of the MLE of model parameters and R. Knowing the asymptotic distribution of R enables us to obtain its corresponding asymptotic confidence interval. The Fisher information matrix of $\Delta = (\alpha_1, \alpha_2, \beta, c, k)$ is given as:

$$I(\Delta) = E \begin{pmatrix} -\frac{\partial^2 l}{\partial \alpha_1^2} & -\frac{\partial^2 l}{\partial \alpha_1 \partial \alpha_2} & -\frac{\partial^2 l}{\partial \alpha_1 \partial \beta} & -\frac{\partial^2 l}{\partial \alpha_1 \partial c} & -\frac{\partial^2 l}{\partial \alpha_1 \partial k} \\ -\frac{\partial^2 l}{\partial \alpha_2 \partial \alpha_1} & -\frac{\partial^2 l}{\partial \alpha_2^2} & -\frac{\partial^2 l}{\partial \alpha_2 \partial \beta} & -\frac{\partial^2 l}{\partial \alpha_2 \partial c} & -\frac{\partial^2 l}{\partial \alpha_2 \partial k} \\ -\frac{\partial^2 l}{\partial \beta \partial \alpha_1} & -\frac{\partial^2 l}{\partial \beta \partial \alpha_2} & -\frac{\partial^2 l}{\partial \beta^2} & -\frac{\partial^2 l}{\partial \beta \partial c} & -\frac{\partial^2 l}{\partial \beta \partial k} \\ -\frac{\partial^2 l}{\partial c \partial \alpha_1} & -\frac{\partial^2 l}{\partial c \partial \alpha_2} & -\frac{\partial^2 l}{\partial c \partial \beta} & -\frac{\partial^2 l}{\partial c^2} & -\frac{\partial^2 l}{\partial c \partial k} \\ -\frac{\partial^2 l}{\partial k \partial \alpha_1} & -\frac{\partial^2 l}{\partial k \partial \alpha_2} & -\frac{\partial^2 l}{\partial k \partial \beta} & -\frac{\partial^2 l}{\partial k \partial c} & -\frac{\partial^2 l}{\partial k^2} \end{pmatrix}.$$

Using the asymptotic distribution of the MLE's and the multivariate central limit theorem, it is shown that as $n \to \infty$, $m \to \infty$,

$$\sqrt{n+m}(\hat{\Delta} - \Delta) \xrightarrow{\mathrm{d}} N(0, I^{-1}(\Delta)),$$

where $\xrightarrow{\mathrm{d}}$ denotes convergence in distribution and $I^{-1}(\Delta)$ denotes the inverse of the Fisher information matrix $I(\Delta)$. To determine the asymptotic normality of

R, we first consider,

$$d^T = \left(\frac{\partial R}{\partial \alpha_1}, \frac{\partial R}{\partial \alpha_2}, \frac{\partial R}{\partial \beta}, \frac{\partial R}{\partial c}, \frac{\partial R}{\partial k}\right),$$

where T denotes the transpose operation and

$$\frac{\partial R}{\partial \alpha_1} = \frac{-\alpha_2}{(\alpha_1+\alpha_2)^2}, \quad \frac{\partial R}{\partial \alpha_2} = \frac{\alpha_1}{(\alpha_1+\alpha_2)^2}, \quad \frac{\partial R}{\partial \beta} = \frac{\partial R}{\partial c} = \frac{\partial R}{\partial k} = 0.$$

With the use of delta method proposed by Krishnamoorthy and Lin (2010), the asymptotic distribution of $\hat{R}$ satisfies,

$$\sqrt{n+m}(\hat{R} - R) \to N(0, \mathrm{Var}(\hat{R})),$$

where,

$$\mathrm{Var}(\hat{R}) \simeq d^T I^{-1}(\Delta) d.$$

Thus an approximate $100(1-\gamma)\%$ confidence interval for R is given by,

$$\left(\hat{R} \pm Z_{\frac{\gamma}{2}} \sqrt{\mathrm{Var}(\hat{R})}\right),$$

where $Z_{\frac{\gamma}{2}}$ is the upper $\frac{\gamma}{2}$ percentile of the standard normal distribution. The components of the Fisher information matrix are given by,

$$
\begin{aligned}
\frac{\partial^2 l}{\partial \alpha_1^2} &= -\frac{n}{\alpha_1^2}. \\
\frac{\partial^2 l}{\partial \alpha_2^2} &= -\frac{m}{\alpha_2^2}, \\
\frac{\partial^2 l}{\partial \alpha_1 \alpha_2} &= 0. \\
\frac{\partial^2 l}{\partial \alpha_1 \partial \beta} &= \sum_{i=1}^{n} [(1+x_i^{-c})^k - 1]^{-\beta} \ln[(1+x_i^{-c})^k - 1]. \\
\frac{\partial^2 l}{\partial \alpha_1 \partial c} &= -\beta k \sum_{i=1}^{n} x_i^{-c} \ln(x_i)(1+x_i^{-c})^{k-1}[(1+x_i^{-c})^k - 1]^{-(\beta+1)}. \\
\frac{\partial^2 l}{\partial \alpha_1 \partial k} &= \beta \sum_{i=1}^{n} (1+x_i^{-c})^k \ln(1+x_i^{-c})[(1+x_i^{-c})^k - 1]^{-(\beta+1)}. \\
\frac{\partial^2 l}{\partial \alpha_2 \partial \beta} &= = \sum_{j=1}^{m} [(1+y_j^{-c})^k - 1]^{-\beta} \ln[(1+y_j^{-c})^k - 1]. \\
\frac{\partial^2 l}{\partial \alpha_2 \partial c} &= -\beta k \sum_{j=1}^{m} y_j^{-c} \ln(y_j)(1+y_j^{-c})^{k-1}[(1+y_j^{-c})^k - 1]^{-(\beta+1)}. \\
\frac{\partial^2 l}{\partial \alpha_2 \partial k} &= \beta \sum_{j=1}^{m} (1+y_j^{-c})^k \ln(1+y_j^{-c})[(1+y_j^{-c})^k - 1]^{-(\beta+1)}. \\
\frac{\partial^2 l}{\partial \beta^2} &= -\frac{(m+n)}{\beta^2} - \alpha_1 \sum_{i=1}^{n} [(1+x_i^{-c})^k - 1]^{-\beta} \ln[(1+x_i^{-c}]^k - 1) \\
&- \alpha_2 \sum_{j=1}^{m} [(1+y_j^{-c})^k - 1]^{-\beta} \ln[(1+y_j^{-c}]^k - 1). \\
\frac{\partial^2 l}{\partial k^2} &= -\frac{m+n}{k^2} - \sum_{i=1}^{n} (1+x_i^{-c})^k [(1+x_i^{-c})^k - 1]^{-\beta-2} \{-[(1+x_i^{-c})^k - 1]^{\beta} \\
&+ (\alpha_1 - [(1+x_i^{-c})^k - 1]^{\beta})\beta + (1+x_i^{-c})^k \alpha_1 \beta^2\} (\ln(1+x_i^{-c})^2) \\
&- \sum_{j=1}^{m} (1+y_j^{-c})^k [(1+y_j^{-c})^k - 1]^{-\beta-2} \{\alpha_2 \beta [1 + (1+y_j^{-c})^k \beta] \\
&- [(1+y_j^{-c})^k - 1]^{\beta}(1+\beta)\} (\ln(1+y_j^{-c}))^2.
\end{aligned}
$$

$$
\begin{aligned}
\frac{\partial^2 l}{\partial\beta\partial c} &= k\sum_{i=1}^{n}\frac{x_i^{-c}\ln(x_i)}{(1+x_i^{-c})} + k\sum_{j=1}^{m}\frac{y_j^{-c}\ln(y_j)}{(1+y_j^{-c})} + \sum_{i=1}^{n}\frac{k(1+x_i^{-c})^{-k-1}x_i^{-c}\ln(x_i)}{[1-(1+x_i^{-c})^{-k}]} \\
&+ \sum_{j=1}^{m}\frac{k(1+y_j^{-c})^{-k-1}y_j^{-c}\ln(y_j)}{[1-(1+y_j^{-c})^{-k}]} \\
&- \alpha_1 k\sum_{i=1}^{n}[(1+x_i^{-c})^k-1]^{-\beta-1}(1+x_i^{-c})^{k-1}x_i^{-c}\ln(x_i) \\
&+ \sum_{i=1}^{n}\ln[(1+x_i^{-c})^k-1]\alpha_1 k\beta[(1+x_i^{-c})^k-1]^{-\beta-1}(1+x_i^{-c})^{k-1}x_i^{-c}\ln(x_i) \\
&- \alpha_2 k\sum_{j=1}^{m}[(1+y_j^{-c})^k-1]^{-\beta-1}(1+y_j^{-c})^{k-1}y_j^{-c}\ln(y_j) \\
&+ \sum_{j=1}^{m}\ln[(1+y_j^{-c})^k-1]\alpha_1 k\beta[(1+y_j^{-c})^k-1]^{-\beta-1}(1+y_j^{-c})^{k-1}y_j^{-c}\ln(y_j). \\
\frac{\partial^2 l}{\partial\beta\partial k} &= -\frac{n+m}{\beta^2} - \sum_{i=1}^{n}\ln(1+x_i^{-c}) - \sum_{j=1}^{m}\ln(1+y_j^{-c}) \\
&- \sum_{i=1}^{n}\frac{(1+x_i^{-c})^{-k}\ln(1+x_i^{-c})}{[1-(1+x_i^{-c})^{-k}]} - \sum_{j=1}^{m}\frac{(1+y_j^{-c})^{-k}\ln(1+y_j^{-c})}{[1-(1+y_j^{-c})^{-k}]} \\
&+ \alpha_1\sum_{i=1}^{n}[(1+x_i^{-c})^k-1]^{-\beta-1}(1+x_i^{-c})^k\ln(1+x_i^{-c}) \\
&- \alpha_1\beta\sum_{i=1}^{n}\ln[(1+x_i^{-c})^k-1][(1+x_i^{-c})^k-1]^{-\beta-1}(1+x_i^{-c})^k\ln(1+x_i^{-c}) \\
&+ \alpha_2\sum_{j=1}^{m}[(1+y_j^{-c})^k-1]^{-\beta-1}(1+y_j^{-c})^k\ln(1+y_j^{-c}) \\
&- \alpha_2\beta\sum_{j=1}^{m}\ln[(1+y_j^{-c})^k-1][(1+y_j^{-c})^k-1]^{-\beta-1}(1+y_j^{-c})^k\ln(1+y_j^{-c}).
\end{aligned}
$$

$$\frac{\partial^2 l}{\partial c^2} = -\frac{m+n}{c^2} - \frac{\sum_{i=1}^{n} x_i^c(1+k\beta)(\ln(x_i))^2}{(1+x_i^{-c})^2}$$
$$- \frac{k\sum_{i=1}^{n}(1+x_i^{-c})^k[(1+x_i^{-c})^k-1]^{-\beta-2}\alpha_1\beta\{k-x_i^c[(1+x_i^{-c})^k-1]+k(1+x_i^{-c})^k\beta\}(\ln(x_i))^2}{(1+x_i^c)^2}$$
$$+ \frac{k^2\sum_{i=1}^{n}(1+\beta)(\ln(x_i))^2}{(1+x_i^c)^2[(1+x_i^{-c})^k-1]^2} - \frac{k(1+\beta)\sum_{i=1}^{n}(-k+x_i^c)(\ln(x_i))^2}{(1+x_i^c)^2[(1+x_i^{-c})^k-1]}$$
$$- \frac{\alpha_2 k\beta\sum_{j=1}^{m}(1+y_j^c)^k[(1+y_j^{-c})^k-1]^{-\beta-2}\{k-y_j^c[(1+y_j^{-c})^k-1]+k(1+y_j^{-c})^k\beta\}(\ln(y_j))^2}{(1+y_j^c)^2}$$
$$- \frac{\sum_{j=1}^{m} y_j^c(1+k\beta)(\ln(y_j))^2}{(1+y_j^{-c})^2} + \frac{k^2\sum_{j=1}^{m}(1+\beta)(\ln(y_j))^2}{(1+y_j^c)^2[(1+y_j^{-c})^k-1]^2}$$
$$- \frac{k(1+\beta)\sum_{j=1}^{m}(-k+y_j^c)(\ln(y_j))^2}{(1+y_j^c)^2[(1+y_j^{-c})^k-1]}.$$

$$\frac{\partial^2 l}{\partial c\partial k} = \frac{1}{(1+x_i^c)}\sum_{i=1}^{n}[(1+x_i^{-c})^k-1]^{-2-\beta}\ln(x_i)\times$$
$$\left\{[(1+x_i^{-c})^k-1]\left([(1+x_i^{-c})^k-1]^{\beta}+(1+x_i^{-c})^k\left([(1+x_i^{-c})^k-1]^{\beta}-\alpha_1\right)\beta\right)\right\}$$
$$+\frac{\sum_{i=1}^{n}[(1+x_i^{-c})^k-1]^{-2-\beta}\ln(x_i)}{(1+x_i^c)}$$
$$\times[k(1+x_i^{-c})^k(-[(1+x_i^{-c})^k-1]^{\beta}+(\alpha_1-[(1+x_i^{-c})^k-1]^{\beta})\beta$$
$$+\alpha_1\beta^2(1+x_i^{-c})^k)\ln(1+x_i^{-c})] + \frac{1}{(1+y_j^c)}\sum_{j=1}^{m}[(1+y_j^{-c})^k-1]^{-2-\beta}\ln(y_j)$$
$$\times\left\{\left[(1+y_j^{-c})^k-1\right]\left(-\alpha_2\beta(1+y_j^c)^k+[(1+y_j^{-c})^k-1]^{\beta}[(1+y_j^{-c})^k\beta+1]\right)\right\}$$
$$+\frac{1}{(1+y_j^c)}\sum_{j=1}^{m}[(1+y_j^{-c})^k-1]^{-2-\beta}\ln(y_j)$$
$$\times\left\{k(1+y_j^{-c})^k\ln(1+y_j^{-c})\left(\alpha_2\beta\left[1+\beta(1+y_j^{-c})^k\right]-\left[(1+y_j^{-c})^k-1\right]^{\beta}(1+\beta)\right)\right\}.$$

6.3.1.2 Bootstrap Confidence Interval

In this section, we propose another approach termed parametric bootstrap method for estimating confidence intervals of R introduced by Efron (1982). This method is particularly useful when the normality assumption is not met, especially in cases where the sample size is small. In such situations, the asymptotic

confidence interval does not perform well. The parametric bootstrap estimates of R, are obtained using the following algorithm.

Algorithm 1

1: Suppose $\underline{x} = (x_1, x_2, ..., x_n)$ and $\underline{y} = (y_1, y_2, ..., y_m)$ be the independent samples taken from WBIII(α_1, β, c, k) and WBIII(α_2, β, c, k), then compute the MLE's ($\hat{\alpha}_1$, $\hat{\alpha}_2$, $\hat{\beta}$, $\hat{c}$, $\hat{k}$) of (α_1, α_2, β, c, k).

2: Generate an independent bootstrap sample (x_1^*, x_2^*, ..., x_n^*) and (y_1^*, y_2^*, ..., y_m^*) from WBIII($\hat{\alpha}_1$, $\hat{\beta}$, $\hat{c}$, $\hat{k}$)and WBIII($\hat{\alpha}_2$, $\hat{\beta}$, $\hat{c}$, $\hat{k}$) respectively, then compute bootstrap estimate of R say $\hat{R}^*$ using (6.2).

3: Step 2 is repeated N times in order to obtain the parametric bootstrap estimates $\hat{R}_1^*, \hat{R}_2^*, ..., \hat{R}_N^*$ of R.

4: Let $h_1(x) = P(\hat{R}^* \leq x)$ be the CDF of $\hat{R}^*$. Define $\hat{R}_{Boot-p}(x) = h_1^{-1}(x)$ for a given x. The approximate $100(1-\gamma)\%$ confidence interval of R is given by,

$$\left(\hat{R}_{Boot-p}\left(\frac{\gamma}{2}\right), \hat{R}_{Boot-p}\left(1-\frac{\gamma}{2}\right)\right).$$

6.3.2 Bayesian estimation of *R*

The Bayes estimation of R is computed in this part under the assumption that both the scale parameter α_1, α_2 and shape parameters β, c, k are random variables. To perform Bayesian estimation, we need to specify the prior distribution for the unknown parameter. Among the informative priors, the gamma distribution is a popular choice due to its flexibility, richness, and computational simplicity. Therefore, we have opted for an independent gamma prior for all the five independent parameters namely $\alpha_1, \alpha_2, \beta, c,$ and k,

$$\begin{aligned}
\pi(\alpha_1) &\propto \alpha_1^{a_1-1}\exp(-b_1\alpha_1); \quad \alpha_1 > 0, a_1 > 0, b_1 > 0,\\
\pi(\alpha_2) &\propto \alpha_2^{a_2-1}\exp(-b_2\alpha_2); \quad \alpha_2 > 0, a_2 > 0, b_2 > 0,\\
\pi(\beta) &\propto \beta^{a_3-1}\exp(-b_3\beta); \quad \beta > 0, a_3 > 0, b_3 > 0,\\
\pi(c) &\propto c^{a_4-1}\exp(-b_4 c); \quad c > 0, a_4 > 0, b_4 > 0,\\
\pi(k) &\propto k^{a_5-1}\exp(-b_5 k); \quad k > 0, a_5 > 0, b_5 > 0,
\end{aligned}$$

where a_i and b_i $(i = 1, 2, 3, 4, 5)$ are the hyper-parameters which is assumed to be known and non-negative. When the hyper parameters are zero, it corresponds

to the case of non-informative priors. Then the gamma prior becomes,

$$\pi(\alpha_t) \propto \frac{1}{\alpha_t}; t = 1, 2.$$

Several studies discuss this non-informative type of gamma prior in real data illustration and simulation processes and it coincides with Jeffrey scale invariant prior. The non-informative prior for the shape parameters β, c, and k can be expressed in the following manner,

$$\begin{aligned} \pi(\beta) &\propto \frac{1}{\beta}, \beta > 0, \\ \pi(c) &\propto \frac{1}{c}, c > 0, \\ \pi(k) &\propto \frac{1}{k}, k > 0. \end{aligned}$$

After assuming the prior distribution of Θ (model vector parameter), the posterior distribution of Θ is given by,

$$\pi^*(\Theta \mid data) \propto L(\Theta \mid data)\pi(\Theta),$$

where $L(\Theta \mid data)$ is the likelihood function and $\pi(\Theta)$ denotes the joint prior distribution. Then the joint posterior density function in the case of informative prior is given by,

$$\begin{aligned} \pi^*(\alpha_1, \alpha_2, \beta, c, k \mid \text{data}) &\propto \alpha_1^{n+a_1-1}\alpha_2^{m+a_2-1}\beta^{n+m+a_3-1}c^{n+m+a_4-1}k^{n+m+a_5-1} \\ &\times \prod_{i=1}^{n} x_i^{-c-1}\frac{(1+x_i^{-c})^{-(k\beta+1)}}{[1-(1+x_i^{-c})^{-k}]^{\beta+1}} \\ &\times \prod_{j=1}^{m} y_j^{-c-1}\frac{(1+y_j^{-c})^{-(k\beta+1)}}{[1-(1+y_j^{-c})^{-k}]^{\beta+1}} \\ &\times e^{-\alpha_1\left(b_1+\sum_{i=1}^{n}[(1+x_i^{-c})^k-1]^{-\beta}\right)-\alpha_2\left(b_2+\sum_{j=1}^{m}[(1+y_j^{-c})^k-1]^{-\beta}\right)} \\ &\times e^{-b_3\beta-b_4c-b_5k}. \end{aligned} \tag{6.11}$$

6.3.2.1 Bayes estimators under Symmetric and Asymmetric loss function

In this section, we deal with both symmetric and asymmetric loss functions. The most commonly used loss function in Bayesian estimation is the symmetric loss function which assigns equal weight to overestimation and underestimating and the squared error loss function (SELF) is one of them. Asymmetric loss functions, like the linex loss function (LLF) can be useful in scenarios where overestimation or underestimation is more significant than the other. The SELF and LLF are defined by,

$$\begin{aligned} L_{SELF}(\theta,\hat{\theta}) &= (\theta-\hat{\theta})^2, \\ L_{LLF}(\theta,\hat{\theta}) &= \exp[v(\theta-\hat{\theta})]-v(\theta-\hat{\theta})-1, \quad v\neq 0. \end{aligned}$$

Then the bayes estimate under SELF and LLF is given by,

$$\hat{R}_{SELF} = \int_0^\infty\int_0^\infty\int_0^\infty\int_0^\infty\int_0^\infty R\pi^*(\alpha_1,\alpha_2,\beta,c,k\mid \text{data})d\alpha_1 d\alpha_2 d\beta dc dk,$$

$$\hat{R}_{LLF}=-\frac{1}{v}\ln\left[\int_0^\infty\int_0^\infty\int_0^\infty\int_0^\infty\int_0^\infty e^{-vR}\pi^*(\alpha_1,\alpha_2,\beta,c,k\mid \text{data})d\alpha_1 d\alpha_2 d\beta dc dk\right],$$

where v is a constant such that $v>0$.

As the Bayes estimators involve integrals for which an analytical solution is impossible, numerical approaches are required to find their solutions. In this regard, MCMC methods have been proposed for Bayesian computation. MCMC involves a random process that selects a new value from the posterior distribution based on the previous value. This repeating approach produces a Markov Chain of values, which represents a sample drawn from the posterior distribution. The commonly used MCMC techniques are the Gibbs sampler and the MH algorithm. The Gibbs sampler is useful when sampling from a multivariate posterior is not possible, but sampling from a conditional distribution for each parameter is possible.

The posterior conditional distribution of $\alpha_1,\alpha_2,\beta,c$ and k are expressed as fol-

lows,

$$\pi_1^*(\alpha_1 \mid \beta, c, k, \text{data}) \propto \alpha_1^{n+a_1-1} \exp\left[-\alpha_1\left(b_1 + \sum_{i=1}^{n}[(1+x_i^{-c})^k - 1]^{-\beta}\right)\right],$$

$$\pi_2^*(\alpha_2 \mid \beta, c, k, \text{data}) \propto \alpha_2^{m+a_2-1} \exp\left[-\alpha_2\left(b_2 + \sum_{j=1}^{m}[(1+y_j^{-c})^k - 1]^{-\beta}\right)\right],$$

$$\begin{aligned}\pi_3^*(\beta \mid \alpha_1, \alpha_2, c, k, \text{data}) \propto{}& \beta^{n+m+a_3-1} \prod_{i=1}^{n} x_i^{-c-1} \frac{(1+x_i^{-c})^{-(k\beta+1)}}{[1-(1+x_i^{-c})^{-k}]^{\beta+1}} \\ &\times \prod_{j=1}^{m} y_j^{-c-1} \frac{(1+y_j^{-c})^{-(k\beta+1)}}{[1-(1+y_j^{-c})^{-k}]^{\beta+1}} \exp[-b_3\beta] \\ &\times \exp\left[-\alpha_1 \sum_{i=1}^{n}[(1+x_i^{-c})^k - 1]^{-\beta} - \alpha_2 \sum_{j=1}^{m}[(1+y_j^{-c})^k - 1]^{-\beta}\right],\end{aligned}$$

$$\begin{aligned}\pi_4^*(c \mid \alpha_1, \alpha_2, \beta, k, \text{data}) \propto{}& c^{n+m+a_4-1} \prod_{i=1}^{n} x_i^{-c-1} \frac{(1+x_i^{-c})^{-(k\beta+1)}}{[1-(1+x_i^{-c})^{-k}]^{\beta+1}} \\ &\times \prod_{j=1}^{m} y_j^{-c-1} \frac{(1+y_j^{-c})^{-(k\beta+1)}}{[1-(1+y_j^{-c})^{-k}]^{\beta+1}} \exp[-b_4 c] \\ &\times \exp\left[-\alpha_1 \sum_{i=1}^{n}[(1+x_i^{-c})^k - 1]^{-\beta} - \alpha_2 \sum_{j=1}^{m}[(1+y_j^{-c})^k - 1]^{-\beta}\right],\end{aligned}$$

$$\begin{aligned}\pi_5^*(k \mid \alpha_1, \alpha_2, \beta, c, \text{data}) \propto{}& k^{n+m+a_5-1} \prod_{i=1}^{n} x_i^{-c-1} \frac{(1+x_i^{-c})^{-(k\beta+1)}}{[1-(1+x_i^{-c})^{-k}]^{\beta+1}} \\ &\times \prod_{j=1}^{m} y_j^{-c-1} \frac{(1+y_j^{-c})^{-(k\beta+1)}}{[1-(1+y_j^{-c})^{-k}]^{\beta+1}} \exp[-b_5 k] \\ &\times \exp\left[-\alpha_1 \sum_{i=1}^{n}[(1+x_i^{-c})^k - 1]^{-\beta} - \alpha_2 \sum_{j=1}^{m}[(1+y_j^{-c})^k - 1]^{-\beta}\right].\end{aligned}$$

Sample of α_1 and α_2 can be easily generated since the posterior distribution of α_1 and α_2 follows gamma distribution. But the posterior PDFs of β, c, k are not

in standard distributional forms, so we cannot directly obtain samples from it. To address this, we utilize the Metropolis sampling method within the Gibbs sampling procedure to generate samples from conditional posterior distributions using a normal proposal distribution. The MH algorithm, originally developed by Metropolis et al. (1953) and later extended by Hastings (1970) is employed to generate samples from an arbitrary probability distribution function. The steps of the simulation process are given in Algorithm 2.

Algorithm 2

1: Set the intial values of $\alpha_1, \alpha_2, b, c, k$ as $(\alpha_1^0, \alpha_2^0, b^0, c^0, k^0)$.

2: Set t = 1.

3: Generate $\alpha_1^{(t)}$ from Gamma$(n + a_1, (b_1 + \sum_{i=1}^{n}[(1 + x_i^{-c^{(t-1)}})^{k^{(t-1)}} - 1]^{-\beta^{(t-1)}}))$.

4: Generate $\alpha_2^{(t)}$ from Gamma$(m + a_2, (b_2 + \sum_{j=1}^{m}[(1 + y_j^{-c^{(t-1)}})^{k^{(t-1)}} - 1]^{-\beta^{(t-1)}}))$.

5: Using the Metropolis method, generate $\beta^{(t)}$from $\pi_3^*(\beta^{(t-1)} \mid \alpha_1^{(t)}, \alpha_2^{(t)}, c^{(t-1)}, k^{(t-1)}, \text{data})$ with normal proposal distribution.

6: Using the Metropolis method, generate $c^{(t)}$ from $\pi_4^*(c^{(t-1)} \mid \alpha_1^{(t)}, \alpha_2^{(t)}, \beta^{(t)}, k^{(t-1)}, \text{data})$ with normal proposal distribution.

7: Using the Metropolis method, generate $k^{(t)}$ from $\pi_5^*(k^{(t-1)} \mid \alpha_1^{(t)}, \alpha_2^{(t)}, \beta^{(t)}, c^{(t)}, \text{data})$ with normal proposal distribution.

8: Compute $R^{(t)}$ from Eq (6.2).

9: Set $t = t + 1$.

10: Repeat steps: 3–9 N times.

11: Then an approximate Bayes estimators of R under SELF and LLF are given by

$$\hat{R}_{SELF} = \frac{1}{N-M}\sum_{i=M+1}^{N} R^i, \tag{6.12}$$

$$\hat{R}_{LLF} = \frac{-1}{v}\log\left[\frac{1}{N-M}\sum_{i=M+1}^{N} e^{-vR^i}\right], \tag{6.13}$$

where M is the burn in period.

6.4 Simulation

A Monte Carlo simulation was conducted to analyze the performance of different proposed estimation methods. The comparison of ML and BEs using informative and non-informative priors under SELF (LLF) is conducted in terms of estimated risk (ER). Additionally, we obtain the coverage probabilities (CP) and confidence lengths (CL) of the asymptotic, bootstrap, and highest posterior density (HPD) credible intervals for informative and non-informative cases. The simulation study is conducted via R software and the nlm function is used to find the estimated values in MLE. The shape parameters β, c and k are held constant at 1 for all cases, and we investigate four different combinations of (α_1, α_2) = (10, 5), (5.6, 6.9), (2, 6) and (0.3, 3), which correspond to R values 0.33, 0.55, 0.75 and 0.90. Sample sizes of (n, m) = (20, 20), (35, 35), (50, 50), (75, 75) and (100, 100) are considered.

Bayes estimators are computed using the M-H algorithm under the SELF and LLF. The hyperparameters of the gamma prior are chosen such that the prior means is equal to the true value of the parameters and the prior variance are equal to 1. This is denoted as Prior 1. When the hyper-parameters are equal to zero, which is the case of a non-informative prior term denoted by Prior 2. The first 7000 iterations are eliminated to reduce the distributions initial influence which is referred to as the burn-in process. R statistical software is used to perform all the simulation calculations. The 95% HPD credible intervals is obtained using the HPDinterval command in R. Tables 6.1, 6.2, 6.3 and 6.4 present the average estimate (AV) of R and risk of MLE and BEs under SELF and LLF for different R values. The CP and CL of the asymptotic, bootstrap and HPD credible intervals are shown in Table 6.5. The ER of SELF and LLF has the form,

$$\begin{aligned} ER_{SELF}(\hat{\theta}) &= \frac{1}{N}\sum_{i=1}^{N}(\theta - \hat{\theta})^2, \\ ER_{LLF}(\hat{\theta}) &= \frac{1}{N}\sum_{i=1}^{N}\exp[v(\theta - \hat{\theta})] - v(\theta - \hat{\theta}) - 1, \end{aligned}$$

where $\hat{\theta}$ is the bayes estimate of θ and N is the number of replications. The following results are obtained from Table 6.1, 6.2, 6.3, 6.4 and 6.5.

- The risk of the proposed estimators decreases as the sample size increases.

- The Bayesian and ML results become more similar as the sample size increases and informative priors outperform non-informative priors and MLE estimators.

- The performance of Bayes estimators under the LINEX loss function outperforms all other estimators. The BEs under the non-informative prior are equally efficient as the MLE in estimating the parameters since the risk values are getting closer as sample size increases.

- The asymmetric loss function shows lower risk values than the symmetric loss function.

- For all estimation techniques, the CL of asymptotic, bootstrap confidence and HPD credible intervals are getting decreased as the sample size increases, indicating estimated reliability is in the most accurate interval.

- Also the CP are getting increased as the sample sizes increases. In terms of CL and CP, boot-p confidence intervals outperform asymptotic confidence intervals. HPD credible intervals obtained using informative priors outperform all other confidence/HPD credible intervals.

The graphical representation of the estimated risk for $R = 0.55$ and $R = 0.75$ is also shown in Figure 6.1. The results stated above can be further confirmed using Figure 6.1.

Table 6.1: AV and estimated risk (ER) of R when $\alpha_1 = 10$ and $\alpha_2 = 5$ (actual value = 0.33).

(n, m)	MLE	Prior 1		Prior 2	
		SEL	LLF	SEL	LLF
(20, 20)	0.3362	0.3528	0.3537	0.4133	0.4099
	0.0049	0.0021	0.0010	0.0131	0.0070
(35, 35)	0.3346	0.3355	0.3361	0.3583	0.3568
	0.0027	0.0013	0.0006	0.0036	0.0019
(50, 50)	0.3370	0.3378	0.3373	0.3334	0.3325
	0.0019	0.0010	0.0005	0.0019	0.0010
(75, 75)	0.3354	0.3352	0.3356	0.3233	0.3226
	0.0013	0.0007	0.0004	0.0014	0.0007
(100, 100)	0.3338	0.3334	0.3330	0.3248	0.3244
	0.0010	0.0007	0.0004	0.0008	0.0004

Table 6.2: AV and estimated risk (ER) of R when $\alpha_1 = 5.6$ and $\alpha_2 = 6.9$ (actual value = 0.55).

(n, m)	MLE	Prior 1		Prior 2	
		SEL	LLF	SEL	LLF
(20,20)	0.5499	0.5815	0.5805	0.6507	0.6481
	0.0059	0.0029	0.0015	0.0149	0.0079
(35,35)	0.5504	0.5800	0.5794	0.6096	0.6082
	0.0034	0.0021	0.0011	0.0060	0.0031
(50,50)	0.5541	0.5669	0.5662	0.5995	0.5980
	0.0022	0.0017	0.0008	0.0051	0.0027
(75,75)	0.5529	0.5697	0.5691	0.5697	0.5691
	0.0016	0.0014	0.0007	0.0014	0.0007
(100,100)	0.5515	0.5521	0.5517	0.5537	0.5530
	0.0012	0.0008	0.0004	0.0013	0.0006

Table 6.3: AV and estimated risk (ER) of R when $\alpha_1 = 0.3$ and $\alpha_2 = 3$ (actual value = 0.90)

(n, m)	MLE	Prior 1		Prior 2	
		SEL	LLF	SEL	LLF
(20,20)	0.9054	0.9079	0.9075	0.933	0.9324
	0.0008	0.0007	0.0003	0.0016	0.0008
(35,35)	0.9069	0.8999	0.8997	0.9316	0.9313
	0.0004	0.0006	0.0003	0.0010	0.0005
(50,50)	0.9087	0.9109	0.9108	0.9233	0.9231
	0.0003	0.0002	0.0001	0.0005	0.0003
(75,75)	0.9086	0.9133	0.9132	0.9147	0.9145
	0.0002	0.0002	0.0001	0.0003	0.0002
(100,100)	0.9084	0.9099	0.9098	0.9089	0.9088
	0.0001	0.0002	0.0001	0.0002	0.0001

Table 6.4: AV and estimated risk (ER) of R when $\alpha_1 = 2$ and $\alpha_2 = 6$ (actual value= 0.75)

(n, m)	MLE	Prior 1		Prior 2	
		SEL	LLF	SEL	LLF
(20,20)	0.7448	0.7650	0.7638	0.7695	0.7680
	0.0036	0.0027	0.0013	0.0034	0.0017
(35,35)	0.7467	0.7615	0.7609	0.7686	0.7675
	0.0020	0.0013	0.0006	0.0025	0.0013
(50,50)	0.7502	0.7611	0.7606	0.7595	0.7588
	0.0013	0.0011	0.0005	0.0015	0.0007
(75,75)	0.7497	0.7451	0.7447	0.7474	0.7469
	0.0009	0.0007	0.0003	0.0009	0.0005
(100,100)	0.7489	0.7459	0.7456	0.7609	0.7605
	0.0007	0.0006	0.0003	0.0009	0.0004

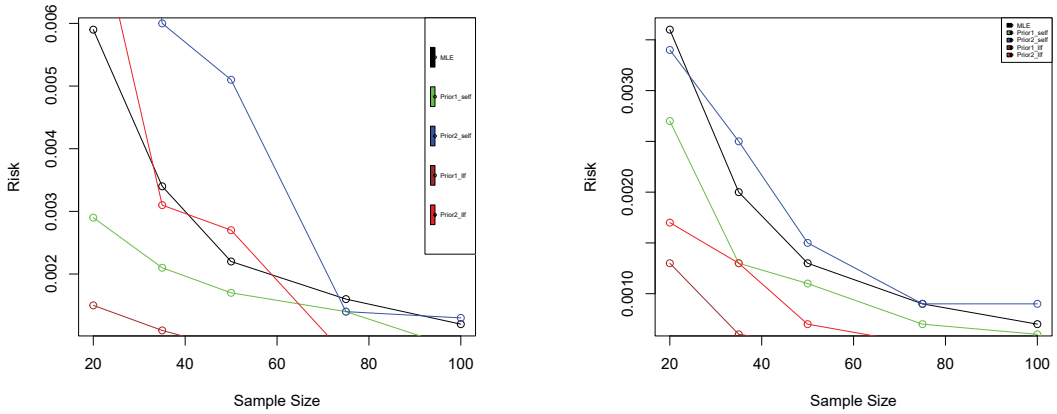

Figure 6.1: Plots representing the estimated risk for $R = 0.55$ and $R = 0.75$.

Table 6.5: CL and CP of 95% asymptotic, bootstrap confidence/HPD credible intervals for different R values.

		MLE		Boot-p		Bayes			
						Prior1		Prior2	
(α_1, α_2)	(n, m)	CL	CP	CL	CP	CL	CP	CL	CP
	(20, 20)	0.2706	0.9390	0.1903	0.92	0.1625	0.95	0.3199	0.951
	(35, 35)	0.2061	0.941	0.1664	0.94	0.1382	0.951	0.2181	0.951
(10, 5)	(50, 50)	0.1737	0.95	0.1521	0.95	0.1166	0.952	0.1644	0.952
	(75, 75)	0.1419	0.958	0.1236	0.959	0.1041	0.952	0.1368	0.952
	(100, 100)	0.1228	0.959	0.1165	0.97	0.1015	0.953	0.1062	0.953
	(20, 20)	0.2995	0.928	0.1945	0.92	0.1745	0.951	0.2807	0.951
	(35, 35)	0.2287	0.938	0.1709	0.93	0.1511	0.951	0.200	0.951
(5.6, 6.9)	(50, 50)	0.192	0.941	0.1456	0.93	0.1501	0.952	0.1989	0.952
	(75, 75)	0.1573	0.945	0.1417	0.99	0.1360	0.953	0.136	0.952
	(100, 100)	0.1365	0.954	0.1319	0.99	0.1140	0.955	0.1375	0.953
	(20, 20)	0.1053	0.941	0.1241	0.951	0.1053	0.963	0.1241	0.951
	(35, 35)	0.0788	0.938	0.0942	0.952	0.1002	0.972	0.0942	0.952
(0.3, 3)	(50, 50)	0.0649	0.936	0.0598	0.952	0.0535	0.974	0.0598	0.952
	(75, 75)	0.0530	0.943	0.0653	0.954	0.0535	0.981	0.0653	0.954
	(100, 100)	0.0461	0.954	0.0608	0.956	0.0511	0.991	0.0608	0.956
	(20, 20)	0.2313	0.934	0.1295	0.90	0.1938	0.951	0.2039	0.951
	(35, 35)	0.1754	0.936	0.1221	0.92	0.1312	0.951	0.1825	0.951
(2, 6)	(50, 50)	0.1459	0.940	0.1138	0.96	0.1207	0.952	0.1497	0.952
	(75, 75)	0.1195	0.944	0.1106	0.96	0.0957	0.953	0.1199	0.953
	(100, 100)	0.1039	0.955	0.1024	0.99	0.092	0.955	0.1156	0.953

6.5 Data Analysis

6.5.1 Aortic luminal diameter Dataset

The first set of data depicts a human abdominal aortic aneurysm, a pathologic dilatation of the abdominal aorta diameter that is a significant source of morbidity and mortality in the United States and across the world as described by Azuma et al. (2011). Nguimkeu et al. (2015) has already examined this dataset to investigate the interval estimation of SSR using independent normal random variables. A new ultrasound-based equipment was used to assess the aortic luminal diameter (ALD) of two groups of individuals. Accurate measurement of its dimension is critical for determining the severity of the disease. The first group included 20 patients with modest aneurysm diameters (the control or low risk group), whereas the second included 20 individuals with big aneurysm diameters (the treatment or high risk group). This work is primarily concerned with determining the diagnostic accuracy of this new instrument in distinguishing between persons with low and high rupture risk. For this, we assume that Y represents the control groups ultrasound measurements and X represents the treatment groups measurements. Then $R = P(X > Y)$ is the probability that the abdominal aortic diameter reading of a patient with a high rupture risk is larger than the abdominal aortic diameter measurement of a patient with a low rupture risk. As a result, it assesses the ultrasound instruments diagnostic accuracy in distinguishing between these two kinds of patient groups. The greater the value of R, the better the instrument distinguishes between the two groups of patients. The ALD dataset is given in 6.6.

Table 6.6: Aortic luminal diameter dataset

X	0.88	1.075	0.997	0.921	1.093	1.154	1.074	1.348	1.153	1.331
	1.132	1.21	1.273	1.412	1.367	1.486	1.427	1.355	1.562	1.761
Y	0.586	0.623	0.552	0.606	0.626	0.586	0.623	0.606	0.634	0.684
	0.684	0.743	0.735	0.712	0.765	0.756	0.82	0.781	0.812	0.879

To determine the suitability of the WBIII distribution for the given data sets, we utilized the K-S statistic in conjunction with p - value, AIC and BIC.

The applicability of the WBIII distribution is compared with the Weibull inverse Lomax (WIL) distribution and the statistic values are given in Table 6.7. Based on the results, the WBIII distribution was found to be a better fit for the data sets as shown in the Table 6.7. Additionally, a P-P plot was used to further demonstrate the fitness of the ALD datasets, which is shown in Figure 6.2.

Table 6.7: Fitting of the ALD datasets.

Data	Model	AIC	BIC	K-S	p - value
X	WBIII	2.848278	6.831207	0.10206	0.9715
	WIL	4.159996	8.142925	0.11419	0.9305
Y	WBIII	-30.60697	-26.62404	0.18255	0.5177
	WIL	-30.12308	-26.14015	0.18041	0.5331

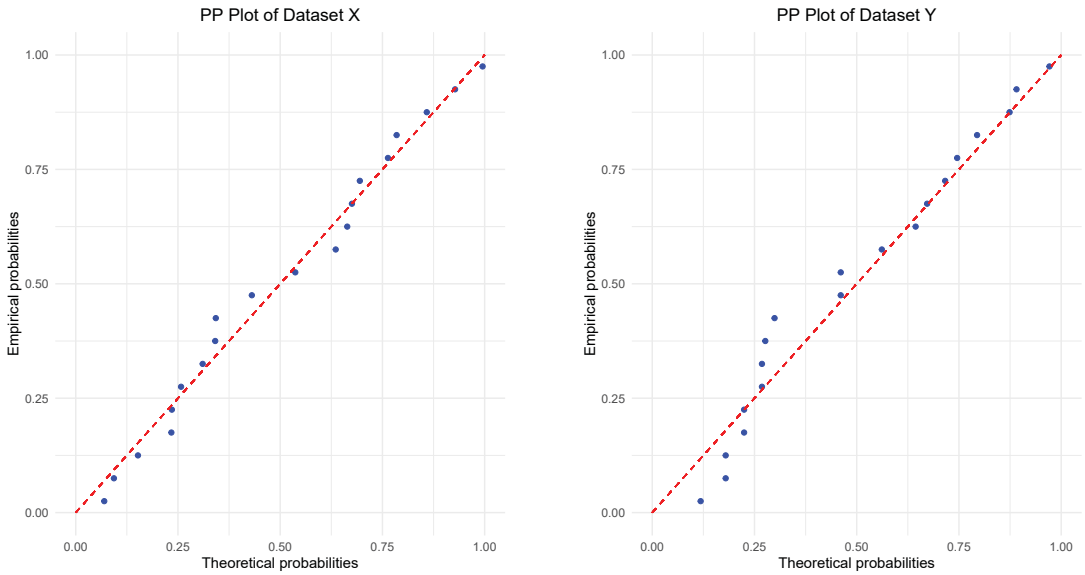

Figure 6.2: P-P plot of the ALD dataset

For the ALD datasets, the point estimate of R is 0.9801 and the corresponding 95% confidence interval of R is (0.9442, 1.0160). The R value shows that the system is 98% reliable in distinguishing between the two types of patients. To create samples from the posterior density, we use the method of M-H to construct a Markov chain of size 18000 and discard the first 17000 observations. The simulation was carried out using R software and we monitored the convergence of the Markov chain using diagnostic tools such as trace plots and running mean plots.

The traceplot is used to demonstrate the convergence of the simulated Markov chains and the running mean plot depicts the graphical representation of the mean of the sampled data. By observing the trace plot and running mean plot in Figure 6.3, it is clear that the chain has either converged or reached stationarity as the number of iterations increased. The corresponding bayes estimate is 0.9805 with an HPDCI of (0.9535, 0.9977).

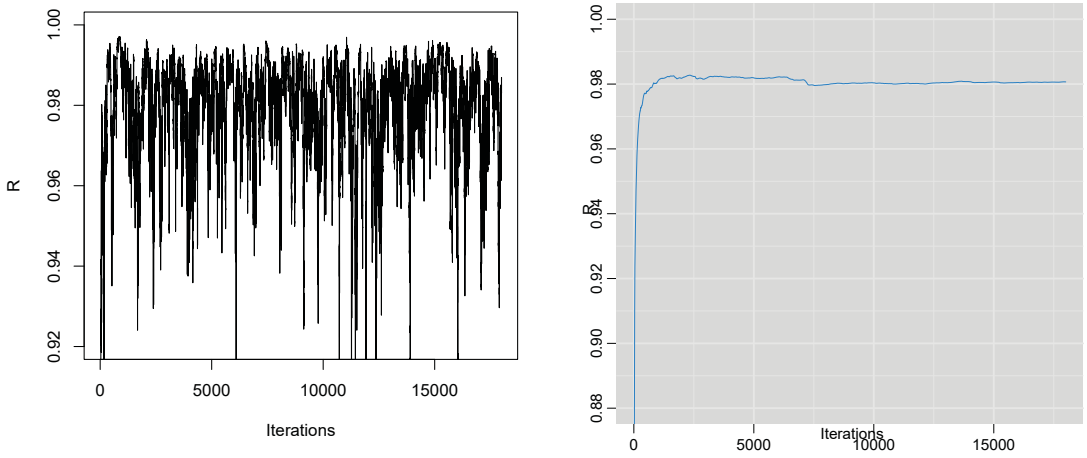

Figure 6.3: Trace plot and Running mean plot for ALD dataset.

6.5.2 Head Neck Cancer Dataset

The second data set consists of patients with two groups who have head and neck cancer which is proposed by Efron (1988). Several authors already modelled this data using inverted gamma distribution (Iranmanesh et al. (2018)), generalized inverse Lindley distribution (Sharma et al. (2015)), inverted exponential distribution (Singh et al. (2015)), inverse Weibill distribution (Yadav et al. (2018)) etc. Also Makkar et al. (2014) have used the log-normal model to analyze the data and discussed its posterior-based inferences. The dataset contains information on the survival rates of two groups of head and neck cancer patients, one receiving radiation (RT) and the other receiving combination radiotherapy and chemotherapy (CT + RT). The aim is to determine if the combination treatment improves patient survival compared to RT alone. The data sets of HNC data are given in Table 6.8

For HNC dataset, the applicability of WBIII distribution is compared with

Table 6.8: Head neck cancer dataset

X	6.53	7	10.42	14.48	16.1	22.7	34	41.55	42	45.28	49.4
	53.62	63	64	83	84	91	108	112	129	133	133
	139	140	140	146	149	154	157	160	160	165	173
	176	218	225	241	248	273	277	297	405	417	420
	440	523	583	594	1101	1146	1146	1417			
Y	12.2	23.56	23.74	25.87	31.98	37	41.35	47.38	55.46	58.36	63.47
	68.46	78.26	74.47	81.43	84	92	94	110	112	119	127
	130	133	140	146	155	159	173	179	194	195	209
	249	281	319	339	432	469	519	633	725	817	1776

Inverse Weibull Distribution (IW) and Burr III Distribution (BIII). The SSR estimation for the inverse Weibull distribution was previously evaluated using this dataset by Yadav et al. (2018). Upon analyzing Table 6.9, it was found that the proposed model had more flexibility compared to the other two distributions.

Table 6.9: Fitting of the HNC data sets.

Data	Model	AIC	BIC	K-S	p - value
X	WBIII	666.6111	674.3384	0.1189	0.4661
	IW	676.6352	680.4989	0.1729	0.0947
	BIII	675.6379	679.5015	0.1687	0.1095
Y	WBIII	562.656	569.7927	0.0596	0.9949
	IW	563.140	566.7086	0.0927	0.8104
	BIII	562.961	566.5294	0.0911	0.8261

Similarly for the head neck cancer data, the estimate of the R is found to be 0.5140 with 95% confidence interval (0.4878, 0.5403). Hence the probability of survival for patients treated with combination therapy (CT+RT) is reliable more than 51% of the time. This suggests that the combination of RT and CT may increase the survival rates for patients with head and neck cancer. Additionally, the corresponding Bayes estimate is 0.5157 with an HPDCI (0.4360, 0.6084). The P-P plot in Figure 6.4 indicates the fitness of the HNC datasets. Meanwhile, Figure 6.5 shows the traceplot and running mean plot of the HNC dataset.

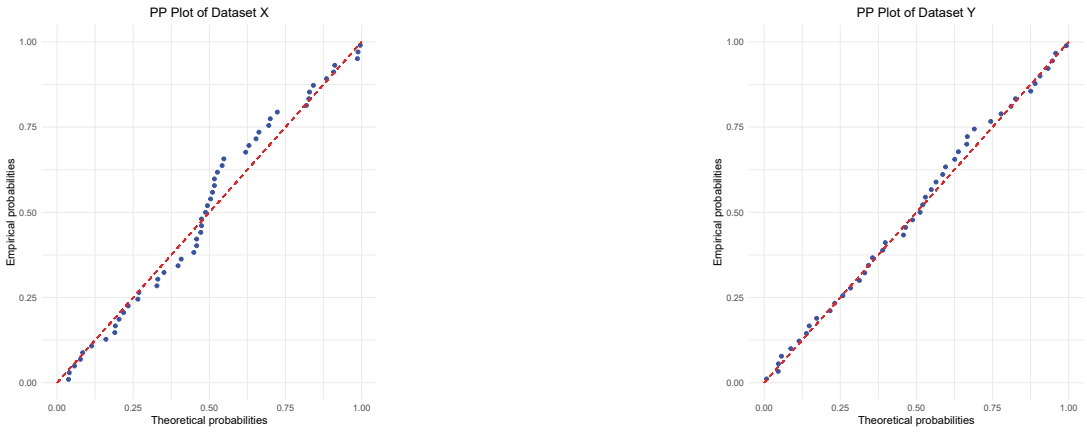

Figure 6.4: P-P plot of the HNC dataset

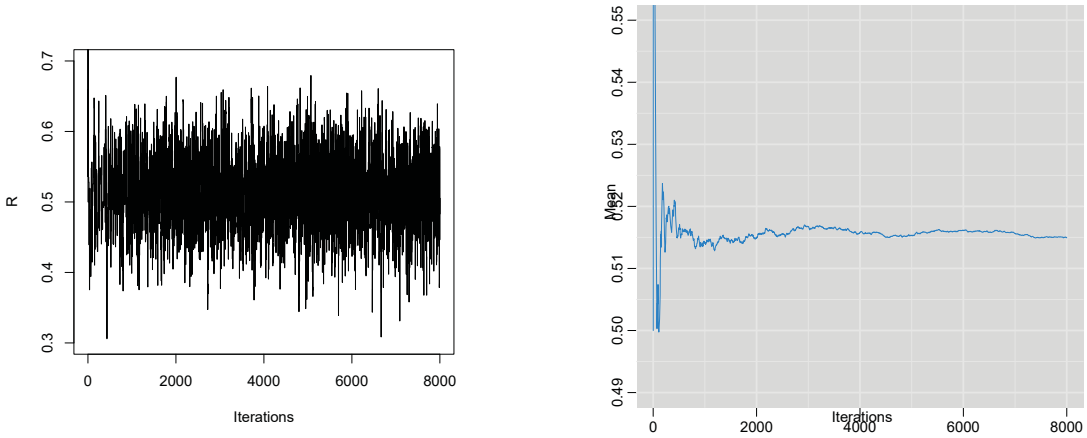

Figure 6.5: Trace plot and Running mean plot for HNC dataset.

6.6 Summary

This Chapter focuses on estimating $R = \mathrm{P}(\mathrm{X} > \mathrm{Y})$, where X and Y are independent WBIII random variables with the same shape but different scale parameters. The estimation of R is done using ML and Bayesian estimation. Bayesien estimation is proposed with non-informative and gamma informative priors having various error loss functions- squared error and linex loss functions. A simulation study is conducted to compare the effectiveness of each proposed method. The results indicates that the Bayes estimator in point estimation and the HPD credible interval in interval estimation based on informative priors are highly reliable and can be used for practical purposes. The relevance of the study is clearly described by using two clinical data sets.

Chapter 7

On Partially Observed Competing Risks Model for Weibull Distribution under Generalized Type-II Hybrid Censoring

7.1 Introduction

In real world scenarios, it is common for an item to be susceptible to multiple causes of failure simultaneously, with the failure likely occurring due to the cause that emerges first. These situations typically fall under the concept of competing risks (CRs), with examples provided in Chapter 1. A conventional approach for modeling lifetime data in the context of CRs is to assume that there is a latent lifetime associated with each of the causes to which the item is subjected, and the observed lifetime of the item is the minimum among these latent lifetimes. Thus, the CR data typically consist of failure times along with an associated indicator variable denoting the causes of failure. Furthermore, these latent lifetimes are persumed to be independent of one another, following either the same or different distributions.

In the majority of existing literature, the discussions are predicated on the assumption that the causes of failures are completely observed for all experimental units. However, in real-world scenarios, the causes of failure are often

only observed for a portion of the failed units due to limitations in cause detection methods, making it impossible to observe all failure causes. This situation, where failure causes are missing for some units, is referred to as partially observed competing risks (POCR). Conducting lifetime studies in such situations presents significant challenges, as making inferences about failure causes is crucial for improving product quality and addressing safety concerns. In the literature, this phenomenon is sometimes referred to as masked data in conjunction with CRs, with the fraction of unknown failure causes termed as masking probability. For example, an industrial machine may fail due to wear and tear, electrical faults, or overheating, but the exact cause may remain unknown due to lack of diagnostic tools, or incomplete maintenance records. If a machine stops and the technician cannot determine whether the failure was caused by an electrical short circuit or overheating, the cause remains ambiguous. These scenarios of POCR require specialized statistical methods to ensure accurate reliability assessments. Several research articles have explored POCR, including, Lodhi et al. (2021) investigated POCR for a general class of inverted exponentiated distributions, while Mahto et al. (2022) focused on POCR for the Kumaraswamy distribution. Almuhayfith et al. 2022 examines inference methods for partially observed failure modes under the assumption that the data follows a Burr XII distribution. Abushal et al. (2022) discussed a CRs model with partially observed failure causes and latent failure times following a Lomax distribution; Dutta et al. (2023) investigated statistical inference for a POCR model when latent failure times follow a general family of inverted exponentiated distributions. Chandra et al. (2023) conducted an analysis for a POCR model utilizing Burr XII distributions under a GPHC scheme and Singh et al. (2024) examines a POCR model for the Chen distribution. Additionally, Dutta et al. (2024) investigated POCR for the Kumaraswamy-G family of distributions under a unified progressive hybrid censoring scheme.

Censoring is often used when it is impractical to record failure times for all units due to time and cost constraints (see Chapter 1 for details). To overcome the limitations of Type-I and Type-II censoring schemes, Chandrasekar et al. (2004) introduced generalized hybrid censoring schemes (GHCS). The experi-

ments under GHCS ensure both proper control within a defined testing period and the occurrence of at least a fixed number of failures. Statistical inference is more efficient under GHCS because it provides a greater number of observed failures. The basic forms of GHCS are categorized as type-I and type-II GHCS, are expressed as follows:

(i). Generalized Type-I Hybrid Censoring Scheme - In the generalized Type-I hybrid censoring scheme (GTIHCS), n experimental units are subjected to a life test. The experimenter pre-selects two numbers, s and m, such that $s < m \leq n$, as well as a time T within the range $(0, \infty)$. If the s^{th} failure occurs before the specified time T, the experiment will be terminated at $T^* = \min(X_m, T)$. If the s^{th} failure occurs after T, the experiment will conclude at T_s, where T_s is the failure time of the s^{th} unit.

(ii). Generalized Type-II Hybrid Censoring Scheme - In a generalized Type-II hybrid censoring scheme (GTIIHCS), a predefined number m (where $m \leq n$) and thresholds time T_1 and T_2 are set, with $T_1 < T_2$. If the m^{th} failure happens prior to T_1, the experiment will conclude at T_1. If the m^{th} failure happens within the interval T_1 to T_2, then the experiment will conclude at T_m. If the m^{th} failure happens beyond T_2, then the experiment will conclude at T_2. In GTIIHCS, the experiment is ensured to conclude by time T_2. Then, the following cases are identified under GTIIHCS.

$$\text{Case I : If } 0 < X_{m:n} < T_1 < T_2, \text{ then } T^* = T_1.$$
$$\text{Case II : If } 0 < T_1 < X_{m:n} < T_2, \text{ then } T^* = X_{m:n}.$$
$$\text{Case III : If } 0 < T_1 < T_2 < X_{m:n}, \text{ then } T^* = T_2.$$

The experiment is designed to ensure that it concludes within a predefined maximum duration, with T_2 serving as the upper limit for the experiment's time-line. The GTIIHCS is highly advantageous in applications like reliability testing, medical devices, and clinical trials. By combining failure-based and time-based stopping rules, it ensures either a pre-specified number of failures or termination within a fixed duration. This flexibility allows GTIIHCS to overcome the limi-tations of traditional Type-I and Type-II censoring schemes. Type-I censoring,

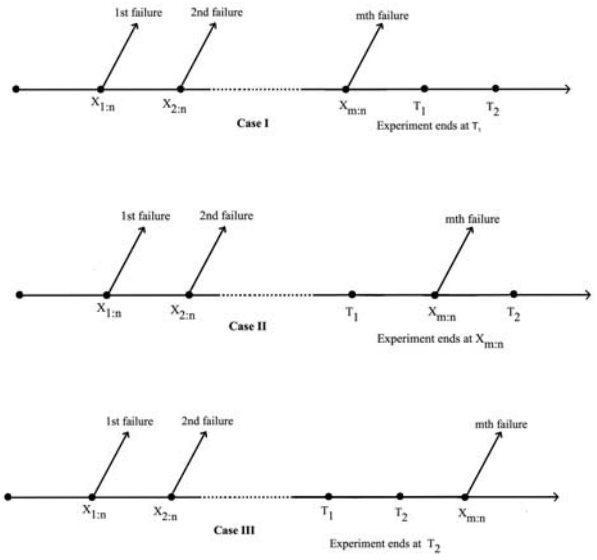

Figure 7.1: Illustration of the generalized type-II hybrid censoring scheme.

which terminates experiments at a fixed time, may result in insufficient failure data and low inference precision, while Type-II censoring ensures a fixed number of failures but often requires excessively long testing periods. GTIIHCS resolves these challenges by balancing test efficiency and data reliability. It provides better control over the testing process and improves the accuracy of statistical inferences, making it an ideal choice for real-world applications with strict time or resource constraints. The visual representation of GTIIHCS is given in Figure 7.1. Numerous researchers have investigated the estimation problem for various statistical models, highlighting the importance of the GTIIHCS. Shafay (2016) examined Bayesian estimation and prediction using GTIIHCS. Mahmoud and Ghazal (2017) estimated the unknown parameters of the exponentiated rayleigh distribution using GTIIHC data. Rabie and Li (2019) derived ML, Bayesian, and E-Bayesian estimators for the unknown shape parameter of the Burr-X distribution under GTIIHCS. Abushal and Al-Zaydi (2024) conducted inference on unknown parameters using GTIIHCS for the inverse Nadarajah–Haghighi distribution in the context of CRs.

This Chapter focuses on developing inference procedures for the Weibull competing risk model within the context of GTIIHCS. Here, we assume the presence of two distinct CR factors influencing the failure of experimental units.

The latent failure times are modeled using Weibull distributions with a common shape parameter α and different scale parameters λ_1 and λ_2, where $\lambda_1 \neq \lambda_2$. Let X_{ji} represent the i^{th} latent failure time under the j^{th} cause, where $i = 1, 2, \ldots, n$ following a Weibull distribution. Then the corresponding PDF and CDF can be expressed as follows:

$$f_j(x; \alpha, \lambda_j) = \alpha\lambda_j x^{\alpha-1} e^{-\lambda_j x^\alpha} \text{ and } F_j(x; \alpha, \lambda_j) = 1 - e^{-\lambda_j x^\alpha};\ x > 0,\ j = 1, 2. \tag{7.1}$$

The structure of this Chapter is organized as follows: Section 7.2 outlines the model assumptions for POCR data under the GTIIHCS framework. Section 7.3 discusses the ML estimation of unknown parameters, along with approximate confidence intervals. Bayesian estimation techniques using the importance sampling method are explored in Section 7.4. Section 7.5 provides a Monte Carlo simulation study, while Section 7.6 includes a real-world example for illustration. Finally, a concluding summary for the Chapter is presented in Section 7.7.

7.2 Model Framework

Consider an experiment where n independent units are tested, with their respective lifetimes denoted by random variables X_1, X_2, ..., X_n. Under the POCR model, we consider two independent causes of failure. Then, the latent failure times resulting from two independent causes of failure for any unit are defined as,

$$X_i = \min\{X_{1i}, X_{2i}\} \quad i = 1, 2, \ldots, n. \tag{7.2}$$

where X_{ji} represents the failure time of the i^{th} unit due to j^{th} cause. Under GTIIHC, if T_1, T_2, and m denote the test duration time and the predetermined number of observed failures, then the experiment concludes at time T^*, which can be expressed as follows for the three scenarios:

$$T^* = \begin{cases} T_1, & 0 < X_{m:n} < T_1, \\ X_{m:n}, & T_1 < X_{m:n} < T_2, \\ T_2, & T_1 < T_2 < X_{m:n}, \end{cases} \tag{7.3}$$

where $X_{1:n}, \ldots, X_{D:n}$ are the GTIIHCS corresponding to $X_1, X_2, \ldots, X_n$. Then the data on POCR under GTIIHCS can be described as follows:

$$\begin{aligned}
&\text{Case I: } (X_{1:n}, \xi_1), \ldots, (X_{m_1:n}, \xi_{m_1}), \text{ if } 0 < X_{m:n} < T_1 \text{ and } T^* = T_1, \\
&\text{Case II: } (X_{1:n}, \xi_1), \ldots, (X_{m:n}, \xi_m), \text{ if } T_1 < X_{m:n} < T_2 \text{ and } T^* = X_{m:n}, \\
&\text{Case III: } (X_{1:n}, \xi_1), \ldots, (X_{m_2:n}, \xi_{m_2}), \text{ if } T_1 < T_2 < X_{m:n} \text{ and } T^* = T_2,
\end{aligned} \tag{7.4}$$

where T^* represents the termination point of the experiment, while m_1 and m_2 are two positive integers, with $x_{m_1:n} < T_1 < x_{m_1+1:n}$ and $x_{m_2:n} < T_2 < x_{m_2+1:n}$. Assume that the causes of failures are independent. Then, the observed failure times are $(x_{1:n}, \xi_1), (x_{2:n}, \xi_2), \ldots, (x_{D:n}, \xi_D)$ and the corresponding cause of failure is represented by an indicator function ξ_i such that $\xi_i = j, \quad j = 1, 2, 3, \quad i = 1, 2, \ldots, D$ where,

$$\xi_i = \begin{cases} 1, & \text{if the failure occurs due to cause 1,} \\ 2, & \text{if the failure occurs due to cause 2,} \\ 3, & \text{if the cause of the failure cannot be determined.} \end{cases}$$

Considering the POCR data in (7.4), then the likelihood function for the observed data $\underline{x} = (x_{1:n}, \xi_1), \ldots, (x_{D:n}, \xi_D)$ can be expressed as,

$$L(\underline{x}) = \frac{n!}{(n-D)!} \prod_{i=1}^{D} \left[f_1(x_i) S_2(x_i)\right]^{I(\xi_i=1)} \left[f_2(x_i) S_1(x_i)\right]^{I(\xi_i=2)} \left[f(x_i)\right]^{I(\xi_i=3)} S(T^*)^{n-D}, \tag{7.5}$$

where $f(.)$ and $S(.)$ are the density and survival functions of $X_i = \min\{X_{1i}, X_{2i}\}$ and D represents the total number of failures under the following cases,

$$D = \begin{cases} m_1, & \text{Case I,} \\ m, & \text{Cases II ,} \\ m_2, & \text{Cases III .} \end{cases}$$

Also, we define the indicator function

$$I(\xi_i = j) = \begin{cases} 1, & \text{if } \xi_i = j, \\ 0, & \text{otherwise.} \end{cases}$$

Thus, $D_1 = \sum_{i=1}^{D} I(\xi_i = 1)$ and $D_2 = \sum_{i=1}^{D} I(\xi_i = 2)$ represent the total number of failures due to cause 1 and cause 2. Also, $D_3 = \sum_{i=1}^{D} I(\xi_i = 3)$ represents the number of failures with unobserved cause. Now, consider that the GTIIHC competing risks data (7.4) are derived from Weibull distributions with two independent failure causes such that $X_{1i} \sim \mathrm{W}(\alpha, \lambda_1)$ and $X_{2i} \sim \mathrm{W}(\alpha, \lambda_2)$ for $i = 1, 2, \ldots, n$. Consequently, the observations $X_i = \min\{X_{1i}, X_{2i}\}$ for $i = 1, 2, \ldots, n$ are also independent and follow Weibull distribution with parameters $(\alpha, \lambda_1+\lambda_2)$.

Remark 1. *If the failure times X_1 and X_2 are i.i.d random variables following Weibull distributions with parameters (α, λ_1) and (α, λ_2) respectively, then the random variable $X = \min(X_1, X_2)$ follows a Weibull distribution with parameters $(\alpha, \lambda_1+\lambda_2)$, where α represents the shape parameter and $(\lambda_1+\lambda_2)$ denotes the scale parameter.*
The reliability function of the random variable X, denoted as $\bar{F}_X(x)$, is provided as follows,

$$\begin{aligned} \bar{F}_X(x) &= P\left(\min(X_1, X_2) > x\right) \\ &= P\left(X_1 > x\right) P\left(X_2 > x\right) \\ &= e^{-(\lambda_1+\lambda_2)x^{\alpha}}. \end{aligned}$$

Then, the corresponding CDF $F_X(x)$ and the PDF $f_X(x)$ are given by,

$$F_X(x) = 1 - e^{-(\lambda_1+\lambda_2)x^{\alpha}} \text{ and } f_X(x) = \alpha(\lambda_1 + \lambda_2)x^{\alpha-1}e^{-(\lambda_1+\lambda_2)x^{\alpha}}.$$

The likelihood functionof λ_1, λ_2 and α can be formulated based on (7.5) as:

$$L(\underline{x}) \propto \alpha^{D}\lambda_1^{D_1}\lambda_2^{D_2}(\lambda_1 + \lambda_2)^{D_3}e^{-(\lambda_1+\lambda_2)(T^*)^{\alpha}(n-D)}\prod_{i=1}^{D} x_i^{\alpha-1}e^{-(\lambda_1+\lambda_2)x_i^{\alpha}}. \qquad (7.6)$$

Thus, certain comments made on this model were considered as,

1. The proposed model indicates that the failure time is noted for certain units with an unknown cause of failure. Then, the latent failure time follows a Weibull distribution with the scale parameter $\lambda_1 + \lambda_2$ and shape parameter α.

2. The observed numbers of failures D_1 and D_2 for the first and second causes follow binomial distributions with sample size (D-D_3) and probability of success $\frac{\lambda_1}{\lambda_1+\lambda_2}$ and $\frac{\lambda_2}{\lambda_1+\lambda_2}$, respectively.

3. The discrete random variable D_3 follows a Bernoulli distribution with a masking probability p, where $0 \leq p \leq 1$. Hence, the values 0 and 1 represent failures with unknown and known causes, respectively.

7.3 ML Estimation

According to Equation (7.6), the log-likelihood function is expressed as follows:

$$\begin{aligned} L(\lambda_1, \lambda_2, \alpha \mid \underline{x}) &= D \ln \alpha + D_1 \ln \lambda_1 + D_2 \ln \lambda_2 + D_3 \ln(\lambda_1 + \lambda_2) \\ &+ (\alpha - 1) \sum_{i=1}^{D} \ln x_i - (\lambda_1 + \lambda_2) Z(\alpha), \end{aligned} \tag{7.7}$$

where $\mathrm{Z}(\alpha) = \sum_{i=1}^{D} x_i^{\alpha} + (n - D)(T^*)^{\alpha}$.

Theorem 5. *Given that $D_j \geq 1$, the MLE of λ_j, when α is known, can be represented as:*

$$\hat{\lambda}_j = \frac{D_j}{Z(\alpha)} \left[\frac{D_3}{D_1 + D_2} + 1 \right], j = 1, 2.$$

Proof. : By taking the derivatives of $L = L(\lambda_1, \lambda_2, \alpha \mid \underline{x})$ in (7.7) with respect to λ_1 and λ_2, and then setting these derivatives to zero, we obtain the following equations,

$$\lambda_j = \frac{D_j}{Z(\alpha)} \left[\frac{D_3}{D_1 + D_2} + 1 \right], j = 1, 2.$$

To demonstrate that the MLEs of $\hat{\lambda}_1$ and $\hat{\lambda}_2$ maximize L for a given α, we proceed as follows.

Let $H(\lambda_1, \lambda_2)$ represent the Hessian matrix of L at (λ_1, λ_2). Given that,
$H_{jj}(\lambda_1, \lambda_2) = \frac{\partial^2 L}{\partial \lambda_j^2} = -\frac{D_j}{\lambda_j^2} - \frac{D_3}{(\lambda_1+\lambda_2)^2}, j = 1, 2.$
$H_{12}(\lambda_1, \lambda_2) = -\frac{D_3}{(\lambda_1+\lambda_2)^2}.$
Thus, the determinant of the Hessian matrix at $(\hat{\lambda}_1, \hat{\lambda}_2)$ is,
$\det(H) = H_{11}(\hat{\lambda}_1, \hat{\lambda}_2)H_{22}(\hat{\lambda}_1, \hat{\lambda}_2) - H_{12}(\hat{\lambda}_1, \hat{\lambda}_2)^2 = \frac{D_1 D_2}{\hat{\lambda}_1^2 \hat{\lambda}_2^2} + \frac{D_1 D_3}{\hat{\lambda}_1^2(\hat{\lambda}_1+\hat{\lambda}_2)^2} + \frac{D_2 D_3}{\hat{\lambda}_2^2(\hat{\lambda}_1+\hat{\lambda}_2)^2} > 0.$
Therefore, $(\hat{\lambda}_1, \hat{\lambda}_2)$ represents a local maximum of L for a given α. As there is no singular point of L and it possesses only one critical point, $\hat{\lambda}_1$ and $\hat{\lambda}_2$ emerge as the absolute maximum of L. Thus, the assertion stands proven. □

Remark 2. *As noted in Theorem 5, at least one failure due to the j^{th} cause is required for the MLE of λ_j to be determined, where j = 1,2. If $D_j = 0$, meaning there are no failures from the j^{th} cause or there is no information available about λ_j from the observed CRs data. Therefore, if $D_j = 0$, the MLE of λ_j does not exist. Also, the ordinary CRs model is achieved when $D_3 = 0$.*

Theorem 6. *Assume that $D_j \geq 1$ for j = 1,2, the MLE of α exists and is unique, which is the solution of the following equation,*

$$\frac{1}{\alpha} + \frac{\sum_{i=1}^{D} \ln x_i}{D} = \frac{Z'(\alpha)}{Z(\alpha)}, \tag{7.8}$$

with $Z'(\alpha) = \sum_{i=1}^{D} x_i^{\alpha} \ln(x_i) + (n - D)T^{*\alpha} \ln(T^*)$.

Proof. By substituting $\hat{\lambda}_j$ for λ_j in (7.7), the profile log-likelihood function of α can be derived as follows.

$$L(\alpha) \propto D \ln \alpha + \alpha \sum_{i=1}^{D} \ln x_i - D \ln Z(\alpha).$$

Then, by differentiating $L(\alpha)$ with respect to α and setting it equal to zero, we obtain the following:

$$\frac{1}{\alpha} + \frac{\sum_{i=1}^{D} \ln x_i}{D} = \frac{Z'(\alpha)}{Z(\alpha)}.$$

Let $G_1(\alpha) = \frac{1}{\alpha} + \frac{\sum_{i=1}^{D} \ln x_i}{D}$ and $G_2(\alpha) = \frac{Z'(\alpha)}{Z(\alpha)}$.
Here $G_1'(\alpha) = -\frac{1}{\alpha^2} < 0$, which implies that $G_1(\alpha)$ is decreasing in the range

$\left(\frac{1}{D}\sum_{i=1}^{D}\ln x_i, \infty\right)$. In the case of $G_2(\alpha)$, we have the following:

$$G_2'(\alpha) = \frac{1}{[Z(\alpha)]^2}\left[\left(\sum_{i=1}^{D} x_i^{\alpha} + (n-D)T^{*^{\alpha}}\right)\left(\sum_{i=1}^{D} x_i^{\alpha}(\ln(x_i))^2 + (n-D)T^{*^{\alpha}}(\ln(T^*))^2\right) - \left(\sum_{i=1}^{D} x_i^{\alpha}\ln(x_i) + (n-D)T^{*^{\alpha}}\ln(T^*)\right)^2\right].$$

Applying the Cauchy–Schwarz inequality, we obtain $G_2^{'}(\alpha) > 0$, indicating that $G_2(\alpha)$ is an increasing function of α with,

$$\lim_{\alpha\to 0} G_2(\alpha) = \frac{1}{n}\left[\sum_{i=1}^{D}\ln x_i + (n-D)\ln T^*\right],$$
$$\lim_{\alpha\to +\infty} G_2(\alpha) = \ln T^*.$$

Also,

$$\lim_{\alpha\to\infty}\frac{G_1(\alpha)}{G_2(\alpha)} = \frac{1}{D}\frac{\sum_{i=1}^{D}\ln x_i}{\ln T^*} < 1.$$

We note that the curves $G_1(\alpha)$ and $G_2(\alpha)$ intersect at a unique point, indicating that the MLE of α exists and is unique. □

Also, it is important to note that the MLE $\hat{\alpha}$ for α does not have any closed-form expression. It can be evaluated using the fixed-point iterative method derived from the non-linear equation (7.8) as,

$$B(\alpha^{(s)}) = \alpha^{(s+1)},$$

where $\left[B(\alpha) = \frac{Z^{'}(\alpha)}{Z(\alpha)} - \frac{\sum_{i=1}^{D}\ln x_i}{D}\right]^{-1}$. Here, $\alpha^{(s)}$ represents the s^{th} iteration of $\hat{\alpha}$. The process is terminated when the difference $\mid \alpha^{(s)} - \alpha^{(s+1)} \mid$ is sufficiently small. Thus, the MLEs of λ_j denoted as $\hat{\lambda}_j$, $j = 1, 2$ can be derived from Theorem 5 as,

$$\hat{\lambda}_j = \frac{D_j}{Z(\hat{\alpha})}\left[\frac{D_3}{D_1 + D_2} + 1\right], j = 1, 2.$$

7.3.1 Approximate Confidence Interval

In this section, we establish approximate confidence intervals (CIs) for the parameters by exploiting the asymptotic normality property of MLEs. Let's assume that $\theta = (\lambda_1,\ \lambda_2,\ \alpha)$, where $\theta_1 = \lambda_1$, $\theta_2 = \lambda_2$, and $\theta_3 = \alpha$. In this case, the observed Fisher information matrix can be expressed as:

$$I(\theta) = \left[-\frac{\partial^2 L(\lambda_1, \lambda_2, \alpha \mid \underline{x})}{\partial\theta_j \partial\theta_s} \right]_{\theta_j = \hat{\theta}_j, j,s=1,2,3},$$

with

$$-\frac{\partial^2 L}{\partial \lambda_1^2} = \left(\frac{D_1}{\lambda_1^2} + \frac{D_3}{(\lambda_1+\lambda_2)^2} \right),$$

$$-\frac{\partial^2 L}{\partial \lambda_2^2} = \left(\frac{D_2}{\lambda_2^2} + \frac{D_3}{(\lambda_1+\lambda_2)^2} \right),$$

$$-\frac{\partial^2 L}{\partial \alpha^2} = \frac{D}{\alpha^2} + (\lambda_1+\lambda_2)\left[\sum_{i=1}^{D} x_i^{\alpha} (\ln x_i)^2 + (n-D)(T^*)^{\alpha} (\ln (T^*))^2 \right],$$

$$-\frac{\partial^2 L}{\partial \lambda_1 \partial \lambda_2} = -\frac{\partial^2 L}{\partial \lambda_2 \partial \lambda_1} = \left(\frac{D_3}{(\lambda_1+\lambda_2)^2} \right),$$

$$-\frac{\partial^2 L}{\partial \lambda_1 \partial \alpha} = -\frac{\partial^2 L}{\partial \alpha \partial \lambda_1} = \sum_{i=1}^{D} x_i^{\alpha} \ln x_i + (n-D)(T^*)^{\alpha} \ln (T^*),$$

$$-\frac{\partial^2 L}{\partial \lambda_2 \partial \alpha} = -\frac{\partial^2 L}{\partial \alpha \partial \lambda_2} = \sum_{i=1}^{D} x_i^{\alpha} \ln x_i + (n-D)(T^*)^{\alpha} \ln (T^*).$$

As established in Theorem 7.63 of Schervish (2012), it can be directly verified that the likelihood function (7.6) meets the regularity conditions, including the existence of continuous second partial derivatives, the interchangeability of differentiation and integration, and a finite mean for the Fisher information matrix, etc. Hence, using the asymptotic theory of MLEs, the approximate distribution of the MLE $\hat{\theta}$ is given by, $\hat{\theta} - \theta \sim N(0, I^{-1}(\theta))$, where $I^{-1}(\theta)$ represents the inverse of the observed information matrix, which is defined as:

$$I^{-1}(\hat{\theta}) = \begin{pmatrix} \text{var}(\hat{\lambda}_1) & \text{cov}(\hat{\lambda}_1, \hat{\lambda}_2) & \text{cov}(\hat{\lambda}_1, \hat{\alpha}) \\ \text{cov}(\hat{\lambda}_2, \hat{\lambda}_1) & \text{var}(\hat{\lambda}_2) & \text{cov}(\hat{\lambda}_2, \hat{\alpha}) \\ \text{cov}(\hat{\alpha}, \hat{\lambda}_1) & \text{cov}(\hat{\alpha}, \hat{\lambda}_2) & \text{var}(\hat{\alpha}) \end{pmatrix}$$

Hence, for any $0 < \nu < 1$, a 100(1-ν)% asymptotic confidence interval (ACI) for θ_j is given by,

$$\left(\hat{\theta}_j - Z_{\nu/2}\sqrt{\text{var}(\hat{\theta}_j)}, \hat{\theta}_j + Z_{\nu/2}\sqrt{\text{var}(\hat{\theta}_j)}\right); j = 1, 2, 3,$$

where $Z_{\nu/2}$ is the upper $\frac{\nu}{2}$ quantile of the standard normal distribution.

7.4 Bayesian Estimation

The Bayesian estimation method serves as a strong alternative to the classical estimation approach by treating unknown parameters as random variables and combining prior knowledge with sample data for inference. This section covers the Bayesian approach for obtaining point and interval estimates of the unknown model parameters. In the Bayesian framework, prior information about the unknown parameter is necessary before making any inferences using the likelihood function. This information can be either complete or incomplete, depending on the choice of the prior distribution. In a non-informative prior, little or no information is available about the unknown parameter, whereas an informative prior provides sufficient information to quantify the uncertainty associated with the parameter. Thus, the prior is chosen in such a way that it does not significantly alter the model estimates or influence the model selection. It is worth noting that there is no well-established method for choosing an appropriate prior in Bayesian analysis. The gamma distribution is highly adaptable, capable of modeling various shapes of the density function. Its density function is log-concave over the interval (0, ∞). Jeffrey's prior can be regarded as a specific case of the gamma prior. The gamma distribution is commonly used as an informative prior in various lifetime models due to its simplicity and ease of computation. Due to the relevance of gamma distributions, several authors have recently employed gamma priors to obtain BEs for the Weibull CR model (see Ashour and Nassar (2017), Chacko and Mohan (2019) etc.). In a similar way, we also consider the gamma priors for the parameters λ_1, λ_2 and α. Then, the joint prior density

function of λ_1, λ_2, and α can be expressed as follows:

$$\pi(\lambda_1, \lambda_2, \alpha) \propto \lambda_1^{a_1-1}\lambda_2^{a_2-1}\alpha^{a_3-1}\exp(-b_1\lambda_1-b_2\lambda_2-b_3\alpha), \text{ for } \lambda_1, \lambda_2, \alpha > 0, a_i, b_i > 0, \tag{7.9}$$

for $i = 1, 2, 3$. Then, the corresponding posterior distribution is formulated as follows:

$$\pi^*(\lambda_1, \lambda_2, \alpha \mid \underline{x}) = \frac{\pi(\lambda_1, \lambda_2, \alpha)L(\lambda_1, \lambda_2, \alpha \mid \underline{x})}{\int_0^\infty \int_0^\infty \int_0^\infty \pi(\lambda_1, \lambda_2, \alpha)L(\lambda_1, \lambda_2, \alpha \mid \underline{x})d\lambda_1 d\lambda_2 d\alpha}.$$

Then, the BEs of any function of λ_1, λ_2 and α, represented as $\eta(\lambda_1, \lambda_2, \alpha)$, under the SELF is given by,

$$\hat{\eta}_{SE} = \frac{\int_0^\infty \int_0^\infty \int_0^\infty \eta(\lambda_1, \lambda_2, \alpha)\pi(\lambda_1, \lambda_2, \alpha)L(\lambda_1, \lambda_2, \alpha \mid \underline{x})d\lambda_1 d\lambda_2 d\alpha}{\int_0^\infty \int_0^\infty \int_0^\infty \pi(\lambda_1, \lambda_2, \alpha)L(\lambda_1, \lambda_2, \alpha \mid \underline{x})d\lambda_1 d\lambda_2 d\alpha}. \tag{7.10}$$

From equation (7.10), it is evident that the BEs of $\eta(\lambda_1, \lambda_2, \alpha)$ with respect to the SELF cannot be obtained explicitly. Hence, an approximation technique like the MCMC technique is needed to compute the desired BEs. The MCMC method can generate samples from the posterior density function (8.13), allowing us to compute the BEs of the unknown parameters and the corresponding credible intervals. This study employs MCMC with importance sampling technique to compute Bayes estimators under the SELF. Based on equations (7.6) and (7.9), the joint posterior density function of λ_1, λ_2, and α can be expressed as follows:

$$\begin{aligned}\pi^*(\lambda_1, \lambda_2, \alpha \mid \underline{x}) &\propto \alpha^{D+a_3-1}\lambda_1^{D_1+a_1-1}\lambda_2^{D_2+a_2-1}(\lambda_1+\lambda_2)^{D_3} \\ &\times \exp\left(-b_1\lambda_1 - b_2\lambda_2 - b_3\alpha + (\alpha-1)\sum_{i=1}^{D}\ln x_i - (\lambda_1+\lambda_2)Z(\alpha)\right).\end{aligned} \tag{7.11}$$

Then, the marginal posterior distributions of λ_1, λ_2 and α from equation (7.11) are expressed as follows:

$$\pi_1^*(\lambda_1 \mid \alpha, \underline{x}) \propto Gamma(D_1 + a_1, b_1 + Z(\alpha)), \tag{7.12}$$

$$\pi_2^*(\lambda_2 \mid \alpha, \underline{x}) \;\; \propto \;\; Gamma(D_2 + a_2, b_2 + Z(\alpha)), \tag{7.13}$$

$$\pi_3^*(\alpha \mid \underline{x}) \;\; \propto \;\; \alpha^{D+a_3-1} \exp\left(-b_3\alpha + \alpha \sum_{i=1}^{D} \ln x_i\right), \tag{7.14}$$

with the associated weight,

$$W(\lambda_1, \lambda_2, \alpha, \mid \underline{x}) = \frac{(\lambda_1 + \lambda_2)^{D_3}}{[b_1 + Z(\alpha)]^{D_1+a_1} [b_2 + Z(\alpha)]^{D_2+a_2}}.$$

Here, we present the importance sampling procedure for generating random samples from posterior distribution and to compute the BEs. The procedure is outlined as follows:

Step1: Set $k = 1$ and start with an initial guess for $\Theta^{(0)} = (\hat{\lambda}_1, \hat{\lambda}_2, \hat{\alpha})$.

Step2: Generate $\lambda_1^{(k)}$ and $\lambda_2^{(k)}$ from the gamma distributions specified in equations (7.12) and (7.13), respectively.

Step3: Generate $\alpha^{(k)}$ from equation (7.14) using the M-H algorithm with a normal proposal distribution with mean $\alpha^{(k-1)}$ and variance σ^2 , where σ^2 is derived from a variance-covariance matrix, as follows:

(a): Generate α^* from the normal distribution $\mathrm{N}(\alpha^{(k-1)}, \sigma^2)$ as the proposal distribution.

(b): Calculate the acceptance probability from equation (7.14) as
$\mathrm{P}(\alpha^*, \alpha^{(k-1)}) = \min\left[1, \frac{\pi_3^*(\alpha^* | \lambda_1^{(k)}, \lambda_2^{(k)}, \underline{x})}{\pi_3^*(\alpha^{(k-1)} | \lambda_1^{(k)}, \lambda_2^{(k)}, \underline{x})}\right]$.

(c): Generate U_k from uniform (0, 1).

(d): If $U_k \leq \mathrm{P}(\alpha^*, \alpha^{(k-1)})$, take $\alpha^{(k)} = \alpha^*$; Otherwise $\alpha^{(k)} = \alpha^{(k-1)}$.

Step4: Assign $k = k + 1$.

Step5: Repeat steps 2 - 4 M times.

Step6: Considering that M^* represents the number of MCMC iterations needed to reach the stationary distribution, the BE of any function $g(\lambda_1, \lambda_2, \alpha)$ of the model parameters under the SELF is given by,

$$\hat{g}_B = \frac{\frac{1}{M-M^*} \sum_{i=M^*+1}^{M} g(\lambda_1^{(i)}, \lambda_2^{(i)}, \alpha^{(i)}) W(\lambda_1^{(i)}, \lambda_2^{(i)}, \alpha^{(i)} \mid \underline{x})}{\frac{1}{M-M^*} \sum_{i=M^*+1}^{M} W(\lambda_1^{(i)}, \lambda_2^{(i)}, \alpha^{(i)} \mid \underline{x})},$$

with the associated posterior variance is,

$$\hat{V}(\lambda_1,\lambda_2,\alpha)=\frac{\frac{1}{M-M^*}\sum_{i=M^*+1}^{M}\left(g(\lambda_1^{(i)},\lambda_2^{(i)},\alpha^{(i)})-\hat{g}_B\right)^2 W(\lambda_1^{(i)},\lambda_2^{(i)},\alpha^{(i)}\mid \underline{x})}{\frac{1}{M-M^*}\sum_{i=M^*+1}^{M} W(\lambda_1^{(i)},\lambda_2^{(i)},\alpha^{(i)}\mid \underline{x})}.$$

7.4.1 Bayesian Credible Interval

As stated in Chen and Shao (1999), the credible interval or HPD credible intervals for any function $g(\lambda_1,\lambda_2,\alpha)$ can be constructed as follows:

Step1: Sort $g(\lambda_1^{(i)},\lambda_2^{(i)},\alpha^{(i)})$ and the corresponding weighted function $w^{(i)}=\frac{W(\lambda_1^{(i)},\,\lambda_2^{(i)},\,\alpha^{(i)}|\underline{x})}{\sum_{i=M^*+1}^{M}W(\lambda_1^{(i)},\,\lambda_2^{(i)},\,\alpha^{(i)}|\underline{x})}$ are denoted as $g_{(i)}$ and $w_{(i)}$ for i $=M^*+1,M^*+2,\ldots,M$, obtained from the importance sampling technique.

Step2: The marginal posterior of g given in the ordered pairs (g_i,w_i) can be defined as follows:

$$\hat{g}(\gamma)=\begin{cases} g_{(1)}, & \text{if } \gamma=0\\ g_{(k)}, & \text{if } \sum_{i=1}^{k-1}w^{(i)}<\gamma<\sum_{i=1}^{k}w^{(i)}\end{cases}$$

Step3: The estimated $100(1-\gamma)\%$ credible interval for $g(\lambda_1,\lambda_2,\alpha)$ is represented as $\left(g\left(\frac{\gamma}{2}\right),g\left(1-\frac{\gamma}{2}\right)\right)$.

Step4: The estimated $100(1-\gamma)\%$ HPD credible interval for $g(\lambda_1,\lambda_2,\alpha)$ is given by $\left(g\left(\frac{L}{M-M^*}\right),g\left(\frac{L+[(1-\gamma)(M-M^*)]}{M-M^*}\right)\right)$, where L ranges from 1 to $\gamma(M-M^*)$. This interval is chosen for having the smallest width among all credible intervals.

7.5 Simulation

In this section, we carry out comprehensive Monte Carlo simulations to assess the effectiveness of the proposed estimation methods under GTIIHCS. The estimated MSEs are used to compare the point estimators of the parameters in CRs models. Similarly, interval estimators are examined based on average lengths (AL) and their associated coverage probabilities (CP). The following algorithm illustrates the steps to generate GTIIHC competing risks data from a Weibull distribution:

1. Generate Type-II censored data from W(α, λ_1+λ_2).

2. For each Type-II data, allocate the cause of failure as either one or two, with probabilities of $\frac{\lambda_1}{\lambda_1+\lambda_2}$ and $\frac{\lambda_2}{\lambda_1+\lambda_2}$ respectively.

3. By comparing T_1, T_2 and $X_{m:n}$ with Type-II censored data, we obtain the Weibull GTIIHC CRs data with sample size D.

4. Partially observed CRs GTIIHC data can be obtained by generating a trial of 0 and 1 of size D using a Bernoulli distribution with parameter p, where $0 < p < 1$ represents the masking probability. If 0 appears, the associated failure cause is treated as unknown, whereas if 1 appears, the failure cause is considered known.

The true values of the model parameters for the selected simulation study are (λ_1, λ_2, α) = (0.4, 0.7, 1.5). Various censoring schemes are examined based on differing values of (n, m, T_1, T_2, p). For each censoring criterion, m values are selected as (15, 20) for sample size $n = 30$, (20, 30) for $n = 40$, and (30, 40) for $n = 60$, with masking probabilities $p = 0.05$ and 0.1. Also, we consider all results for prefixed time constraints (T_1, T_2) = (0.4, 1) and (0.2, 1.3). Here, BEs are evaluated considering both IP and a NIP. The results of simulations for each point and interval estimate, based on 10,000 repetitions, are displayed in Tables 7.1 - 7.4. Interval estimates are computed using a nominal significance level of 0.05. Based on Tables 7.1 - 7.4, the following conclusions have been drawn:

- The average MSE of both the MLEs and BEs decline with increasing values of n and m.
- Also, the MSE of the MLE and Bayesian estimates increases as the masking probability p is permitted to increase.
- The average MSE values decrease as the values of the prefixed time increase.
- In terms of MSEs, the BEs under IP outperform the MLEs and the BEs under NIP.
- As the values of n amd m increase, the AL of the confidence intervals decreases.
- The AL of the intervals increase as the masking probability p increases, while keeping n and m constant.

- Similarly, the CPs of these intervals closely approximate the nominal significance level in most instances. This behavior persists as p increases.

Table 7.1: Average estimates (AEs) and mean squared errors (MSEs) for the parameters (λ_1, λ_2, α) = (0.4, 0.7, 1.5) with (T_1, T_2) = (0.4, 1).

			MLE			IP			NIP		
p	n	m	λ_1	λ_2	α	λ_1	λ_2	α	λ_1	λ_2	α
0.05	30	15	0.5037	0.8989	1.7190	0.3967	0.6898	1.5761	0.3886	0.6849	1.5984
			0.1061	0.3017	0.2092	0.0329	0.0598	0.0824	0.0340	0.0613	0.0898
		20	0.4545	0.7983	1.6518	0.4083	0.7233	1.5168	0.4195	0.7295	1.5053
			0.0389	0.0902	0.1305	0.0269	0.0483	0.0706	0.0287	0.0507	0.0779
0.1	30	15	0.5039	0.8987	1.7190	0.4020	0.7010	1.5717	0.3982	0.6856	1.6184
			0.1079	0.3049	0.2092	0.0335	0.0631	0.0826	0.0345	0.0647	0.0924
		20	0.4620	0.7897	1.6677	0.4163	0.7313	1.5185	0.4203	0.7365	1.5352
			0.0405	0.0908	0.1401	0.0273	0.0493	0.0743	0.0290	0.0516	0.0806
0.05	40	20	0.4660	0.8097	1.6497	0.3823	0.6577	1.5587	0.3830	0.6586	1.5952
			0.0513	0.1046	0.1355	0.0217	0.0396	0.0590	0.0224	0.0432	0.0652
		30	0.4347	0.7618	1.6205	0.4119	0.7244	1.4315	0.4160	0.7163	1.4578
			0.0220	0.0387	0.0865	0.0187	0.0329	0.0441	0.0193	0.0336	0.0449
0.1	40	20	0.4670	0.8087	1.6497	0.3815	0.6733	1.5814	0.3778	0.6728	1.5839
			0.0520	0.1064	0.1355	0.0234	0.0404	0.0615	0.0236	0.0475	0.0669
		30	0.4333	0.7632	1.6205	0.4190	0.7302	1.4375	0.4188	0.7267	1.4551
			0.0226	0.0394	0.0865	0.0194	0.0336	0.0443	0.0198	0.0350	0.0469
0.05	60	30	0.4343	0.7672	1.5909	0.3762	0.6470	1.4011	0.3599	0.6521	1.3809
			0.0229	0.0580	0.0782	0.0132	0.0217	0.0206	0.0139	0.0247	0.0337
		40	0.4197	0.7336	1.5692	0.3964	0.6828	1.5052	0.4061	0.7049	1.5249
			0.0129	0.0246	0.0558	0.0117	0.0199	0.0201	0.0125	0.0216	0.0234
0.1	60	30	0.4343	0.7672	1.5909	0.3691	0.6349	1.3956	0.3603	0.6179	1.3724
			0.0249	0.0587	0.0782	0.0236	0.0230	0.0241	0.0286	0.0250	0.0345
		40	0.4191	0.7343	1.5692	0.3915	0.7031	1.5096	0.3961	0.7062	1.5468
			0.0133	0.0250	0.0558	0.0198	0.0212	0.0340	0.0231	0.0234	0.0357

Table 7.2: ALs and CPs for the parameters (λ_1, λ_2, α) = (0.4, 0.7, 1.5) with (T_1, T_2) = (0.4, 1).

			ACI			IP HPD			NIP HPD		
p	n	m	λ_1	λ_2	α	λ_1	λ_2	α	λ_1	λ_2	α
0.05	30	15	0.9878	1.4544	1.6142	0.5226	0.5918	1.0826	0.6415	0.8162	1.1727
			0.95	0.97	0.95	0.93	0.93	0.92	0.92	0.93	0.93
		20	0.7069	0.9680	1.3529	0.5113	0.5887	0.9354	0.5011	0.7056	1.0604
			0.96	0.97	0.96	0.93	0.94	0.95	0.94	0.92	0.94
0.1	30	15	0.9995	1.4633	1.6142	0.5740	0.8212	1.1511	0.6548	0.8665	1.3794
			0.94	0.96	0.95	0.93	0.92	0.91	0.93	0.94	0.95
		20	0.7229	0.9706	1.3417	0.5297	0.6991	1.1130	0.5629	0.7929	1.3811
			0.95	0.97	0.96	0.94	0.93	0.94	0.92	0.95	0.95
0.05	40	20	0.7605	1.0698	1.3397	0.4894	0.6586	1.0024	0.4939	0.7059	1.1663
			0.95	0.97	0.96	0.91	0.92	0.93	0.93	0.95	0.95
		30	0.5626	0.7548	1.1052	0.4871	0.6254	0.8388	0.4762	0.6273	1.1475
			0.95	0.96	0.95	0.92	0.93	0.94	0.94	0.96	0.97
0.1	40	20	0.7717	1.0768	1.3397	0.5303	0.5643	1.0686	0.5311	0.6542	1.1822
			0.95	0.97	0.96	0.96	0.95	0.96	0.97	0.95	0.96
		30	0.5711	0.7626	1.1052	0.5284	0.6128	0.8880	0.5301	0.6648	0.8747
			0.95	0.96	0.95	0.95	0.95	0.96	0.96	0.95	0.97
0.05	60	30	0.5683	0.8010	1.0549	0.4178	0.5420	0.8219	0.4235	0.5221	0.8662
			0.95	0.96	0.96	0.94	0.95	0.97	0.93	0.94	0.95
		40	0.4530	0.6071	0.8908	0.3318	0.5027	0.7334	0.3710	0.4938	0.7369
			0.95	0.95	0.95	0.95	0.95	0.96	0.94	0.95	0.95
0.1	60	30	0.5769	0.8075	1.0549	0.4293	0.5689	1.0030	0.4305	0.5737	0.8716
			0.96	0.96	0.96	0.96	0.95	0.94	0.95	0.97	0.93
		40	0.4603	0.6133	0.8908	0.3594	0.5295	0.7362	0.3934	0.5862	0.7818
			0.95	0.96	0.95	0.97	0.96	0.95	0.96	0.96	0.95

Table 7.3: Average estimates (AEs) and mean squared errors (MSEs) for the parameters (λ_1, λ_2, α) = (0.4, 0.7, 1.5) with (T_1, T_2) = (0.2, 1.3)

			MLE			IP			NIP		
p	n	m	λ_1	λ_2	α	λ_1	λ_2	α	λ_1	λ_2	α
0.05	30	15	0.4983	0.8736	1.7104	0.3904	0.7101	1.5092	0.4003	0.7283	1.4997
			0.1027	0.2583	0.2196	0.0325	0.0632	0.0715	0.0334	0.0652	0.0734
		20	0.4435	0.787	1.6461	0.3994	0.7292	1.5747	0.3999	0.7563	1.6326
			0.0399	0.0968	0.1296	0.0248	0.0449	0.0725	0.0271	0.0535	0.0758
0.1	30	15	0.4988	0.8732	1.7100	0.3802	0.6944	1.5136	0.3841	0.7134	1.5559
			0.1043	0.2597	0.2196	0.0338	0.0647	0.0754	0.0364	0.0694	0.0856
		20	0.4447	0.7858	1.6461	0.4102	0.7428	1.5689	0.4169	0.7453	1.6126
			0.0413	0.0979	0.1296	0.0249	0.0488	0.0817	0.0275	0.0542	0.0951
0.05	40	20	0.4644	0.8112	1.6494	0.3823	0.6577	1.5495	0.3923	0.6702	1.5645
			0.0514	0.1060	0.1356	0.0217	0.0396	0.0550	0.0222	0.0397	0.0574
		30	0.4180	0.7465	1.5922	0.3986	0.6969	1.4519	0.3953	0.7124	1.4813
			0.0198	0.0351	0.0708	0.0160	0.0264	0.0420	0.0161	0.0300	0.0478
0.1	40	20	0.4632	0.8123	1.6494	0.3971	0.6859	1.5448	0.3909	0.6567	1.5974
			0.0516	0.1094	0.1356	0.0230	0.0410	0.0561	0.0231	0.0417	0.0586
		30	0.4173	0.7472	1.5922	0.4138	0.7199	1.4315	0.4155	0.7542	1.4961
			0.0204	0.0357	0.0708	0.0170	0.0291	0.0441	0.0185	0.0334	0.0509
0.05	60	30	0.4377	0.7636	1.5906	0.3606	0.6597	1.3831	0.3535	0.6470	1.4107
			0.0295	0.0489	0.0779	0.0131	0.0246	0.0332	0.0232	0.0480	0.0225
		40	0.4172	0.7270	1.5594	0.4136	0.6957	1.5234	0.3971	0.7174	1.5086
			0.0147	0.0251	0.0533	0.0115	0.0194	0.0203	0.0119	0.0216	0.0331
0.1	60	30	0.4376	0.7638	1.5906	0.3696	0.6582	1.3761	0.3555	0.6349	1.3516
			0.0299	0.0495	0.0779	0.0136	0.0248	0.0346	0.0249	0.0507	0.0890
		40	0.4176	0.7267	1.5594	0.4214	0.6873	1.5694	0.3987	0.7128	1.5251
			0.0152	0.0255	0.0533	0.0130	0.0197	0.0206	0.0226	0.0379	0.0371

Table 7.4: ALs and CPs for the parameters (λ_1, λ_2, α) = (0.4, 0.7, 1.5) with (T_1, T_2) = (0.2, 1.3).

			ACI			IP HPD			NIP HPD		
p	n	m	λ_1	λ_2	α	λ_1	λ_2	α	λ_1	λ_2	α
0.05	30	15	0.8914	1.3991	1.6049	0.5019	0.7000	1.0809	0.5610	0.7090	1.0840
			0.94	0.97	0.95	0.94	0.93	0.95	0.94	0.92	0.93
		20	0.6772	0.9301	1.2922	0.4756	0.6384	0.9512	0.4963	0.7028	1.0228
			0.95	0.96	0.95	0.93	0.95	0.93	0.94	0.93	0.94
0.1	30	15	0.9703	1.3037	1.6049	0.7011	0.8945	1.7862	0.6236	0.9388	1.9115
			0.93	0.98	0.97	0.92	0.93	0.94	0.93	0.92	0.95
		20	0.6869	0.9323	1.2922	0.6682	0.8506	1.0655	0.5016	0.7262	1.0829
			0.93	0.97	0.94	0.93	0.94	0.95	0.94	0.94	0.96
0.05	40	20	0.7582	1.0711	1.3391	0.4309	0.6003	0.7913	0.4401	0.6036	0.9484
			0.95	0.96	0.96	0.96	0.94	0.95	0.94	0.93	0.96
		30	0.5115	0.6877	1.0030	0.4200	0.5833	0.9790	0.4318	0.5874	0.8318
			0.94	0.96	0.95	0.97	0.95	0.96	0.95	0.94	0.95
0.1	40	20	0.7670	1.0800	1.3391	0.4423	0.6061	0.8004	0.4434	0.6085	0.9761
			0.94	0.96	0.96	0.93	0.95	0.95	0.94	0.96	0.94
		30	0.5197	0.6946	1.0030	0.4323	0.5813	0.9286	0.4348	0.5939	0.8458
			0.96	0.96	0.96	0.94	0.96	0.94	0.95	0.97	0.92
0.05	60	30	0.5725	0.7965	1.0546	0.4178	0.5027	0.8662	0.4200	0.4902	0.8668
			0.94	0.97	0.97	0.95	0.94	0.96	0.94	0.93	0.92
		40	0.4414	0.5898	0.8641	0.3576	0.4576	0.7681	0.3381	0.4933	0.7287
			0.93	0.96	0.95	0.93	0.98	0.97	0.94	0.93	0.97
0.1	60	30	0.5810	0.8031	1.0546	0.4305	0.5731	1.0038	0.4499	0.5860	0.8721
			0.95	0.97	0.97	0.96	0.95	0.96	0.93	0.96	0.93
		40	0.4491	0.5953	0.8641	0.4067	0.5295	0.8327	0.4076	0.5352	0.8649
			0.93	0.96	0.95	0.95	0.94	0.95	0.97	0.95	0.96

7.6 Data Analysis

In this section, we explore a real data set for illustrative purposes, derived from an experiment by Dr. H.E. Walburg Jr. at the Oak Ridge National Laboratory (refer to Hoel (1972)). A set of male mice was administered a radiation dose of 300 roentgens at the age of 5-6 weeks. The causes of death were categorized into three groups: (1) Thymic Lymphoma, (2) Reticulum Cell Sarcoma, and (3) Other causes. For our analysis, we have designated Reticulum Cell Sarcoma as Cause-1 and grouped all other causes together as Cause-2. The data is shown in Table 7.5. For computational simplicity, we analyzed the data after dividing it by 1000. The transformed data sets are assumed to follow a Weibull distribution with a scale parameter $\lambda_1 + \lambda_2$ and a shape parameter α.

Table 7.5: Autopsy Results for 99 RFM conventional male mice exposed to a radiation dose of 300 roentgens dose at 5-6 weeks of age.

Cause of Death	**Mice ID Numbers**
Thymic Lymphoma	159, 189, 191, 198, 200, 207, 220, 235, 245, 250, 256, 261, 265, 266, 280, 343, 356, 383, 403, 414, 428, 432
Reticulum Cell Sarcoma	317, 318, 399, 495, 525, 536, 549, 552, 554, 557, 558, 571, 586, 594, 596, 605, 612, 621, 628, 631, 636, 643, 647, 648, 649, 661, 663, 666, 670, 695, 697, 700, 705, 712, 713, 738, 748, 753
Other Causes	40, 42, 51, 62, 163, 179, 206, 222, 228, 252, 249, 282, 324, 333, 341, 366, 385, 407, 420, 431, 441, 461, 462, 482, 517, 517, 524, 564, 567, 586, 619, 620, 621, 622, 647, 651, 686, 761, 763

A GoF test was conducted to evaluate whether the Weibull distribution is a suitable model for the given datasets. Specifically, the K-S statistic, along with the corresponding p - value, was used to assess the fit. The results of the GoF test were compared with those from the Lognormal, Chen, and inverted exponential distributions. These datasets were previously analyzed in CRs scenarios using the Chen (Al-Bossly (2022)) and inverted exponential Farghal et al. (2023) distributions under different censoring schemes. Table 7.6 demonstrates that the proposed model exhibits greater flexibility than the other three distributions. We also provide Q-Q plots in Figure 7.2. These graphs demonstrate

that the considered model offers a relatively good fit for the two data sets under examination.

Table 7.6: GoF of datsets.

	Dataset 1		Dataset 2	
	K-S	p - value	K-S	p -value
Weibull	0.0733	0.9773	0.0817	0.8095
Lognormal	0.1701	0.1974	0.1086	0.4675
Inverted exponetial	0.1006	0.7993	0.1507	0.1248
Chen	0.0759	0.9691	0.0848	0.7716

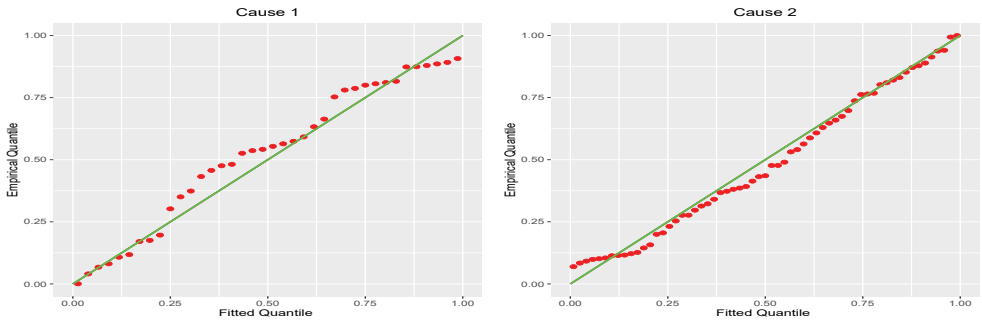

Figure 7.2: Q-Q plots for the dataset with two different causes.

With $n = 99$, $m = 55$, $T_1 = 0.45$, $T_2 = 0.6$ and $p = 0.1$ given, the CRs for GTIIHCS are summarized in Table 7.7. Due to insufficient data, some randomly chosen failure causes are marked as missing, indicated by 0. In this context, 1 represents the first cause, 2 the second, and 0 an unobserved cause. Based on the data, we note the values (D_1, D_2, D_3, D) as (7, 44, 4, 55). For the data provided, we compute the ML estimates for the unknown parameters, along with the corresponding 95% confidence intervals. Figure 7.3 presents the profile log-likelihood of α. Upon visual examination, these plots reveal that the profile likelihood is unimodal, suggesting a unique maximum.

Table 7.7: Partial competing risk censored data with failure time and cause of failure for n = 99 and m = 55.

(0.04, 2)	(0.2, 2)	(0.252, 0)	(0.333, 2)	(0.414, 2)	(0.517, 2)
(0.042, 2)	(0.206, 2)	(0.256, 2)	(0.341, 2)	(0.42, 2)	(0.517, 2)
(0.051, 2)	(0.207, 2)	(0.261, 2)	(0.343, 2)	(0.428, 2)	(0.524, 2)
(0.062, 2)	(0.22, 2)	(0.265, 2)	(0.356, 2)	(0.431, 2)	(0.525, 1)
(0.159, 1)	(0.222, 0)	(0.266, 2)	(0.366, 2)	(0.432, 2)	(0.536, 1)
(0.163, 2)	(0.228, 2)	(0.28, 2)	(0.383, 2)	(0.441, 2)	
(0.179, 0)	(0.235, 2)	(0.282, 2)	(0.385, 2)	(0.461, 0)	
(0.189, 2)	(0.245, 2)	(0.317, 1)	(0.399, 1)	(0.462, 2)	
(0.191, 2)	(0.249, 2)	(0.318, 1)	(0.403, 2)	(0.482, 2)	
(0.198, 2)	(0.25, 2)	(0.324, 2)	(0.407, 2)	(0.495, 1)	

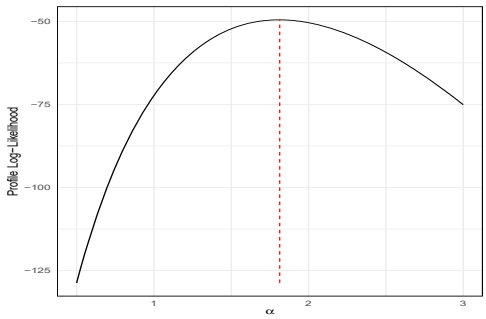

Figure 7.3: Plots of profile log-likelihood of α for the real data.

In the absence of prior information for the unknown parameters, we utilize NIPs to compute BEs and determine the associated HPD credible intervals. The results of the ML estimates and approximate confidence intervals, as well as the BEs and HPD intervals, are shown in Table 7.8. Moreover, we observe that the Bayesian credible intervals for parameters, based on NIPs, have shorter lengths compared to MLE based asymptotic confidence intervals. In order to assess the convergence of the MCMC technique for the given datasets, the trace and density graphs for the three parameters are provided in Figures 7.4.

Table 7.8: Point and interval estimates (with interval lengths in brackets) of the unknown parameters of the Weibull distribution for a real dataset under POCR data

	λ_1	λ_2	α
ML Estimates	0.3466	2.1790	1.8097
BEs	0.1862	1.1809	1.0851
ACI	(0.0673, 0.6259)[0.5586]	(1.2357, 3.1222)[1.8864]	(1.3729, 2.2466)[0.8737]
HPD	(0.1112, 0.2548)[0.1436]	(0.9787,1.4297)[0.4510]	(0.9797, 1.2113)[0.2316]

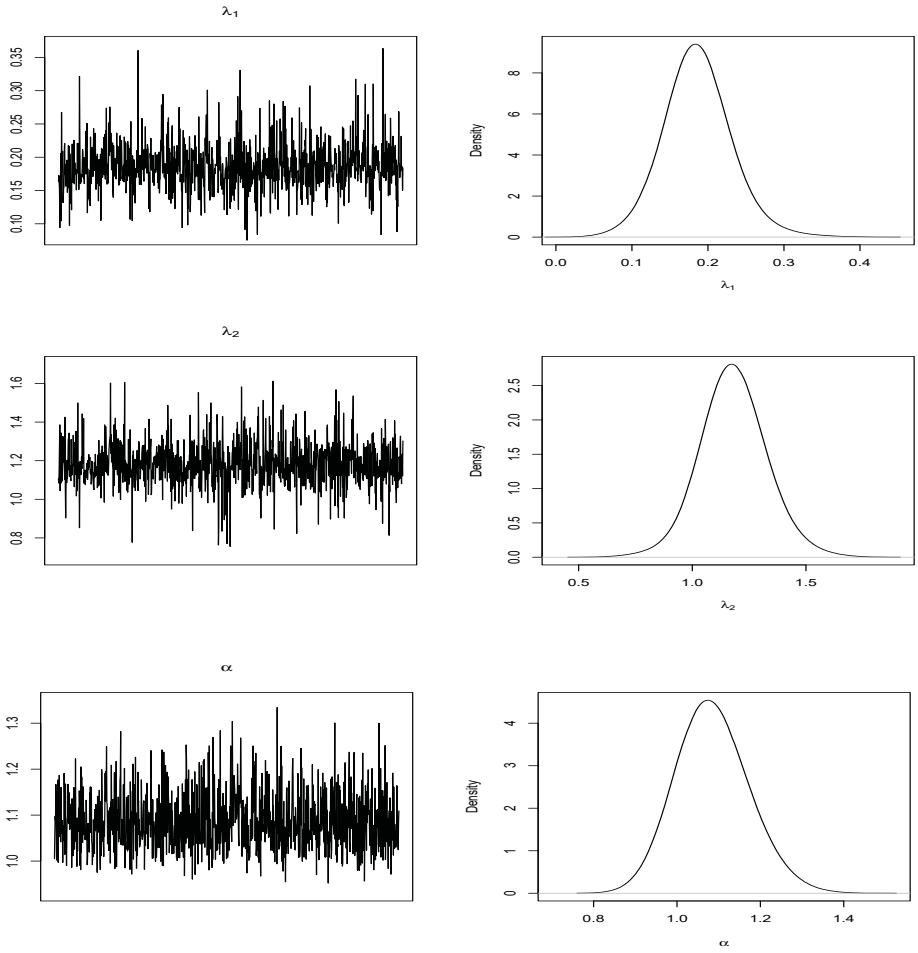

Figure 7.4: Trace and density plots of MCMC samples for the parameters under the POCRs in real life data.

7.7 Summary

This Chapter investigates a generalization of the CRs problem, known as POCR, where data are obtained using GTIIHC. Various inferences for the unknown parameters of Weibull distributions are obtained using both classical and Bayesian approaches. A comprehensive simulation study is conducted to evaluate the proposed model, and an illustrative real data analysis is also provided. The simulation results suggest that Bayesian methods outperform classical methods. A key observation is that higher masking probabilities degrade the performance of the estimators. This implies that the presence or absence of failure causes significantly impacts the lifetime analysis of units where multiple causes of failure are possible.

Chapter 8

Inference on Multicomponent Stress-Strength Reliability using Progressively First-Failure Censored data from Weibull Distribution

8.1 Introduction

The traditional single component stress-strength model, expressed as $R = P(X > Y)$, can be extended to multicomponent systems. These MSS models are increasingly recognized for their ability to model complex systems, gaining attention in reliability engineering, survival analysis, and risk assessment. A detailed overview of MSS models and their applications is presented in Chapter 1.

Researchers have primarily examined the MSS reliability model under the assumption that the strength components are i.i.d. random variables. However, this assumption is not applicable when the component architectures differ. In fact, even among identical objects made from the same material, variations in strength can occur. For instance, the structure of the jute technical fiber in the breaking strength experiment relies on several parallel short ultimate cells embedded in a non-cellulose matrix, resembling multiple fiber reinforced composites (see Xia et al. 2009). Hence, the strengths of the components become non-

identical. These illustrations imply that assuming non-identical strength factors is a more practical approach for real-world scenarios. Research on the reliability of non-i.i.d MSS is limited. Rasethuntsa and Nadar 2018 focused on MSSR using the Kumaraswamy distribution for non-identical strength components. Kohansal et al. (2021) investigated stress-strength parameters in multicomponent systems with non-identical strengths using bathtub shaped distribution. More recently, Demiray and Kızılaslan (2024) estimated MSSR under a proportional hazard rate model, while Saini et al. (2024) analyzed MSSR based on PC data from the Kumaraswamy distribution.

Let's now look at a system comprising $\mathrm{k} = (k_1, k_2, \ldots, k_m)$ components. The k_i components in this system are of type i, where $i = 1, 2, \ldots, m$. Assume that the CDF of the strengths of type i components is $F_i(.)$. Furthermore, it is assumed that all components are subjected to a common stress Y with CDF $F_Y(.)$. Under this condition, the system remains reliable as long as at least $\mathrm{s} = (s_1, s_2, \ldots, s_m)$ of the k strength components exceed the applied stress. Rasethuntsa and Nadar (2018) refined (1.9) to develop an appropriate model, expressed as follows:

$$R_{\mathrm{s,k}} = \sum_{p_1=s_1}^{k_1} \cdots \sum_{p_m=s_m}^{k_m} \left(\prod_{i=1}^{m} \binom{k_i}{p_i} \right) \int_{-\infty}^{\infty} \prod_{i=1}^{m} \left((1 - F_i(y))^{p_i} \left(F_i(y)\right)^{k_i - p_i} \right) dF_Y(y). \tag{8.1}$$

Here the summation extends over $0 \leq p_i \leq k_i$ for all $i = 1, 2, \ldots, m$, such that $s \leq \sum_{i=1}^{m} p_i \leq k$.

Due to computational complexity, this paper focuses on a system with two types of components, i.e., $\mathrm{k} = (k_1, k_2)$ and $\mathrm{s} = (s_1, s_2)$. Hence, the multi-component reliability for a system with two non-identical strength component can be derived from (8.1) as follows:

$$\begin{aligned} R_{s_1,s_2,k_1,k_2} &= \sum_{p_1=s_1}^{k_1} \sum_{p_2=s_2}^{k_2} \binom{k_1}{p_1} \binom{k_2}{p_2} \int_{-\infty}^{\infty} (1 - F_1(y))^{p_1} \left(F_1(y)\right)^{k_1 - p_1} \\ &\times (1 - F_2(y))^{p_2} \left(F_2(y)\right)^{k_2 - p_2} dF_Y(y). \end{aligned} \tag{8.2}$$

The aforementioned model simplifies when $k_2 = 0$, resulting in the multicompo-

nent system with i.i.d. components established by Bhattacharyya and Johnson (1974).

Censoring plays a significant role in real-life testing scenarios, as we often face limitations in the number of test units or cannot include all of them due to constraints like time and budget. Various censoring methods have been discussed in literature, including Type I, Type II, progressive, random, and first failure censoring schemes, which are utilized in life testing experiments. Cohen (1963) introduced the concept of progressive censoring, which permits the removal of items before the life testing experiments conclude. Balasooriya (1995) proposed a new censoring method referred to as the first-failure censoring scheme. This scheme involves organizing test units into several groups, each containing a collection of items, and conducting the experiment until the first failure occurs within each group. Wu and Kus (2009) merged the principles of progressive and first failure censoring, creating what they termed the progressive first failure censoring scheme (PFFCS). Over the past ten years, these PFFCS have garnered considerable attention in research. For comprehensive information on this topic, one can refer to works by Soliman et al. (2012), Kumar et al. (2015), Krishna et al. (2017), Saini et al. (2021), Fathi et al. (2024), and others.

The definition of the PFFCS can be described as follows: Consider N groups undergoing a life test, with each group consisting of l items. Throughout the experiment, R_1 groups are randomly eliminated when the first failure $X_{1:n:N:l}$ occurs in addition to the group with the failed item. Likewise, R_2 groups are removed when the second failure $X_{2:n:N:l}$ occurs along with the corresponding group, and this pattern continues until the n^{th} failure is observed. The sample resulting from the recorded failure times, where $X_{1:n:N:l} < X_{2:n:N:l} < ... < X_{n:n:N:l}$, constitute progressively first failure-censored sample under the progressive censoring scheme represented as $R = (R_1, R_2, ..., R_n)$, where $N = n + R_1 + R_2 + ... + R_n$.

This Chapter presents the classical and Bayesian estimation procedures for the MSSR with non-identical strength component based on the Weibull (W) distribution, under a PFFC scheme. The PDF and CDF of the two-parameter

$W(\alpha, \lambda)$ distribution are expressed as follows:

$$f(x;\alpha,\lambda) = \alpha\lambda x^{\alpha-1}e^{-\lambda x^{\alpha}}, x>0, \alpha>0, \lambda>0. \tag{8.3}$$

$$F(x;\alpha,\lambda) = 1-e^{-\lambda x^{\alpha}}, x>0, \alpha>0, \lambda>0. \tag{8.4}$$

Let $X=(x_1, x_2, \ldots, x_{k_1})$ be k_1 strength components following a W(α, λ_1), and $Z=(z_1, z_2, \ldots, z_{k_2})$ be k_2 strength components from W(α, λ_2). Assume the independent stress variable Y follows W(α, λ_3). Using Equations (8.2), (8.3), and (8.4), the MSSR for non-identical strength components from the W distribution can be defined as follows:

$$\begin{aligned}
R_{s_1,s_2,k_1,k_2} &= \sum_{p_1=s_1}^{k_1}\sum_{p_2=s_2}^{k_2}\binom{k_1}{p_1}\binom{k_2}{p_2}\int_0^{\infty} e^{-p_1\lambda_1 y^{\alpha}}\left(1-e^{-\lambda_1 y^{\alpha}}\right)^{k_1-p_1} e^{-p_2\lambda_2 y^{\alpha}} \\
&\times \left(1-e^{-\lambda_2 y^{\alpha}}\right)^{k_2-p_2}\alpha\lambda_3 y^{\alpha-1}e^{-\lambda_3 y^{\alpha}}dy \quad \text{put}: \ t=e^{-y^{\alpha}} \\
&= \sum_{p_1=s_1}^{k_1}\sum_{p_2=s_2}^{k_2}\binom{k_1}{p_1}\binom{k_2}{p_2}\lambda_3 \\
&\times \int_0^1 t^{\lambda_1 p_1+\lambda_2 p_2+\lambda_3-1}\left(1-t^{\lambda_1}\right)^{k_1-p_1}\left(1-t^{\lambda_2}\right)^{k_2-p_2}dt. \\
&= \sum_{p_1=s_1}^{k_1}\sum_{p_2=s_2}^{k_2}\sum_{q_1=0}^{k_1-p_1}\sum_{q_2=0}^{k_2-p_2}\binom{k_1}{p_1}\binom{k_2}{p_2}\binom{k_1-p_1}{q_1}\binom{k_2-p_2}{q_2}(-1)^{q_1+q_2} \\
&\times \frac{\lambda_3}{\lambda_1(p_1+q_1)+\lambda_2(p_2+q_2)+\lambda_3}.
\end{aligned} \tag{8.5}$$

The organization of the Chapter is outlined as follows: In Section 8.2, we explore the statistical inference of R_{s,k_1,k_2} under the assumption of an unknown common parameter α. Both MLE and Bayesian estimation techniques are used for this purpose. Section 8.3 broadens the inference to a more general scenario, again applying both MLE and Bayesian methods to estimate R_{s,k_1,k_2}. Section 8.4 presents the outcomes of a simulation study, while Section 8.5 illustrates the application of the proposed methods to latest real data. The concluding remarks are summarized in Section 8.6.

8.2 Inference of R_{s,k_1,k_2} when α is Unknown

8.2.1 MLE of R_{s,k_1,k_2}

In this section, we aim to determine the MLEs of α, λ_1, λ_2 and λ_3 in order to derive the MLE for MSSR R_{s,k_1,k_2}. Let $\{Y_1,\ldots,Y_n\}$, $\{X_{i1},\ldots,X_{ik_1}\}$ and $\{Z_{i1},\ldots,Z_{ik_2}\}$, $i=1,\ldots,n$, be three PFFC samples of stress and strength components from W(α, λ_3), W(α, λ_1) and W(α, λ_2) with schemes $(N,n,l_1,S_1,\ldots,S_n)$, $(K_1,k_1,l_2,R_{i1},\ldots,R_{ik_1})$ and $(K_2,k_2,l_3,Q_{i1},\ldots,Q_{ik_2})$, respectively. Then, the multicomponent data are structured as follows:

$$X=\begin{pmatrix} X_{11} & X_{12} & \cdots & X_{1k_1}\\ \vdots & \vdots & \ddots & \vdots\\ X_{n1} & X_{n2} & \cdots & X_{nk_1}\end{pmatrix},\quad Z=\begin{pmatrix} Z_{11} & Z_{12} & \cdots & Z_{1k_2}\\ \vdots & \vdots & \ddots & \vdots\\ Z_{n1} & Z_{n2} & \cdots & Z_{nk_2}\end{pmatrix},\quad Y=\begin{pmatrix} Y_1\\ Y_2\\ \vdots\\ Y_n\end{pmatrix}.$$

The following is the likelihood equation for the aforementioned data:

$$\begin{aligned} L(\lambda_1,\lambda_2,\lambda_3,\alpha\mid data) = c_1 l_1^n \prod_{i=1}^{n}\Bigg[&\Big(c_2 l_2^{k_1}\prod_{j_1=1}^{k_1} f(x_{ij_1})\left(1-F(x_{ij_1})\right)^{l_2(R_{j_1}+1)-1}\Big)\\ &\times\Big(c_3 l_3^{k_2}\prod_{j_2=1}^{k_2} f(z_{ij_2})\left(1-F(z_{ij_2})\right)^{l_3(Q_{j_2}+1)-1}\Big)\\ &\times f(y_i)\left(1-F(y_i)\right)^{l_1(S_i+1)-1}\Bigg].\\ =&c_1 l_1^n c_2^n l_2^{nk_1} c_3^n l_3^{nk_2}\alpha^{nk_1+nk_2+n}\lambda_1^{nk_1}\lambda_2^{nk_2}\lambda_3^n\\ &\times\prod_{i=1}^{n}\prod_{j_1=1}^{k_1} x_{ij_1}^{\alpha-1}\prod_{i=1}^{n}\prod_{j_2=1}^{k_2} z_{ij_2}^{\alpha-1}\prod_{i=1}^{n} y_i^{\alpha-1}\\ &\times e^{-\lambda_1\sum_{i=1}^{n}\sum_{j_1=1}^{k_1} x_{ij_1}^{\alpha} l_2(R_{j_1}+1)} e^{-\lambda_2\sum_{i=1}^{n}\sum_{j_2=1}^{k_2} z_{ij_2}^{\alpha} l_3(Q_{j_2}+1)}\\ &\times e^{-\lambda_3\sum_{i=1}^{n} y_i^{\alpha} l_1(S_i+1)}, \end{aligned} \tag{8.6}$$

where $c_1=N(N-S_1-1)\cdots(N-S_1-\cdots-S_{n-1}-n+1)$, $c_2=K_1(K_1-R_1-1)\cdots(K_1-R_1-\cdots-R_{k_1-1}-k_1+1)$ and $c_3=K_2(K_2-Q_1-1)\cdots(K_2-Q_1-\cdots-Q_{k_2-1}-k_2+1)$ represent the normalizing constants. Ignoring the additive

constant, the log-likelihood function from (8.6) is,

$$\begin{aligned} L(\lambda_1, \lambda_2, \lambda_3, \alpha \mid data) &= (nk_1 + nk_2 + n)\log(\alpha) + nk_1 \log(\lambda_1) \\ &+ n\log(\lambda_3) + nk_2 \log(\lambda_2) \\ &+ (\alpha - 1)\left(\sum_{i=1}^{n}\sum_{j_1=1}^{k_1} \log(x_{ij_1}) + \sum_{i=1}^{n}\sum_{j_2=1}^{k_2} \log(z_{ij_2}) + \sum_{i=1}^{n} \log(y_i)\right) \\ &- \lambda_1 \sum_{i=1}^{n}\sum_{j_1=1}^{k_1} x_{ij_1}^{\alpha} l_2(R_{j_1} + 1) - \lambda_2 \sum_{i=1}^{n}\sum_{j_2=1}^{k_2} z_{ij_2}^{\alpha} l_3(Q_{j_2} + 1) \\ &- \lambda_3 \sum_{i=1}^{n} y_i^{\alpha} l_1(S_i + 1). \end{aligned} \tag{8.7}$$

The MLE's of α, λ_1, λ_2 and λ_3, represented as $\hat{\alpha}$, $\hat{\lambda}_1$, $\hat{\lambda}_2$ and $\hat{\lambda}_3$, respectively, can be derived by solving the following equations,

$$\frac{\partial L}{\partial \lambda_1} = \frac{nk_1}{\lambda_1} - \sum_{i=1}^{n}\sum_{j_1=1}^{k_1} x_{ij_1}^{\alpha} l_2(R_{j_1} + 1), \tag{8.8}$$

$$\frac{\partial L}{\partial \lambda_2} = \frac{nk_2}{\lambda_2} - \sum_{i=1}^{n}\sum_{j_2=1}^{k_2} z_{ij_2}^{\alpha} l_3(Q_{j_2} + 1), \tag{8.9}$$

$$\frac{\partial L}{\partial \lambda_3} = \frac{n}{\lambda_3} - \sum_{i=1}^{n} y_i^{\alpha} l_1(S_i + 1), \tag{8.10}$$

$$\begin{aligned} \frac{\partial L}{\partial \alpha} &= \frac{nk_1 + nk_2 + n}{\alpha} + \sum_{i=1}^{n}\sum_{j_1=1}^{k_1} \log(x_{ij_1}) + \sum_{i=1}^{n}\sum_{j_2=1}^{k_2} \log(z_{ij_2}) + \sum_{i=1}^{n} \log(y_i) \\ &- \lambda_1 \sum_{i=1}^{n}\sum_{j_1=1}^{k_1} x_{ij_1}^{\alpha} \log(x_{ij_1}) l_2(R_{j_1} + 1) - \lambda_2 \sum_{i=1}^{n}\sum_{j_2=1}^{k_2} z_{ij_2}^{\alpha} \log(z_{ij_2}) l_3(Q_{j_2} + 1) \\ &- \lambda_3 \sum_{i=1}^{n} y_i^{\alpha} \log(y_i) l_1(S_i + 1). \end{aligned} \tag{8.11}$$

Equations (8.8), (8.9) and (8.10) are used to obtain,

$$\begin{aligned} \hat{\lambda}_1(\alpha) &= \frac{nk_1}{\sum_{i=1}^{n}\sum_{j_1=1}^{k_1} x_{ij_1}^{\alpha} l_2(R_{j_1} + 1)}, \\ \hat{\lambda}_2(\alpha) &= \frac{nk_2}{\sum_{i=1}^{n}\sum_{j_2=1}^{k_2} z_{ij_2}^{\alpha} l_3(Q_{j_2} + 1)}, \\ \hat{\lambda}_3(\alpha) &= \frac{n}{\sum_{i=1}^{n} y_i^{\alpha} l_1(S_i + 1)}. \end{aligned}$$

Further, the value of $\hat{\alpha}$ is determined through numerical methods, such as the Newton-Raphson method, on (8.11). Also, by using the invariance property of MLE, we get,

$$\begin{aligned}\hat{R}_{s,k_1,k_2} &= \sum_{p_1=s_1}^{k_1}\sum_{p_2=s_2}^{k_2}\sum_{q_1=0}^{k_1-p_1}\sum_{q_2=0}^{k_2-p_2}\binom{k_1}{p_1}\binom{k_2}{p_2}\binom{k_1-p_1}{q_1}\binom{k_2-p_2}{q_2}(-1)^{q_1+q_2}\\ &\times \frac{\hat{\lambda}_3}{\hat{\lambda}_1(p_1+q_1)+\hat{\lambda}_2(p_2+q_2)+\hat{\lambda}_3}.\end{aligned}$$

8.2.2 Asymptotic Confidence Interval

In this section, we utilized the asymptotic normality property of MLEs to construct an ACI for R_{s,k_1,k_2}. If $\hat{\mu} = (\hat{\lambda}_1,\ \hat{\lambda}_2,\ \hat{\lambda}_3,\ \hat{\alpha})$ are the MLEs of $\mu = (\lambda_1,\ \lambda_2,\ \lambda_3,\ \alpha)$, then the observed Fisher information matrix is provided by $I(\hat{\mu}) = [I_{ij}]_{\mu=\hat{\mu}} = \left[-\frac{\partial^2 L}{\partial\mu_i\partial\mu_j}\right]_{\mu=\hat{\mu}}$, $i,j = 1,2,3,4$, where,

$$\begin{aligned}I_{11} &= \frac{\partial^2 L}{\partial\lambda_1^2} = \frac{nk_1}{\lambda_1^2}, \quad I_{22} = \frac{\partial^2 L}{\partial\lambda_2^2} = \frac{nk_2}{\lambda_2^2}, \quad I_{33} = \frac{\partial^2 L}{\partial\lambda_3^2} = \frac{n}{\lambda_3^2},\\ I_{12} &= I_{21} = 0, \quad I_{13} = I_{31} = 0, I_{23} = I_{32} = 0,\\ I_{14} &= \sum_{i=1}^{n}\sum_{j_1=1}^{k_1} x_{ij_1}^{\alpha}\log(x_{ij_1})l_2(R_{j_1}+1) = I_{41},\\ I_{24} &= \sum_{i=1}^{n}\sum_{j_2=1}^{k_2} z_{ij_2}^{\alpha}\log(z_{ij_2})l_3(Q_{j_2}+1) = I_{42},\\ I_{34} &= \sum_{i=1}^{n} y_i^{\alpha}\log(y_i)l_1(S_i+1) = I_{43},\\ I_{44} &= \frac{nk_1+nk_2+n}{\alpha^2} + \lambda_1\sum_{i=1}^{n}\sum_{j_1=1}^{k_1} x_{ij_1}^{\alpha}\log^2(x_{ij_1})l_2(R_{j_1}+1)\\ &+ \lambda_2\sum_{i=1}^{n}\sum_{j_2=1}^{k_2} z_{ij_2}^{\alpha}\log^2(z_{ij_2})l_3(Q_{j_2}+1) + \lambda_3\sum_{i=1}^{n} y_i^{\alpha}\log^2(y_i)l_1(S_i+1).\end{aligned}$$

The delta method is used to determine the variance of $\hat{R}_{s,k_1,k_2}$ as follows:

$$\begin{aligned}\mathrm{Var}(\hat{R}_{s,k_1,k_2}) &= \left(\frac{\partial R_{s,k_1,k_2}}{\partial \lambda_1}\right)^2 [I^{-1}]_{11} + \left(\frac{\partial R_{s,k_1,k_2}}{\partial \lambda_2}\right)^2 [I^{-1}]_{22} \\ &+ \left(\frac{\partial R_{s,k_1,k_2}}{\partial \lambda_3}\right)^2 [I^{-1}]_{33} + 2\left(\frac{\partial R_{s,k_1,k_2}}{\partial \lambda_1}\right)\left(\frac{\partial R_{s,k_1,k_2}}{\partial \lambda_2}\right)[I^{-1}]_{12} \\ &+ 2\left(\frac{\partial R_{s,k_1,k_2}}{\partial \lambda_1}\right)\left(\frac{\partial R_{s,k_1,k_2}}{\partial \lambda_3}\right)[I^{-1}]_{13} + 2\left(\frac{\partial R_{s,k_1,k_2}}{\partial \lambda_2}\right)\left(\frac{\partial R_{s,k_1,k_2}}{\partial \lambda_3}\right)[I^{-1}]_{23}.\end{aligned}$$

Thus, a $100(1-\xi)\%$ ACI for R_{s,k_1,k_2} can be formulated as:

$$\left(\hat{R}_{s,k_1,k_2} - z_{\xi/2}\sqrt{\mathrm{Var}(\hat{R}_{s,k_1,k_2})}, \quad \hat{R}_{s,k_1,k_2} + z_{\xi/2}\sqrt{\mathrm{Var}(\hat{R}_{s,k_1,k_2})}\right),$$

where z_ξ represents the $100(1-\xi)^{th}$ percentile of the $N(0,1)$.

8.2.3 Bayesian Estimation of R_{s,k_1,k_2}

In this section, we derive the Bayesian estimation of R_{s,k_1,k_2} along with its associated credible interval, using the SELF. Assuming that λ_1, λ_2, λ_3 and α all have independent gamma densities, let's say that $\lambda_1 \sim \Gamma(a_1, b_1)$, $\lambda_2 \sim \Gamma(a_2, b_2)$, $\lambda_3 \sim \Gamma(a_3, b_3)$, $\alpha \sim \Gamma(a_4, b_4)$ have the following PDFs:

$$\begin{aligned}\pi_1(\lambda_1) &\propto \lambda_1^{a_1-1} e^{-b_1\lambda_1}, \quad \lambda_1 > 0,\ a_1 > 0,\ b_1 > 0, \\ \pi_2(\lambda_2) &\propto \lambda_2^{a_2-1} e^{-b_2\lambda_2}, \quad \lambda_2 > 0,\ a_2 > 0,\ b_2 > 0, \\ \pi_3(\lambda_3) &\propto \lambda_3^{a_3-1} e^{-b_3\lambda_3}, \quad \lambda_3 > 0,\ a_3 > 0,\ b_3 > 0, \\ \pi_4(\alpha) &\propto \alpha^{a_4-1} e^{-b_4\alpha}, \quad \alpha > 0,\ a_4 > 0,\ b_4 > 0.\end{aligned}$$

Then the joint posterior density function of λ_1, λ_2, λ_3 and α is given by,

$$\pi(\lambda_1, \lambda_2, \lambda_3, \alpha \mid \text{data}) = \frac{L(\lambda_1,\lambda_2,\lambda_3,\alpha|\text{data})\,\pi_1(\lambda_1)\,\pi_2(\lambda_2)\,\pi_3(\lambda_3)\,\pi_4(\alpha)}{\int_0^\infty \int_0^\infty \int_0^\infty \int_0^\infty L(\lambda_1,\lambda_2,\lambda_3,\alpha|\text{data})\,\pi_1(\lambda_1)\,\pi_2(\lambda_2)\,\pi_3(\lambda_3)\,\pi_4(\alpha) d\lambda_1 d\lambda_2 d\lambda_3 d\alpha}. \tag{8.12}$$

The BE presented in (8.12) is not solvable through analytical methods. As a result, the MCMC approach is employed to determine the BE. The posterior

distribution outlined in (8.12) can be expressed simply as:

$$\begin{aligned}
\pi(\lambda_1,\lambda_2,\lambda_3,\alpha \mid \text{data}) &\propto \alpha^{nk_1+nk_2+n+a_4-1}\lambda_1^{nk_1+a_1-1}\lambda_2^{nk_2+a_2-1}\lambda_3^{n+a_3-1} \\
&\times \prod_{i=1}^{n}\prod_{j_1=1}^{k_1} x_{ij_1}^{\alpha-1}\prod_{i=1}^{n}\prod_{j_2=1}^{k_2} z_{ij_2}^{\alpha-1}\prod_{i=1}^{n} y_i^{\alpha-1} \\
&\times e^{-\lambda_1\left[b_1+\sum_{i=1}^{n}\sum_{j_1=1}^{k_1} x_{ij_1}^{\alpha} l_2(R_{j_1}+1)\right]} e^{-\lambda_2\left[b_2+\sum_{i=1}^{n}\sum_{j_2=1}^{k_2} z_{ij_2}^{\alpha} l_3(Q_{j_2}+1)\right]} \\
&\times e^{-\lambda_3\left[b_3+\sum_{i=1}^{n} y_i^{\alpha} l_1(S_i+1)\right]} e^{-b_4\alpha}. \qquad (8.13)
\end{aligned}$$

The conditional posterior densities of the parameters λ_1, λ_2, λ_3 and α are derived from (8.13), as,

$$\begin{aligned}
\lambda_1 \mid \alpha, data &\sim \Gamma\left(nk_1+a_1, b_1+\sum_{i=1}^{n}\sum_{j_1=1}^{k_1} x_{ij_1}^{\alpha} l_2(R_{j_1}+1)\right), \\
\lambda_2 \mid \alpha, data &\sim \Gamma\left(nk_2+a_2, b_2+\sum_{i=1}^{n}\sum_{j_2=1}^{k_2} z_{ij_2}^{\alpha} l_3(Q_{j_2}+1)\right), \\
\lambda_3 \mid \alpha, data &\sim \Gamma\left(n+a_3, b_3+\sum_{i=1}^{n} y_i^{\alpha} l_1(S_i+1)\right) \\
\pi(\alpha \mid \lambda_1,\lambda_2,\lambda_3, data) &\sim \alpha^{nk_1+nk_2+n+a_4-1}\prod_{i=1}^{n}\prod_{j_1=1}^{k_1} x_{ij_1}^{\alpha-1}\prod_{i=1}^{n}\prod_{j_2=1}^{k_2} z_{ij_2}^{\alpha-1}\prod_{i=1}^{n} y_i^{\alpha-1} \\
&\times e^{-\lambda_1\left[b_1+\sum_{i=1}^{n}\sum_{j_1=1}^{k_1} x_{ij_1}^{\alpha} l_2(R_{j_1}+1)\right]} e^{-\lambda_2\left[b_2+\sum_{i=1}^{n}\sum_{j_2=1}^{k_2} z_{ij_2}^{\alpha} l_3(Q_{j_2}+1)\right]} \\
&\times e^{-b_4\alpha-\lambda_3\left[b_3+\sum_{i=1}^{n} y_i^{\alpha} l_1(S_i+1)\right]}.
\end{aligned}$$

It is evident that random samples can be generated effectively from the posterior PDFs of λ_1, λ_2 and λ_3. However, since $\pi(\alpha \mid \lambda_1,\lambda_2,\lambda_3,data)$ does not correspond to a commonly recognized distribution, direct sampling from it is unfeasible. Thus, the Gibbs sampling algorithm is implemented using the M-Hs method as follows:

1. Begin with the initial values $(\lambda_1^0,\lambda_2^0,\lambda_3^0,\alpha^0)$.
2. Set $t=1$.
3. Generate $\alpha^{(t)}$ from $\pi\left(\alpha \mid \lambda_1^{(t-1)},\lambda_2^{(t-1)},\lambda_3^{(t-1)},\text{data}\right)$ using the M-H method with $N\left(\alpha^{(t-1)},1\right)$ as the proposal distribution.
4. Generate $\lambda_1^{(t)}$ from $\Gamma\left(nk_1+a_1, b_1+\sum_{i=1}^{n}\sum_{j_1=1}^{k_1} x_{ij_1}^{\alpha} l_2(R_{j_1}+1)\right)$.

5. Generate $\lambda_2^{(t)}$ from $\Gamma\left(nk_2 + a_2, b_2 + \sum_{i=1}^{n}\sum_{j_2=1}^{k_2} z_{ij_2}^{\alpha} l_3(Q_{j_2}+1)\right)$.
6. Generate $\lambda_3^{(t)}$ from $\Gamma\left(n + a_3, b_3 + \sum_{i=1}^{n} y_i^{\alpha} l_1(S_i+1)\right)$.
7. Compute $\widehat{R}_{s,k_1,k_2}^{(t)}$ using the formula provided in Equation (8.5).
8. Set $t = t + 1$.
9. Repeat steps 3 to 8 for T times.

Thus, the BE of R_{s,k_1,k_2} under SELF can be derived using the following expression:

$$\widehat{R}_{s,k_1,k_2}^{MC} = \frac{1}{T}\sum_{t=1}^{T} R_{s,k_1,k_2}^{(t)}.$$

The HPD credible intervals for the system reliability R_{s,k_1,k_2} can now be constructed using the algorithm introduced by Chen and Shao (1999).

8.3 Inference of R_{s,k_1,k_2} in General Case

8.3.1 MLE of R_{s,k_1,k_2}

Assume three independent random variables with distinct unknown parameters are $X \sim W(\alpha_1, \lambda_1)$, $Z \sim W(\alpha_2, \lambda_2)$ and $Y \sim W(\alpha_3, \lambda_3)$. The multi-component reliability for Weibull distribution with two non-identical component strengths can be attained by using (8.3) and (8.4) as,

$$\begin{aligned} R_{s,k_1,k_2} = &\sum_{p_1=s_1}^{k_1}\sum_{p_2=s_2}^{k_2}\binom{k_1}{p_1}\binom{k_2}{p_2}\int_0^{\infty} e^{-p_1\lambda_1 y^{\alpha_1}}\left(1-e^{-\lambda_1 y^{\alpha_1}}\right)^{k_1-p_1} e^{-p_2\lambda_2 y^{\alpha_2}} \\ &\times\left(1-e^{-\lambda_2 y^{\alpha_2}}\right)^{k_2-p_2}\alpha_3\lambda_3 y^{\alpha_3-1}e^{-\lambda_3 y^{\alpha_3}}dy. \end{aligned}$$

It is evident that the numerical approach is needed to solve this integral. Now, let us consider $\{Y_1,\ldots,Y_n\}$, $\{X_{i1},\ldots,X_{ik_1}\}$ and $\{Z_{i1},\ldots,Z_{ik_2}\}$,$i = 1,\ldots,n$, be three PFFC samples from W(α_1, λ_1), W(α_2, λ_2) and W(α_3, λ_3) with corresponding schemes $(N, n, l_1, S_1, \ldots, S_n)$, $(K_1, k_1, l_2, R_{i1}, \ldots, R_{ik_1})$ and $(K_2, k_2, l_3, Q_{i1}, \ldots, Q_{ik_2})$, respectively. Then, the likelihood function can be de-

terminedd as follows:

$$\begin{aligned} L(\alpha_1,\alpha_2,\alpha_3,\lambda_1,\lambda_2,\lambda_3 \mid data) &= c_1 l_1^n c_2^n l_2^{nk_1} c_3^n l_3^{nk_2} \alpha_1^{nk_1} \alpha_2^{nk_2} \alpha_3^n \lambda_1^{nk_1} \lambda_2^{nk_2} \lambda_3^n \\ &\times \prod_{i=1}^{n}\prod_{j_1=1}^{k_1} x_{ij_1}^{\alpha_1-1} \prod_{i=1}^{n}\prod_{j_2=1}^{k_2} z_{ij_2}^{\alpha_2-1} \prod_{i=1}^{n} y_i^{\alpha_3-1} \\ &\times e^{-\lambda_1 \sum\limits_{i=1}^{n}\sum\limits_{j_1=1}^{k_1} x_{ij_1}^{\alpha_1} l_2(R_{j_1}+1)} e^{-\lambda_2 \sum\limits_{i=1}^{n}\sum\limits_{j_2=1}^{k_2} z_{ij_2}^{\alpha_2} l_3(Q_{j_2}+1)} \\ &\times e^{-\lambda_3 \sum\limits_{i=1}^{n} y_i^{\alpha_3} l_1(S_i+1)}. \end{aligned}$$

The MLEs of λ_1, λ_2 and λ_3 denoted by $\hat{\lambda}_1$, $\hat{\lambda}_2$ and $\hat{\lambda}_3$ are are obtained by,

$$\begin{aligned} \hat{\lambda}_1(\alpha_1) &= \frac{nk_1}{\sum\limits_{i=1}^{n}\sum\limits_{j_1=1}^{k_1} x_{ij_1}^{\alpha_1} l_2(R_{j_1}+1)}, \quad \hat{\lambda}_2(\alpha_2) = \frac{nk_2}{\sum\limits_{i=1}^{n}\sum\limits_{j_2=1}^{k_2} z_{ij_2}^{\alpha_1} l_3(Q_{j_2}+1)} \\ \hat{\lambda}_3(\alpha_3) &= \frac{n}{\sum\limits_{i=1}^{n} y_i^{\alpha_3} l_1(S_i+1)}. \end{aligned}$$

Additionally, the MLEs of α_1, α_2 and α_3 can be attained by solving the following equations, respectively,

$$\begin{aligned} \frac{\partial L}{\partial \alpha_1} &= \frac{nk_1}{\alpha_1} + \sum_{i=1}^{n}\sum_{j_1=1}^{k_1} \log(x_{ij_1}) - \lambda_1 \sum_{i=1}^{n}\sum_{j_1=1}^{k_1} x_{ij_1}^{\alpha_1} \log(x_{ij_1}) l_2(R_{j_1}+1), \\ \frac{\partial L}{\partial \alpha_2} &= \frac{nk_2}{\alpha_2} + \sum_{i=1}^{n}\sum_{j_2=1}^{k_2} \log(z_{ij_2}) - \lambda_2 \sum_{i=1}^{n}\sum_{j_2=1}^{k_2} z_{ij_2}^{\alpha_2} \log(z_{ij_2}) l_3(Q_{j_2}+1), \\ \frac{\partial L}{\partial \alpha_3} &= \frac{n}{\alpha_3} + \sum_{i=1}^{n} \log(y_i) - \lambda_3 \sum_{i=1}^{n} y_i^{\alpha_3} \log(y_i) l_1(S_i+1). \end{aligned}$$

Now by, considering the invariance property of the MLE, we have,

$$\begin{aligned} \widehat{R}_{s,k_1,k_2} = \sum_{p_1=s_1}^{k_1}\sum_{p_2=s_2}^{k_2} \binom{k_1}{p_1}\binom{k_2}{p_2} \int_0^{\infty} e^{-p_1\widehat{\lambda}_1 y^{\widehat{\alpha}_1}} \left(1-e^{-\widehat{\lambda}_1 y^{\widehat{\alpha}_1}}\right)^{k_1-p_1} e^{-p_2\widehat{\lambda}_2 y^{\widehat{\alpha}_2}} \\ \times \left(1-e^{-\widehat{\lambda}_2 y^{\widehat{\alpha}_2}}\right)^{k_2-p_2} \widehat{\alpha}_3\widehat{\lambda}_3 y^{\widehat{\alpha}_3-1} e^{-\widehat{\lambda}_3 y^{\widehat{\alpha}_3}} dy. \end{aligned} \tag{8.14}$$

8.3.2 Bayesian Estimation of R_{s,k_1,k_2}

In this section, we derive the Bayesian estimation and the associated credible interval for R_{s,k_1,k_2}, under the SELF. Assume that, the unknown parameters $\lambda_1, \lambda_2, \lambda_3, \alpha_1, \alpha_2$ and α_3 follows independent gamma distabution with parameters (a_1, b_1), (a_2, b_2), (a_3, b_3), (a_4, b_4), (a_5, b_5) and (a_6, b_6). Under the SELF, the BE of R_{s,k_1,k_2} and its corresponding credible interval are derived. Then, the joint posterior density function of $\lambda_1, \lambda_2, \lambda_3, \alpha_1, \alpha_2$ and α_3 can be expressed as follows:

$$\begin{aligned}\pi(\lambda_1, \lambda_2, \lambda_3, \alpha_1, \alpha_2, \alpha_3 \mid \text{data}) &\propto L(\lambda_1, \lambda_2, \lambda_3, \alpha_1, \alpha_2, \alpha_3 \mid \text{data}) \\ &\times \pi_1(\lambda_1)\pi_2(\lambda_2)\pi_3(\lambda_3)\pi_4(\alpha_1)\pi_5(\alpha_2)\pi_6(\alpha_3). \quad (8.15)\end{aligned}$$

Equation (8.15) clearly indicates that the BEs for the parameters cannot be expressed in a closed form. Thus, the MCMC method is utilized. The posterior PDFs for $\lambda_1, \lambda_2, \lambda_3, \alpha_1, \alpha_2, \alpha_3$ are presenred as follows:

$$\begin{aligned}\lambda_1 \mid \alpha_1, data &\sim \Gamma(nk_1 + a_1, b_1 + \sum_{i=1}^{n}\sum_{j_1=1}^{k_1} x_{ij_1}^{\alpha_1} l_2(R_{j_1}+1)), \\ \lambda_2 \mid \alpha_2, data &\sim \Gamma(nk_2 + a_2, b_2 + \sum_{i=1}^{n}\sum_{j_2=1}^{k_2} z_{ij_2}^{\alpha_2} l_3(Q_{j_2}+1)), \\ \lambda_3 \mid \alpha_3, data &\sim \Gamma(n + a_3, b_3 + \sum_{i=1}^{n} y_i^{\alpha_3} l_1(S_i+1), \\ \pi(\alpha_1 \mid \lambda_1, data) &\propto \alpha_1^{nk_1+a_4-1} \prod_{i=1}^{n}\prod_{j_1=1}^{k_1} x_{ij_1}^{\alpha_1-1} e^{-b_4\alpha_1 - \lambda_1 \sum\limits_{i=1}^{n}\sum\limits_{j_1=1}^{k_1} x_{ij_1}^{\alpha_1} l_2(R_{j_1}+1)}, \\ \pi(\alpha_2 \mid \lambda_2, data) &\propto \alpha_2^{nk_2+a_5-1} \prod_{i=1}^{n}\prod_{j_1=2}^{k_2} z_{ij_2}^{\alpha_2-1} e^{-b_5\alpha_2 - \lambda_2 \sum\limits_{i=1}^{n}\sum\limits_{j_2=1}^{k_2} z_{ij_2}^{\alpha_2} l_3(Q_{j_2}+1)}, \\ \pi(\alpha_3 \mid \lambda_3, data) &\propto \alpha_3^{n+a_6-1} \prod_{i=1}^{n} y_i^{\alpha_3-1} e^{-b_6\alpha_3 - \lambda_3 \sum\limits_{i=1}^{n} y_i^{\alpha_3} l_1(S_i+1)}.\end{aligned}$$

It is evident that random samples can be readily produced from the posterior PDFs of λ_1, λ_2 and λ_3. However, since $\pi(\alpha_1 \mid \lambda_1, data)$, $\pi(\alpha_2 \mid \lambda_2, data)$ and $\pi(\alpha_3 \mid \lambda_3, data)$ do not correspond to standard distributions, generating random samples from them directly is not feasible. Consequently, we apply the M-H

method to implement the Gibbs sampling algorithm in the following manner:

1. Begin with the initial values $(\lambda_1^0, \lambda_2^0, \lambda_3^0, \alpha_1^0, \alpha_2^0, \alpha_3^0)$.

2. Set $t = 1$.

3. Generate $\alpha_1^{(t)}$ from $\pi\left(\alpha_1 \mid \lambda_1^{(t-1)}, \text{data}\right)$ using the M-H method with $N\left(\alpha_1^{(t-1)}, 1\right)$ as the proposal distribution.

4. Generate $\alpha_2^{(t)}$ from $\pi\left(\alpha_2 \mid \lambda_2^{(t-1)}, \text{data}\right)$ using the M-H method with $N\left(\alpha_2^{(t-1)}, 1\right)$ as the proposal distribution.

5. Generate $\alpha_3^{(t)}$ from $\pi\left(\alpha_3 \mid \lambda_3^{(t-1)}, \text{data}\right)$ using the M-H method with $N\left(\alpha_3^{(t-1)}, 1\right)$ as the proposal distribution.

6. Generate $\lambda_1^{(t)}$ from $\Gamma\left(nk_1 + a_1, b_1 + \sum_{i=1}^{n}\sum_{j_1=1}^{k_1} x_{ij_1}^{\alpha_1} l_2(R_{j_1} + 1)\right)$.

7. Generate $\lambda_2^{(t)}$ from $\Gamma\left(nk_2 + a_2, b_2 + \sum_{i=1}^{n}\sum_{j_2=1}^{k_2} z_{ij_2}^{\alpha_2} l_3(Q_{j_2} + 1)\right)$.

8. Generate $\lambda_3^{(t)}$ from $\Gamma\left(n + a_3, b_3 + \sum_{i=1}^{n} y_i^{\alpha_3} l_1(S_i + 1)\right)$.

9. Compute $\widehat{R}_{s,k_1,k_2}^{(t)}$ using the formula provided in Equation (8.14).

10. Set $t = t + 1$.

11. Repeat steps 3 to 10 for T times.

Thus, the BE of R_{s,k_1,k_2} under SELF can be derived using the following expression:

$$\widehat{R}_{s,k_1,k_2}^{MC} = \frac{1}{T}\sum_{t=1}^{T} R_{s,k_1,k_2}^{(t)}.$$

Chen and Shao (1999) proposed a method for constructing credible intervals, and using their approach, we derive a $100(1-\xi)\%$ HPD interval for R_{s,k_1,k_2}.

8.4 Simulation

A Monte Carlo simulation study is conducted to compare various point and interval estimators, including MLE, BEs, ACI and the HPD credible interval of MSSR R_{s,k_1,k_2}. The comparison of point estimators is based on their average absolute biases and MSEs, while interval estimators are evaluated regarding their average lengths (ALs) and coverage probabilities (CPs). The PFFC schemes are utilized on two distinct types of non-identical strength variables, X and Z, as well as the stress variable Y. This simulation study incorporates various PFFC schemes, which are detailed in Table 8.1. The notations like (0*5, 6) is used for (0, 0, 0, 0, 0, 6). The minimum number of required strength components considered is $s_1 = s_2 = 2$. When the common shape parameter α is unknown,

Table 8.1: Various censoring schemes considered in the simulation study.

(K_1, k_1)		CS	(K_2, k_2)		CS	(N, n)		CS
(12, 6)	R_1	(0*5, 6)	(12, 6)	Q_1	(0*5, 6)	(12, 6)	S_1	(0*5,6)
(12,6)	R_2	(6, 0*5)	(12, 6)	Q_2	(6, 0*5)	(12, 6)	S_2	(6,0*5)
(12, 6)	R_3	(1*6)	(12, 6)	Q_3	(1*6)	(12, 6)	S_3	(1*6)
(20, 10)	R_4	(0*9, 10)	(20, 10)	Q_4	(0*9, 10)	(20, 10)	S_4	(0*9, 10)
(20, 10)	R_5	(10,0*9)	(20, 10)	Q_5	(10, 0*9)	(20, 10)	S_5	(10,0*9)
(20, 10)	R_6	(1*10)	(20, 10)	Q_6	(1*10)	(20, 10)	S_6	(1*10)

we analyze true parameter values (α, λ_1, λ_2, λ_3) = (1, 2, 2, 2). We derive ML and BEs for R_{s,k_1,k_2}, focusing on average absolute bias and MSE. We also calculate 95% ACIs and HPD credible intervals and evaluate their CLs and CPs. The BE is obtained under the SELF framework, considering both informative (Prior 1) and non-informative (Prior 2) priors. For the IP, hyperparameters are set such that the mean aligns with the true values. In the second scenario, the simulation results are generated by considering distinct unknown α_1, α_2 and α_3 parameters. The simulation results are generated using the parameter values (α_1, α_2, α_3, λ_1, λ_2, λ_3) = (2, 3, 4, 1, 1, 1). Simulation results are shown in Tables 8.2 - 8.5. From the simulation tables, it is evident that Bayesian estimations outperform classical estimation methods. Also, as the sample size increases, the results of the MLE and the NIP case become closer. Additionally, 95% asymptotic and

Table 8.2: The average absolute biases and MSEs of the MLE and BEs of R_{s,k_1,k_2} under various censoring schemes, when α is unknown

					MCMC			
			MLE		Prior1		Prior2	
(l_1, l_2, l_3)	CS	R	Bias	MSE	Bias	MSE	Bias	MSE
(2,2,2)	(R_1, Q_1, S_1)	0.6243756	0.1180590	0.0218988	0.1029812	0.0164511	0.1179428	0.0197226
	(R_1, Q_2, S_3)		0.1165723	0.0213331	0.1121637	0.0187090	0.1146896	0.0197659
	(R_3, Q_2, S_1)		0.1111735	0.0193113	0.1090763	0.0184481	0.1162459	0.0200530
	(R_2, Q_3, S_1)		0.1112867	0.0193841	0.1101718	0.0188759	0.1209598	0.0211965
	(R_2, Q_2, S_2)		0.1167791	0.0213591	0.1210277	0.0210076	0.1218153	0.0220526
	(R_3, Q_3, S_3)		0.1173212	0.0215801	0.0968019	0.0142759	0.1184722	0.0202040
	(R_1, Q_1, S_4)		0.0931330	0.0119930	0.0823111	0.0101089	0.0954789	0.0140251
	(R_2, Q_2, S_5)		0.0976130	0.0132729	0.0894638	0.0117769	0.0883199	0.0124873
	(R_3, Q_3, S_6)		0.0875336	0.0118929	0.0788735	0.0103089	0.0950276	0.0139334
	(R_1, Q_1, S_5)		0.0898275	0.0122730	0.0831111	0.0112160	0.0904217	0.0121669
	(R_1, Q_1, S_6)		0.0882567	0.0120107	0.0842632	0.0119100	0.0886065	0.0126103
	(R_2, Q_2, S_4)		0.0875168	0.0119646	0.0855836	0.0118523	0.0989433	0.0136834
	(R_2, Q_2, S_6)		0.0882891	0.0160581	0.0933437	0.0127732	0.0888291	0.0128897
	(R_3, Q_3, S_4)		0.0874586	0.0119129	0.0786607	0.0097221	0.1045442	0.0165030
	(R_3, Q_3, S_5)		0.0920571	0.0135586	0.0926132	0.0133044	0.0947298	0.0140034
	(R_2, Q_3, S_6)		0.0916489	0.0133686	0.0913907	0.0125264	0.0923773	0.0134876
	(R_1, Q_2, S_5)		0.0994436	0.0141891	0.0881385	0.0119314	0.0966619	0.0140907
	(R_3, Q_1, S_4)		0.1052023	0.0155172	0.0895370	0.0121409	0.0931057	0.0123833
	(R_4, Q_4, S_1)	0.7566644	0.1060281	0.0163607	0.0861684	0.0106990	0.1307951	0.0253036
	(R_5, Q_5, S_2)		0.1052934	0.0161233	0.1068240	0.0157255	0.1370960	0.0265250
	(R_6, Q_6, S_3)		0.1056211	0.0162260	0.1037596	0.0145943	0.0979303	0.0152661
	(R_4, Q_4, S_4)		0.0834975	0.0104700	0.0729291	0.0084200	0.0784914	0.0101593
	(R_5, Q_5, S_5)		0.0829912	0.0103083	0.0789045	0.0088920	0.0847741	0.0105822
	(R_6, Q_6, S_6)		0.0832352	0.0103822	0.0741370	0.0081478	0.0857527	0.0110663
	(R_4, Q_5, S_6)		0.0830099	0.0103025	0.0784172	0.0088737	0.0807198	0.0109312
	(R_6, Q_5, S_4)		0.0826623	0.0101806	0.0788284	0.0088357	0.0740281	0.0088448
	(R_5, Q_6, S_4)		0.0826671	0.0101937	0.0751838	0.0082542	0.0876844	0.0119314

HPD intervals for R_{s,k_1,k_2} were established. Notably, the HPD credible intervals exhibited the smallest ALs across the different cases, as shown in Table 8.3 and 8.5. Also, within Bayes estimation, IPs outperformed their non-informative case, with Prior 1 in both cases offering the smallest credible intervals with the most CPs. Furthermore, the general trends observed in Table 8.2 - 8.5 indicate that, when the values of s and k remain constant, a larger sample size n leads to reductions in both the MSEs and the ALs of the intervals, alongside an increase in CPs. Similarly, when s and n are held constant, increasing the value of k results in lower MSEs and shorter ALs, accompanied by improved CPs.

Table 8.3: Average confidence length and coverage probabilities for estimators of R_{s,k_1,k_2} under various censoring schemes α is unknown

		MLE		Prior 1		Prior2	
(l_1, l_2, l_3)	CS	AL	CP	AL	CP	AL	CP
(2,2,2)	(R_1, Q_1, S_1)	0.666610	0.961	0.429074	0.96	0.493796	0.955
	(R_1, Q_2, S_3)	0.637037	0.954	0.434558	0.945	0.505192	0.943
	(R_3, Q_2, S_1)	0.648517	0.956	0.434288	0.966	0.503170	0.931
	(R_2, Q_3, S_1)	0.648709	0.954	0.432471	0.968	0.510722	0.925
	(R_2, Q_2, S_2)	0.607469	0.934	0.433352	0.923	0.501002	0.921
	(R_3, Q_3, S_3)	0.634488	0.95	0.438555	0.937	0.505676	0.924
	(R_1, Q_1, S_4)	0.525007	0.976	0.372720	0.975	0.433610	0.935
	(R_2, Q_2, S_5)	0.478624	0.956	0.388986	0.953	0.435631	0.941
	(R_3, Q_3, S_6)	0.501177	0.967	0.370532	0.946	0.430271	0.955
	(R_1, Q_1, S_5)	0.478624	0.956	0.388986	0.945	0.435631	0.938
	(R_1, Q_1, S_6)	0.508586	0.973	0.372243	0.957	0.431469	0.932
	(R_2, Q_2, S_4)	0.513785	0.974	0.365535	0.958	0.419412	0.924
	(R_2, Q_2, S_6)	0.502023	0.966	0.367823	0.949	0.417364	0.957
	(R_3, Q_3, S_4)	0.514939	0.973	0.369563	0.955	0.418455	0.925
	(R_3, Q_3, S_5)	0.475561	0.957	0.379482	0.935	0.430061	0.924
	(R_2, Q_3, S_6)	0.501315	0.966	0.364343	0.944	0.422575	0.931
	(R_1, Q_2, S_5)	0.478226	0.958	0.372405	0.956	0.427320	0.948
	(R_3, Q_1, S_4)	0.519338	0.973	0.368234	0.945	0.428296	0.951
	(R_4, Q_4, S_1)	0.576304	0.952	0.383649	0.923	0.424449	0.932
	(R_5, Q_5, S_2)	0.537375	0.924	0.376367	0.963	0.426126	0.922
	(R_6, Q_6, S_3)	0.552092	0.933	0.386785	0.928	0.424596	0.932
	(R_4, Q_4, S_4)	0.459579	0.965	0.372178	0.955	0.441166	0.951
	(R_5, Q_5, S_5)	0.430369	0.941	0.375130	0.928	0.426945	0.934
	(R_6, Q_6, S_6)	0.441987	0.954	0.371444	0.941	0.434410	0.926
	(R_4, Q_5, S_6)	0.445738	0.955	0.368670	0.957	0.429658	0.945
	(R_6, Q_5, S_4)	0.450530	0.967	0.362405	0.945	0.432502	0.955
	(R_5, Q_6, S_4)	0.450498	0.972	0.369912	0.954	0.423213	0.952

Table 8.4: The average absolute biases and MSEs of the MLE and BEs of R_{s,k_1,k_2} under various censoring schemes in general case.

					MCMC			
			MLE		Prior1		Prior2	
(l_1, l_2, l_3)	CS	R	Bias	MSE	Bias	MSE	Bias	MSE
(2,2,2)	(R_1, Q_1, S_1)	0.616621	0.154919	0.032919	0.114618	0.020082	0.142505	0.029282
	(R_1, Q_2, S_3)		0.141110	0.028477	0.104183	0.016414	0.127756	0.023925
	(R_3, Q_2, S_1)		0.157730	0.032030	0.108411	0.017841	0.143462	0.029516
	(R_2, Q_3, S_1)		0.151337	0.031527	0.109614	0.018152	0.137937	0.027427
	(R_2, Q_2, S_2)		0.122265	0.021981	0.099032	0.014939	0.113511	0.019297
	(R_3, Q_3, S_3)		0.138213	0.027146	0.103619	0.016427	0.125714	0.023337
	(R_1, Q_1, S_4)		0.131348	0.025459	0.097792	0.014504	0.111537	0.018980
	(R_2, Q_2, S_5)		0.138287	0.029957	0.112345	0.017944	0.162935	0.042947
	(R_3, Q_3, S_6)		0.125656	0.023991	0.078647	0.009047	0.137651	0.028631
	(R_1, Q_1, S_5)		0.130058	0.026490	0.097482	0.013575	0.145697	0.034259
	(R_1, Q_1, S_6)		0.134100	0.027532	0.097567	0.013546	0.153677	0.036988
	(R_2, Q_2, S_4)		0.131762	0.027341	0.109107	0.016684	0.155458	0.039036
	(R_2, Q_2, S_6)		0.129199	0.026804	0.106432	0.015922	0.155175	0.039079
	(R_3, Q_3, S_4)		0.115036	0.019523	0.091530	0.012867	0.122157	0.020614
	(R_3, Q_3, S_5)		0.090390	0.012834	0.082606	0.010638	0.111880	0.017531
	(R_2, Q_3, S_6)		0.102299	0.015876	0.087949	0.011925	0.107387	0.016467
	(R_1, Q_2, S_5)		0.091441	0.012993	0.082427	0.010655	0.084177	0.011045
	(R_3, Q_1, S_4)		0.112197	0.018964	0.092539	0.013119	0.121651	0.020399
	(R_4, Q_4, S_1)	0.804811	0.128167	0.022929	0.104487	0.017789	0.143776	0.025020
	(R_5, Q_5, S_2)		0.098529	0.013822	0.087368	0.011781	0.109426	0.015851
	(R_6, Q_6, S_3)		0.115772	0.018490	0.095507	0.014756	0.131762	0.021431
	(R_4, Q_4, S_4)		0.087848	0.012036	0.077854	0.009425	0.082470	0.010365
	(R_5, Q_5, S_5)		0.105199	0.016564	0.086663	0.011524	0.111880	0.017531
	(R_6, Q_6, S_6)		0.093897	0.013716	0.088519	0.012052	0.090929	0.012677
	(R_4, Q_5, S_6)		0.106059	0.016846	0.093108	0.013236	0.106393	0.016404
	(R_6, Q_5, S_4)		0.114729	0.019354	0.089659	0.012256	0.130082	0.022985
	(R_5, Q_6, S_4)		0.101552	0.015715	0.084388	0.010950	0.085728	0.011226

Table 8.5: Average confidence length and coverage probabilities for estimators of R_{s,k_1,k_2} under various censoring schemes in general case.

		MLE		Prior 1		Prior2	
(l_1, l_2, l_3)	CS	AL	CP	AL	CP	AL	CP
(2,2,2)	(R_1, Q_1, S_1)	0.646238	0.890	0.562007	0.951	0.611250	0.942
	(R_1, Q_2, S_3)	0.560796	0.893	0.516959	0.952	0.558417	0.943
	(R_3, Q_2, S_1)	0.605598	0.895	0.555159	0.958	0.591623	0.944
	(R_2, Q_3, S_1)	0.592704	0.899	0.539805	0.953	0.580502	0.944
	(R_2, Q_2, S_2)	0.491394	0.898	0.496559	0.953	0.5197355	0.942
	(R_3, Q_3, S_3)	0.554253	0.891	0.548115	0.952	0.5566527	0.948
	(R_1, Q_1, S_4)	0.527299	0.894	0.471014	0.956	0.481715	0.945
	(R_2, Q_2, S_5)	0.401142	0.902	0.377709	0.955	0.374064	0.949
	(R_3, Q_3, S_6)	0.459505	0.905	0.428520	0.956	0.443219	0.951
	(R_1, Q_1, S_5)	0.437243	0.901	0.401451	0.961	0.417316	0.955
	(R_1, Q_1, S_6)	0.477797	0.896	0.454436	0.958	0.460214	0.953
	(R_2, Q_2, S_4)	0.508840	0.896	0.461124	0.960	0.466009	0.957
	(R_2, Q_2, S_6)	0.447460	0.890	0.412165	0.964	0.424807	0.955
	(R_3, Q_3, S_4)	0.514030	0.891	0.461007	0.953	0.465600	0.947
	(R_3, Q_3, S_5)	0.418114	0.892	0.387607	0.950	0.391161	0.944
	(R_2, Q_3, S_6)	0.453496	0.894	0.410762	0.958	0.428047	0.953
	(R_1, Q_2, S_5)	0.422833	0.896	0.391299	0.956	0.407200	0.955
	(R_3, Q_1, S_4)	0.522018	0.901	0.463787	0.949	0.480329	0.950
	(R_4, Q_4, S_1)	0.540120	0.905	0.395477	0.951	0.569717	0.947
	(R_5, Q_5, S_2)	0.413028	0.911	0.349002	0.952	0.459477	0.946
	(R_6, Q_6, S_3)	0.476318	0.899	0.367416	0.948	0.572056	0.944
	(R_4, Q_4, S_4)	0.462127	0.903	0.508852	0.949	0.551236	0.947
	(R_5, Q_5, S_5)	0.401862	0.906	0.347234	0.953	0.399440	0.946
	(R_6, Q_6, S_6)	0.486280	0.899	0.409537	0.952	0.494558	0.946
	(R_4, Q_5, S_6)	0.472790	0.895	0.409356	0.951	0.491649	0.947
	(R_6, Q_5, S_4)	0.526393	0.902	0.454656	0.955	0.554662	0.948
	(R_5, Q_6, S_4)	0.524658	0.904	0.448085	0.954	0.559950	0.943

8.5 Data Analysis

This section provides an analysis of real data sets, specifically examining the monthly water capacity of the Shasta Reservoir in California, USA. These

datasets are available at the following link: `https://cdec.water.ca.gov/dynamicapp/QueryMonthly?s=SHA`. Drought significantly affects agricultural production, so assessing its probability of occurance is critical for farmers. Here, we consider that a drought will not occur if, in at least two of the next five years, a reservoir's water capacity in July and August exceeds the water level recorded in December of the previous year. This framework allows us to interpret the multi-component reliability value, considering two non-identical strength components represents the probability of not experiencing a drought. Estimating this probability is essential because drought can lead to reduced crop yields and livestock challenges due to insufficient rainfall. It also negatively impacts pasture growth, lowering fodder availability from crop residues. By understanding this probability, we can effectively implement preventative measures against drought damage, ensuring the protection of essential equipment from potential harm.

The complete datasets includes Y_1 is the capacity for December 1983, with $X_{11}, X_{12}, \ldots, X_{15}$ and $Z_{11}, Z_{12}, \ldots, Z_{15}$ for July and August capacities from 1984 to 1988. Y_2 covers December 1989, while $X_{21}, X_{22}, \ldots, X_{25}$ and $Z_{21}, Z_{22}, \ldots, Z_{25}$ indicate the capacities for July and August from 1990 to 1994. This pattern continues, with Y_7 representing December 2019, and $X_{71}, X_{72}, \ldots, X_{75}$ and $Z_{71}, Z_{72}, \ldots, Z_{75}$ showing capacities for July and August from 2020 to 2024. All data points were divided by the total capacity of the reservoir, which is 4,552,000 acre-feet, to simplify the computations. Then, the water capacity for July, August and December from 1983 to 2024 is as follows:

$$X = \begin{pmatrix} 0.788093 & 0.503537 & 0.768453 & 0.575556 & 0.446463 \\ 0.452761 & 0.336938 & 0.481297 & 0.858913 & 0.626028 \\ 0.823240 & 0.646955 & 0.911108 & 0.816548 & 0.729613 \\ 0.681662 & 0.779254 & 0.615619 & 0.799476 & 0.831308 \\ 0.418677 & 0.510939 & 0.843836 & 0.886407 & 0.718595 \\ 0.346010 & 0.437245 & 0.778641 & 0.865924 & 0.691332 \\ 0.588313 & 0.319420 & 0.369728 & 0.854569 & 0.758084 \end{pmatrix}$$

$$Z = \begin{pmatrix} 0.726164 & 0.423814 & 0.715158 & 0.463687 & 0.363359 \\ 0.371905 & 0.291173 & 0.414087 & 0.753984 & 0.538082 \\ 0.722614 & 0.561238 & 0.813964 & 0.755238 & 0.668612 \\ 0.605979 & 0.715851 & 0.529519 & 0.718754 & 0.742026 \\ 0.345076 & 0.425335 & 0.767070 & 0.795065 & 0.613911 \\ 0.294835 & 0.392917 & 0.688100 & 0.796703 & 0.591255 \\ 0.516476 & 0.269552 & 0.349297 & 0.775703 & 0.660655 \end{pmatrix} \quad Y = \begin{pmatrix} 0.759556 \\ 0.451150 \\ 0.717855 \\ 0.656033 \\ 0.391938 \\ 0.367614 \\ 0.731547 \end{pmatrix}$$

First, we will perform the K-S GoF test to determine whether the given three datasets align with the W distribution. The findings from the K–S tests are presented in Table 8.6. The p - values clearly indicate that the W distribution is a suitable fit for X, Z and Y datasets. The P-P plots for datasets X, Z, and Y, shown in Fig 8.1, indicate that the W distribution is a strong fit for these data sets. We now explore three distinct censoring schemes for demonstrative

Table 8.6: The MLEs of the unknown parameters and the corresponding K-S statistic values and p - values for datasets X, Z and Y.

	α	λ	K-S	p - value
Y	4.418362	7.056069	0.23954	0.7369
X	4.377022	4.205485	0.14242	0.4364
Z	3.997394	5.988052	0.16291	0.2793

purposes. The first scheme represents a complete sample, while the remaining two involve PFFC samples, detailed as follows:

$$\begin{aligned} \text{Complete Case} : R &= Q = [0,0,0,0,0] \quad S = [0,0,0,0,0,0,0] \\ &\quad (k_1 = k_2 = 5, \quad n = 7, \quad s_1 = s_2 = 2 \text{ and } s_1 = s_2 = 1). \\ \text{Scheme 1} : R &= Q = [1,0,1] \quad S = [0,0,0,0,2] \\ &\quad (k_1 = k_2 = 3, \quad n = 5, \quad s_1 = s_2 = 2 \text{ and } s_1 = s_2 = 1). \\ \text{Scheme 2} : R &= Q = [0,0,1,0] \quad S = [0,1,0,0,0,0] \\ &\quad (k_1 = k_2 = 4, \quad n = 6, \quad s_1 = s_2 = 2 \text{ and } s_1 = s_2 = 1). \end{aligned}$$

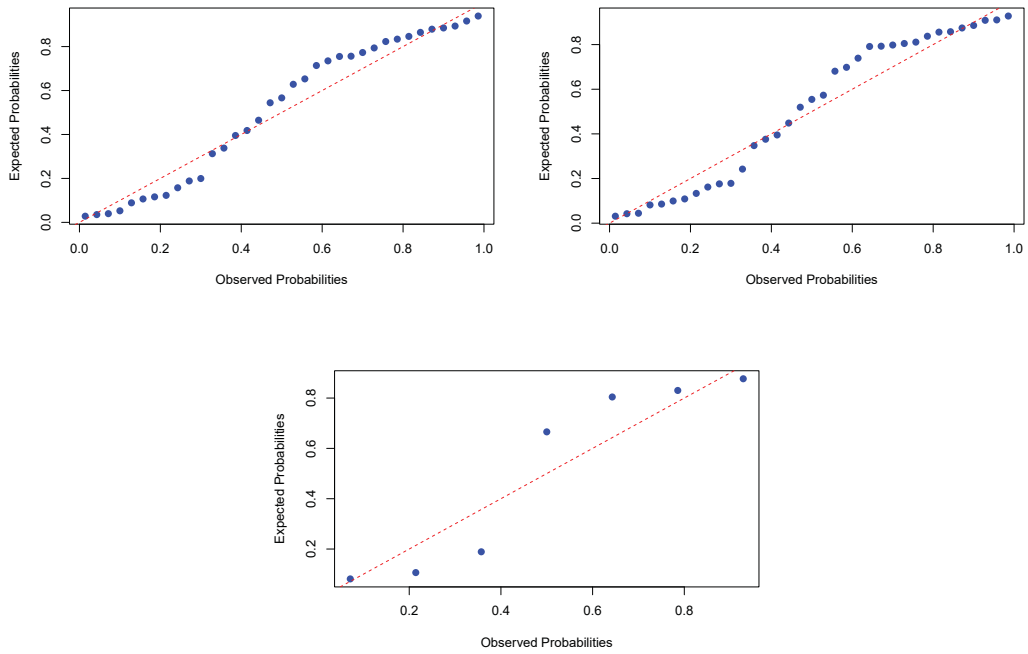

Figure 8.1: P-P plot for X, Z and Y datasets.

The PFFC data obtained using Scheme 1 are as follows:

$$X = \begin{pmatrix} 0.446463 & 0.575556 & 0.768453 \\ 0.336938 & 0.481297 & 0.626028 \\ 0.646955 & 0.816548 & 0.823240 \\ 0.615619 & 0.779254 & 0.799476 \\ 0.418677 & 0.718595 & 0.843836 \end{pmatrix} \quad Z = \begin{pmatrix} 0.363359 & 0.463687 & 0.715158 \\ 0.291173 & 0.414087 & 0.538082 \\ 0.561238 & 0.722614 & 0.755238 \\ 0.529519 & 0.715851 & 0.718754 \\ 0.345076 & 0.613911 & 0.767070 \end{pmatrix}$$

$$Y = \begin{pmatrix} 0.367614 \\ 0.391938 \\ 0.451150 \\ 0.656033 \\ 0.717855 \end{pmatrix}$$

Also, the PFFC data obtained using Scheme 2 are as follows:

$$X = \begin{pmatrix} 0.446463 & 0.503537 & 0.575556 & 0.788093 \\ 0.336938 & 0.452761 & 0.481297 & 0.858913 \\ 0.615619 & 0.681662 & 0.779254 & 0.831308 \\ 0.418677 & 0.510939 & 0.718595 & 0.886407 \\ 0.346010 & 0.437245 & 0.691332 & 0.865924 \\ 0.319420 & 0.369728 & 0.588313 & 0.854569 \end{pmatrix}$$

$$Z = \begin{pmatrix} 0.363359 & 0.423814 & 0.463687 & 0.726164 \\ 0.291173 & 0.371905 & 0.414087 & 0.753984 \\ 0.529519 & 0.605979 & 0.715851 & 0.742026 \\ 0.345076 & 0.425335 & 0.613911 & 0.795065 \\ 0.294835 & 0.392917 & 0.591255 & 0.796703 \\ 0.269552 & 0.349297 & 0.516476 & 0.775703 \end{pmatrix} \quad Y = \begin{pmatrix} 0.367614 \\ 0.391938 \\ 0.656033 \\ 0.717855 \\ 0.731547 \\ 0.759556 \end{pmatrix}$$

Then, we compute the ML and BEs with NIP, along with their credible intervals using complete and PFF censored samples and the results are presented in Table 8.7 and 8.8. In comparing the two censoring schemes, it is evident that both classical and BEs demonstrate that Scheme 2 consistently yields smaller standard errors compared to Scheme 1. Also, to assess the diagnostics of the MCMC technique, the trace plots and running mean plot of complete sample data are presented in Figure 8.2. These figure indicates that the MCMC chains are converging to their stationary distributions.

Table 8.7: The parameter estimates from the ML and Bayesian methods under different schemes.

	Common Case		Scheme 1		Scheme 2	
	MLE	BE	MLE	BE	MLE	BE
α_1	4.3758	4.3531	4.9363	4.9477	3.7757	3.7353
α_2	3.9972	3.9772	4.2342	4.2469	3.4464	3.4785
α_3	4.4186	4.4525	3.4231	3.3165	4.8921	4.9344
λ_1	4.2041	4.1950	3.3525	3.4637	3.6699	3.6524
λ_2	5.9879	6.0382	4.3639	4.6417	5.0345	5.1944
λ_3	7.0543	7.9145	3.7291	3.9489	7.2429	8.9203

Table 8.8: The MLE and BEs (with standard errors), along with the ACI and HPD intervals of R_{s,k_1,k_2} based on the real dataset.

.

		MLE	ACI	BE	HPD
Complete Case	$R_{2,2,5,5}$	0.6207(0.1390)	(0.3482, 0.8931)	0.5926(0.1327)	(0.3318,0.8306)
	$R_{1,1,5,5}$	0.8128(0.1050)	(0.5403, 1.085)	0.7827(0.1106)	(0.5526, 0.9561)
Scheme 1	$R_{2,2,3,3}$	0.5015(0.1532)	(0.2012,0.8018)	0.4743(0.1475)	(0.1889,0.7294)
	$R_{1,1,3,3}$	0.7299(0.1515)	(0.4330, 1.0269)	0.6774(0.1409)	(0.3821, 0.9308)
Scheme 2	$R_{2,2,4,4}$	0.4318(0.1489)	(0.1400,0.7235)	0.4187(0.1382)	(0.1565, 0.6857)
	$R_{1,1,4,4}$	0.7106(0.1289)	(0.4580, 0.9632)	0.6744(0.1219)	(0.4199, 0.9104)

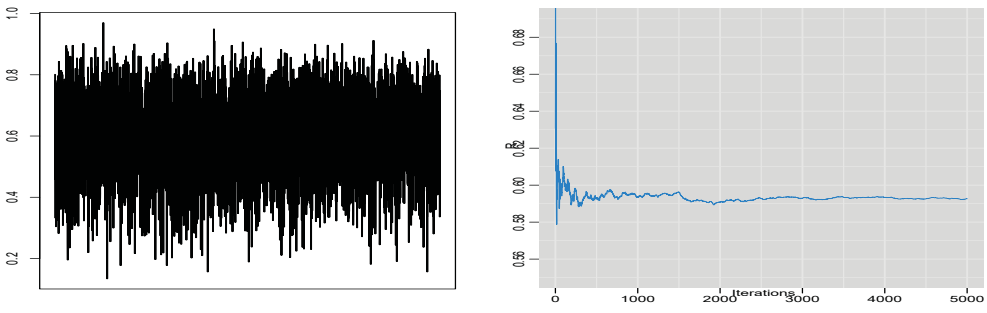

Figure 8.2: Trace plot and Running mean plot of complete sample for the real dataset.

8.6 Summary

This Chapter presents various estimates of MSSR involving two non-identical strength component for Weibull distributions, utilizing the PFFC framework. We obtained estimates of the reliability R_{s,k_1,k_2} based on the Weibull distribution through both classical and Bayesian methods. Using the SELF approach, we derived the BE for R_{s,k_1,k_2}. Additionally, we calculated the 95% ACI and HPD intervals for the unknown parameters. The simulation results show that as the sample size grows, the performance of the proposed estimators for R_{s,k_1,k_2} generally improves. The simulation findings indicated that BEs outperformed classical estimates. Finally, the applicability of the model is demonstrated using a recent dataset.

Chapter 9

Conclusion

Lifetime data analysis is essential in reliability engineering, survival analysis, and related fields. It measures the time until the key events occur, such as system failures, disease recurrences, or treatment successes. Accurate modeling of this data is crucial for predicting outcomes and making informed decisions. However, lifetime data often exhibit complexities such as skewness, heavy-tailed distributions, and varying hazard rate behaviors, which cannot be adequately modeled by traditional distributions alone. This highlights the need for flexible models that are capable of capturing these distributional features and diverse failure patterns. Accurate modeling of lifetime data thus plays a pivotal role in drawing reliable conclusions, estimating risk, and enhancing the reliability and performance of systems across multiple disciplines.

A wide variety of lifetime distributions are available in the literature to address the challenges associated with modeling time-to-event data. Among them, the Weibull and Burr III distributions stand out for their ability to accommodate a broad spectrum of hazard rate shapes and distributional features. The Weibull distribution is particularly renowned for its capacity to model increasing, decreasing, and constant hazard rates, making it especially effective in diverse reliability contexts. In contrast, the Burr III distribution is well-suited for modeling heavy-tailed behavior and a wide range of failure patterns, including unimodal and decreasing hazard functions, thereby providing excellent fit to complex real-world lifetime data. Owing to their adaptability, analytical tractability, and practical relevance, the Weibull and Burr III distributions serve as the foundation of this

thesis. The entire work is centered on the application and extension of these two distributions to develope new statistical models, address intricate reliability problems, and propose meaningful solutions for analyzing lifetime data across various domains.

In real-world lifetime and reliability data analysis, probability density and distribution functions are often complex or lack closed-form expressions. In such situations, QFs offer a practical and flexible approach for modeling real-life data, especially when traditional methods fail to provide desired results. In Chapter 2, a new family of distributions is proposed using a QF defined as the sum of the QFs of the Burr III and Weibull distributions. The Chapter presents several distributional characteristics and reliability properties that highlight the theoretical strength of the proposed model. Parameters are estimated using both the Method of LSE and MLM, which are efficient and practical techniques for quantile-based modeling. The effectiveness of the model is validated using two real-world datasets, demonstrating its appropriateness in the field of reliability. Overall, this Chapter emphasizes the growing importance of quantile-based approaches and their practical relevance in modern statistical applications.

Chapter 3 introduces a new distribution based on the Weibull and Burr III distributions within a CRs framework. This model addresses the limitations of the parent distributions in capturing complex hazard behaviors, such as non-monotonic and bathtub-shaped failure rates. Its structural properties are analyzed, proving it to be mathematically manageable and applicable in various real-world scenarios. A simulation study evaluates the ML estimators, supporting the distribution's efficacy in modeling complex lifetime data. Applications to real datasets reveal the enhanced ability of the proposed distribution to closely reflect the underlying structure and behavior of complex lifetime data, demonstrating its practical relevance in diverse applied settings. This Chapter lays a foundation for extending the model to more generalized forms and exploring its applicability across broader lifetime data scenarios in future research.

Chapter 4 examined the survival measures of the OBIIIW distribution through a comparative analysis of the ANNs model and MLE approach. Both methods yielded consistent results, confirming the effectiveness of the OBIIIW

distribution for real-world data modeling. The ANN model, in particular, demonstrated high predictive accuracy and low error rates, highlighting its effectiveness for both optimization and prediction tasks. Overall, the findings indicate that the ANN model is well-suited for handling intricate data structures and serves as a powerful analytical tool in clinical and biomedical research. Thus, ANN can be effectively applied to real-life datasets that exhibit complex behavior, offering a reliable and efficient approach to data-driven modeling and prediction.

Flexible regression models are crucial for analyzing censored lifetime data and addressing bathtub-shaped hazard rates commonly found in reliability and survival studies. In Chapter 5, a new location-based regression model called the LOBIIIW regression model is introduced to meet these challenges. This model uses the strengths of both the Burr III and Weibull distributions, making it well-suited for complex lifetime data. Parameter estimation is done using ML and jackknife methods under right-censoring, yielding reliable estimates across different sample sizes. The model's effectiveness is illustrated through a real censored dataset, demonstrating its ability to detect influential observations and provide accurate fits. This Chapter highlights the importance of integrating diagnostic tools in flexible regression models to enhance the reliability of findings in survival and reliability research.

SSR analysis is essential for determining the ability of a system or component to operate effectively under different stress conditions. In Chapter 6, the SSR measure $R = P(X > Y)$ is investigated, where X and Y are assumed to follow independent Weibull-Burr III distributions. The Chapter employs both ML and Bayesian estimation under informative and non-informative prior assumptions. The performance of the ML and Bayes estimators is evaluated using the SELF and LLF, demonstrating their accuracy and efficiency. The usefulness of the proposed methodology is supported through its application to real-world datasets, confirming its flexibility and practical relevance in SSR modeling across a wide range of domains.

Chapters 7 and 8 extend inference procedures based on the Weibull distribution, addressing CRs and MSSR under different censoring schemes. Chapter 7 considers CRs with partially observed failure causes under GTIIHCS, while

Chapter 8 deals with MSSR using PFF censored data, where strength components are not identical. Both Chapters employ ML and Bayesian estimation techniques, with the performance of the estimators validated through extensive simulations and applications to real-life datasets. The results demonstrate the flexibility, and practical effectiveness of Weibull-based models in handling complex censoring structures and providing reliable inference in diverse lifetime data scenarios.

In summary, this thesis contributes significantly to the modeling and application of lifetime data using Weibull and Burr III distributions by introducing new distributional families, advanced regression structures, and frameworks for CRs and SSR, all rooted in these flexible models. Through the use of ML, Bayesian, and machine learning methods, the research effectively addresses the complexities of real-world data. The findings provide valuable insights into complex survival behaviors and enhance reliability analysis, offering both theoretical advancements and practical tools for fields such as engineering, biostatistics, and medical research. These contributions open promising directions for future research in flexible lifetime modeling and advanced inference techniques.

Chapter 10

Recommendations

This research leads us to recommend the following directions for future work.

- Developing a framework for time series quantile forecasting and present a novel quantile regression model based on the Burr III Weibull quantile function.
- Analysis of classical and Bayesian estimation in the proposed Burr III-Weibull quantile function.
- Perform a thorough analysis utilising ANNs and MLE with the recently suggested Burr III-Weibull Distribution.
- Develop a location-scale regression model based on the newly proposed Burr III Weibull Distribution.
- Development of dependent stress-strength reliability using Weibull and Burr III distribution.
- Exploring the applicability of Burr III and Weibull distributions in step-stress, one-shot device models, generalized shock models etc.
- Analysis of Burr III distribution using progressive Type II censoring scheme under competing risk models.
- Analysis of multicomponent stress-strength reliability using the Burr III distribution under progressive first failure censoring schemes.

Deepthy G. S. Statistical modelling and applications using Weibull and Burr III distributions. Department of Statistics St. Thomas College (Autonomous) University of Calicut.

UNIVERSITY OF CALICUT

CERTIFICATE ON PLAGIARISM CHECK

1.	Name of the Research Scholar	Deepthy G.S	
2.	Title of thesis / dissertation	Statistical Modelling and Applications Using Weibull and Burr III Distributions	
3.	Name of the Supervisor	Dr Nicy Sebastian	
4.	Department/Institution	Research Scholar,Department of Statistics,St.Thomas College,Thrissur	
5.	Similar content (%) identified	Non Core	Core
		Introduction/ Theoretical overview/Review of literature/ Materials & Methods/ Methodology	**Analysis/Result/Discussion / Summary/Conclusion/ Recommendations**
		5	**4**
	Acceptable maximum limit (%)	10	10
6.	Software used	iThenticate	
7.	Date of verification	02.06.2025	

**Report on plagiarism check, specifying included/excluded items with % of similarity to be attached.*

Checked by (with name, designation & signature) Dr. Nasirudheen. T, Assistant Librarian, University of Calicut, Kerala.

Name and signature of the Researcher Deepthy G.S Deepthy

Name and signature of the Supervisor. Dr. Nicy Sebastian

The Doctoral Committee* has verified the report on plagiarism check with the contents of the thesis, as summarized above and appropriate measures have been taken to ensure originality of the Research accomplished herein.

02-06-25

Name & Signature of the HoD/HoI (Chairperson of the Doctoral Committee)

Dr. Martin K. A.
Principal-in-Charge
St Thomas College (Autonomous)
Thrissur - 680 001

**In case of languages like Malayalam, Tamil etc..on which no software is available for plagiarism check, a manual check shall be made by the Doctoral Committee for which an additional certificate has to be attached.*

References

Aboul-Fotouh Salem, S., Abo-Kasem, O. E., & Abdelgaied Khairy, A. (2024). Inference for generalized progressive hybrid type-ii censored weibull lifetimes under competing risk data. Computational Journal of Mathematical and Statistical Sciences, 3(1), 177–202.

Abushal, T. A., & AL-Zaydi, A. M. (2024). Statistical inference of inverted nadarajah–haghighi distribution under type-ii generalized hybrid censoring competing risks data. Journal of Engineering Mathematics, 144(1), 24.

Abushal, T. A., Soliman, A., & Abd-Elmougod, G. (2022). Inference of partially observed causes for failure of lomax competing risks model under type-ii generalized hybrid censoring scheme. Alexandria Engineering Journal, 61(7), 5427–5439.

Agiwal, V. (2023). Bayesian estimation of stress strength reliability from inverse chen distribution with application on failure time data. Annals of Data Science, 10(2), 317–347.

Ahmad, H. H., Almetwally, E. M., & Ramadan, D. A. (2022). A comparative inference on reliability estimation for a multi-component stress-strength model under power lomax distribution with applications. AIMS Math, 7, 18050–18079.

Ahmad, Z., Ilyas, M., & Hamedani, G. G. (2019). The extended alpha power transformed family of distributions: properties and applications. Journal of Data Science, 17(4), 726 -741.

Akaike, H. (1973). Information theory and an extension of the maximum likelihood principle. In B.n. petrov and f. csaki eds., 2nd international symposium on information theory (p. 267-281).

Al-Babtain, A. A., Elbatal, I., & Almetwally, E. M. (2022). Bayesian and non-bayesian reliability estimation of stress-strength model for power-modified lindley distribution. Computational Intelligence and Neuroscience, 2022(1), 1154705.

Al-Bossly, A. (2022). Inference of competing risks chen lifetime populations under type-i censoring scheme when causes of failure are partially observed. Alexandria Engineering Journal, 61(12), 12991–12999.

Algarni, A., Almarashi, A. M., Okasha, H., & Ng, H. K. T. (2020). E-bayesian estimation of chen distribution based on type-i censoring scheme. Entropy, 22(6), 636.

Almalki, S. J., & Yuan, J. (2013). A new modified weibull distribution. Reliability Engineering & System Safety, 111, 164–170.

Almarashi, A. M., Algarni, A., & Abd-Elmougod, G. A. (2020). Statistical analysis of competing risks lifetime data from nadarajaha and haghighi distribution under type-ii censoring. Journal of Intelligent & Fuzzy Systems, 38(3), 2591–2601.

Almongy, H. M., Almetwally, E. M., Aljohani, H. M., Alghamdi, A. S., & Hafez, E. (2021). A new extended rayleigh distribution with applications of covid-19 data. Results in Physics, 23, 104012.

Almuhayfith, F. E., Darwish, J. A., Alharbi, R., & Marin, M. (2022). Burr xii distribution for disease data analysis in the presence of a partially observed failure mode. Symmetry, 14(7), 1298.

Ariana, M., Vaferi, B., & Karimi, G. (2015). Prediction of thermal conductivity of alumina water-based nanofluids by artificial neural networks. Powder Technology, 278, 1–10.

Ashour, S., & Nassar, M. (2017). Inference for weibull distribution under adaptive type-i progressive hybrid censored competing risks data. Communications in Statistics-Theory and Methods, 46(10), 4756–4773.

Azuma, J., Maegdefessel, L., Kitagawa, T., Dalman, R. L., McConnell, M. V., & Tsao, P. S. (2011). Assessment of elastase-induced murine abdominal aortic aneurysms: Comparison of ultrasound imaging with in situ video microscopy. BioMed Research International, 2011(1), 252141.

Balasooriya, U. (1995). Failure–censored reliability sampling plans for the exponential distribution. Journal of Statistical Computation and Simulation, 52(4), 337–349.

Barbiero, A. (2013). Inference on reliability of stress-strength models for poisson data. Journal of Quality and Reliability Engineering, 2013(1), 530530.

Barros, M., Paula, G. A., & Leiva, V. (2008). A new class of survival regression models with heavy-tailed errors: robustness and diagnostics. Lifetime data analysis, 14, 316–332.

Berger, J. O. (2013). Statistical decision theory and bayesian analysis. Springer Science & Business Media, New York.

Berger, J. O., & Sun, D. (1993). Bayesian analysis for the poly-weibull distribution. Journal of the American Statistical Association, 88(424), 1412–1418.

Bhattacharyya, G., & Johnson, R. A. (1974). Estimation of reliability in a multicomponent stress-strength model. Journal of the American Statistical Association, 69(348), 966–970.

Birnbaum, Z., & McCarty, R. (1958). A distribution-free upper confidence bound for $pr\{Y < X\}$, based on independent samples of x and y. The Annals of Mathematical Statistics, 558–562.

Birnbaum, Z., et al. (1956). On a use of the mann-whitney statistic. In Proceedings of the third berkeley symposium on mathematical statistics and probability (Vol. 1, pp. 13–17).

Biswas, A., Chakraborty, S., & Mukherjee, M. (2021). On estimation of stress–strength reliability with log-lindley distribution. Journal of Statistical Computation and Simulation, 91(1), 128–150.

Block, H. W., Savits, T. H., & Singh, H. (1998). The reversed hazard rate function. Probability in the Engineering and informational Sciences, 12(1), 69–90.

Bocchetti, D., Giorgio, M., Guida, M., & Pulcini, G. (2009). A competing risk model for the reliability of cylinder liners in marine diesel engines. Reliability Engineering & System Safety, 94(8), 1299–1307.

Bourguignon, M., Silva, R. B., & Cordeiro, G. M. (2014). The weibull-g family of probability distributions. Journal of data science, 12(1), 53–68.

Box, G. E., & Tiao, G. C. (2011). Bayesian inference in statistical analysis. John Wiley & Sons, New York.

Burr, I. W. (1942). Cumulative frequency functions. The Annals of mathematical statistics, 13(2), 215–232.

Carrasco, J. M., Ortega, E. M., & Cordeiro, G. M. (2008). A generalized modified weibull distribution for lifetime modeling. Computational Statistics & Data Analysis, 53(2), 450–462.

Carrasco, J. M., Ortega, E. M., & Paula, G. A. (2008). Log-modified weibull regression models with censored data: Sensitivity and residual analysis. Computational statistics & data analysis, 52(8), 4021–4039.

Chacko, M., & Mohan, R. (2019). Bayesian analysis of weibull distribution based on progressive type-ii censored competing risks data with binomial removals. Computational Statistics, 34, 233–252.

Chandra, N. K., & Roy, D. (2001). Some results on reversed hazard rate. Probability in the Engineering and informational Sciences, 15(1), 95–102.

Chandra, P., Mahto, A. K., & Tripathi, Y. M. (2023). Inference for a competing risks model with burr xii distributions under generalized progressive hybrid censoring. Brazilian Journal of Probability and Statistics, 37(3), 566–595.

Chandrasekar, B., Childs, A., & Balakrishnan, N. (2004). Exact likelihood inference for the exponential distribution under generalized type-i and type-ii hybrid censoring. Naval Research Logistics (NRL), 51(7), 994–1004.

Chen, M. H., & Shao, Q. M. (1999). Monte carlo estimation of bayesian credible and hpd intervals. Journal of computational and Graphical Statistics, 8(1), 69–92.

Chung, W. K. (1982). Some stress-strength reliability models. Microelectronics Reliability, 22(2), 277–280.

Cohen, A. C. (1963). Progressively censored samples in life testing. Technometrics, 5(3), 327–339.

Çolak, A. B., Sindhu, T. N., Lone, S. A., Akhtar, M. T., & Shafiq, A. (2024). A comparative analysis of maximum likelihood estimation and artificial neural network modeling to assess electrical component reliability. Quality and Reliability Engineering International, 40(1), 91–114.

Collett, D. (2023). Modelling survival data in medical research. Chapman and Hall, London.

Cook, R. D. (1977). Detection of influential observation in linear regression. Technometrics, 19(1), 15–18.

Cordeiro, G. M., Gomes, A. E., & da Silva, C. Q. (2014). Another extended burr iii model: some properties and applications. Journal of Statistical Computation and Simulation, 84(12), 2524–2544.

Cox, D. R. (1959). The analysis of exponentially distributed life-times with two types of failure. Journal of the Royal Statistical Society Series B: Statistical Methodology, 21(2), 411–421.

Cramer, E., & Schmiedt, A. B. (2011). Progressively type-ii censored competing risks data from lomax distributions. Computational Statistics & Data Analysis, 55(3), 1285–1303.

Dagum, C. (2008). A new model of personal income distribution: specification and estimation. In Modeling income distributions and lorenz curves (pp. 3–25). Springer, New York.

Deepthy, G., Anakha, K., & Nicy, S. (2025). Inference on partially observed competing risks models using generalized type-ii hybrid censoring scheme. Austrian Journal of Statistics, 54(4), 117–135.

Deepthy, G., Areekara, S., & Sebastian, N. (2024). A comprehensive analysis using maximum likelihood estimation and artificial neural networks for modeling arthritic pain relief data. Stochastics and Quality Control.

Deepthy, G., Sebastian, N., & Chandra, N. (2023). Applications of burr iii-weibull quantile function in reliability analysis. Statistical Theory and Related Fields, 7(4), 296–308.

Demiray, D., & Kızılaslan, F. (2024). Reliability estimation of a consecutive k-out-of-n system for non-identical strength components with applications to wind speed data. Quality Technology & Quantitative Management, 21(1), 111–146.

Dey, S., Mazucheli, J., & Anis, M. (2017). Estimation of reliability of multicomponent stress-strength for a kumaraswamy distribution. Communications in Statistics-Theory and Methods, 46(4), 1560–1572.

Domma, F. (2010). Some properties of the bivariate burr type iii distribution. Statistics, 44(2), 203–215.

Du, Y., & Gui, W. (2022). Statistical inference of burr-xii distribution under adaptive type ii progressive censored schemes with competing risks. Results in Mathematics, 77(2), 81.

Dutta, S., & Kayal, S. (2024). Estimation and prediction for burr type iii distribution based on unified progressive hybrid censoring scheme. Journal of Applied Statistics, 51(1), 1–33.

Dutta, S., Ng, H. K. T., & Kayal, S. (2023). Inference for a general family of inverted exponentiated distributions under unified hybrid censoring with partially observed competing risks data. Journal of Computational and Applied Mathematics, 422, 114934.

Dutta, S., Ng, H. K. T., & Kayal, S. (2024). Inference for kumaraswamy-g family of distributions under unified progressive hybrid censoring with partially observed competing risks data. Statistica Neerlandica, 78(4), 719–742.

Efron, B. (1982). The jackknife, the bootstrap and other resampling plans. Society for industrial and applied mathematics, Philadelphia.

Efron, B. (1988). Logistic regression, survival analysis, and the kaplan-meier curve. Journal of the American statistical Association, 83(402), 414–425.

Eliwa, M., Altun, E., Alhussain, Z. A., Ahmed, E. A., Salah, M. M., Ahmed, H. H., & El-Morshedy, M. (2021). A new one-parameter lifetime distribution and its regression model with applications. Plos one, 16(2), e0246969.

Epstein, B. (1954). Truncated life tests in the exponential case. The Annals of Mathematical Statistics, 555–564.

Falgore, J. Y., & Doguwa, S. I. (2020). The inverse lomax-g family with application to breaking strength data. Asian Journal of Probability and Statistics, 8(2), 49–60.

Farghal, A.-W. A., Badr, S. K., Abu-Zinadah, H., & Abd-Elmougod, G. A. (2023). Analysis of generalized inverted exponential competing risks model in presence of partially observed failure modes. Alexandria Engineering Journal, 78, 74–87.

Fathi, A., Farghal, A.-W. A., & Soliman, A. A. (2024). Inference on weibull inverted exponential distribution under progressive first-failure censoring with

constant-stress partially accelerated life test. Statistical Papers, 65(8), 5021–5053.

Finkelstein, M. S. (2002). On the reversed hazard rate. Reliability Engineering & System Safety, 78(1), 71–75.

Fleming, T. R., & Harrington, D. P. (2013). Counting processes and survival analysis (Vol. 625). John Wiley & Sons, New York.

Gadde, D. S. R. (2012). Estimation of reliability in multicomponent stress-strength based on generalized exponential distribution. Revista Colombiana de Estadística.

Ganji, M., Bevrani, H., Golzar, N. H., & Zabihi, S. (2016). The weibull-rayleigh distribution, some properties, and applications. Journal of Mathematical Sciences, 218(3), 269–277.

Gaver, D. P., & Lewis, P. A. (1980). First-order autoregressive gamma sequences and point processes. Advances in Applied Probability, 12(3), 727–745.

Gilchrist, W. (2000). Statistical modelling with quantile functions. Chapman and Hall/CRC, New York.

Gillariose, J., & Tomy, L. (2023). On an extension of the two-parameter lindley distribution. Reliability: Theory & Applications, 18(1 (72)), 385–402.

Glänzel, W. (1987). A characterization theorem based on truncated moments and its application to some distribution families. In Mathematical statistics and probability theory: volume b statistical inference and methods proceedings of the 6th pannonian symposium on mathematical statistics, bad tatzmannsdorf, austria, september 14–20, 1986 (pp. 75–84).

Govindarajulu, Z. (1977). A class of distributions useful in life testing and reliability with applications to nonparametric testing. In The theory and applications of reliability with emphasis on bayesian and nonparametric methods (pp. 109–129). Elsevier.

Gupta, R. D., & Kundu, D. (1998). Hybrid censoring schemes with exponential failure distribution. Communications in Statistics-Theory and Methods, 27(12), 3065–3083.

Hachen Jr, D. S. (1988). The competing risks model: A method for analyzing processes with multiple types of events. Sociological Methods & Research, 17(1), 21–54.

Hankin, R. K., & Lee, A. (2006). A new family of non-negative distributions. Australian & New Zealand Journal of Statistics, 48(1), 67–78.

Haq, M. A. u., Hashmi, S., Aidi, K., Ramos, P. L., & Louzada, F. (2020). Unit modified burr-iii distribution: Estimation, characterizations and validation test. Annals of Data Science, 1–26.

Hashimoto, E. M., Ortega, E. M., Cancho, V. G., & Cordeiro, G. M. (2010). The log-exponentiated weibull regression model for interval-censored data. Computational statistics & data analysis, 54(4), 1017–1035.

Hassan, A. S., Elsherpieny, E., & Aghel, W. E. (2023). Statistical inference of the burr type iii distribution under joint progressively type-ii censoring. Scientific African, 21, e01770.

Hastings, W. K. (1970). Monte carlo sampling methods using markov chains and their applications. Biometrika, 57, 97-109.

Hastings Jr, C., Mosteller, F., Tukey, J. W., & Winsor, C. P. (1947). Low moments for small samples: a comparative study of order statistics. The Annals of Mathematical Statistics, 18(3), 413–426.

Hoel, D. G. (1972). A representation of mortality data by competing risks. Biometrics, 475–488.

Hosking, J. R. (1990). L-moments: analysis and estimation of distributions using linear combinations of order statistics. Journal of the Royal Statistical Society Series B: Statistical Methodology, 52(1), 105–124.

Huang, S., & Oluyede, B. O. (2014). Exponentiated kumaraswamy-dagum distribution with applications to income and lifetime data. Journal of Statistical Distributions and Applications, 1, 1–20.

Hyun, S., Lee, J., & Yearout, R. (2016). Parameter estimation of type-i and type-ii hybrid censored data from the log-logistic distribution. Industrial and systems engineering review, 4(1), 37–44.

Iranmanesh, A., Fathi Vajargah, K., & Hasanzadeh, M. (2018). On the estimation of stress strength reliability parameter of inverted gamma distribution. Mathematical Sciences, 12, 71–77.

Jamal, F., Abuzaid, A. H., Tahir, M. H., Nasir, M. A., Khan, S., & Mashwani, W. K. (2021). New modified burr iii distribution, properties and applications. Mathematical and Computational Applications, 26(4), 82.

Jamal, F., Nasir, M. A., Tahir, M., & Montazeri, N. H. (2017). The odd burr-iii family of distributions. Journal of Statistics Applications and Probability, 6(1), 105–122.

Jayakumar, K., & Babu, M. G. (2015). Some generalizations of weibull distribution and related processes. Journal of Statistical Theory and Applications, 14(4), 425–434.

Kalbfleisch, J. D., & Prentice, R. L. (2011). The statistical analysis of failure time data. John Wiley & Sons, New York.

Karim, M. R., Islam, M. A., et al. (2019). Reliability and survival analysis. Springer.

Kilai, M., Waititu, G. A., Kibira, W. A., Abd El-Raouf, M., & Abushal, T. A. (2022). A new versatile modification of the rayleigh distribution for modeling covid-19 mortality rates. Results in Physics, 35, 105260.

Kleiber, C. (2003). Statistical size distributions in economics and actuarial sciences. John Wiley &Sons, Inc, Hoboken, N J.

Klein, J. P., & Moeschberger, M. L. (2006). Survival analysis: techniques for censored and truncated data. Springer Science & Business Media, New York.

Kohansal, A. (2019). On estimation of reliability in a multicomponent stress-strength model for a kumaraswamy distribution based on progressively censored sample. Statistical Papers, 60, 2185–2224.

Kohansal, A., Fernández, A. J., & Pérez-González, C. J. (2021). Multicomponent stress–strength parameter estimation of a non-identical-component strengths system under the adaptive hybrid progressive censoring samples. Statistics, 55(4), 925–962.

Koley, A., & Kundu, D. (2017). On generalized progressive hybrid censoring in presence of competing risks. Metrika, 80, 401–426.

Koley, A., Kundu, D., & Ganguly, A. (2017). Analysis of type-ii hybrid censored competing risks data. Statistics, 51(6), 1304–1325.

Krishna, H., Dube, M., & Garg, R. (2017). Estimation of p (y¡ x) for progressively first-failure-censored generalized inverted exponential distribution. Journal of Statistical Computation and Simulation, 87(11), 2274–2289.

Krishnamoorthy, K., & Lin, Y. (2010). Confidence limits for stress–strength reliability involving weibull models. Journal of Statistical Planning and Inference, 140(7), 1754–1764.

Krishnamoorthy, K., Mukherjee, S., & Guo, H. (2007). Inference on reliability in two-parameter exponential stress–strength model. Metrika, 65, 261–273.

Kumar, K., Krishna, H., & Garg, R. (2015). Estimation of p (y¡ x) in lindley distribution using progressively first failure censoring. International Journal of System Assurance Engineering and Management, 6, 330–341.

Kundu, D., & Basu, S. (2000). Analysis of incomplete data in presence of competing risks. Journal of Statistical Planning and Inference, 87(2), 221–239.

Kundu, D., & Gupta, R. D. (2005). Estimation of $p[y < x]$ for generalized exponential distribution. Metrika, 61(3), 291–308.

Kundu, D., & Gupta, R. D. (2006). Estimation of $p[y < x]$ for weibull distributions. IEEE Trans. Reliab., 55(2), 270–280.

Lai, C. D., & Xie, M. (2006). Stochastic ageing and dependence for reliability. Springer Science & Business Media, New York.

Lawless, J. F. (1982). Parametric regression models. Statistical Models and Methods for Lifetime Data, 6, 269–339.

Lawless, J. F. (2011). Statistical models and methods for lifetime data. John Wiley & Sons, New York.

Lee, C., Famoye, F., & Olumolade, O. (2007). Beta-weibull distribution: some properties and applications to censored data. Journal of modern applied statistical methods, 6, 173–186.

Lee, E. T., & Wang, J. (2003). Statistical methods for survival data analysis (Vol. 476). John Wiley & Sons, Germany.

Lindsay, S., Wood, G., & Woollons, R. (1996). Modelling the diameter distribution of forest stands using the burr distribution. Journal of applied statistics, 23(6), 609–620.

Lio, Y., Tsai, T.-R., Wang, L., & Cecilio Tejada, I. P. (2022). Inferences of the multicomponent stress–strength reliability for burr xii distributions. Mathematics, 10(14), 2478.

Lipsitz, S. R., Laird, N. M., & Harrington, D. P. (1990). Using the jackknife to estimate the variance of regression estimators from repeated measures studies. Communications in Statistics-Theory and Methods, 19(3), 821–845.

Liu, M. C., Kuo, W., & Sastri, T. (1995). An exploratory study of a neural network approach for reliability data analysis. Quality and Reliability Engineering International, 11(2), 107–112.

Lodhi, C., Tripathi, Y. M., & Wang, L. (2021). Inference for a general family of inverted exponentiated distributions with partially observed competing risks under generalized progressive hybrid censoring. Journal of Statistical Computation and Simulation, 91(12), 2503–2526.

Mahmoud, M., & Ghazal, M. (2017). Estimations from the exponentiated rayleigh distribution based on generalized type-ii hybrid censored data. Journal of the Egyptian Mathematical Society, 25(1), 71–78.

Mahto, A. K., Lodhi, C., Tripathi, Y. M., & Wang, L. (2022). Inference for partially observed competing risks model for kumaraswamy distribution under generalized progressive hybrid censoring. Journal of Applied Statistics, 49(8), 2064–2092.

Makkar, P., Srivastava, P. K., Singh, R., & Upadhyay, S. (2014). Bayesian survival analysis of head and neck cancer data using lognormal model. Communications in Statistics-Theory and Methods, 43(2), 392–407.

Manly, B. F. (2018). Randomization, bootstrap and monte carlo methods in biology. chapman and hall/CRC, New York.

Marshall, A. W., & Olkin, I. (1997). A new method for adding a parameter to a family of distributions with application to the exponential and weibull families. Biometrika, 84(3), 641–652.

McCullagh, P. (2019). Generalized linear models. CRC Press, Routledge.

Meeker, W. Q. (1984). A comparison of accelerated life test plans for weibull and lognormal distributions and type i censoring. Technometrics, 26(2), 157–171.

Metropolis, N., Rosenbluth, A. W., Rosenbluth, M. N., Teller, A. H., & Teller, E. (1953). Equation of state calculations by fast computing machines. The journal of chemical physics, 21(6), 1087–1092.

Mielke Jr, P. W. (1973). Another family of distributions for describing and analyzing precipitation data. Journal of Applied Meteorology, 275–280.

Mills, J. P. (1926). Table of the ratio: area to bounding ordinate, for any portion of normal curve. Biometrika, 18(3), 395–400.

Modi, K., & Gill, V. (2020). Unit burr-iii distribution with application. Journal of Statistics and Management Systems, 23(3), 579–592.

Mudholkar, G. S., & Hutson, A. D. (1996). The exponentiated weibull family: some properties and a flood data application. Communications in Statistics-Theory and Methods, 25(12), 3059–3083.

Nadar, M., & Kızılaslan, F. (2015). Estimation of reliability in a multicomponent stress-strength model based on a marshall-olkin bivariate weibull distribution. IEEE Transactions on Reliability, 65(1), 370–380.

Nadarajah, S., & Kotz, S. (2008). Strength modeling using weibull distributions. Journal of mechanical science and technology, 22, 1247–1254.

Nair, N. U., & Sankaran, P. (2009). Quantile-based reliability analysis. Communications in Statistics-Theory and Methods, 38(2), 222–232.

Nair, N. U., Sankaran, P., & Balakrishnan, N. (2013). Quantile-based reliability analysis. Springer, New York.

Nair, N. U., Sankaran, P., & Kumar, B. V. (2008). Total time on test transforms of order n and their implications in reliability analysis. Journal of Applied Probability, 45(4), 1126–1139.

Nasir, M. A., Korkmaz, M. C., Jamal, F., & Yousof, H. M. (2018). On a new weibull burr xii distribution for lifetime data. Sohag Journal of Mathematics, 5(2), 47–56.

Nassar, M., & Elshahhat, A. (2024). Estimation procedures and optimal censoring schemes for an improved adaptive progressively type-ii censored weibull distribution. Journal of Applied Statistics, 51(9), 1664–1688.

Nguimkeu, P., Rekkas, M., & Wong, A. (2015). Interval estimation of the stress-strength reliability with independent normal random variables. Communications in Statistics-Theory and Methods, 44(6), 1210–1221.

Nikulin, M. S. (1973). Chi-square test for continuous distributions with location and scale parameters. Teoriya Veroyatnostei i ee Primeneniya, 18(3), 583–591.

Olobatuyi, K. (2017). A new class of generalized burr iii distribution for lifetime data. arXiv preprint arXiv:1701.00403.

Ortega, E. M., Cordeiro, G. M., Campelo, A. K., Kattan, M. W., & Cancho, V. G. (2015). A power series beta weibull regression model for predicting breast carcinoma. Statistics in medicine, 34(8), 1366–1388.

Ortega, E. M., Cordeiro, G. M., Pascoa, M. A., & Couto, E. V. (2012). The log-exponentiated generalized gamma regression model for censored data. Journal of Statistical Computation and Simulation, 82(8), 1169–1189.

Ortega, E. M., Paula, G. A., & Bolfarine, H. (2008). Deviance residuals in generalised log-gamma regression models with censored observations. Journal of Statistical Computation and Simulation, 78(8), 747–764.

Pareek, B., Kundu, D., & Kumar, S. (2009). On progressively censored competing risks data for weibull distributions. Computational Statistics & Data Analysis, 53(12), 4083–4094.

Pescim, R. R., Ortega, E. M., Cordeiro, G. M., & Alizadeh, M. (2017). A new log-location regression model: estimation, influence diagnostics and residual analysis. Journal of Applied Statistics, 44(2), 233–252.

Pescim, R. R., Ortega, E. M., Cordeiro, G. M., Demtriod, C. G., & Hamedani, G. (2013). The log-beta generalized half-normal regression model. Journal of Statistical Theory and Applications, 12(4), 330–347.

Prudnikov, A. P., Brychkov, I. A., & Marichev, O. I. (1986). Integrals and series: special functions (Vol. 2). CRC press, New York.

Rabie, A., & Li, J. (2019). E-bayesian estimation based on burr-x generalized type-ii hybrid censored data. Symmetry, 11(5), 626.

Ramberg, J. S. (1975). A probability distribution with applications to monte carlo simulation studies. In A modern course on statistical distributions in

scientific work: Volume 2—model building and model selection proceedings of the nato advanced study institute held at the university of calgary, calgary, alberta, canada july 29–august 10, 1974 (pp. 51–64).

Ramberg, J. S., & Schmeiser, B. W. (1972). An approximate method for generating symmetric random variables. Communications of the ACM, 15(11), 987–990.

Rao, G. S., & Kantam, R. (2008). Estimation of reliability in multicomponent stress-strength model: Log-logistic distribution. parameters, 1, 2.

Rao, G. S., Mbwambo, S., & Josephat, P. (2019). Estimation of stress–strength reliability from exponentiated inverse rayleigh distribution. International Journal of Reliability, Quality and Safety Engineering, 26(01), 1950005.

Rao, K. C., & Robson, B. (1974). A chi-squabe statistic for goodies-of-fit tests within the exponential family. Communications in Statistics-Theory and Methods, 3(12), 1139–1153.

Rasethuntsa, T. R., & Nadar, M. (2018). Stress–strength reliability of a non-identical-component-strengths system based on upper record values from the family of kumaraswamy generalized distributions. Statistics, 52(3), 684–716.

Rodriguez, R. N. (1977). A guide to the burr type xii distributions. Biometrika, 64(1), 129–134.

Saboor, A., Bakouch, H. S., & Khan, M. N. (2016). Beta sarhan–zaindin modified weibull distribution. Applied Mathematical Modelling, 40(13-14), 6604–6621.

Saini, S., Chaturvedi, A., & Garg, R. (2021). Estimation of stress–strength reliability for generalized maxwell failure distribution under progressive first failure censoring. Journal of Statistical Computation and Simulation, 91(7), 1366–1393.

Saini, S., Patel, J., & Garg, R. (2024). Statistical inference on multicomponent stress–strength reliability with non-identical component strengths using progressively censored data from kumaraswamy distribution. Soft Computing, 28(17), 9317–9339.

Saini, S., Tomer, S., & Garg, R. (2022). On the reliability estimation of multi-component stress–strength model for burr xii distribution using progressively first-failure censored samples. Journal of Statistical Computation and Simulation, 92(4), 667–704.

Sankaran, P., Nair, N. U., & Midhu, N. (2016). A new quantile function with applications to reliability analysis. Communications in statistics-Simulation and Computation, 45(2), 566–582.

Sankaran, P. G., & Dileep Kumar, M. (2018). A new class of quantile functions useful in reliability analysis. Journal of statistical Theory and Practice, 12, 615–634.

Schervish, M. J. (2012). Theory of statistics. Springer Science & Business Media, New York.

Schwarz, G. (1978). Estimating the dimension of a model. The annals of statistics, 461–464.

Shafay, A. (2016). Bayesian estimation and prediction based on generalized type-ii hybrid censored sample. Journal of Statistical Computation and Simulation, 86(10), 1970–1988.

Shafiq, A., Çolak, A. B., Lone, S. A., Sindhu, T. N., & Muhammad, T. (2024). Reliability modeling and analysis of mixture of exponential distributions using artificial neural network. Mathematical Methods in the Applied Sciences, 47(5), 3308–3328.

Shafiq, A., Çolak, A. B., & Naz Sindhu, T. (2021). Designing artificial neural network of nanoparticle diameter and solid–fluid interfacial layer on single-walled carbon nanotubes/ethylene glycol nanofluid flow on thin slendering needles. International Journal for Numerical Methods in Fluids, 93(12), 3384–3404.

Shafiq, A., Çolak, A. B., Sindhu, T. N., Lone, S. A., & Abushal, T. A. (2023). Modeling and survival exploration of breast carcinoma: a statistical, maximum

likelihood estimation, and artificial neural network perspective. Artificial Intelligence in the Life Sciences, 4, 100082.

Shafiq, A., Çolak, A. B., Sindhu, T. N., Lone, S. A., Alsubie, A., & Jarad, F. (2022). Comparative study of artificial neural network versus parametric method in covid-19 data analysis. Results in Physics, 38, 105613.

Shafiq, A., Çolak, A. B., Sindhu, T. N., & Muhammad, T. (2022). Optimization of darcy-forchheimer squeezing flow in nonlinear stratified fluid under convective conditions with artificial neural network. Heat Transfer Research, 53(3).

Shafiq, A., Çolak, A. B., Swarup, C., Sindhu, T. N., & Lone, S. A. (2022). Reliability analysis based on mixture of lindley distributions with artificial neural network. Advanced Theory and Simulations, 5(8), 2200100.

Shao, Q., Chen, Y. D., & Zhang, L. (2008). An extension of three-parameter burr iii distribution for low-flow frequency analysis. Computational Statistics & Data Analysis, 52(3), 1304–1314.

Sharma, V. K., Singh, S. K., Singh, U., & Agiwal, V. (2015). The inverse lindley distribution: a stress-strength reliability model with application to head and neck cancer data. Journal of Industrial and Production Engineering, 32(3), 162–173.

Silva, G. O., Ortega, E. M., Cancho, V. G., & Barreto, M. L. (2008). Log-burr xii regression models with censored data. Computational statistics & data analysis, 52(7), 3820–3842.

Silva, G. O., Ortega, E. M., & Cordeiro, G. M. (2009). A log-extended weibull regression model. Computational statistics & data analysis, 53(12), 4482–4489.

Sindhu, T. N., Çolak, A. B., Lone, S. A., Shafiq, A., & Abushal, T. A. (2024). A decreasing failure rate model with a novel approach to enhance the artificial neural network's structure for engineering and disease data analysis. Tribology International, 192, 109231.

Sindhu, T. N., Shafiq, A., & Huassian, Z. (2024). Generalized exponentiated unit gompertz distribution for modeling arthritic pain relief times data: classical approach to statistical inference. Journal of Biopharmaceutical Statistics, 34(3), 323–348.

Singh, D. P., Jha, M. K., Tripathi, Y., & Wang, L. (2022). Reliability estimation in a multicomponent stress-strength model for unit burr iii distribution under progressive censoring. Quality Technology & Quantitative Management, 19(5), 605–632.

Singh, K., Kumar Mahto, A., & Mani Tripathi, Y. (2024). On partially observed competing risks model for chen distribution under generalized progressive hybrid censoring. Statistica Neerlandica, 78(1), 105–135.

Singh, S. K., Singh, U., Yaday, A., & Viswkarma, P. (2015). On the estimation of stress strength reliability parameter of inverted exponential distribution. International Journal of Scientific World, 3(1), 98–112.

Soliman, A. A., Abd-Ellah, A. H., Abou-Elheggag, N. A., & Abd-Elmougod, G. A. (2012). Estimation of the parameters of life for gompertz distribution using progressive first-failure censored data. Computational Statistics & Data Analysis, 56(8), 2471–2485.

Susam, S. O., & Hudaverdi, B. (2024). Stress–strength reliability for electricity systems based on the bernstein copula approximation. Energy Sources, Part B: Economics, Planning, and Policy, 19(1), 2411532.

Tadikamalla, P. R. (1980). A look at the burr and related distributions. International Statistical Review/Revue Internationale de Statistique, 337–344.

Therneau, T. M., Grambsch, P. M., & Fleming, T. R. (1990). Martingale-based residuals for survival models. Biometrika, 77(1), 147–160.

Usman, R. M., & Haq, M. A. u. (2019). Some remarks on odd burr iii weibull distribution. Annals of Data Science, 6, 21–38.

Varadhan, R., Weiss, C. O., Segal, J. B., Wu, A. W., Scharfstein, D., & Boyd, C. (2010). Evaluating health outcomes in the presence of competing risks: a review of statistical methods and clinical applications. Medical care, 48(6), S96–S105.

Waini, I., Ishak, A., & Pop, I. (2021). Dufour and soret effects on al2o3-water nanofluid flow over a moving thin needle: Tiwari and das model. International Journal of Numerical Methods for Heat & Fluid Flow, 31(3), 766–782.

Weibull, W. (1951). A statistical distribution function of wide applicability. Journal of applied mechanics, 18(3), 293-297.

Wingo, D. (1983). Maximum likelihood methods for fitting the burr type xii distribution to life test data. Biometrical journal, 25(1), 77–84.

Wu, S.-J., & Kuş, C. (2009). On estimation based on progressive first-failure-censored sampling. Computational Statistics & Data Analysis, 53(10), 3659–3670.

Xavier, T., & Jose, J. K. (2021a). Estimation of reliability in a multicomponent stress–strength model based on power transformed half-logistic distribution. International Journal of Reliability, Quality and Safety Engineering, 28(02), 2150009.

Xavier, T., & Jose, J. K. (2021b). A study of stress-strength reliability using a generalization of power transformed half-logistic distribution. Communications in Statistics-Theory and Methods, 50(18), 4335–4351.

Xia, Z., Yu, J., Cheng, L., Liu, L., & Wang, W. (2009). Study on the breaking strength of jute fibres using modified weibull distribution. Composites Part A: Applied Science and Manufacturing, 40(1), 54–59.

Xie, M., & Lai, C. D. (1996). Reliability analysis using an additive weibull model with bathtub-shaped failure rate function. Reliability Engineering & System Safety, 52(1), 87–93.

Xie, M., Tang, Y., & Goh, T. N. (2002). A modified weibull extension with bathtub-shaped failure rate function. Reliability Engineering & System Safety, 76(3), 279–285.

Yadav, A. S., Singh, S. K., & Singh, U. (2018). Estimation of stress–strength reliability for inverse weibull distribution under progressive type-ii censoring scheme. Journal of Industrial and Production Engineering, 35(1), 48–55.

Yadav, S., Singh, S. K., & Kaushik, A. (2024). Parameter estimation of burr type-iii distribution under generalized progressive hybrid censoring scheme. Japanese Journal of Statistics and Data Science, 1–52.

Yakubu, A., & Doguwa, S. I. (2017). On the properties of the weibull-burr iii distribution and its application to uncensored and censored survival data. CBN Journal of Applied Statistics, 8(2), 91–116.

Yu, H. F., & Peng, C. Y. (2013). Estimation for weibull distribution with type ii highly censored data. Quality Technology & Quantitative Management, 10(2), 193–202.

Zellner, A. (1986). Bayesian estimation and prediction using asymmetric loss functions. Journal of the American Statistical Association, 81(394), 446–451.

Zhang, L., Xu, A., An, L., & Li, M. (2022). Bayesian inference of system reliability for multicomponent stress-strength model under marshall-olkin weibull distribution. Systems, 10(6), 196.

Zheng, Y., Ye, T., & Gui, W. (2024). Parameter estimation of inverted exponentiated half-logistic distribution under progressive type-ii censored data with competing risks. American Journal of Mathematical and Management Sciences, 43(1), 21–39.

Zhu, T. (2020). Statistical inference of weibull distribution based on generalized progressively hybrid censored data. Journal of Computational and Applied Mathematics, 371, 112705.

List of Presentations

1. Deepthy G. S presented a paper on "BurrIII-Weibull Distribution; Properties And Its Applications" in National Seminar in Applied Statistics and Symposium on Stochastic Modelling organized by Department of Statistics and B.Voc Data Science, St.Thomas' College (Autonomous), Thrissur during 4 - 6 February 2020.

2. Deepthy G. S presented a paper on "Burr III Weibull Distribution: properties, applications and characterizations" in Eighth International Conference on Statistics for Twenty-first Century-2022 organized by the International Statistics Fraternity(ISF), School of Physical and Mathematical Sciences and Department of Statistics, University of Kerala, Trivandrum during during 16 - 19 December, 2022.

3. Deepthy G. S presented a paper on "Estimation of Stress Strength Reliability for Weibull Burr III Distribution" in International Conference on Knowledge Discoveries on Statistical Innovations & Recent Advances in Optimization (ICON-KSRAO), Department of Statistics, Andra University, Visakhapatnam on 29^{th} & 30th December 2022.

4. Deepthy G. S presented a paper on "A comparative analysis of maximum likelihood estimation and artificial neural network for modeling clinical data." in Ninth International Conference on "Statistics for Twenty-first Century-2023 organized by International Statistics Fraternity(ISF), Department of Statistics and School of Physical and Mathematical Sciences, University of Kerala, Trivandrum during 15 - 18 December, 2023.

5. Deepthy G. S presented a paper on "On Log Odd Burr III Weibull distribution", International Conference on Recent Advances of Probability and Statistics in Interdisciplinary Research (RAPSIR-2024) organized by Department of Statistics, Faculty of Science, University of Allahabad, Prayagraj, India in Conjunction with 43rd Annual Convention of Indian Society for Probability and Statistics (ISPS) during 06-08 February 2024.

6. Deepthy G. S presented a paper on "Inference for partially observed competing risks model for Weibull distribution under Generalized Type-II Hybrid censoring" in the International Conference on Advanced Data Analytics and Statistics (ICADS 2025) organized by the Department of Statistics, Vimala College (Autonomous), Thrissur in association with The Kerala Statistical Association (KSA) during 23 - 25 January 2025.

List of published/ accepted papers

- Deepthy, G. S., Sebastian, N. & Rison, R. (2021). Some Properties and Applications of Burr III-Weibull Distribution. Applied Statistical Techniques and Stochastic Modelling, Nicy Sebastian and Sajesh T A, Proceedings of National Seminar in Applied Statistics and Symposium on Stochastic Modelling, Publication Division-St.Thomas College Thrissur, 2020, 97-112.

- Deepthy, G. S. & Sebastian, N. (2022). A New Life Time Distribution: Burr III Modified Weibull Distribution And Its Application in Burn in Process. *Reliability: Theory & Applications*, 17 (1(67)), 76-86.

- Deepthy, G. S., Sebastian, N. & Chandra, N. (2023). Applications of Burr III-Weibull quantile function in reliability analysis. *Statistical Theory and Related Fields*, 7(4), 296-308, DOI: 10.1080/24754269.2023.2201096.

- Deepthy, G. S., Areekara, S. & Sebastian, N. (2024). A Comprehensive Analysis Using Maximum Likelihood Estimation and Artificial Neural Networks for Modeling Arthritic Pain Relief Data. *Stochastics and Quality Control*, 40(1), 15-32. https://doi.org/10.1515/eqc-2024-0023.

- Deepthy, G. S., Anakha, K. K., & Nicy, S. (2025). Inference On Partially Observed Competing Risks Models Using Generalized Type-II Hybrid Censoring Scheme. *Austrian Journal of Statistics*, 54(4), 117–135.

- Deepthy, G. S., Lakshmi R., & Nicy Sebastian. On Log Odd Burr III Weibull Regression Model and its Application in Survival Analysis, Accepted in *Statistics and Applications*.

- Deepthy, G. S., Sebastian, N. & Chandra, N. Estimation of Stress-Strength Reliability Using Weibull Burr III Model and its Applications in Clinical Trial Data, Communicated in *Monte Carlo Methods and Applications*.

- Deepthy, G. S., Sebastian, N., Sini K.P. & Anakha, K. K. Characteristics and Goodness-of-Fit of the Burr III Weibull Distribution with Applications to COVID-19 Mortality Rates, Communicated in *Asian Journal of Statistical Sciences*.

- Deepthy, G. S., & Sebastian, N. Inference on Multi-Component Stress-Strength Reliability with Non-Identical Component Strengths Using progressively first-failure censored Data from the Weibull Distribution, Communicated in *Journal of Statistical Computation and Simulation*.